Uncertainties in Long-term Management of Water Resources

Golnaz Jahanshahi

School of Engineering
Newcastle University, UK

A Thesis submitted for the degree of
Doctor of Philosophy

June 2018

Abstract

A reliable supply of water to communities, industry and agriculture is crucial for a healthy population, and a successful economy. Long-term management of water resources poses significant challenges for decision makers due to uncertainties. Natural variability in hydrological processes, as well as future changes in climate, land use, demography and other socio economic factors are placing increased pressure on water resources and pose a threat to water security.

The release of probabilistic climate information, such as the UKCP09 scenarios, provides improved understanding of some uncertainties associated with climate model projections. This has motivated a more rigorous approach to dealing with other uncertainties in order to understand the sensitivity of investment decisions to future uncertainty and identify adaptation options that are as far as possible robust.

To understand the implications of this range of uncertainties, a novel integrated systems model has been developed that couples simulations of weather under current and future climates, catchment hydrology, and the water resources system. This systems model was used to assess the likelihood and magnitude of water scarcity. Uncertainty and sensitivity analyses were undertaken to assess the implications of uncertainties on water scarcity, and to subsequently identify water resources management options that are robust to these uncertainties. The integrated systems model has been applied in the Thames catchment which supplies the city of London, UK. This region has some of the lowest rainfalls in the UK, the largest and fastest growing population, and is therefore particularly sensitive to water availability.

Results indicate that by the 2080s, when accounting for all uncertainties considered here, there may not be a considerable change in total amount of rainfall relative to the control period (1961-1990). However as a result of an increase in temperature, the annual mean PET is expected to increase by 26.6%. Based on the results, a 24.0% and 1.3% reduction in annual mean daily flow and subsurface storage are projected to occur in the Thames catchment respectively. Moreover, a 1083.0% increase in the total number of drought days relative to the control period (1961-1990) is expected under current population and climate trends by 2080s.

Water scarcity in London is most sensitive to climate and population change, and so investment in monitoring to reduce these uncertainties would help improve the robustness of investment decisions. A portfolio of adaptation measures, that includes a combination of desalination plant with capacity of 150 Ml/d, constructing a new

reservoir with 100 Mm^3 capacity and 40.0% reduction in leakage, is required to reduce the drought risks. However, sensitivity testing shows that measures taken to reduce per capita water demand are more robust to future uncertainties than major engineering interventions.

Acknowledgments

I would like to express my sincere gratitude to my supervisor Professor Richard Dawson, for his fantastic guidance, enthusiasm and continued support throughout my PhD. Without his guidance and persistent help this thesis would not have been possible. My sincere thanks also goes to Dr Claire Walsh, Dr Elizabeth Lewis and Professor Chris Kilsby for their supervision and continued guidance during my PhD.

I would also like to thank Dr Stephen Birkinshaw, for his help with SHETRAN calibration and troubleshooting, and also Vassilis Glenis for his help and patience with updating UKCP09 WG.

I am also grateful to my friends Catherine Hands, Jasmine Black and Shaun Brown for their constant support and also for making my time in Newcastle fun and fulfilling.

My heartfelt thanks goes to my parents Simin Jalili and Mohammad Vali Jahanshahi and my brother Reza, for all of their unconditional love, encouragement, support and faith in me. I would also like to thank my auntie and friend, Mahboubeh Bakhtiari for her love and constant support. And most of all, I am sincerely grateful to my loving, supporting, encouraging and patient husband Reza Ramezani for his remarkable support during my PhD journey. Thank you!

Contents

List of Figures

List of Tables

Chapter 1

Introduction

This thesis shows how uncertainty and sensitivity analysis can be used to make more robust decisions about water resources. A methodology is developed to create an integrated systems' model that couples simulations of weather under current and future climates, catchment hydrology and the water resources system. This systems' model is used to assess the likelihood and magnitude of water scarcity. Uncertainty and sensitivity analyses are undertaken to assess the implications of uncertainties on water scarcity, and to subsequently identify water resources management options that are robust to these uncertainties. The method is demonstrated on the Thames Catchment which supplies the city of London, UK. This region has some of the lowest rainfalls in the UK, the largest and fastest growing population, and is therefore particularly sensitive to water availability. This introduction sets out the rationale, aim and objectives of this work.

1.1 Background

Climate change affects the whole world and in the coming decades hotter, drier summers, wetter, colder winters, degraded water quality and higher sea levels are projected. The impact of climate change on increasing the frequency and intensity of extreme weather incidence, floods and drought, creates a global threat to water resources which should be dealt with equally. A reliable supply of water to communities, industry and agriculture is crucial for a healthy population, and a successful economy. It has been reported by World Economic Forum (2016), that the water crises will be one of the most "impactful" global risks for years to come. By definition, global risk is considered to be a cluster of uncertainties which when occur can affect regions, countries or vast populations within the next decade. According to the predictions by World Economic Forum (2016), water crises can effectively lead to a large displacement of populations against their will, social instability in the destination of immigration, shortage of food supply (agricultural production), creating obstacles for future urbanization and also creating health risks (e.g. outbreak of deadly diseases).

Reports indicate that almost one billion people do not have access to clean water and nearly 40% of people in the world do not have access to water for one month every year (WEF 2016). These examples show that the water crises is not only a problem of future but also a current global threat. Given these threats (which potentially can turn into devastating trends in the long term) it will become nearly impossible to live without effective water management plans. Long-term management of water resources poses significant challenges for decision makers due to a range of uncertainties. Natural variability in hydrological processes, as well as future changes in climate, land use, demography and other socio economic factors are placing increased pressure on water resources and pose a threat to water security.

Effective management of water resources requires a long-term perspective (Hall et al. 2012). This necessitates consideration of future uncertainties such as the impacts of climatic and non-climatic drivers e.g. change in population, land use, demand and technology. Due to these broad uncertainties and the difficulty in representing and modelling the real world, the accurate prediction of climate change impacts is extremely challenging. Wilby and Dessai (2010) describe this process as creating a "cascade of uncertainty" which shows the aggregated uncertainties inherent in the modelling process. Each step in the analysis from predicting future society, greenhouse emission scenarios, global and regional climate change, local climate impact models through to adaptation strategies, are not only affected by uncertainty from preceding steps but also add new uncertainties into the analysis.

Another challenge to long-term management of water resources is the slow response of the system to policies. Water companies are globally under pressure to improve their management framework used for decision making to identify the most reliable and cost-effective water management options to tackle uncertainties. Although, there are many efforts to account for the future uncertainty in water resources management plans, still it is not clear to what extent these frameworks may be effective.

Uncertainty estimation is important for future predictions of climate change and its impact on water resources management, future global policies and capital investments. Uncertainty analysis has valuable implications for policy makers and managers of environmental systems. In another word, having the knowledge of these uncertainties can help to accurately improve the robustness of investment decisions and reduce the risk of failure in tackling water shortages.

1.2 Challenges for Thames catchment

The Thames catchment, located in south east of the UK, supplies water for the city of London. This region has unique conditions including the lowest rainfall in the UK, the largest and fastest growing population, making it extremely sensitive to water availability. This region also plays a very important role in the economy of the UK,

as well as internationally (Wade, 1999). Historically, this region was rich in natural resources such as water to sufficiently meet demands. However, as a result of climate and demographic change, this region has been classified as a seriously water stressed part of UK (Defra 2008). The projected increase in temperature, change in rainfall patterns, land use change, demographic and economic shifts may increase the demand for water and put more pressure on water resources in this area (UKCIP 2008; WWAP 2009). Hence, due to large uncertainty and inability in precisely modelling the real world conditions in this region, managing water resources in Thames area has become challenging for both water companies and decision makers making it a significant and highly suitable location to trial the new approaches.

The projected reduction in water availability emerges from comprehensive studies to understand to what extend the water resources is affected by hydrological characteristics of Thames basin (Diaz-Nieto & Wilby 2005, Manning et al. 2009). During last few decades a number of studies have been conducted to investigate the impact of climate change on water resources and to address the uncertainty based decision makings in this region (e.g. Wilby & Harris 2006; New et al. 2007; Manning et al. 2009; Brown & Wilby 2012; Matrosov et al. 2013; Borgomeo et al. 2014; Walsh et al. 2016). These studies used different methodologies to assess the sustainability of water resources in this area. For instance, Wilby and Harris (2006), New et al (2007) and Manning et al (2009) used probabilistic frameworks to assess uncertainties in climate change impacts on River Thames flow projections. As noted by Wilby and Harris (2006), low flows in Thames catchment are more sensitive to climate change scenarios and downscaling of Global climate Models (GCM), rather than hydrological model parameters and choice of emission scenarios. In addition, New et al (2007) illustrated that the information from probabilistic approaches are suitable for risk based adaptation assessments and different approaches for probabilistic analysis may lead to different risk based decisions. Manning et al (2009) projected a reduction in future water availability in this catchment and noted different downscaling methods may lead to different flow predictions, which originated from their difference in predicting Potential evapotranspiration (PET).

In this study, to understand the implications of the range of long-term uncertainties, a novel integrated systems model is developed that couples simulations of weather under current and future climates, catchment hydrology, and the water resources system. Different to previous studies, a spatial weather generator and a physically based spatially distributed hydrological model are used to better represent both the climatological and land cover heterogeneity of the catchment. This, then, is coupled to a rule-based water resource model in order to simulate the water availability and frequency of water shortage in the catchment. This integrated systems' model is used to assess the likelihood and magnitude of water scarcity. Uncertainty and sensitivity analyses are undertaken to assess the implications of uncertainties on water scarcity, and to subsequently identify water resources management options that are robust to

these uncertainties.

This integrated systems' model is applied in a real-world water resources management case study of the Thames catchment, however it can be implemented for catchments nationally and internationally. In addition, the presented integrated model can be adapted to incorporate other weather generators, hydrological models and water resources models.

1.3 Aim and objectives

The aim of this research is to provide insights into uncertainties in long-term management of water resources to enable more robust planning and decision making. The method will be demonstrated on the Thames catchment, a region which is pressured by population growth, climate change and other socio economic drivers. This aim will be achieved through the following objectives:

1. Develop a systems' model that couples rainfall, catchment hydrology, water resources and consumption for the Thames catchment.
2. Identify and quantify key uncertainties in long-term water resources management.
3. Test a range of adaptation options and assess their robustness to these uncertainties.
4. Stress test the system model to analyse the impacts of uncertainties and sensitivities of water resources in the Thames catchment.

1.4 Thesis outline

This thesis contains 7 chapters, including this introduction chapter.

Chapter 2 provides an overview of the research literature related to this study. It discusses the impacts of climate change, globally, and in the UK, and to address the Objective 2, various sources of uncertainty in managing water resources. Furthermore, a range of models used for simulating future climate, river flows and available water resources are also discussed in this chapter. This is followed by the potential methods and approaches used for handling uncertainty and decision making under uncertainty. The uncertainties in long-term management of water resources are quantified in subsequent chapters.

Chapter 3 presents a novel integrated systems framework to assess the implications of long-term uncertainties in water resources management which addresses Objective 1. This chapter also introduces a real world case study of the Thames catchment. It is also describes the UK Climate Projections (UKCP09) Spatial Weather Generator that provides time series of rainfall and PET. This is coupled with a physically based

hydrological model of SHETRAN that simulates river flow in the catchment and drives a rule-based water resources management model of LARaWaRM which quantifies resultant daily water availability of the system. Both models are described in detail.

Chapter 4 discusses climate change impact assessment on meteorological and hydrological characteristics of the Thames catchment. This is followed by the projection of the future change in total reservoir storage, frequency of drought days and testing different demand and supply adaptation options to tackle water shortage in 2020s, 2050s, and 2080s. This chapter addresses Objectives 1 and 3.

Chapter 5 presents the uncertainty and sensitivity analyses to assess the impact of uncertainties and sensitivities of water resources in Thames catchment. This chapter discusses the impacts of different land use, demand, leakage and population change scenarios on total reservoir storage and frequency of drought days in the catchment. This chapter addresses Objective 4.

Chapter 6 discusses and analyses the implications of the results presented in Chapter 5. This chapter presents two combinations of uncertainties that are at the low and high plausible extremities of water availability. The robustness of different adaptation options, under current and future climate changes, against these extremities are considered. Sensitivity testing of the water resource model is also used to help explain the results. This chapter also addresses Objective 4.

Chapter 7 reflects on the main conclusions of this study, considering its limitations and setting out future research challenges.

Chapter 2

Literature Review

2.1 Background

2.1.1 Global impact of climate change

Climate change affects the whole world and over coming decades hotter, drier summers, wetter, colder winters, a reduction in water quality and an increase in sea levels are projected. Moreover, the impact of climate change on water availability makes it a serious threat to water resources which should be dealt with equally seriously.

Over the last quarter of a century the global average temperature has increased by 0.2 °C per decade (Jenkins et al. 2009). This rise in global temperature is mainly caused by the increase in the emission of greenhouse gasses from human activities, such as burning fossil fuels (Stott et al. 2000, IPCC 2007, Jenkins et al. 2009).

Based on reports, 2015 and 2016 were the warmest years on record since 1850 and 2017 is predicted to be very warm globally (Met Office 2016). In 2016, the global mean temperature was 0.84 $\pm$ 0.12 °C higher than 1961-1990 and 1 °C above preindustrial levels, which is the highest level recorded since 1850. For 2017 it has been predicted that the average temperature will reach 0.75 $\pm$ 0.12 °C higher than 1961-1990 levels. The chance of global average temperature dropping to below that of 2015 an 2016 is very unlikely (less than 5% chance).

2.1.2 Climate change in the UK

2.1.2.1 The climate during the past century

Global warming has already impacted the climate of the UK (Murphy et al. 2009, Met Office 2016):

- Since 1981, there has been a 1.1 °C increase in temperature across the UK and 2015 was known as the warmest and fourth wettest year in a series from 1910.

- Since 1980, there has been around a 0.8 °C increases in temperatures in Scotland and Northern Ireland.
- Since 1766, rainfall totals have increased in winter and reduced in summer generally (there has been no significant change in annual mean precipitation in England and Wales).
- Over the last four decades, the amount of winter rainfall has increased over all regions of the UK. Also, except for the North East of England and North Scotland, the rest of the UK have experienced less rainfall in summer.
- Over the last three decades, there has been a 0.7 °C increase in sea-surface temperature around the UK.
- Over the 20^{th} century, the sea level around the UK has risen by 1mm/y.

2.1.2.2 Climate during the next century

The UK climate Impacts Programme (UKCIP) (Jenkins et al. 2010) has projected the probable changes in UK climate by the 2080s (relative to a 1961-1990 baseline) with a medium emissions scenario. These projections are:

- The mean temperature is expected to increase during the summer and winter but with little change in spring. Southern parts of the UK are expected to have up to 4.2 °C increase in mean temperature during the summer, with a minimum expected change of 2.5 °C for the Scottish islands.
- The mean daily maximum temperature is expected to increase in all areas of the UK. During the summer, this increase is up to 5.4 °C in southern part of UK and 2.8 °C in northern parts of England.
- Mean daily maximum temperature is expected to range between 1.5 °C and 2.5 °C during winter.
- The warmest day of summer varies for different parts of the UK but it ranges between +2.4 °C to +4.8 °C.
- There will be an increase in the mean daily minimum temperature in the UK ranging from 2.1 °C to 3.5 °C depending on the location.
- Changes in annual precipitation will be very small.
- Winter precipitation is expected to increase by +33% over the west of the UK and change by -11 to +7% in the Scottish highlands.
- The amount of precipitation in summer is expected to decrease by -40% in southern England.

According to UK Climate Projections (Jenkins et al. 2010), an increase of global temperature by 2 °C may lead to serious impacts such as hotter summers and milder winters, as well as sea level rise and melting of the polar ice. Global warming may also lead to changes in the pattern of precipitation, causing more rain in winter and less in summer. It is therefore likely that more droughts, floods and heavy rainfall will be experienced in the future.

2.1.3 Climate change projections

Ocean-atmosphere General Circulation Models (GCM) are used to make projections about future climates. GCMs are used for projecting all global variables. To assess the impacts of climate change, GCM results should be downscaled to regional scales. For the purposes of this project, the GCM outputs need to be downscaled for input into hydrological models which require a much higher resolution. This downscaling adds an extra layer of uncertainties to the projections. GCMs are more reliable at the global scale than the regional scales which are needed for the water resources decision making process.

Climate models are the only way to predict the future changes of the climate system. These models, based on the physical processes of the Earth and atmosphere, mathematically calculate the future of climate changes due to human activities. A lack of knowledge about the Earth and climate system and the inability to model the climate system may affect the accuracy of climate models and cause some inevitable uncertainties to be raised by them (Murphy et al. 2009).

According to Murphy et al. (2009) the future emission of greenhouse gases is highly dependent on population, technical development and human activities. As a result, it seems impossible to predict the amount of future emissions precisely and it may cause more uncertainty in climate projections.

2.1.4 London and south-east England water challenges

The south-east of England is one of the driest and fastest growing parts of the UK. It plays a very important role in the economy of the UK as a whole (Wade et al. 1999). According to the Office for National Statistics (ONS) Region and Country Profiles analysis released in Oct 2013, 15% of the UK economic output is produced in south-east. The south-east of England, which covers 19,100 km^2 contains 14% of the total UK population (8.7 million by mid-2012) (ONS 2013).

The potential impacts of climate change on the south-east of England have been discussed since 1995 (Wade et al. 1999). The south-east of England has a high concentration of population and traffic which increases the greenhouse gas (GHG) emissions. In the past, this region was rich enough in natural resources such as water to sufficiently meet demands, but currently as a result of social and environmental changes, water resources in south-east England are under pressure and this area is

already known as a "water stress area" (Defra 2008).

The impacts of climate change, population change, migration, age distribution, demographic and economic shifts, poverty and also changes in life style in south-east England may increase the demand for water and put more pressure on water resources in this area (UKCIP 2008, WWAP 2009). In addition, land use change as a result of population growth, migration and urbanization may cause additional pressure on surface and groundwater resources (WWAP 2009).

The main potential impacts of climate change predicted to occur in south-east England by the 2080s are:

- Warmer summers and colder winters
- Drier summers and wetter winters
- Sunnier summers and higher evaporation
- Increase in wind speed and risk of severe storms
- Increase in sea level as a result of thermal expansion of sea water and melting of ice

A set of possible future climate scenarios have been projected for the south-east of England by 2080s, relative to 1961-1990. For instance, under a medium emission scenario annual temperature is expected to increase by 2.8-3.2 °C. Summer mean temperature is likely to increase 3.9°C. Moreover a 23% decrease in summer mean rainfall. Moreover, under a medium emissions scenario, the annual rainfall in south-east England is expected to increase by 2-5% contributed to by a 20% increase in winter mean precipitation and a 22% decrease in summer mean rainfall (Defra 2009, Wade et al. 1999).

2.1.5 Thames basin water challenges

The Thames region is one of the driest in the UK and hence sensitive to water availability. In addition, it is one of the fastest growing parts of the UK and plays an important economic role. As can be seen from Figure 2.1 this region has been classified as a "Serious" water stressed part of the UK which has lower than average rainfall and very large demand (EA 2007, Hall et al. 2009, Thames Water 2013).

Future urban growth in the Thames catchment will mostly take place in Thames Gateway, Olympic Park, Oxford, Swindon and Reading areas which may lead to an increase in the population in the basin which urges the necessity of managing land and water resources in this area (BGS 2015*a*).

Average water demand for London is 168 l/p/d, whereas the national average water consumption is 147 l/p/d (Thames Water 2013). All of the new homes built in this area should follow Building Regulation Part G, which is a joint statement from Defra and Communities and Local Government (Fowler et al. 2007), to reduce the potable water consumption to 125 l/p/d. According to Thames water, private

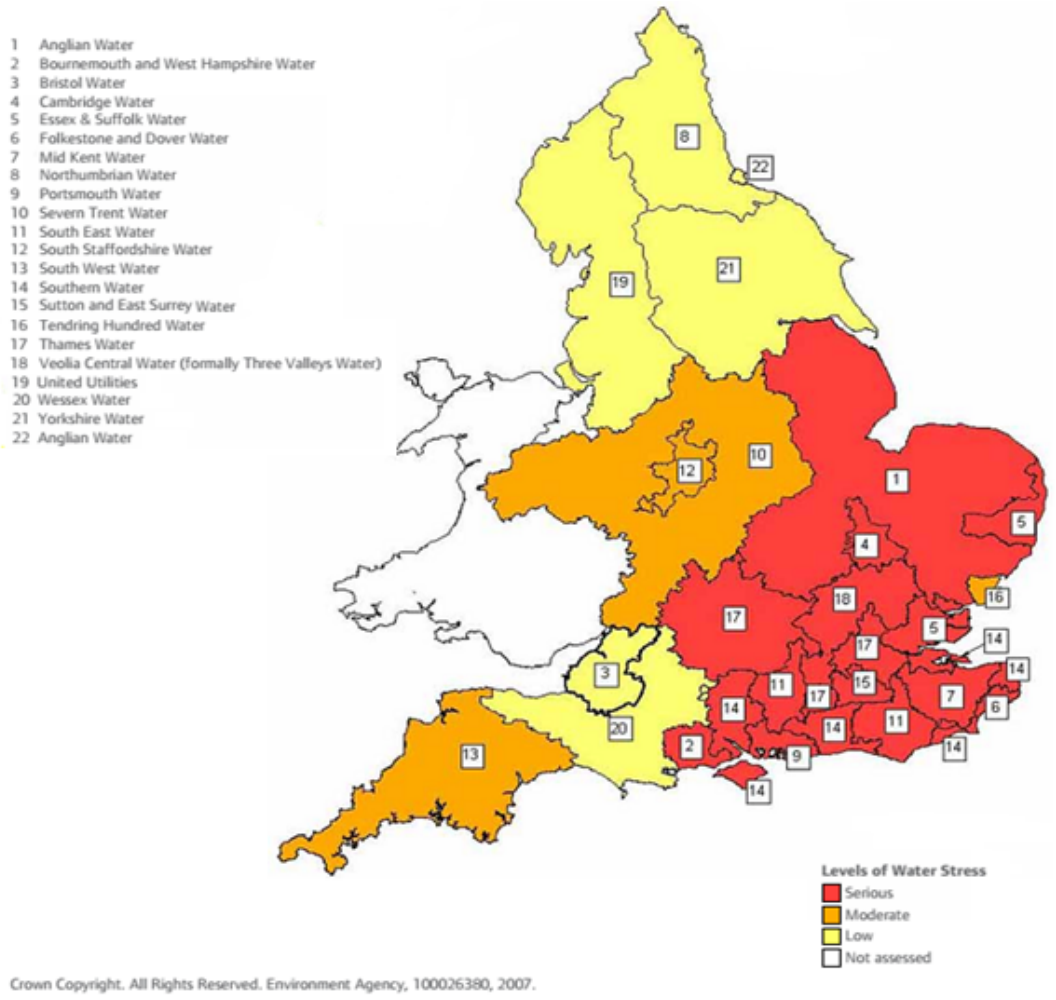

Figure 2.1: Map of water stressed areas (EA 2007).

properties that follow the Code for Sustainable Homes can achieve consumption of as little as 80 l/p/d (Thames Water 2013).

Based on Thames Water 2013, "The actual delivered Per Capita Consumption (PCC) will be influenced by occupancy and the water use behaviour of the occupants. This means that for an "average" home, with "average" occupancy and behaviour, the water consumption should be in the region of 125 l/p/d."

2.1.6 Drought in Thames catchment

Frequency of the occurrence of droughts, rainfall reduction and increasing the temperature during that last decades shows that the UK, especially south-east areas, are very prone to drought. The future climate projections (Murphy et al. 2009) indicate that the UK could experience more seasonality in rainfall (less in summer and more during winter) and higher temperatures. These predictions, along with current observations during the last decades, increase the concern about the sensitivity of water resources in the area and the importance of applying a wide range of modelling to develop a water resources management plan which is more robust to future uncertainties (Thames Water 2013).

Drought is one of the consequences of climate change in England which has an important role in water management planning in England, especially during the past quarter century (Miller & Yates 2006). Three types of drought are commonly identified: meteorological drought, agricultural drought and hydrological drought. For meteorological drought there would be a reduction in amount of rainfall, and if the soil moisture drops during the growing season, there will be an agricultural drought. When there is a shortfall in surface runoff and groundwater levels hydrological drought occurs (Marsh et al. 2007, Rodda & Marsh 2011).

Supply of water in the Thames catchment is highly dependent on surface water. Approximately 80% of required water in this area is abstracted from the Thames river and the remaining 20% is abstracted from groundwater (Thames Water 2013). In fact, during drought when the surface water is limited, groundwater aquifers in this area have an important role in supplying water. The level of water in aquifers is lowered during summer. The aquifers are recharged over winter and depleted (by abstraction or evaporation) during warm seasons.

According to Thames Water, five hyrological droughts occurred in the Thames catchment over the last century. These droughts happened in; 1920-21, 1933-34, 1943-44, 1975-76, 2004-06 (Marsh et al. 2007, Rodda & Marsh 2011) and 2010-2012 (Kendon et al. 2013). The occurrence of these severe droughts put unexpected pressure on water resources and forced water supply companies to consider the impacts of global climate change and choose an appropriate adoption plan to cope with the following droughts successfully (Miller & Yates 2006).

The drought of 1975-1976 lasted for 16 months (from May 1975 to Aug 1976), this

was the driest drought during the previous 250 years which intensely affected both surface water and groundwater (Rodda & Marsh 2011). The last drought in the south-east of the UK occurred in 2010- 2012. It lasted for 2 years (from April 2010 to March 2012) and was the driest drought over the 128 years record for the Thames catchment (Thames Water 2013). All three types of drought have been identified in the 2010-2012 drought. Rainfall reduction during this drought was ranked as one of the most remarkable phenomenons in England and Wales in the last century. The impacts of this drought on agriculture, low flow and reservoir and groundwater storages was severe (Kendon et al. 2013).

2.1.7 Water resources planning guidelines in UK

According to Wade et al. (1999), the drought of 1995 in UK led to more attention being paid to water resources planning and to the publication of the Water Resources Planning Guidelines (WRPG) by the Environment Agency. Water companies have the responsibility to provide required water and as a result they must strive to maintain a balance between the demand and supply of water. For this reason, the Environment Agency has introduced guidelines for water resources planning which should be followed by all companies to help them to develop their plans to make sure that they cover all of the requirements. The Water Resources Planning guidelines help the companies to develop their water resources management plan according to the Water Industry Act 19911 (EA 2012).

In fact, the water resources plan shows how a company intends to keep the balance between water demands and supply. This plan should be set by estimating the demand through consideration of the impacts of climate change during the following 25 years. Firstly, based on Defra/Welsh Assembly Government current demand policy, a baseline forecast of demand should be presented by companies (EA 2012). In preparing the baseline forecast, the possible impacts of climate change on supply and demand for water should be considered by companies. Figure 2.2 illustrates the components of water resources plan as proposed by the Environment Agency (2012).

Moreover, companies should make projections allowing for a suitable level of headroom to deal with uncertainty over the next 25 years. As noted by EA (2012) "headroom is a buffer between supply and demand designed to cater for specified uncertainties". In this way, the surplus or deficit of water can be calculated annually which is referred to as the baseline supply-demand balance. This shows the future situation in a company with respect to having an excess or a shortage of water. In the case of a deficit of water, companies should use the most beneficial and cost effective water management option to meet the predicted demand. This may lead to the preparation of a final supply-demand balance to show how they intend to meet the differences by their preferred option (EA 2012).

A company water resources management plan should contain (EA 2012):

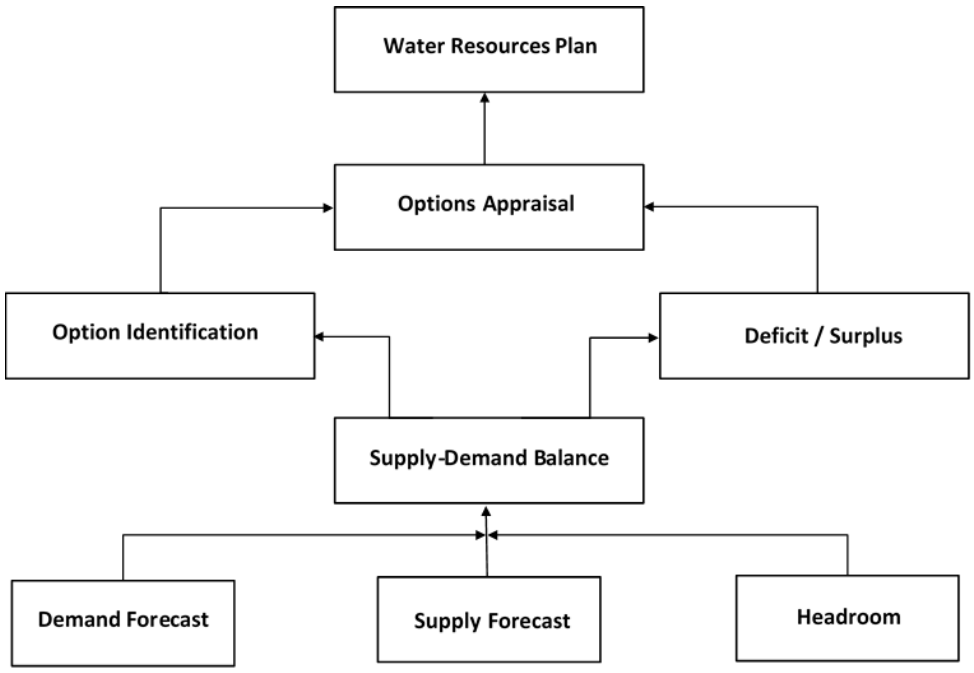

Figure 2.2: Components of a water resources plan (EA 2012).

- The reasons that show why this plan was chosen as the preferred one
- The details of the underlying assumptions in this plan
- A clear demonstration of how the system works
- The flexibility or robustness of the plan to risk and uncertainty resulting from climate change.
- Finally the chosen water resources plan should be submitted to the Secretary of State or the Welsh Minster, as appropriate. This plan is reviewed by the relevant minster and any mistakes are reported to the company for revision.

2.1.8 Challenges in water resources projections

One of the most important limitations for successful hydrological simulation is the fact that climate and hydrological data such as precipitation, evaporation and observed flow data are continuous and variable (temporally and spatially). As a result, there is a doubt that the observed hydro-climate data cannot represent the future data. Some of the sources of uncertainties have been listed below (Wilby 2005, Serrat-Capdevila et al. 2011):

- Socio economic factors:
    1. Change in population as a result of immigration and growing the population
    2. Change in demand
    3. Change in catchment hydrology as a result of land use change

- Input data (climate change projections)
- Choice of model calibration period
- Structure of model formulation (recharge, runoff and evapotranspiration)
- Non-uniqueness of model parameter sets
- Choice of emission scenario
- Climate model ensemble member
- Downscaling technique
- Issues related to boundaries and scales (including soil parameters)

Challenges in water resources projections can be divided to three main groups including supply-side, demand-side and modelling uncertainties:

2.1.8.1 Supply-side uncertainties

Climate change and global warming threaten the ecological and hydrological pattern which may lead to increased temperatures, changes in crop patterns and pollution of water resources. Climate change may affect the volume and seasonal variability of river discharge and the rate of sedimentation in rivers. These changes can gradually put more pressure on available water resources and increase the risk and uncertainties (Defra 2008, WWAP 2009).

Natural variability can be one of the drivers of uncertainty in water availability. The uncertainty in supplying water can be caused by internal or external natural variability. Natural internal factors are related to the climate system and are caused by the variable nature of the climate system which is not following a specific rule and is highly uncertain. These factors range from the storms that affect the regional weather to the changes that happen on a larger scale of seasons and years. Natural external factors are caused by factors from outside of the climate system. Changes in solar radiation and aerosols emitted from volcanic activities can be pointed to as examples of these external factors (Murphy et al. 2009).

For the past three decades, the issue of nonstationarity has caused many concerns for hydrologists and water resources managers (Salas et al. 2012). In the past, the design and management of water systems were based on stationarity assumptions and relied on past hydrological records. In fact, there was an assumption that all natural variables such as annual flood peak were time invariant and could be estimated from the hydrological records. However, As a result of human disturbance and climate change Stationarity is dead and as a result the historical records cannot represent the future any more (Milly et al. 2008). This Nonstationarity is caused by:

1. Land cover and land use changes, which have been caused by human interfaces, and may affect the water supply, water quality (Milly et al. 2008) and rainfall-runoff relationships (Salas et al. 2012).

2. Major natural events such as forest fires and volcanic explosions may cause changes in the composition of the soil surface and the air (Salas et al. 2012).

3. In global climate and hydrology the issue of nonstationarity is mainly caused by the low-frequency components of oceanic-atmospheric phenomena such as Pacific Decadal Oscillation (PDO), El Nino/Southern Oscillation, Atlantic Multidecadal Oscillation (AMO) and Arctic Oscillation (Salas et al. 2012).

4. Global warming is a result of increase in greenhouse gas concentrations and it may cause changes to oceanic and atmospheric processes and affects the hydrologic cycle (Salas et al. 2012).

2.1.8.2 Demand-side uncertainties

Land use changes, changes in population and demand, economic growth and water use efficiency are some examples of socio economic drivers that may have significant effects on future water stress. The population growth, increasing demand and water abstractions are known as the most important factors in increasing global water stress (Shiklomanov & Rodda 2003, Alcamo et al. 2007).

Global warming, urbanization, demographic changes and rising living standards increase the demand for food, water and other services which cause more pressure on land, water and other energy sources, can be counted as main sources of demand uncertainty (Defra 2008, WWAP 2009). It has also been estimated that the water stress by 2025 will be mostly caused by increasing water demand than climate change (Vorosmarty et al. 2000, Alcamo et al. 2007). According to Oki et al. (2003), by 2050 the effect of population growth on increasing water stress will be more than the impacts of economic and technological change.

Climate change may also alter the abstraction of water and put extra pressure on surface and ground water resources. The domestic, agriculture and industry sectors have important roles in increasing water abstraction. The abstracted water is mostly used by domestic sectors and growing income is the most effective factor in domestic water consumption. According to Alcamo et al. (2007), water abstraction has an increasing trend in developing countries. While, in industrialized countries as a result of technological improvement water abstraction is reduced. Alcamo et al. (2007) claimed that the impacts of increasing the incomes is stronger than the population effects.

2.1.8.3 Modelling uncertainties

For dealing with the changing climate and extracting the required projections, a number of methods such as Ocean- atmospheric General Circulation Models (GCM) have been identified. According to the UK Climate Projections science report, the spatial resolution of the third Met Office coupled ocean-atmosphere GCM, HadCM3, is 2.5° latitude by 3.75° longitude over land areas, and it also includes 19 vertical levels

in the atmosphere and four layers in the soil, while according to Fowler et al. (2007) the required resolution for hydrological resolution is 0.125° latitude and longitude (Salath 2003, Fowler et al. 2007). However, GCMs are more reliable at the global scale than regional scales, which are needed for water resources decision making. For regional scales the GCM output should be downscaled to the local scales. This downscaling adds an extra layer of uncertainties to the projections.

Model inter-comparison projects such as CMIP5, CMIP3, ENSEMBLES, and ClimatePrediction.net have been used to investigate and reduce the impacts of uncertainties in climate models (Brown & Wilby 2012). Based on Wilby and Harris (2006), in comparison with uncertainty from emission scenarios, the choice of GCM is the most important source of uncertainty. According to Kundzewicz and Stakhiv (2010) in order to reduce the uncertainties in water resources adaptation and management options more research is required to be done with the GCMs projections accuracy (Kundzewicz & Stakhiv 2010, Salas et al. 2012).

Boberg and Christensen (2012) believe that simulating the current climate by a known model and correcting the biases with observations, may lead to reduce the spread of uncertainties (Boberg & Christensen 2012, Brown & Wilby 2012). Wilby (2005) showed that the choice of emission scenario, downscaling technique, lack of proper understanding of physical processes or our inability to represent them properly (especially in boundaries of scale), choice of model calibration period, structure of model formulation (recharge, runoff and evapotranspiration) and non-uniqueness of model parameter sets may also cause additional uncertainties (Wilby 2005).

2.2 Modelling

2.2.1 Weather generator

GCMs provide weather variables information at a global scale (50,000 km^2). However, for assessing the impact of climate change on water resources finer resolutions and more detailed data are required. As a result, the output from GCMs need to be downscaled to higher resolutions. This downscaling can be achieved statistically or dynamically. There are many tools available for the statistical downscaling of GCM outputs. For example, the Statistical Down Scaling Model (SDSM), developed by Wilby et al. (2002), generates single-site daily time series of weather variables for current and future climate change scenarios. This model use statistical downscaling method to downscale the variables from GCM outputs which can be used either as a stochastic weather generators to produce weather variables or as a statistical downscaling model to downscale the GCM outputs for catchments that has required observed data (Wilby & Dawson 2013). The Model for Assessment of Greenhouse Gas Induced Climate Change/ Scenario Generator (MAGICC/SCENGEN) (Wigley & Raper 1987, Hulme

et al. 2000) is a free carbon cycle-climate model which takes in different greenhouse gas emission scenarios and predicts global change in mean temperature and sea levels. This model was used in the 1999 IPCC assessment report and has been updated accordingly since then (Meinshausen et al. 2011). The Climate Information Portal (CIP) is a web based portal that provides meteorological information for the whole of Africa, including precipitation, maximum and minimum temperature station data. This portal has been developed by the University of Cape Town, who downscaled climate data by merging climatic information from the GHCN and WMO. For each station, this portal provides the users with information about monthly observed data (historical), historical average seasonality and downscaled future climate projections (based on CMIP3 and CMIP5) (CIP 2015).

Other statistical downscaling tools include WGEN, which is a stochastic weather generator developed in the US (Richardson & Wright 1984) to generate daily precipitation, temperature (max and min) and also solar radiation. This model uses first order Markov chain gamma distribution to predict dry or wet days as well as the amount of precipitation (not the time series) and other variables which are all correlated to occurrence of rainfall. The Long Ashton Research Weather Generator (LARS-WG) is another example of stochastic weather generator that was developed with the purpose of climate impact assessments (Racsko et al. 1991, Semenov & Barrow 1997). This model uses semi empirical distribution of wet and dry series to generate daily time series of weather variables such as precipitation, temperature (min and max) and solar radiation. Semenov et al. (1998) compared the performance of LARS-WG with WGEN on 18 different sites in USA, Europe and Asia. The authors believed that because LARS-WG applies semi empirical distribution and use more parameters, this model can simulate the historical data better and as a result performs more accurately than the WGEN. So LARS-WG is more appropriate to be used for hydrological studies in new sites (Semenov et al. 1998).

Neyman-Scott Rectangular Pulses (NSRP) (Cowpertwait et al. 1996*a*,*b*) is another stochastic model that generates more detailed (hourly) time series of rainfall and other weather variables. This model can be used for a single or combination of catchments, as well as ungauged catchments where the observed data are not sufficient. More importantly this model's use of event clustering can simulate extreme events while previous WGs were not able to model the extreme events (e.g. extreme rainfall) (Kilsby et al. 2007). This model has been extended to spatial-temporal model (STNSRP) by Cowpertwait et al. (2002) which takes advantage of stochastic point process to model the variables both spatially and temporally (Cowpertwait et al. 2002).

UK Climate Projections (UKCP09) (Murphy et al. 2009) use stochastic models to provide probabilistic climate projections under three emission scenarios (low, medium, high) for whole UK with 25 km resolutions. UKCP09 is used to create current and potential future time series of rainfall and other meteorological variables that can be used as input for hydrological models to simulate the hydrological behaviour of

specific catchment (Kilsby et al. 2007, Glenis et al. 2015, Beven 2012). This climate model, uses Bayesian framework and based on the perturbed physics ensemble (PPE) from HadCM3 GCM (UK Met Office) and multi-model ensembles (MME), with considering the structural error in climate model, creates probabilistic climate projections. 11 runs of regional climate model (RCM) are used to downscale the climate variables from global scale to 25 km resolutions (Murphy et al. 2009, Glenis et al. 2015). The UKCP09 weather generator (UKCP09 WG), uses change factors derived statically from UKCP09 climate projections and generates hourly or daily time series of weather variables with higher spatial and temporal resolutions of 5x5 km (Kilsby et al. 2007, Jones et al. 2009, Murphy et al. 2009, Jenkins et al. 2009, Glenis et al. 2015). The UKCP09 WG will be described in more details in Chapter 3.

The UKCP09 spatial WG uses regression and inverse-distance weighting to interpolate measured data from stations to gridded format, while CEH have developed a 1km gridded daily rainfall dataset (CEH GEAR, Gridded Estimates of daily and monthly Areal rainfall (1890-2015)) for the UK, which is also based on Met office observed database but uses natural neighbour interpolation to generate gridded rainfall time series are freely available for download. CEH-GEAR is free however the UKCP09 data are not (Tanguy et al. 2014).

2.2.2 Hydrological models

Nobody knows what is exactly happening underground in the real world. Because of the complexity of details and the ambiguity of the hydrological system, it is not possible to precisely reproduce and model all the details of the rainfall-runoff process. Despite of all the advances in measurement techniques in monitoring the subsurface of ground, such as remote sensing and radar, still the information and knowledge about the actual hydrological process in the environment is limited. As a result, hydrological models are not able to model all the details, they only can approximately predict the rainfall-runoff process in the catchment. Hence there is considerable uncertainty in hydrological model projections. The uncertainty can be quantified using various techniques such as Monte Carlo analysis. As a result of these uncertainties, risk assessment framework are required for decision making (Beven 2012).

Our knowledge about hydrological systems is limited, but by using hydrological models we will be able to analyse, study and reproduce past hydrological events, as well as predict future hydrological events. The hydrological models demonstrate the actual complex hydrological system in a very simple way. These models also make it possible to evaluate the impacts of physical changes that human have made to environment and finally help to improve our knowledge about the hydrological system (Freeze & Harlan 1969).

Hydrological model have been classified in several ways (OConnell 1991, Wheater et al. 1993, Singh et al. 1999) but are generally classified based on (Beven 2012):

- The mathematical logic they are based on (e.g. deterministic or stochastic models)
- The way they discretely consider the catchment (e.g. Lumped, semi-distributed, spatially distributed models)
- The structure of the model (e.g. Empirical, conceptual, physically based models)

2.2.2.1 Mathematical models

Hydrological models can be classified based on the mathematical model they are following. In this case they can be deterministic or stochastic. In deterministic models, for each set of input only one possible set of output is available. Which means that in deterministic model, there is always one unique relationship between input, parameters and output (Beven 2012).

In stochastic models (called probabilistic/ statistical model), for each set of inputs, there are many sets of possible outputs. In other words, in a stochastic model for a given set of inputs, a different set of outputs are randomly generated which shows the uncertainty and error in input, parameters and boundary conditions. The uncertainty in prediction of hydrological response can be presented and quantified by probability distributions (Beven 2012).

2.2.2.2 Spatial discretisation of catchment

In lumped models the catchment is treated as a single homogeneous unit, and variables are averaged over the whole catchment area. While, in distributed models a catchment is divided into numerous grids and equations are solved for each grid cell and parameters are local averages over each grid square. Distributed models are more accurate because of the spatial description of the catchment (Beven 2012). The accuracy of prediction increases if the model can be fully validated by observations (Bormann et al. 2009).

To overcome the complexity of distributed models, semi distributed models have proposed. Semi distributed models lie between conceptual and fully distributed models. In this type of model, a catchment is divided into sub catchments and each of these are treated as a lumped basin. Hydrological processes in each of sub catchments are simulated by using Geographical information systems (GIS) and Hydrological Response Units (HRU) which can be formed by combination of spatial soil, land use and topography databases (Bormann et al. 2009, Beven 2012).

2.2.2.3 Structure of hydrological models

From a structural point of view, hydrological models are differentiated as empirical, conceptual and physically based models.

Empirical models:

Empirical models, which are also called data driven models, are only based on measured observations of input and output to a catchment. In fact, in empirical models

a catchment is assumed to be a black box and only includes the mathematical equations and statistical concepts between observed input (rainfall) and output (discharge) and all the other hydrological processes in the catchment are excluded (Beven 2012). Hence this model is only valid within the catchment boundary.

The empirical model is the oldest approach in hydrological modelling (Beven 2012). Rainfall-runoff modelling has a long history and the first hydrological model was proposed by an Irish engineer (Mulvany 1850). This model has a simple equation which calculates the peak hydrograph for a catchment by inputting the catchment area, maximum average rainfall intensity in catchment and an empirical coefficient. This coefficient can be calculated from observed rainfall and peak discharge in the catchment, which is not constant and can be different for different storm events. This model is an example of the empirical approach which is based on the rational relationship between amount of discharge, size of catchment and intensity of rainfall. Hence, this has been known as Rational Method. There are some difficulties in calculating the coefficient for catchments which do not have enough observations and also for future storm events. Because this model only predicts the peak flow, it can only be used in small impermeable catchments (Beven 2012).

Unit Hydrograph (UH) (Sherman 1932), ARMA (Autoregressive Moving Average) (Box & Jenkins 1976), Artificial Neutral Network (ANN) (Garcia-Bartual 2002) and Data-based Mechanistic (DBM) model (Young & Beven 1994) are other examples of empirical approached models. In the latter model, available observed data indicates the structure of the model which needs to be evaluated and considered only if there is a mechanistic explanation (interpretation) for the suggested model. Hence, this model has some disadvantages, such as:

- The observed data can have errors, some areas do not have reliable observed data, so if the available observed data is wrong, the model will be wrong too. As a result these errors can increase the uncertainty in hydrological models result.

- The empirical model is based on observation input and output to the catchment, while eliminating the physical features. As a result of climate change and land use changes, using only historical data might not be so helpful in predicting hydrological systems.

Lumped conceptual models:

Conceptual models, sometimes called "grey box" models, use physical laws in a highly simplified way, they simulate the physical process by using simple mathematical equations. Some of the parameters used in conceptual models are not physically meaningful. In other words, those parameters cannot directly be measured, they need to be estimated by calibration against observed data (Wheater et al. 1993).

The first conceptual model developed by Norman Crawford and Ray Linsely at Stanford University is the Stanford Watershed Model (SWM) (Crawford & Linsley

1966). This model has 35 parameters, most have physical characteristics and only a few of them need to be estimated by calibration (Beven 2012). The Sacramento model (Burnash et al. 1973), SSARR (Rockwood 1968) and Tank (Sugawara et al. 1983) are some examples of conceptual models.

CATCHMOD is another example of a lumped conceptual model, developed by UK Environment Agency (Wilby et al. 1994) and has been used for climate change impact studies and water resources planning in the Thames catchment and elsewhere (Davis 2001, Wilby 2005, Wilby & Harris 2006, New et al. 2007, Manning et al. 2009). This hydrological model takes in daily time series of rainfall and potential Evapotranspiration (PET) (mm/day/km^2) and outputs daily time series of flows (cumecs) at the catchment.

The Xinanjiang (Zhao et al. 1995), ARNO (Todini 1996) or Variable Infiltration Capacity (VIC) (Wood et al. 1992) are other examples of conceptual semi distributed hydrological models. The Xinanjiang model (Zhao et al. 1995), which originated in China, is an explicit soil moisture accounting (ESMA) model. In ESMA models, the soil moisture is modelled by considering connected reservoirs and a few simple equations that control transfer between them (Beven, 2012).

ARNO (Todini 1996) is another example of conceptual model which is also classified as semi distributed model. This model was first applied on the river ARNO in Italy and is mostly used in real time flood forecasting, land surface and soil components in global climate models (GCMs) (Todini 1996, Beven 2012). In this model the catchment is divided into sub catchments based on natural sub basin boundaries. ARNO is a large-scale hydrological model that apples various modules (e.g. soil moisture balance, evapotranspiration, snowmelt, groundwater and routing of flow) to represent the hydrological process. The soil moisture balance module used by ARNO is based on the Xinanjiang model which was developed by Zhao (1995) that applies the probability distribution function for soil moisture capacity (or uses the soil moisture distribution function).

Wood et al. (1992) increased the number of soil layers in the ARNO model and developed the Variable Infiltration Capacity model (VIC) which considers heterogeneity of soil storage and formation of fast runoff in the catchment and can be applied on large scale catchments (Wood et al. 1992, Liang et al. 1994). All of these models are based on a distribution function curve which shows the connection between soil storage capacity and extension of saturated area (Beven 2012). The parameterization of these models is estimated based on observed data.

TOPMODEL is another semi-distributed conceptual model (Beven & Kirkby 1979). This model is based on a distribution function approach uses the topographical data to spatially show the hydrological behaviour of the catchment. This model uses a topographical index distribution, which is a parameter based on physical characteristics and can only be used for small hill slope catchments (Franchini et al. 1996, Beven 2012).

In summary, in comparison with conceptual models, semi distributed models takes advantage of using more physically meaningful parameters. In fact, semi distributed models are physically based models with less spatial complexity than a fully distributed model. This type of model mostly uses a distribution function to show the non linearities of run off formation in a simpler way than fully distributed models, hence semi distributed models are much easier in terms of calibration. The distribution in semi distribution models can be based on (Beven 2012) :

- Statistical description: Probability Distributed Model (Moore and Clarke, 1981; Moore, 2007)
- Simple functional form, distribution function curve : The Xinanjiang (Zhao et al. 1995), Arno (Todini 1996) or Variable Infiltration Capacity (VIC) (Wood et al. 1992)
- Physical, index of hydrological similarity, topographical index : TOPMODEL (Beven & Kirkby 1979)

Physically based spatially distributed (PBSD) models:

Freeze and Harlan (1969) presented a blueprint paper to develop physically based mathematical hydrological model which is the basis for most of the physically based models. In this hydrological model all surface and subsurface flow processes such as overland and channel flow, infiltration, groundwater flow etc., are defined by partial differential equations based on continuity of mass and energy. These equations and the boundary conditions, which represent the shape of the hydrological catchment, comprise the hydrological model runs on a computer. These models use a three dimensional grid network to simulate the catchment. Mathematical equations are solved by numerical techniques (Freeze & Harlan 1969). Since then, based on Freeze and Harlan's (1969) blueprint, several other physically distributed models have been developed. SHE (Systme Hydrologique Europen; European Hydrological System) model was developed by three European organisations; the Institute of Hydrology (UK), SOGREAH (Saltelli et al. 2010) and Danish Hydraulic Institute (Denmark) (Abbott et al. 1986). Each of these organisation were responsible for developing a part of this model. Components such as interception, evaporation, snowmelt, overland and channel flow, unsaturated and saturated subsurface flow can be modelled by SHE. Table 2.1 summarized the equations and organizations that developed each of these components (Abbott et al. 1986).

Physically based distributed models try to replicate the hydrological processes in a catchment, hence this type of model is more complex than other hydrological models (empirical and conceptual). The development of SHE as physically based spatially distributed model (PBSD), made it possible to spatially model a catchment to understand the spatial distribution of the catchment characteristics, simulate the impacts of physically and meteorological changes in the catchment, and give the model a high degree of flexibility in terms of updating the new hydrological features of

	Snowmelt	Interception	Evaporation	Overland & Channel flow	Unsaturated zone flow	Saturated zone flow	FRAME
Institute of Hydrology (UK)	Energy budget method	Rutter Accounting Procedure	Penman Monteith equation				
SOGREAH				Simplification of St. Venant equation			
Danish Hydraulic Institute (Denmark)					One dimensional Richards equation	Two dimensional Boussinesq equation	Central control components

Table 2.1: Components of SHE hydrological model (Abbott et al. 1986)

the catchment. Compared to conceptual and empirical models, for the calibration of physically based models less lengthy hydrometeorological data is required (Abbott et al. 1986).

The performance of these models is highly related to the availability of measured data. A large amount of data is required in physically based modelling, and some of this data is not easy to be measured. Advances in measurement techniques such as using radars and remote sensing can be helpful in reducing the uncertainty caused by the lack of measurements.

In physically based models, the catchment is divided into grid squares which makes it possible to predict and evaluate the impacts of future changes on each of the grid cells in the catchment. These changes can be caused artificially (land use changes such as deforestation and urbanization), or seasonally (changes in land cover as a result of seasonal crops and vegetations).

Sources of uncertainty in simulation by PBSD models:

- This type of model needs a large amount of data that needs to be physically measured. The availability and accuracy of these data may cause uncertainty.
- The land phase measurement usually has point scale which may be different with the scales of the grids used in the model. The accuracy of the SHE model, depends on the grid size (Xevi et al. 1997, Beven 2012).
- Because knowledge of the actual hydrological system is limited, the hydrological process may not adequately represent the actual system and that can be counted as another source of uncertainty.

The IHDM (Institute of Hydrology Distributed Model) developed by Institute of Hydrology in UK (Calver & Wood 1995), THALES model (Grayson et al. 1995) and CSIRO TOPOG-dynamic model (Vertessy et al. 1993) were developed in Australia, are other examples of physically based distributed models.

The SHE model is a starting point for developing other PBSD models such as MIKE SHE (Refsgaard & Storm 1995) and SHETRAN (Ewen et al. 2000). MIKE SHE is a comprehensive PBSD model that provides 3 dimensional simulations of surface and subsurface water flow and contaminant transport in a catchment (Singh et al. 1999, Refsgaard & Storm 1995). This model is more suitable for small catchments and for water resources management for irrigation planning (Yang et al. 2000).

SHETRAN (Ewen et al. 2000) is a PBSD hydrological model that provides a 3D detailed visualization of temporal and spatial description of hydrological processes in the catchment. SHETRAN is based on the SHE hydrological model and follows Freeze and Harlans blueprint. This hydrological model was funded by United Kingdom Nirex Limited (NIREX) for their research to evaluate the safety of using deep underground radioactive wastes storage that led to the development of reactive solute transport component in SHETRAN model. This model uses a finite difference method to

solve the partial differential equations, used for physically spatially simulation of the coupled surface/subsurface water flow, sediment transport and reactive solute transport in a catchment. This model is described in more details in Chapter 3.

SHETRAN has three main components: water flow, sediment transport and contaminant transport. For water flow, SHETRAN simulates coupled surface water flow (overland and in streams) and subsurface water flow (unsaturated and saturated zones such as confined, unconfined and perched aquifers). According to Ewen et al. (2000), SHETRAN can be used for a single or group of catchments. In SHETRAN, catchment is simulated as a series of columns. Each column consists of number of grid cells, that each of them may represent different types of soil. In this hydrological model flow can move in three dimensions, exchanging vertically or laterally between maximum two cells in neighbouring columns (Ewen et al. 2000).

Most of the equations used in water flow simulation, such as equations used for canopy interception of rainfall, evapotranspiration, overland flow and channel flow are similar to the SHE hydrological model (see Table 2.1) (Abbott et al. 1986). But the subsurface saturated run off component is modelled by variably saturated flow equation proposed by Parkin (1996). As Ewen et al. (2000) claimed, SHETRAN is a flexible and powerful hydrological model that can be used for managing water resources (surface and groundwater) and assessing the environmental impacts of climate change and land use changes. Setting up SHETRAN for a new catchment is very time consuming (at least a few weeks) (Ewen et al. 2000). Hence, Birkinshaw et al. (2010) developed the Graphical User Interface (GUI) that accelerates the process of preparing input data for simulating water flow by SHETRAN. For using GUI, only DEM data and catchment Mask are mandatory, providing vegetation and soil data are optional as they can be accessed from soil and vegetation library (Birkinshaw et al. 2010).

From the literature, lumped conceptual models simulates observations well, however because they are not physically based they are assumed to be less accurate in future prediction of catchment hydrology (Beven 2012). While, spatially physically based model are not able to simulate the observations precisely, they are more helpful in future prediction of environment impacts (Beven & Binley 1992).

The choice of model highly depends on data availability, scale and purpose of hydrological modelling (Bormann et al. 2009). In ungauged catchments and where less data are available, using lumped or semi distributed models is more reasonable. At the regional scale, lumped and semi distributed conceptual models are more practical than fully distributed models in terms of calibration and validation. At the local scale, spatially distributed models are more appropriate, especially if studying the land use changes is important (Bormann et al. 2009). Viney et al. (2005) proposed the ensemble approach which combines lumped conceptual models with spatially physically based models to improve the performance of hydrological models. Using an ensemble approach makes it possible to take advantages of both type of hydrological model

which may lead to reduced uncertainty in simulated results and increases the accuracy of future predictions (Viney et al. 2005, Bormann et al. 2009).

2.2.3 Water resources models

Water resources models are important tools for simulating the water resources system which are used for planning and managing the water system, analysing the operational systems and predicting the performance of water system in future, for instance during drought or flooding (Loucks et al. 1981, Loucks & Van Beek 2005). For these aims two types of approaches are available; optimization or a rule-based approach (Matrosov & Harou 2010).

The first type of modelling water resources is by using optimisation algorithms to simulate the water system. These types of models are easier to be programmed but they are not able to consider and model all the operational details in the system (Loucks & Van Beek 2005, Matrosov & Harou 2010). WATHNET (Kuczera 1992), AQUATOOL (Andreu et al. 1996), OASIS (Randall et al. 1997), MISER (Fowler et al. 1999), MODSIM (Labadie et al. 2000), RIVERWARE (Zagona et al. 2001), MIKE BASIN (Jha & Gupta 2003), CALSIM (Draper et al. 2004), WEAP (Yates et al. 2005) and REALM (Perera et al. 2005) are examples of optimization simulation that used for modelling water resources management. (For more information about the optimisation approach read Labadie (2004) and Wurbs (2005)).

Ruled-based modelling is another type of water resources modelling which is a computer based model that simulates the operating rules in water system by programming codes using ”loops” and ”if else” statements. This group of models are complicated to program, however they are more user friendly as the rules can be changed according to user preference, they can be run for long time series and are very reliable in simulating the water systems (Loucks & Van Beek 2005, Matrosov & Harou 2010). WRAP (Wurbs 2005), HEC-ResSim (Klipsch & Hurst 2007), AQUATOR (Oxford Scientific Software 2008), WaterWare (Cetinkaya et al. 2008), WARGI-SIM (Sechi & Sulis 2009), IRAS-2010 (Matrosov & Harou 2010) are examples of rule-based water resources management models.

AQUATOR (Oxford Scientific Software 2008) is a piece of water resources modelling software that has been developed for water companies in the UK, such as the Environment Agency (EA) and Thames water, to model the water system to evaluate the performance of the system in providing enough water for the customers to meet all the water demands in the area.

Interactive River Aquifer Simulation 2010 (IRAS-2010) is an example of a rule-based water resources management model which is based on the Interactive River-Aquifer Simulation (IRAS) model, developed by Loucks et al. (1995) at Cornell University. In 2010, this model was updated by Matrosov and Harou for the Thames catchment (Matrosov & Harou 2010). IRAS-2010 is an open source water resources model, that

simulates the Thames catchment as a group of nodes and links which represent the storage (reservoir, lakes, etc) and demand consumption sites, and links represent the pipes or canals that transfer water between the nodes (Matrosov & Harou 2010, Borgomeo et al. 2014).

The London Area Rapid Water Resources Model (LARaWaRM) is another rule-based water resources management model developed in MATLAB. This model simulates water flows, water consumption, water storages and single and joint reservoir releases in interlinked surface and ground water system. By using this model, probabilistic climate change scenarios and different population demand assumptions can be analysed and also the benefits of different decision adaptation options such as no adaptation, new reservoir, desalination plant, demand management and reducing leakage can be quantified. This model is explained in more details in Chapter 3.

2.3 Uncertainty handling

Uncertainty estimation is important for future predictions of climate change and its impact on water resources management, future global policies and capital investments. Uncertainty analysis has valuable implications for policy makers and managers of environmental system. There are many different definition of uncertainty but generally the outcomes and events that cannot be predicted with certainty are called uncertainty (Loucks & Van Beek 2005).

2.3.1 Uncertainty in model outputs

To predict the performance indicators of the water resources system in future, the environmental system needs to be simulated. The simulation models are used as a primary tool to estimate the possible impacts of climate change. Due to the complexity of the nature and lack of knowledge, the simplification of the real system is necessary for modelling of the water resources system. As a result this prediction is not precise. The modeller tries their best to make the simulations more accurate by doing more research and collecting and analysing valuable data. The simulated results from models may not be perfect but they are expected to be fairly similar to the observed value. This is because the models are simplification of real world and as a result of that models are not able to reproduce every details exactly as it happens in reality.

The sources of uncertainty in model outcome which are mainly caused by a lack of knowledge and the inability to predict ahead of the time are presented in Figure 2.3 and described in details as follows:

- Information uncertainty: Lack of knowledge about the accuracy of measured historical (hydrological and meteorological) data in the past, as well as natural variability (temporal and spatial) and unpredictable change in frequency and

amount of rainfall, temperature, evapotranspiration, water consumption in the future. This type of uncertainty is a part of natural system which cannot be reduced (Loucks & Van Beek 2005)

- Model Uncertainty: Lack of knowledge may cause outputs from a model which is simplification of real world be different with the historical data. This uncertainty can be reduced by additional research and further measurements (Loucks & Van Beek 2005). This uncertainty is associated with:

  - Parameter uncertainty: Lack of knowledge about the value of the parameters that represent the dynamic of a process and/or characteristics of the location, boundary of the domain of interest and initial condition which prescribe the value of the variables at the beginning of the simulation (Loucks & Van Beek 2005, Curry & Webster 2011).

  - Structural uncertainty: Inability in perfect representation of physical processes of the real system in the model (Loucks & Van Beek 2005, Curry & Webster 2011, IPCC 2007).

  - Numerical error: Errors in numerical methods used in model algorithms. For better simulating the real system, complex models are used which introduce another level of uncertainty and error to the outputs (Loucks & Van Beek 2005).

- Decision uncertainty: Inability to predict the future response of water resources system as well as policies and decisions that will be made by organizations and individuals about operating infrastructures such as reservoirs (Loucks & Van Beek 2005).

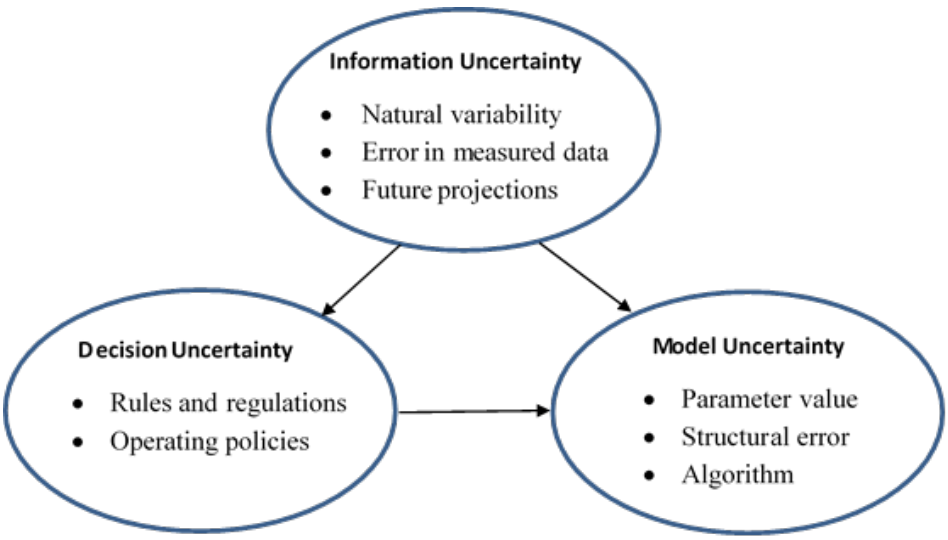

Figure 2.3: Sources of uncertainty in model outcome

2.3.2 Sensitivity and uncertainty analysis

Uncertainty analysis quantifies the range of possible outcomes and uncertainty in output of the models which is caused by uncertainty in inputs (Saltelli et al. 2010, O'Hagan et al. 2006). Studies done about uncertainties show that input data and parameter uncertainty are the most important source of uncertainty in hydrological modelling (IWR 2008). Sensitivity analysis is also used to conduct the uncertainty analysis (Uusitalo et al. 2015). Sensitivity analysis quantifies uncertainty in model outputs depends on parameters and inputs. As noted by Saltelli et al. (2010), the sensitivity analysis indicates how uncertainty in models outputs are related to uncertainty in input and other factors. Although uncertainty and sensitivity are different by definition, they often shares similar mathematical techniques (Pianosi et al. 2016). For instance, Monte Carlo simulation and Generalised Likelihood Uncertainty Estimation (GLUE) (Beven & Binley 1992) are used for both uncertainty and sensitivity analysis (Pianosi et al. 2016).

As noted by Pianosi et al. (2016), using sensitivity and uncertainty together offers valuable information about the performance of the model, as for instance sensitivity analysis shows the inputs which outputs are most sensitive to. In contrast, uncertainty analysis shows whether the outputs given from sensitivity analysis fall within the expected range of model output.

For sensitivity analysis, to monitor the sensitivity of model outputs the model is run for various input data and parameters in their acceptable range, the amount of change in output values indicates the uncertainty and sensitivity of the model outputs to parameters values. For instance, if altering the input data leads to a considerable change in outputs, the uncertainty to parameters values is large. In contrast, if the changes in output is small, the uncertainty in input values, and in other words, the sensitivity of the model output to input values is relatively small (Uusitalo et al. 2015). Although sensitivity analysis used for assessing uncertainty in input values and model parameters, for structural uncertainty the model outputs need to be compared with actual observations. Because required observed data are not always available, expert judgement is necessary for structural uncertainty evaluation (O'Hagan 2012, Uusitalo et al. 2015). Various methods are used for uncertainty and sensitivity analysis such as:

Monte Carlo Simulation (MCS): MCS is one of the sampling techniques used extensively in uncertainty analysis. This method uses uniform random sampling of parameters and according to their probability distribution number of model parameters will be simulated and generated. The Monte Carlo simulation is a computer intensive technique and generally after enough number of runs the results produced by this method will be accurate (Beven 2012). MCS has also used as a sampling method for sensitivity analysis (Yang 2011).

Probability theory: Uncertainties can be represented by probabilistic approaches. In this method, the probability of an event is represented by the frequency of

occurrence of that event. For instance, when a range of an input is available the probability of an event can be identified as a ratio of the number of the times that event occurs to the total number of the inputs. This method estimates the uncertainties of model output for given uncertain input. In fact in this model, uncertainties of input data are described by probability distribution and the aim is to calculate probability distribution of the outputs of the model (IWR 2008).

Non-probabilistic methods (fuzzy set and possibility theory): The possibility theory is based on the possibility of events and their fuzzy sets and was proposed by Zadeh (1978). A fuzzy set is a non-probabilistic method for analysing uncertainties. This method is used mostly where only a few numbers of observations are available and statistical measurements are difficult to evaluate (Beven 2012). According to Zadeh (1978), fuzzy measures are defined as a simple function of errors between observed and predicted variables. When the error is zero or is in the range of zero, then the fuzzy measure is assumed to be at the maximum level. By increasing the error, the fuzzy measures are reduced and for the maximum level of errors the fuzzy measures are reduced to zero.

Interval probability theory (IPT): This theory is used for uncertain inference, which can be used in knowledge-based systems to measure the evidential support. An interval number represents the features of incompleteness and fuzziness in a simple manner. In interval theory of probability, degree of dependence between evidence is introduced by parameter of ρ (Cui & Blockley 1990, Hall et al. 1999).

Latin Hypercube Simulation (LHS): The LHS method (McKay et al. 1979) estimates the statistics of each output by dividing the probability distribution of each basic variable into N ranges with an equal probability (1/N) of occurrence. This method is more accurate than MCS in estimations of an output statistics (IWR 2008).

Point Estimation Methods: The point-probability distribution is used in this method to estimate the statistical moments of outputs (mean and covariance). For a given number of runs the statistical moments of model output can be estimated with this model. In this method the sample of parameters depends on the number of parameters (IWR 2008).

One-at-a-time and All-at-a-time sensitivity measures: The one-at-a-time method is the simplest method used for sensitivity analysis that only varies one parameter at a time, while the other parameters are kept constant at their current level. In this method, the uncertainty can be shown with quantifying the change in output of the model. This method can be used for a sensitivity ranking in which the value of one parameter changes by a specific percentage and changes in output values are quantified (Hamby 1994). This type of analysis is called local sensitivity as it only considers sensitivity over a specific value chosen for the parameter and not over the whole value distribution of input parameter. The latter analysis is called global sensitivity analysis. Local sensitivity analysis mostly uses One-at-a-time method (Pianosi et al. 2016, Hamby 1994). All-at-a-time is another method that combination of

input parameters are changes at a time, so the changes in outputs show the interaction of different parameters in the model. This method can be used for either local or global sensitivity analysis (Pianosi et al. 2016).

Statistical techniques for sensitivity analysis: Analysis of variance (ANOVA) developed by Ronald Fisher (1918), is a statistical model used to analyse the differences between means and variances between and among groups. Variance-based sensitivity analysis (VBSA) is a model independent method that can be used for sensitivity analysis of model output. In contrast with standardised regression and correlation coefficient, the non-linear and non-monotonic relationships between input and output of a model can be accurately found by VBSA approach (Saltelli et al. 2010, Hamm et al. 2006).

Approximate numerical methods (Generalised Likelihood Uncertainty Estimation-GLUE): Generalised Likelihood Uncertainty Estimation (GLUE) method, which was firstly proposed by Beven and Binely (1992), is an approximate numerical method that uses the results from Monte Carlo simulation and is used to estimate the uncertainties caused by hydrological models and parameters (Beven 2012). In this method there is an assumption that there is no single optimal model and this method is based on the equifinality concept that there can be a range of input parameters and models which may have the right sort of response for an application. In GLUE methodology, by using Monte Carlo simulation and based on the observed parameters values random parameter sets are generated to be used in each model and by comparing the results with the available calibration data the likelihood can be measured (Anderson 1999, Beven 2012).

Information-Gap (Info-Gap): Info-Gap is another method used for uncertainty and sensitivity analysis. Info-Gap is a non-probabilistic technique that is used for quantification of uncertainty and optimization of robustness to failure. This model is very useful in decision making in highly uncertain circumstances that in spite of the lack of information, decision makers need to make a realistic decision to wisely tackle with the management problems (Hipel & Ben-Haim 1999).

2.3.3 Review of previous studies

The increasing need for managing environments under uncertainty leads to the growth of studies conducted to investigate uncertainty based decision making. For instance, Wilby and Harris (2006), used a probabilistic framework to assess uncertainties in climate change impacts on the River Thames flow projections by the 2080s. They found that low flows are more sensitive to climate change scenarios and downscaling of GCMs rather than the CATCHMOD hydrological model parameters and emission scenarios.

In addition, New et al. (2007) used a probabilistic approach from multi model climate ensembles to assess uncertainty in impacts of climate change over regional

and local scales. New et al. (2007) used climate model climateprediction.net and CATCHMOD and focused on the Thames River. Their results showed that the information from using a probabilistic approach is more informative than using scenario based approaches (Carter et al. 2001, New et al. 2007) which are suitable for risk based adaptation assessments. Also different approaches for probabilistic analysis may lead to different risk based decisions.

Dessai and Hulme (2007), identified robust adaptation strategies to assess climate change in the east of the UK. The RCM was found to be the main source of uncertainty in in this study. Based on their study, due to using the driest model (HadCM3) and large size of supply adaptation option, the water resources, in this area remained robust to uncertainties. As noted by Dessai and Hulmi (2007), finding robust adaptation is not easy. Robust adaptation to climate change uncertainties is usually costly and needs to be negotiated between decision makers and stakeholders.

Manning et al. (2009), used multi models ensemble to provide probabilistic climate change information to assess water resources in the Thames catchment. As noted by Manning et al. (2009), different downscaling methods may lead to different flow prediction, which is originated in their difference in predicting PET. The results shows a reduction in predicted water availability in this catchment.

Lopez et al. (2009) used an ensemble of climate models to assess impacts of climate change on water supply and adaptation. They focused on the south-west of England. Their results indicated that the wider range of information given from climate model ensembles, in understanding the future impacts, is more helpful for decision makers than the information from single model scenarios. Burke and Brown (2010) used ensembles to asses uncertainty in the frequency of drought occurrence in the UK. The results indicated the increase in occurrence of drought by the end of 21th century.

Christensen et al. (2012) used UKCP09 to project the impact of climate change on river flows in UK for the 2020s. The GLUE methodology and also LHS approach were adapted for uncertainty handling. Their results showed reduction in future flow, simulated by CATCHMOD, in most of the UK and uncertainty presented in future flow projections is mainly from the uncertainty in climate projections.

Harris et al. (2013) also used the UKCP09 WG for robustness analysis of the North Strafforshire WRZ in the 2080s and noted that uncertainty caused by climate model parametrization is greater than uncertainty from emission scenarios. It is also stated that uncertainty in overall flow and water shortage is mostly originated from uncertainty in climate model parametrization rather than choice of emission scenario.

These studies used varied methods to investigate the impacts of climate change on water resources considering uncertainties and they all had a similar conclusion that uncertainty in climate change impact assessment is large and inevitable. Furthermore, downscaling and climate models lead to a large uncertainty in future flow projections and also the impact projections are very sensitive to structure and parametrization of climate models. These are originated in an inability to exactly model the climatological

and hydrological process of the real world. As noted by Wilby and Dessai (2010), there is "cascade of uncertainty" in modelling process which means choosing different scenarios for future, e.g. future society which is unknown, introduces new level of uncertainty to the system which flows through into the next step (e.g. emission scenario). Therefore, uncertainty in each step not only brings a new level to the system, but also is affected by uncertainty from previous step as well.

2.3.4 Adaptation planning under climate change uncertainty

Long-term management of water resources poses significant challenges for decision makers due to uncertainties. Long-term decisions regarding future investments e.g. construction new infrastructures are costly. As noted by Hallegatte (2009) these important decisions cannot be easily made due to the uncertainty in future climate conditions. Hence, given the complexity of the future climate conditions, and the fact that investing in supply adaptation options, such as constructing a new reservoir, is costly, it becomes crucial for decision makers to consider the uncertainty in future changes, and also increase their knowledge about climatic and non-climatic drivers to evaluate and update their decisions over the time (Hallegatte 2009, Curry & Webster 2011).

During the last few decades, in order to manage uncertainty in long-term climate projections, many techniques and approaches have been adapted. Based on the literature, "top-down" or "Scenario-led" method is one of the approaches traditionally used for adaptation decision making (Wilby & Dessai 2010, Brown & Wilby 2012) which start from downscaling the GCM to generate the RCM, which is then fed into the impact models to provide estimates of the impacts of climate change on the hydrological characteristics of the catchment. As noted by Wilby and Dessai(2010) the outcome of this approach contains a "cascade of uncertainties" which is in fact the aggregated uncertainties inherent in each step of the modelling process. Stakhiv (2011) also believed that information provided by GCMs which contain a cascade of uncertainties are not reliable to be used for decision making. In fact Stakhiv (2011) suggested that "adaptive management" is a suitable tool to assess adaptation options regarding stress testing and monitoring the performance and vulnerability of existing water infrastructure system.

Brown and Wilby (2012), also demonstrated climate stress testing or vulnerability analysis as an alternative approach for decision making under climate change. Brown et al. (2012) demonstrated the decision-scaling method to provide the required information about sensitivity of a system to future climate for decision makers. A "scenario-neutral" approach is another method based on sensitivity analysis which was presented by Prudhomme et al. (2010). These methods, called "Bottom-up meets Top-down" methods (Brown & Wilby 2012) are unlike top-down methods, which mainly focus on the sensitivity of catchments to a wide range of possible climate

changes rather than outcomes of scenarios. In these methods, first the problems are identified and then by stress testing the system, the performance of the system to different climatic and non climatic variables are assessed and finally the GCM climate projections are used to evaluate the future risk (Brown & Wilby 2012).

Robust decision making (RDM) is another quantitative approach to make decisions under deep uncertainty. This approach supports decision makers in evaluating adaptive strategies to eventually decide the most effective and robust option (Lempert et al. 2006, Lempert & Groves 2010). As noted by Lempert et al. (2006) the robust option is the one which is most reliable and flexible to unforeseen future climate condition. The RDM approach was fist adapted by Lempert and Groves (2010) to assess the impacts of climate change on Californian water resources system (Lempert & Groves 2010). The RDM approach in conjunction with Info-Gap Decision making has also been used by Matrosov et al. (2013) to find the most robust water supply option for Thames catchment, using UKCP09 and CATCHMOD. Risk-based decision making is also another approach presented by Bormogeo et al. (2014) for the Thames catchment, using UKCP09 and non-stationary probabilistic climate scenarios, and CATCHMOD to simulate inflows.

Dynamic robustness or managed adaptive approach is another alternative approach to deal with deep uncertainty in future conditions. The dynamic approaches such as those proposed by Haasnoot et al. (2013), and Ranger et al. (2013) provide an opportunity for decision makers to dynamically identify a wider range of uncertainties, and by sequencing of options as adaptation pathways, explore more flexible and profitable short-term and long-term adapting plans over time.

The narrative scenarios and storylines of future climatic and non-climatic changes (Clark et al. 2016, Yates et al. 2015) also been used as alternative approach for stress testing the water supply system and adaptation options. In this method different combinations of plausible future climatic and non-climatic scenarios are considered to provide meaningful information for decision makers. These set of scenarios can be used to analyse the performance of possible adaptation options in planning and managing of the water resources.

2.4 Summary

This chapter provided an overview of the research literature related to this study. This literature review summarised the impacts of climate change, globally, and in the UK. Furthermore, various sources of uncertainty in managing water resources, a range of models used for simulating future climate, river flows and available water resources were presented in this chapter. This was followed by the potential methods and approaches used for handling uncertainty and decision making under uncertainty.

The implications of the key uncertainties in long-term management of water resources are explored in this thesis with a novel method using a coupled system of

models that includes a weather generator, simulations of catchment hydrology and the water resources system. This integrated systems model are presented in Chapter 3.

Chapter 3

Integrated Systems Framework

3.1 Overview

This chapter presents a novel integrated systems framework to assess the implications of long-term uncertainties in water resources management. This chapter demonstrates this integrated systems model for a real world case study of the Thames catchment which is one of the most water scarce basins in the UK. Furthermore, the chapter introduces the choice of models used in this study. These are a spatial Weather Generator (UKCP09) that provides time series of rainfall and PET; a physically based hydrological model, SHETRAN, that simulates river flows in the catchment which drives a rule-based water resources management model, LARaWaRM which quantifies resultant daily water availability of the system. This coupled system of models are set up for the Thames catchment and the performance of each of these models is evaluated by validating their outputs against observed data, which is also presented in this chapter

3.2 Overview of the integrated systems framework

In this study, to understand the implications of the range of long-term uncertainties, a novel integrated systems model is developed that couples simulations of weather under current and future climates, catchment hydrology, and the water resources system. The framework of the integrated systems model is presented in Figure 3.1. The main steps to create the integrated system are as follows:

Step 1: Climate scenario and weather generator model are used to provide daily series of potential weather variables (e.g. rainfall and Potential Evapotranspiration (PET)), to drive the hydrological model.

Step 2: The generated meteorological time series are used as input for hydrological model to simulate the current and future daily river flows within the catchment.

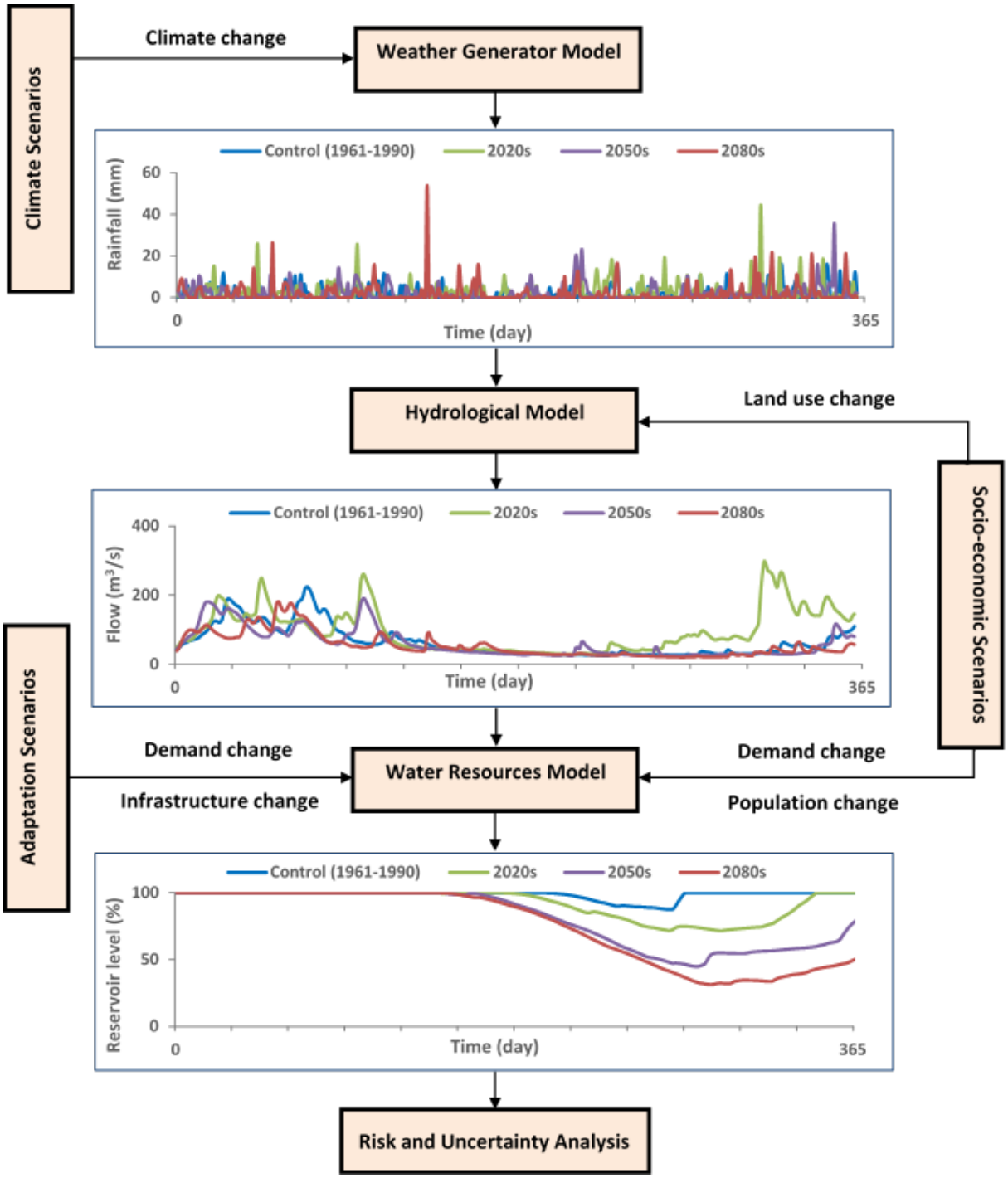

Figure 3.1: Integrated systems framework for risk and uncertainty analysis. The proposed integrated system models consists of a coupled system of models that includes a weather generator that provides time series of rainfall, this drives a hydrological model that simulates daily river flows in the catchment, and a water resources model which quantifies resultant daily water availability.

Step 3: The synthetic flow time series simulated by the hydrological model are used to drive a water resources model in order to predict the daily water availability in the water resources zone and assess the likelihood and consequences of water scarcity in the catchment.

Step 4: Sensitivity and uncertainty analysis water resources management options that are robust to uncertainties are identified.

Step 5: Different sources of uncertainty such as climatic (climate models and emission scenarios) and non-climatic (socio economic scenarios: land use, population and demand change) drivers are accommodated in the framework and by repeating the previous steps they can be analysed individually and/or in combination. Also the benefits of different demand and supply adaptation options are tested and the most robust adaptation options chosen.

The proposed integrated systems model can be implemented for any catchments within the UK and internationality, and also can be adapted for different weather generators, hydrological and water resources models. For this study, the integrated systems model is developed for a real-world water resources management case study of the Thames catchment, which is one of the most water scarce basins in the UK.

3.3 Thames catchment

This project is undertaken in the Thames catchment, a region which supplies water to the city of London, UK. The Thames Basin is the largest basin (9948 km^2) in the South East of England which covers the most populated area in the UK (Thames Water 2013). GLA (2014), predict London's population to increase from current 8.1 million at present to between 10.1 - 10.7 million by 2041. On average Londoners consume 168 l/p/d water which is higher than the average UK consumption (147 l/p/d). Due to experiencing hotter weather and increasing living standards, the consumption of water is expected to increase in the future.

The River Thames is the second longest river in the UK (346 km). It rises from Jurassic limestones of the Cotswold Hills in Gloucestershire and flows eastward, passing through Oxford, Reading, The Chilterns, London and finally joins the North Sea at its estuary. The River Thames between its source and Teddington is usually non-tidal, from Teddington Lock to the Thames Estuary, river is tidal as it receives tides from North Sea. The non-tidal part of Thames catchment is managed by the Environment Agency (EA) (BGS 2015*b*). This study focuses on the non-tidal part of Thames which is where the water resources are abstracted.

The average annual rainfall in this area is 737 mm, while the annual average of rainfall in England and Wales is 897 mm (Thames Water 2013). In fact, this area is the

most water scarce part of UK which has lower than average rainfall and very large demand (EA 2007). Two thirds of the rainfall in this area is evaporated or transpired. The remaining 246 mm is effective rainfall of which 55% abstracted and most used for public supply including household and non-household demands (Thames Water 2013).

In the Thames catchment, water supplies come from a combination of surface water and groundwater resources. Surface water is the primary source of water which provides approximately 80% of the total supplied water. The remaining 20% is abstracted from groundwater aquifers. The groundwater in this area yields from boreholes distributed over the basin. During droughts, when the surface water is limited, water is mainly supplied from groundwater aquifers (Thames Water 2013). There are three groundwater aquifers in this catchment, including the Chalk, the Oolitic limestones of the Jurassic and the Greensand. Figure 3.2 shows major groundwater aquifers of the Thames catchment.

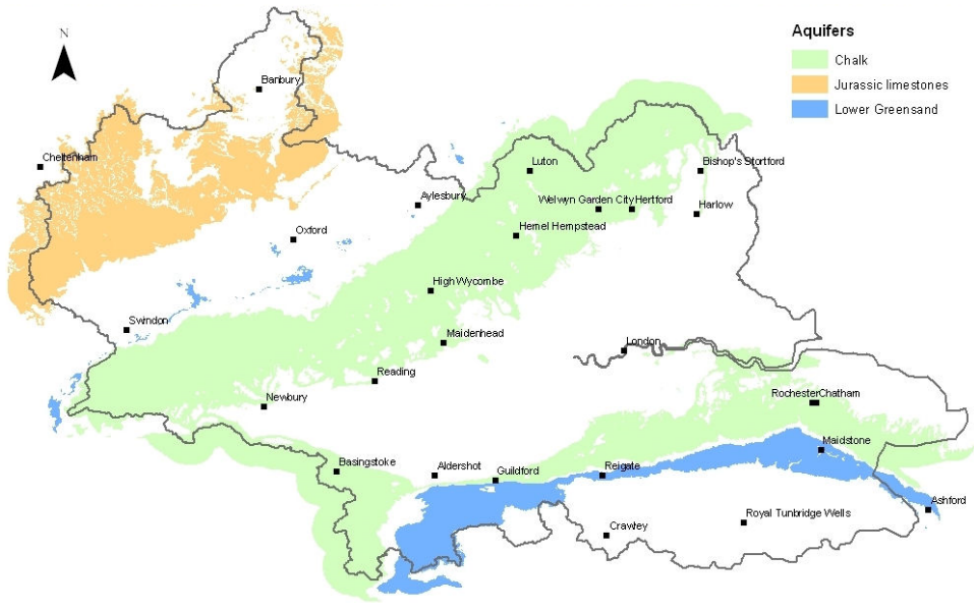

Figure 3.2: Major aquifers of the Thames catchment (BGS 2015*a*).

There is a chain of reservoirs in Lee Valley, supplied by the River Lee and a group of reservoirs in south west of London, supplied by the River Thames. In Thames catchment the water is abstracted from the Lee and the Thames River and diverted to the reservoirs. The abstraction from the rivers is subject to meet the minimum environmental flows and maximum daily abstraction in the river. These limitations are indicated in the Lower Thames Operating Agreements (LTOA) which is between Thames Water Utilities Ltd (TWUL) and the EA. The Lower Thames control Diagram (LTCD) dictates some restrictions on abstraction from River Thames at Teddington Weir. These restrictions range between 300 Ml/d and 800 Ml/d which depend on storage level in the reservoir (LAgS) and time of the year. The LTCD (see Figure 3.3) indicates the target flow curves and the restriction levels (Level 1 to Level 4).

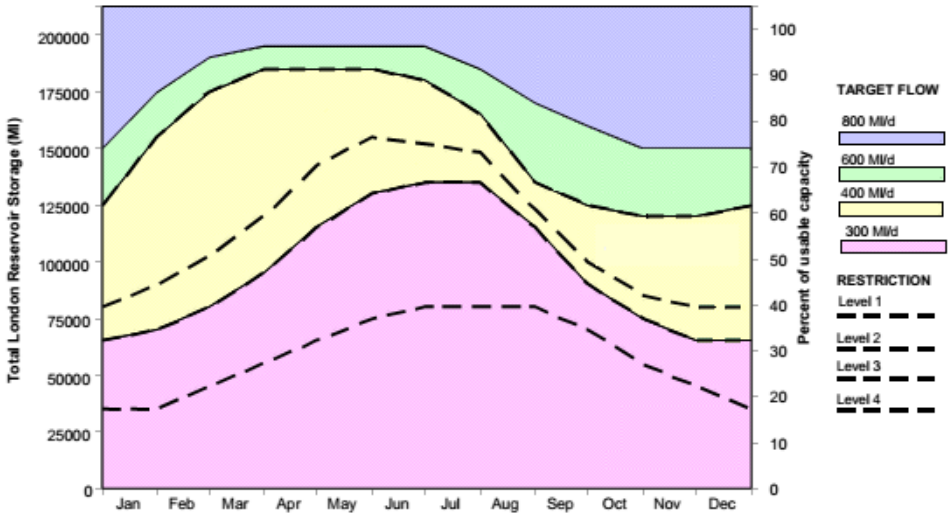

Figure 3.3: Lower Thames Control Diagram (Thames Water 2013).

The application of target flow curves depends upon level of storage in the reservoir, and time of the year. Target flow curves with an annual profile indicates the minimum environmental flow that should be remain in the River Thames. When the reservoir is full, the target flow is 800 Ml/d. By reducing the total reservoir level, the target flow level also drops. This means that more water is allowed to be abstracted from the river to preserve the storage level in the reservoir. The minimum target flow for Teddington flow is 300 Ml/d. As reservoir levels drop, more strict restrictions are imposed on customer demand. There is also a daily maximum abstraction of 5455 Ml/day and a total annual abstraction license of 665388 Ml.

Table 3.1 shows the Target level of services (LoS), Demand saving (DS) restrictions and the maximum frequencies of occurrence of these restrictions.

Level of Services	Frequency of Occurrence (in average)	Water Use Restrictions
Level 1	1 year in 5	Intensive media campaign
Level 2	1 year in 10	Sprinkler/ unattended hosepipe ban Enhanced media campaign
Level 3	1 year in 20	Temporary use ban Ordinary Drought Order/permits
Level 4	Never	Rota Cuts and Standpipe Emergency Drought Order

Table 3.1: Level of services and water use restrictions (Thames Water 2013)

In Thames basin, in addition to surface water and ground water sources, there are two backup storage schemes used in during dry periods. This backup storage includes North London Artificial Recharge Scheme (NLARS) and the West Berkshire Ground

Water Scheme (WBGW). The NLARS is an aquifer storage refilled by excess treated water that is pumped to the ground in north London and the WBGW is another aquifer storage which is only available during extreme droughts. These backup storages are used when reservoir storage drops below Level 4 of the control diagram threshold and target flow drops below 400 Ml/d.

In order to better represent the study area, the Thames catchment is divided to two sub-catchments including Thames at Kingston (including upper and Lower Thames) and Lee at Feildes Weir. Figure 3.4 illustrates the boundaries of these sub catchments. Characteristics of the Kingston and Lee sub-catchments are described in Table 3.2.

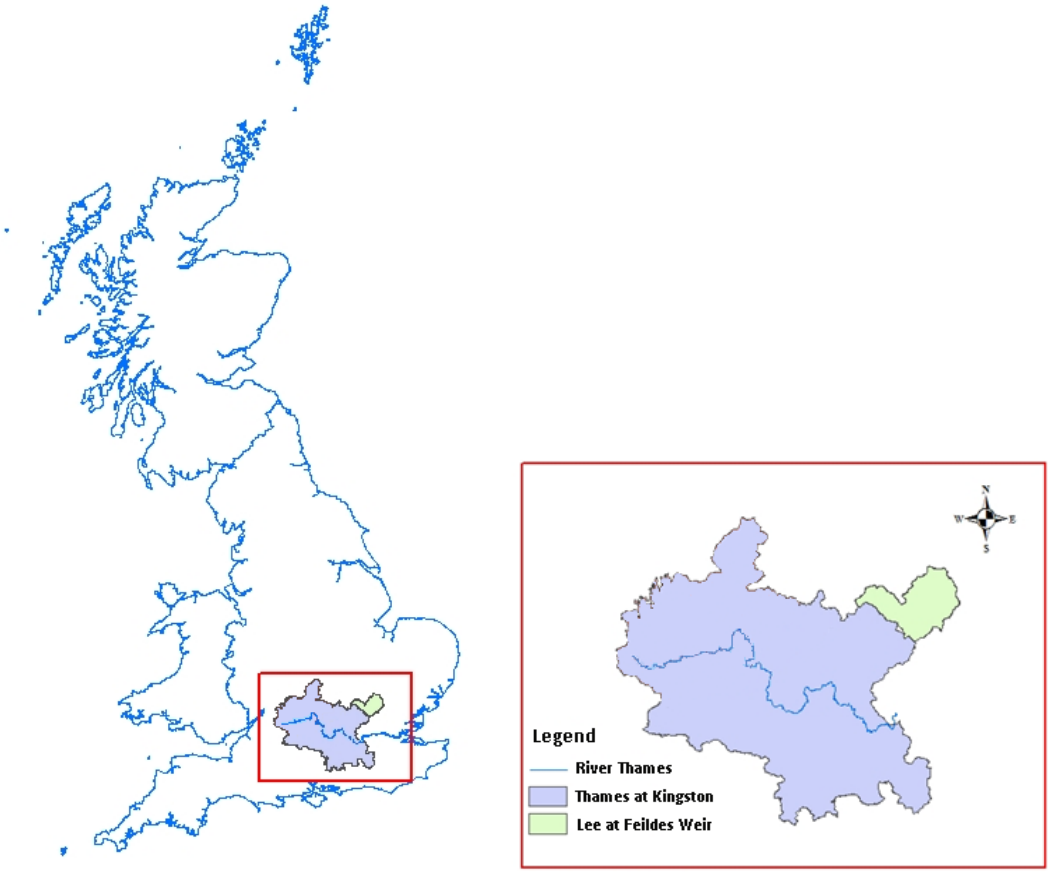

(a) (b)

Figure 3.4: The study area of the Thames Catchment.

Gauge station	Period of report	Catchment area (km^2)	Catchment description
Thames at Kingston	1883-2012	9948	Chalk and Oolites
Lee at Feildes Weir	1879-2012	1036	Chalk catchment with extensive Drift cover

Table 3.2: Thames sub catchments descriptions (NRFA 2012)

3.4 Climate change projections and Weather Generator

Global climate models (GCM) provide projections of climate variables under different emission scenarios at the global scale. For climate impact studies, higher resolution models and analysis are required, hence the outputs from GCMs need to be downscaled to regional scales (RCM). The UK Climate Projections (UKCP09) (Murphy et al. 2009) is a standard tool that projects the national future climate for the UK and provides improved understanding of some uncertainties inherent in climate models. It uses 11 members of Met Office RCM ensembles (HadRM3) to downscale the GCM to provide probabilistic projections at 25 km resolution, (Murphy et al. 2009). As noted by Murphy (2009), by using these 11 member HadRM3 based perturbed physics ensembles (PPE), UKCP09 better samples the parameter uncertainties in downscaling processes. Moreover, UKCP09 also uses multi-model ensembles, consisting of 12 other climate models to sample structural uncertainty due to modelling errors. The UKCP09 climate projections is a useful tool for the climate change impact assessments and has been extensively used for water resources management and decision making studies within the UK (e.g. Harris et al. 2013; Christierson et al. 2012; Manning et al. 2009; Matrosov et al. 2013; Borgomeo et al. 2014; Walsh et al. 2016).

For local climate change impact studies a higher resolution than 25 km is required. The UKCP09 Weather Generator (UKCP09 WG) simulates the synthetic time series of meteorological variables at 5 km resolution. This WG uses a stochastic (random) method to generate the daily time series of weather variables, for current and future climate (Kilsby et al. 2007). In UKCP09 WG, the future climates are defined with change factors at monthly time steps which are obtained from UKCP09 probabilistic projections, by measuring the difference between the statistics of the current value and the projected future value of a weather variable (Jones et al. 2009).

UKCP09 WG is currently the best available tool to be used for this study, where a stochastic rainfall model is required which can be perturbed for future climates. This weather generator produces future daily or hourly time series of rainfall which match basic summary statistics of future projections at the daily level, such as the mean, standard deviation and proportion of dry days. However, the model is not directly parameterised using seasonal or interannual properties, although generated series are reasonably consistent with the baseline observed climate data (Jones et al. 2009). Hence, the model is not capable of generating future series with a specified (increased or decreased) long-term variability which for instance can be used for analysing multi season droughts. There are monthly rainfall modelling frameworks which can reproduce multi-site monthly total rainfall for drought analysis, as demonstrated by Serinaldi and Kilsby (2012), but these models cannot currently project future changes in variability. Even if a model were available with this capability, there is currently no climate model which can reliably reproduce multi season drought characteristics of rainfall for the baseline, and hence cannot be relied upon to predict future variability.

Moreover, even if climate models could reliably reproduce the atmospheric circulation, there are severe limits imposed on validating their reproduction of extreme drought behaviour due to short observed records.

In UKCP09 WG, rainfall is the primary variable which means that first, the UKCP09 climate projections, generates the daily sequence of rainfall and then based on the simulated rainfall, the other variables such as mean daily temperature, vapour pressure and sunshine are generated. The generated time series are stationary which means they are all statistically consistent with real observed weather (Jones et al. 2009). The WG is calibrated by observed daily rainfall and other variables for the baseline climate 1961-1990.

The single-site UKCP09 WG is the original implementation of the UKCP09 WG, which uses single-site Neyman Scott Rectangular Plus (NSRP) model to provide the synthetic time series of climate variable at 5 km resolution (Jones et al. 2009) rainfall model. The spatial UKCP09 WG is an upgraded version of this WG which uses Spatial Temporal NSRP (STNRP) model (Cowpertwait 1995, Burton et al. 2008) which produces time series of meteorological variables such as rainfall, temperature, vapour pressure, wind, sunshine duration as well as PET, for each grid cells. The PET calculated by spatial UKCP09 WG with FAO-modified (Food and Agriculture Organization of the United Nation) version of Penman-Monteith method (Allen et al. 1998). All of these meteorological variables are internally consistent for each grid cell (Kilsby et al. 2007). As described by Burton et al (2013), the advantage of using spatial temporal weather generator is that it can simulate the weather scenarios for current and future projections, of any location and on a regular grid, rather than single or multi sites. Hence, using spatial UKCP09 WG in this project is advantageous as the simulated weather scenarios can be easily coupled with spatially distributed hydrological model of SHETRAN. It is recommended by UKCP09 WG guidelines (UKCP09 UI 2009) to use a minimum of 100 runs (random samples) to sustain the probabilistic nature of sampled datasets. Each of these runs are treated as an independent event and they all are statistically consistent. Although, for any day, the value of the generated weather variables are different, the underlying statistic for all the runs are the same. For daily data the length of these runs must be between 30 and 100 years (UKCP09 UI 2009).

In this study, the initial analysis conducted to assess the validation of UKCP09 WG, revealed that this WG was not acceptable in term of validation. For instance in October, there was more than 20% difference between simulated and observed rainfall for Kingston catchment. After further investigation it became apparent that for 1961-1990, monthly mean rainfall used for parametrisation of UKCP09 WG did not match the observed rainfall provided by Met Office for 5 km reference dataset. Revealing this issue led to updating the data used to parametrise UKCP09 WG. The new version of spatial UKCP09 WG (SWG: new version of spatial UKCP09) is wholly consistent with national gridded rainfall data set provided by Met Office. In this study, the new

version of weather generator is used, which limits the ability to compare this work with past studies (e.g. Walsh et al. 2016).

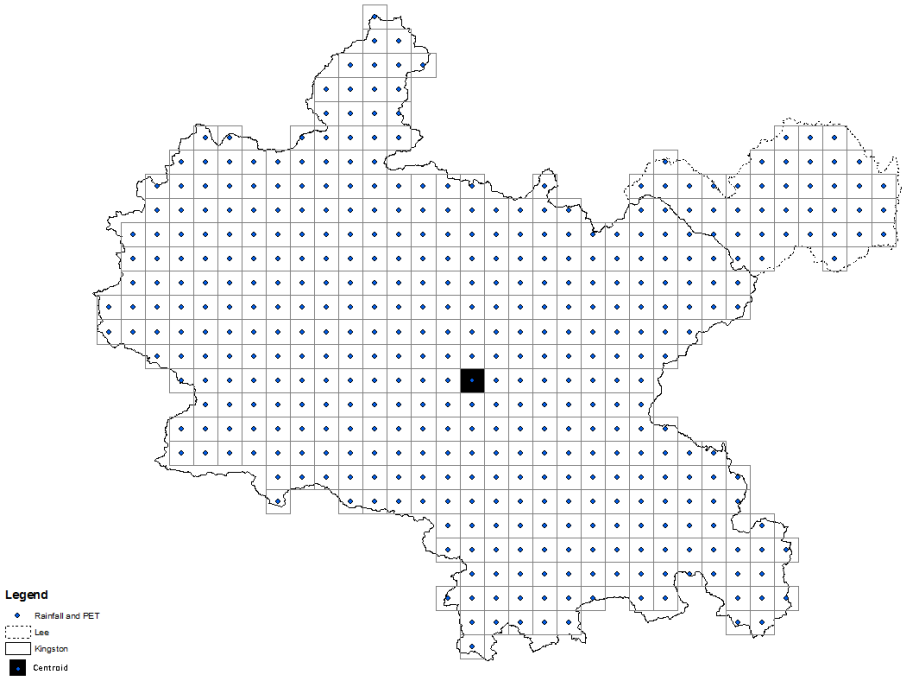

Figure 3.5: Rainfall grids (5×5 km) in Thames catchment used in spatial UKCP09 WG.

3.4.1 Validation of spatial UKCP09 WG

In order to choose the most suitable WG for the Thames catchment, both single-site (SSWG) and spatial UKCP09 WG (SWG) were considered. For the single-site WG (SSWG), the SWG runs only for the centroid grid, which represents the whole Thames catchment. Therefore, in this study, the SWG is run once for all of the grid cells within the Thames catchment and once for the centroid cell only. Figure 3.5 shows all the grid cells and also the centroid grid of the Thames catchment.

For running the SWG, the grid cells IDs within the catchment, the emission scenarios, time slice, the number of simulations as well as length of time series should be specified. In this study 100 runs of 100-year in length gridded daily simulations of control (1961-1990) and future time slices of 2020s, 2050s, and 2080s, under medium emission scenario were generated and used to represent the whole basin. For SWG, the 100 runs of 100-year gridded daily simulations were generated for all of the grids.

In order to assess the performance of spatial UKCP09 WG (SWG) in reproducing the 1961-1990 observed rainfall for each sub-catchments, the simulated rainfall for control runs are validated against the relevant daily observed rainfall time series provided by Met Office. In this chapter, only the 100 runs of 100-year-long control scenarios are discussed. The outputs for future scenarios are discussed in the next chapter (Chapter 4).

3.4.1.1 Validation of UKCP09 WG for Kingston sub-catchment

For this study, 100 runs of a 100-year-long gridded rainfall time series were generated by the SSWG and SWG, as baseline scenarios. The outputs from the weather generator are text files contain time series of different meteorological variables such as rainfall and PET. The simulated rainfall and PET time series were extracted from WG outputs for each sub-catchments.

Figure 3.6 shows boxplots[1] representing the performance of SSWG and SWG for average values of simulated rainfall against the observed values, for Kingston, 1961-1990. The results show that SWG better simulated the observed rainfall for control scenario. As it can be seen from this figure, across the year the median of average observed values fall within the simulated range from SWG. While, for SSWG the observed values are generally greater than the simulated range, except for June in which observed rainfall is within the simulated range.

Although the SWG better simulates the actual rainfall, there is a 9.0% underestimation in monthly mean rainfall for July and 5.0% overestimation in October. Not to mention that these amount of difference in actual and simulated variables are still in an acceptable range. Hence, in terms of validation, the results from SWG are valid and acceptable.

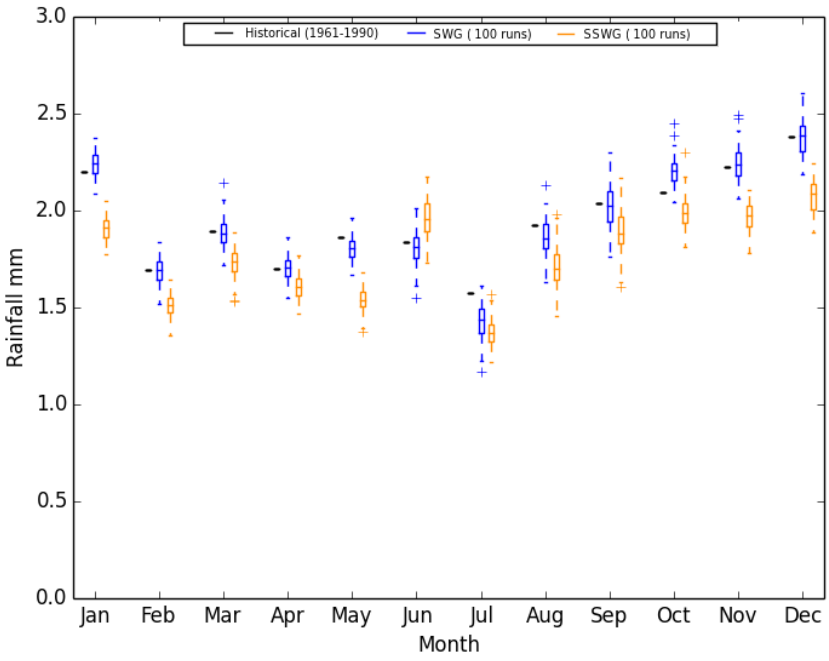

Figure 3.6: Boxplots of mean daily rainfall for historical (1961-1990) and simulated values from SWG and SSWG control scenario, Kingston sub-catchment.

[1]Each of the boxplots indicates the median, 25th, and 75th percentile values. Whiskers show the 1.5 times of inter quartiles (IQRs), the difference between 25th and 75th percentile values. The small crosses are outliners, which are any points of data that lies below (25th percentile - 1.5 IQRs) or above (75th percentile + 1.5 IQRs).

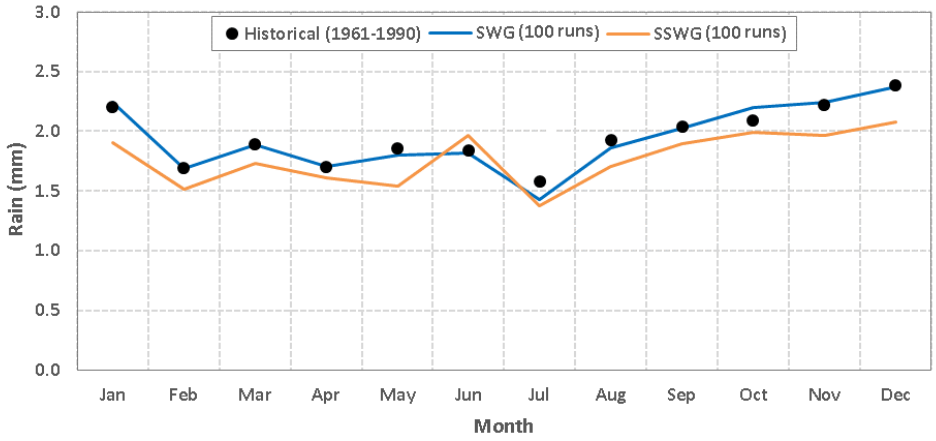

Figure 3.7: Mean daily rainfall comparison between historical (1961-1990) and simulated values from SWG and SSWG control scenario, Kingston sub-catchment.

Figure 3.7 illustrates the comparison between average simulated values and observed rainfall for Kingston. As it can be seen the results from SWG better represents the actual observed data for 1961-1990. More details about the difference and % change within simulated and observed rainfall are listed in Table A.1.

The difference between average of daily observed rainfall over 30 years and average of the 100 simulated 100-year-long daily rainfall from SWG is only 0.01 mm (1.94 mm for SWG vs 1.95 for observed). While for SSWG this value is 1.77 mm which is nearly 9.0% lower than the observed one.

In the UK, PET for hydrological models is produced by the Met Office Rainfall and Evapotranspiration Calculation System (MORECS) which provides estimates of precipitation, evapotranspiration and soil moisture at 40 $\times$ 40 km resolution for the whole of the UK (Hough & Jones 1997, Kay et al. 2013). For this project, a 5 $\times$ 5 km resolution is required therefore, historical PET is calculated using FAO Penman-Monteith (Allen et al. 1998) from observed variables provided by the Met Office. The calculated PET within each sub catchments have been validated against MORECS annual mean PET for Thames catchment. Here, the 100 runs of 100-year-long time series of simulated PET are generated by SWG.

The boxplots of daily mean PET in Kingston have been illustrated in Figure 3.8. This figure compares the range of simulated PET against historical values. For simulated PET, the values are from 100 runs of 100-year-long time series provided from SWG outputs. As it can be seen, there is an underestimation in simulating PET during spring and summer (from April to September) while the PET has been overestimated for the rest of the year. Overall, the difference between SSWG and historical is always greater than the difference between SWG and the historical.

Figure 3.9 compares the average of historical PET with simulated values. As it can be seen, the maximum difference between historical and simulated PET are in June and January. More details about this comparison are listed in Table A.2. For SWG,

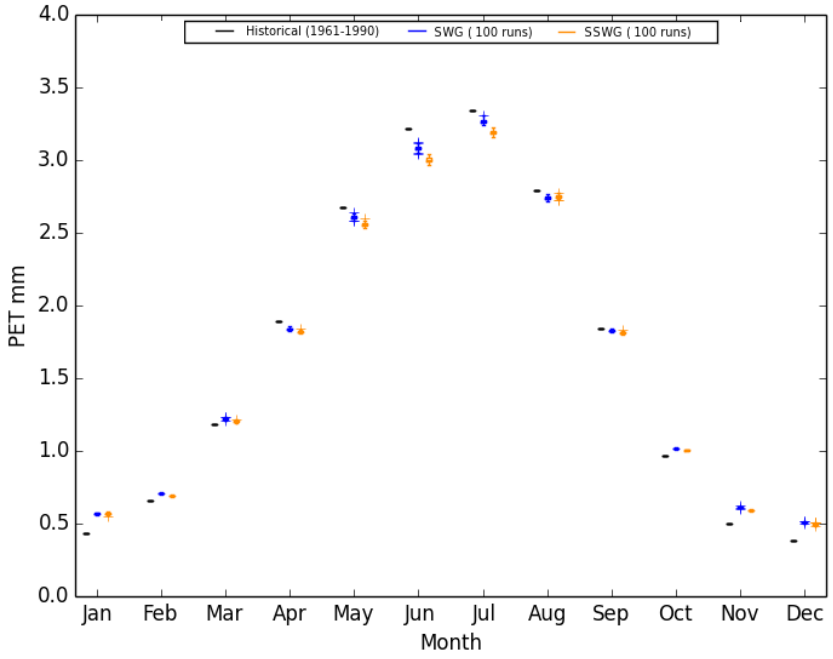

Figure 3.8: Boxplots of mean daily PET for historical (1961-1990) and simulated values from SWG and SSWG control scenario, Kingston sub-catchment.

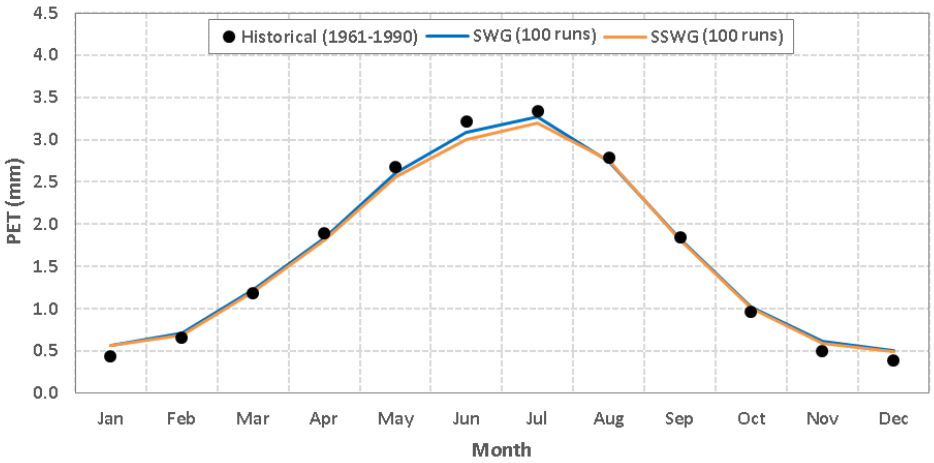

Figure 3.9: Mean daily PET comparison between historical (1961-1990) and simulated values from SWG and SSWG control scenario, Kingston sub-catchment.

there is 0.14 mm underestimation and 0.13 mm overestimation in June and January respectively. This difference for SSWG ranged between -0.22 and 0.13 mm. Similar to SWG, there is 0.13 mm overestimation in PET from SSWG while the difference between historical and simulated PET with SSWG is higher in June (-0.22 mm).

Similar to rainfall, the difference between average annual PET between SWG and historical is 0.01 mm which shows that the SWG PET is only 0.5% higher than the historical PET. While this difference between historical and centroid is -0.02 mm which also shows that there is 0.9% underestimation in SSWG. As a result, although the difference between historical and simulated PET from both spatial and SSWG are slim, still the SWG better simulates PET for Kingston.

3.4.1.2 Validation of UKCP09 WG for Lee sub-catchment

Figure 3.10 compares the performance of SSWG and also SWG for average values of simulated rainfall against the observed values, for the Lee sub-catchment, 1961-1990. As it can be seen from this figure, across the year the median of average observed values fall within the simulated range from SWG. In contrast, for SSWG the observed value is generally greater than the simulated range, except in July where SSWG underestimates the rainfall. The results show that SWG better simulates the observed rainfall for control scenario.

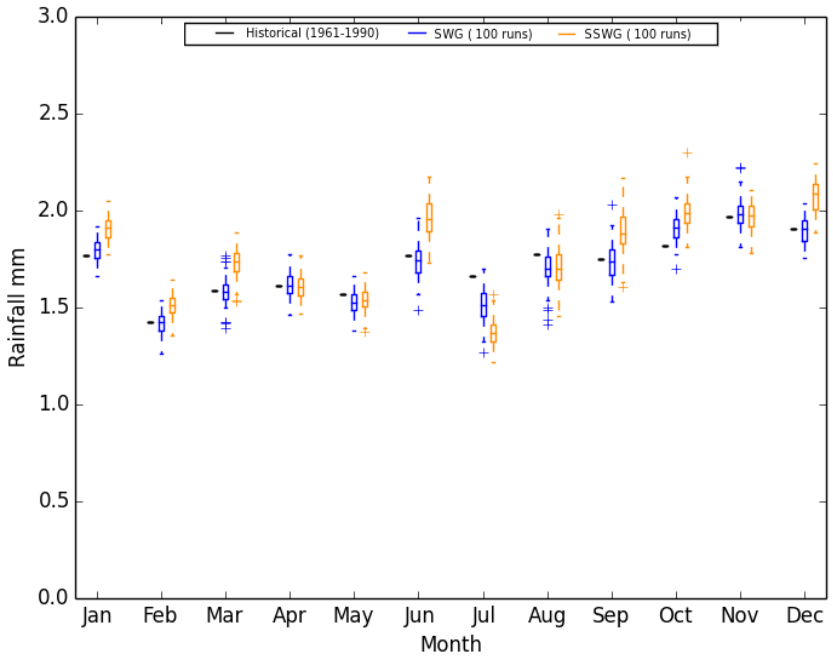

Figure 3.10: Boxplots of mean daily rainfall for historical (1961-1990), SWG and SSWG control scenario, Lee sub-catchment.

Figure 3.11 compares the average of historical and simulated values of rainfall in each month. For SWG, the simulated values are closer to historical rainfall values. The maximum difference between the spatial and historical rainfall values are in July and

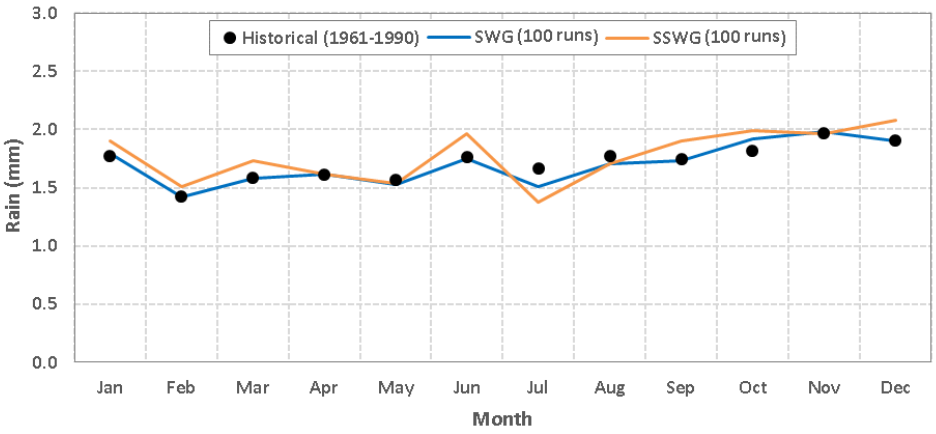

Figure 3.11: Mean daily rainfall comparison between historical (1961-1990) and simulated values from SWG and SSWG control scenario, Lee sub-catchment.

October. While for SSWG, there is a large overestimation in rainfall values in most of the months. The only exception is July which there is 11.2% underestimation in rainfall compared to observed values.

Table A.3 lists more details about the difference in historical and simulated rainfall values. In the Lee sub-catchment, similar to Kingston, there is 9.0% underestimation in monthly mean rainfall for July and 5.0% overestimation in October. More investigations showed that these errors in July and October are consistent in all the grids and the whole Thames catchment itself. This shows a systematic error in the weather generator which is highlighted as an important source of uncertainty in projecting the future climate in this study.

The comparison between simulated rainfall and historical values shows 0.01 mm underestimation in the average of annual rainfall for SWG, while the single site shows 0.06 mm overestimation in the annual rainfall values. As a result, it can be concluded that the SWG better simulates the rainfall for Lee sub-catchment.

Figure 3.12 shows the boxplots of daily mean PET in the Lee sub-catchment. This figure by comparing the range of simulated PET against historical values, illustrates the performance of weather generators in simulating the PET. From the boxplots it can be seen that, the average of PET simulated by weather generators are not very close to the historical values. The simulation by SSWG is even worse than SWG. Similar to Kingston sub-catchment, the results from weather generators show underestimation in PET values during spring and summer while these values are overestimated for autumn and winter. Generally, the difference between SSWG and historical values is always greater than the difference between historical and SWG.

Figure 3.13 shows monthly comparison between averages of PET simulated by the weather generators against historical values. For SWG the difference between historical and simulated values, ranges between -0.05 mm and 0.17 mm. The underestimation occurs only in three months from April to June. The maximum

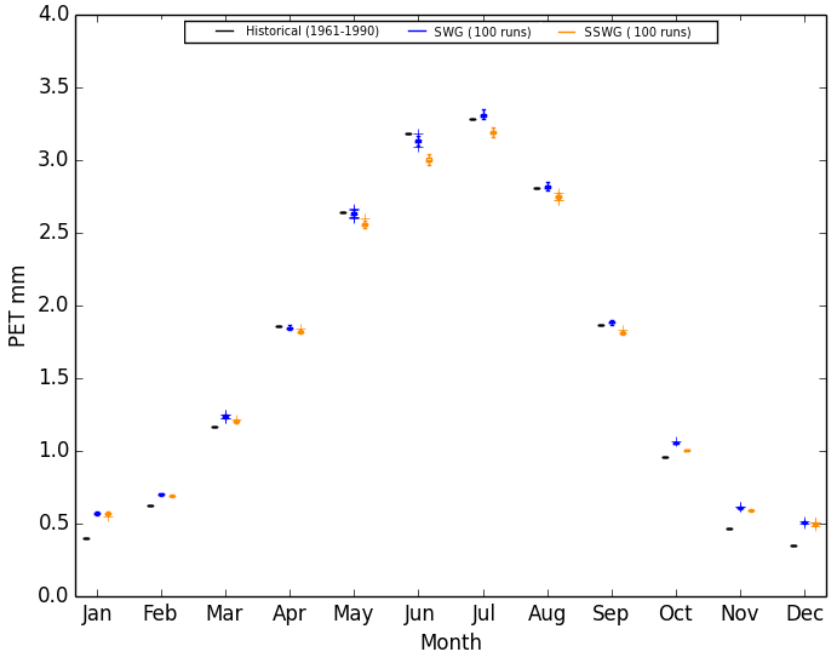

Figure 3.12: Boxplots of mean daily PET for historical (1961-1990), SWG and SSWG control scenario, Lee sub-catchment.

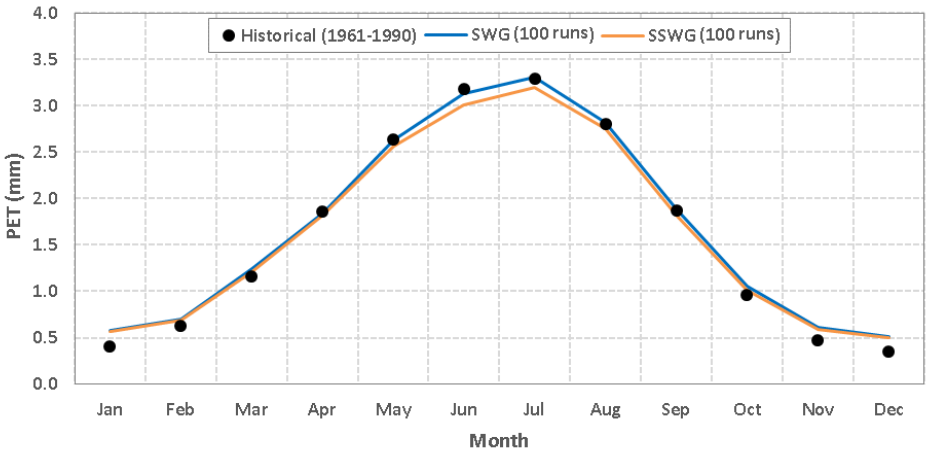

Figure 3.13: Mean daily PET comparison between historical (1961-1990) and simulated values from SWG and SSWG control scenario, Lee sub-catchment.

underestimation is in June (-0.05 mm), and the greatest overestimation, with +0.17 mm difference, happens in January. More details are tabulated in Table A.4.

For SSWG the difference ranges between -0.18 and 0.17. There is an underestimation in half of the year, from April to September, and the maximum difference with 0.18 mm occurs in June. There is overestimation in the rest of the months, January with 0.17 mm has the greatest overestimation. For annual rainfall, the average of rainfall given from SSWG is 1.64 mm which shows that there is only 0.01 mm between SSWG and historical. While for SWG, this difference is around 0.06 mm. This shows that in annual scale the SSWG better simulates the PET while in monthly scale the performance of SWG is better than single site.

3.5 Hydrological model

The synthetic rainfall and PET time series are then used as input for the hydrological model to simulate the current and future daily discharge of the catchment. Initially in this study, the conceptual hydrological model CATCHMOD was used to simulate the discharge in Kingston and Lee sub-catchments (Walsh et al. 2016). However, given the ability to modify model parameters is crucial for this uncertainty analysis, it became apparent that CATCHMOD was not adequate for this study and the proposed uncertainty analysis (e.g. land use change uncertainty). Conceptual hydrological models, when compared with the physically based, are assumed to be less accurate to predict future characteristics of the catchment, and they may not be robust under climate change (Beven, 2000). While, physically-based spatially-distributed (PBSD) models are more reliable when modifying model parameters and so they are better suited to future prediction of environmental change (Breuer et al. 2009, Beven 2012).

Although, physically based hydrological models such as SHETRAN are very data intensive, they are more suitable for uncertainty analysis, as they better capture the spatial characteristics of the catchment compared to conceptual models (Beven 2012). Not to mention that when SHETRAN couples with a spatial weather generator it better represents spatial heterogeneity. Hence, it was decided to use the physically-based spatially-distributed model SHETRAN (Ewen & Parkin 1996) as an alternative hydrological model to simulate the flow in Thames catchment. However, given the complexity of the SHETRAN model, along with the size of the catchment, model run times were increased from a matter of minutes to over 30 days per simulation. As a result, it was decided to reduce the resolution from 1 km to 5 km. Reducing the resolution led to a significant reduction in run time for the Thames sub-catchment. After reducing the resolution, each run for Kingston took 4 hours and for Lee took only 30 minutes.

3.5.1 SHETRAN hydrological model

SHETRAN is a physically-based spatially-distributed (PBSD) model (Ewen & Parkin 1996, Ewen et al. 2000, Birkinshaw et al. 2010) which can be used to study hydrological and environmental impacts of climate change and land use change. In fact, this model can be used for a single catchment or a group of catchments which are connected contiguously (Ewen et al. 2000). Using SHETRAN in this study makes it possible to extend this project from Thames catchment to whole the South East region in the future.

SHETRAN is a fully distributed model which considers the basin as a group of grids, columns and stream links. Each of the grids has a column consisting of various cells located one above the other which represent the soil or geology and land use associated with each cell. The rivers are modelled as a network of streams, each of the rivers are simulated along the edges of the grids. This column approach couples the surface and subsurface, makes it possible to model the transfer of water vertically and horizontally. SHETRAN can model groundwater systems including perched aquifers and confined aquifers.

The SHETRAN hydrological model is very data intensive and it usually takes several weeks to create the preliminary data sets for a new catchment. As noted by Ewen and Parkin (1996) the initial values for the parameters of the physically based hydrological model such as SHETRAN, are chosen based on the literature, field measurements of the physical properties and also expert knowledge of the modellers. The authors present "blind validation" approach for using models on the condition of change. In this study the preliminary data sets for Thames catchment was provided from previous study conducted in by Lewis (2016).

Unlike lumped conceptual models, physically based distributed models, in theory, do not need calibration. In principle, SHETRAN is a physically based model with parameters explicitly related to physical processes that can be determined a priori from spatial data sets. By representing the physical processes (e.g. infiltration, saturation, vertical and lateral flows, transpiration etc.) explicitly, the catchment response to rainfall and evaporation forcing is constrained and more robust to variation in the forcing than if described in one lumped process. Thus, physically-based models can potentially avoid the situation where the flexible nature of a lumped parameterization provides capability for model fitting along with the potential for over-fitting to the calibration data set, resulting in less robust model for perturbed conditions outside the range of the observed period. Key model parameters (e.g. depth of aquifer) are not time-varying, and largely are independent from climate conditions. However, in many cases, some adjustment to parameter values is necessary. For instance, for catchments with significant groundwater systems, such as the Thames catchment, information on the aquifer extent and porosity is limited and so some calibration is necessary. In this study, because the value of the calibrated parameters is within the bound of physical

values, there is some confidence that these parameters are applicable in the future as well.

It is very important to define the boundary of a catchment carefully as it can become one of the main sources of uncertainty (Shaw et al. 2010). This affects the evaluation of input rainfall and output discharge of the catchment. Knowledge about geology, topography and boundaries of the catchment has important role in assessing the water resources of the study area. Digital Elevation Model (Singh et al. 2004) is widely used to plot the catchment area on a topographical map, provides a better understanding of impacts of neighbour catchments hydrology or water budget of the study area. For instance in the Pang catchment, the river is a chalk stream which depends on groundwater, much of the groundwater drains into the River Thames and not the Pang river (Shaw et al. 2010).

3.5.2 Required data for SHETRAN set up

In SHETRAN, all the physically based properties (surface and subsurface) of the model should be specified for each of the grid cells. Datasets required for each of the grids are as follows:

- Digital Elevation Models (DEMs)
- Geology
- Soil properties
- Land cover map
- Rainfall
- Potential evapotranspiration (PET)

In order to simulate the discharge in Thames catchment, 5 km spatial resolution and a daily time step were chosen. The selected spatial resolution is a compromise to shorten the simulation times. For Thames catchment, SHETRAN is set up individually for each of the sub-catchments of Kingston and Lee. For this aim, all the required data need to be collected and stored in an acceptable format to be integrated into the hydrological model.

The following distributed datasets are used to set up SHETRAN for the Thames catchment:

Digital elevation model (OS landform)

Digital Elevation Model used in this study is based on Ordnance Survey (OS) landform panorama data which was downloaded for 20×20 km tiles for whole UK. Using ArcGIS, this was resampled to 5 km resolutions for Thames catchment. Another required data for running SHETRAN is the river channels in the catchment. In SHETRAN, minimum elevation in each grid cell is considered as river channel. Hence,

in order to model the rivers within the Thames catchment, a DEM map with minimum elevation (with 5 km resolution) was generated with ArcGIS.

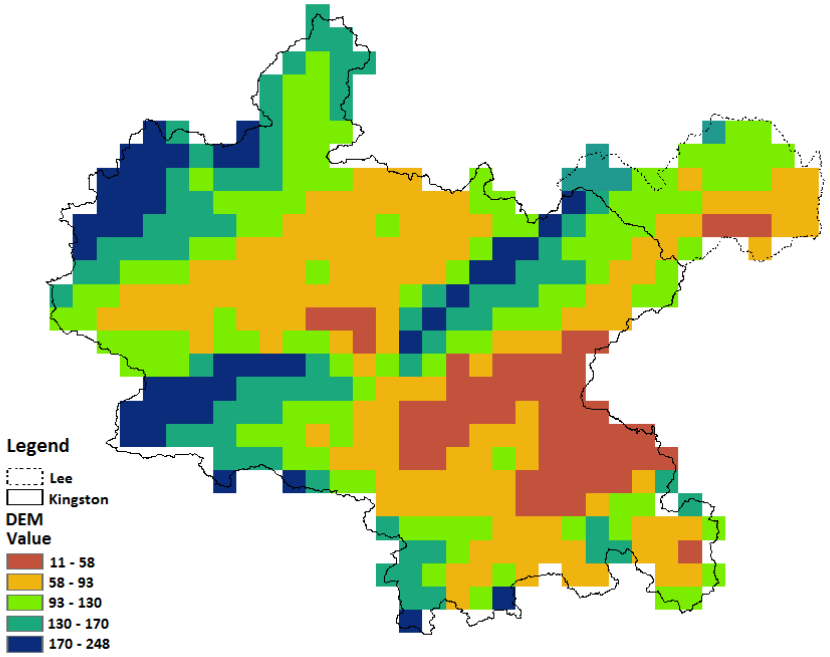

Figure 3.14: DEM map for the Thames catchment.

Geology and soil

In SHETRAN, subsurface is modelled as a group of columns, consist of various cells located one above the other which represents the soil or rock associated with each grid cell. Information such as dominant topsoil and subsoil texture, depth of each layer, saturated water conductivity, residual and saturated soil content need to be specified for each of these layer. For this study, these parameters were provided by the European Soil Database (ESDB) v2.0. $1km \times 1km$ (Europen Soil Data 2006).

For better representation of the characteristics of the catchment, geological information about aquifer properties of the catchment need to be provided. This information was taken from British Geological Survey (BGS 2015*a*) 1:625000 scale digital hydrogeological map (BGS 2014). The subsurface map for the Thames catchment was created from combining ESDB and BGS hydrogeological layers.

Land Cover map

Land cover map for Thames catchment was derived from CEH land cover map (LMC) 2007, 1 km raster data sets (Morton et al, 2011). The LMC is produced from satellite images containing 23 land cover classes. These land cover classes have been simplified to only 7 classes to be used by SHETRAN. The land cover classes used by SHETRAN are arable, bare ground, grass, deciduous forest, ever green forest, shrub and urban (Birkinshaw et al. 2011).

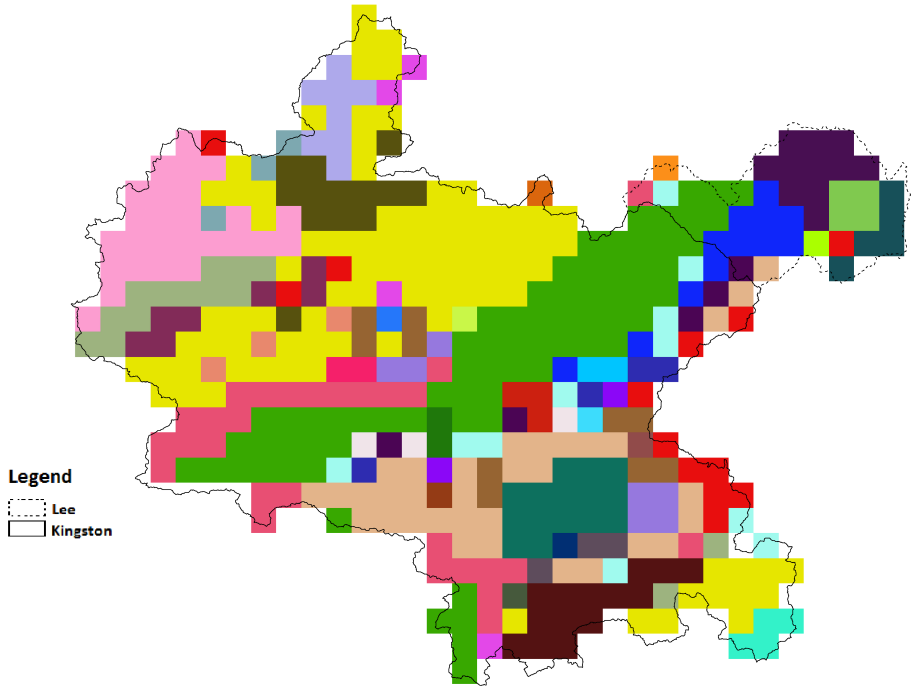

Figure 3.15: Subsurface map for the Thames catchment. This map created from combining ESDB and BGS hydrogeology layers, and different colors indicate different soil categories consist of various combinations of soil properties. In Thames catchment the dominant soil categories are 22 (dark green), 192 (yellow) and 25 (pink). Both categories 22 and 25 include highly productive (chalk) aquifers, while no aquifer is present for category 192. The soil type for category 22 is silty clay loam, for 192 is sandy loam and for 25 is silt loam.

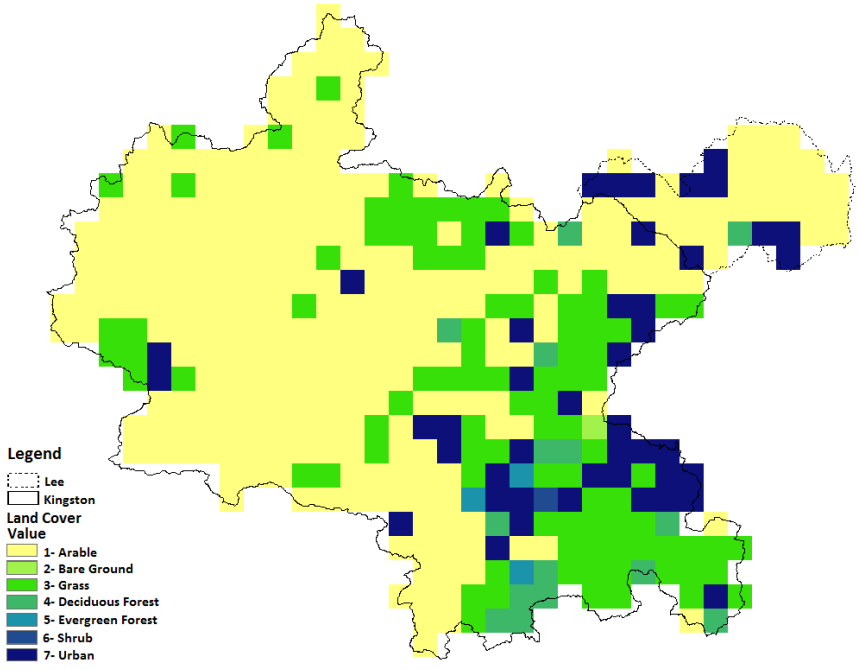

Figure 3.16: Land cover map for the Thames catchment.

Rainfall and Potential Evapotranspiration (PET) data

Daily time series of rainfall and PET precipitation for Thames catchment are generated by SWG and SSWG and discussed in section 3.4.1. The SWG generates a text file (contains time series of the weather variables such as rainfall and PET) for each of the runs, and for each of the grid ID within the catchment. While for running SHETRAN, for each of the runs, there should be a single file contains all the grid IDs within each sub-catchment. Hence, to meet the required format for SHETRAN, a python script was written to join the time series of all the grids of each of the sub-catchments, in a single csv file.

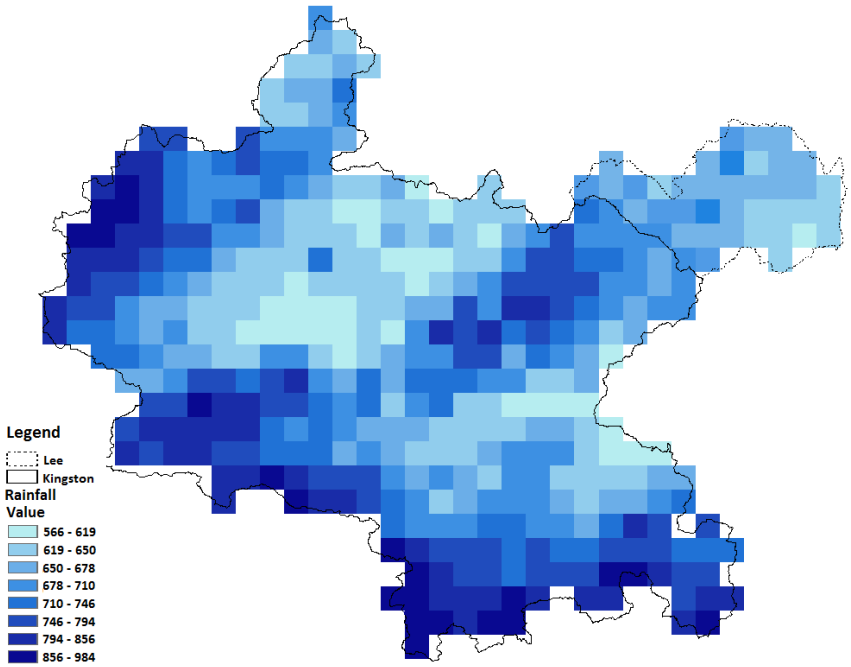

Figure 3.17: Annual rainfall total for the Thames catchment.

3.5.3 Calibration and validation of SHETRAN for Thames catchment

After setting up the SHETRAN, the next stage is parameter calibration. In order to reduce the uncertainty in the values for the parameters, the hydrological model should be calibrated against measured data for the catchment, and also to test the fitness of the hydrological model in predicting the impacts of changes in land use and climate, the hydrological model need to be validated (Ewen & Parkin 1996).

In this study, SHETRAN is calibrated for the period of 1991-2001 (11 years). For calibration, the results given from SHETRAN are compared with the historical discharges measured for the same time period. The time series of observed flow data in Thames catchment are obtained from National River Flow Archive (NRFA) for stations 39001 and 38001, Kingston and Lee respectively (NRFA 2012). Because the flow in Thames River is highly influenced by human activities, only naturalized flows were considered.

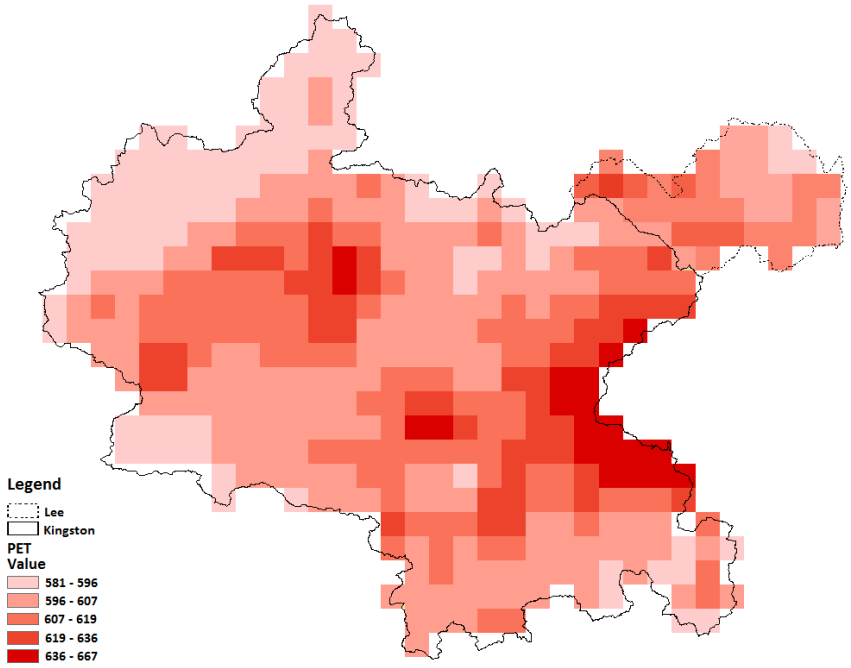

Figure 3.18: Annual PET total for the Thames catchment.

The simulated discharge are from running SHETRAN with inputs from observed rainfall and PET for 1991-2001. All the initial parameters values to run SHETRAN are chosen based on its guideline [2]. For calibration, the value of input parameters were manually adjusted to get the best fit between observed and simulated discharge. The value of the parameters were based on expert knowledge of Dr Stephen Birkinshaw. As reported in the literature, following parameters are considered in course of calibration of SHETRAN (Birkinshaw et al. 2011, 2014, Mourato et al. 2015):

- Ratio of actual/potential evapotranspiration for each land cover type (AE/PE)
- Depth of aquifer associated with each soil type
- Strickler overland flow (inverse of Manning's Roughness Coefficient)
- Saturated hydraulic conductivity (Ks)

The next step after calibration, is validation. In order to test the fitness of the hydrological model in predicting the impacts of changes in land use and climate, the hydrological model need to be validated (Ewen & Parkin 1996). The aim of validation is to make sure that simulations from hydrological model are valid for future time periods. Hence, for validation the SHETRAN was run for an independent period of 1961-1990. The running process is similar to calibration, but this time the meteorological input data are for 1961-1990 time period. The simulated discharge are compared with measured flow provided by NRFA for this time period.

In order to measure the performance of hydrological model in simulating real historical discharge, different statistical metrics are used (Hall 2001, Krause et al. 2005,

[2]http://research.ncl.ac.uk/shetran/SHETRAN%20V4%20User%20Guide.pdf.

Moriasi et al. 2007). One of these statistical measures which is widely reported in hydrological literature is Nash-Sutcliffe Efficiency (NSE) (Nash & Sutcliffe 1970). NSE is calculated as:

$$NSE = 1 - \frac{\sum_{i=1}^{n} \left(O_i - S_i\right)^2}{\sum_{i=1}^{n} \left(O_i - \overline{O}\right)^2} \tag{3.1}$$

Where O is observed, S is simulated and $\overline{O}$ is mean observed values. The range of NSE lies between -∞ to 1. NSE of 1 indicates the simulated and observed values perfectly match, while NSE of lower than zero indicates that the mean of observed value can be a better predictor. Here, the NSE value greater than 0.65 has been considered as good simulation (Singh et al. 2004, Moriasi et al. 2007). Although NSE is widely used in hydrology, this metric has some limitations. It squared the difference between observed and simulated value, which leads to overestimation during peak flows and underestimation during low flows (Krause et al. 2005). Hence, in conjunction with NSE, other metrics such as modified NSE and RMSE are also considered.

The Modified NSE which has been recommended by Krause et al. (2005) is as follows:

$$ModifiedNSE_j = \frac{\sum_{i=1}^{n} |O_i - S_i|^j}{\sum_{i=1}^{n} |O_i - \overline{O}|^j} with j \in N \tag{3.2}$$

As it has been noted by Krause et al. (2005), if j=1 the overestimation of peak flows reduces which gives a better overall evaluation of hydrological models.

The other metric used in this study is Root Mean Square Error (RMSE) (Singh et al. 2004, Moriasi et al. 2007).

$$RMSE = \sqrt{\frac{1}{N} \sum_{i=1}^{n} \left(S_i - O_i\right)^2} \tag{3.3}$$

For RMSE the value of 0 shows a perfect fit between simulation and observed values and the RMSE values less than half the standard deviation of the observed data can be considered as an acceptable value (Singh et al. 2004).

3.5.3.1 Calibration and validation analysis for Thames at Kingston

The results of SHETRAN simulation for Kingston sub-catchment are shown in Figure 3.19. In calibration period (1991-2001) the comparison between daily observed and simulated discharge gives NSE of 0.9, Modified NSE of 0.73 and RMSE of 8.98. These metrics are listed in Table 3.3. The given results show that the time series of the simulated discharge represent observed values well. As it can be seen in Figure 3.19, especially the low flows are reasonably well captured by the model.

The validation is carried out for 1961-1990 gives NSE of 0.78, modified NSE of 0.61 and RMSE of 8.88. The NSE for validation is less than the calibration period. More

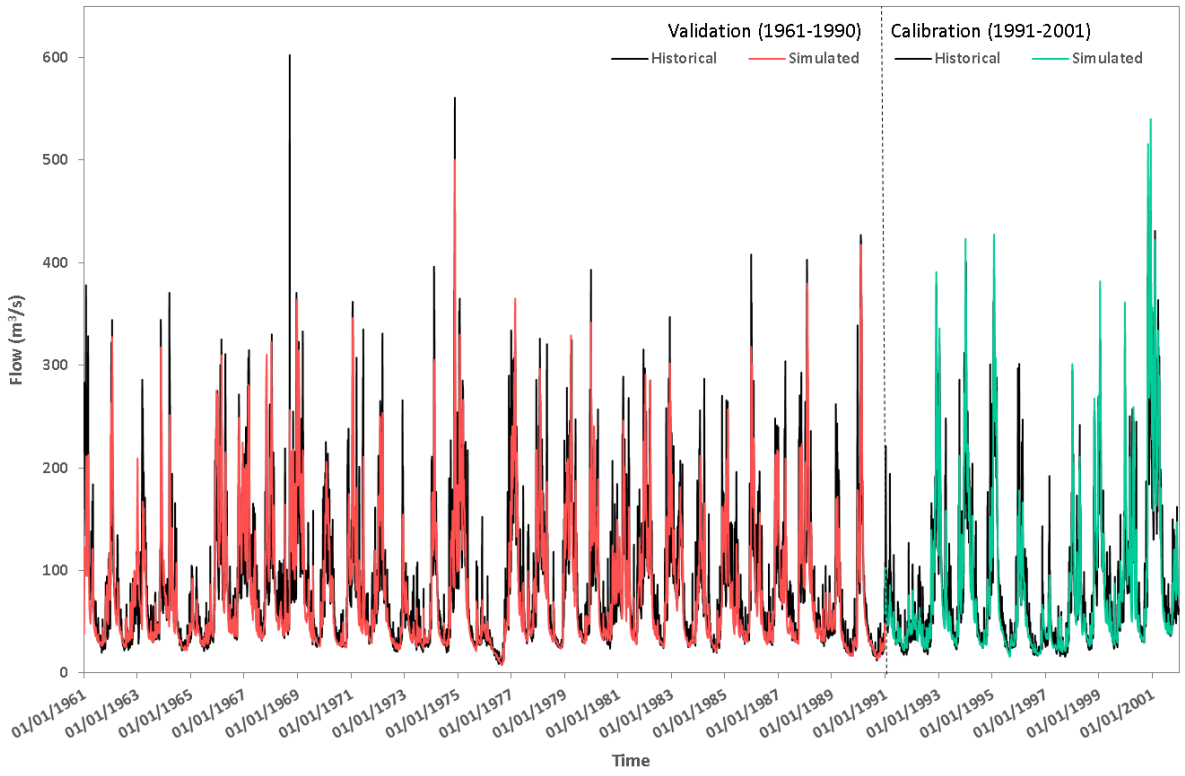

Figure 3.19: Calibration and validation for Kingston sub-catchment.

	Time period	NSE	Modified NSE	RMSE
Calibration	1.1.1991-31.12.2001	0.90	0.73	8.98 (<42.9/2)
Validation	1.1.1961-31.12.1990	0.78	0.61	8.88 (<37.3/2)

Table 3.3: Calibration and validation for Kingston sub-catchment

investigations show that the total PET, rainfall and runoff for validation period is less than the calibration period (see Table 3.4). Because the basis for modelling, the evapotranspiration and discharge, are unchanged in the model, the drop in NSE for validation, from 0.9 to 0.78, has occurred. As it can be seen in Figure 3.19, in validation period the low flow, especially the 1976 drought, is well captured by the simulation.

	Rainfall (mm)	PET (mm)	Runoff (mm)
1961-1990	713.56	607.24	258.35
1991-2001	762.30	639.19	267.58

Table 3.4: Annual mean total rainfall, PET and run-off in Kingston sub-catchment

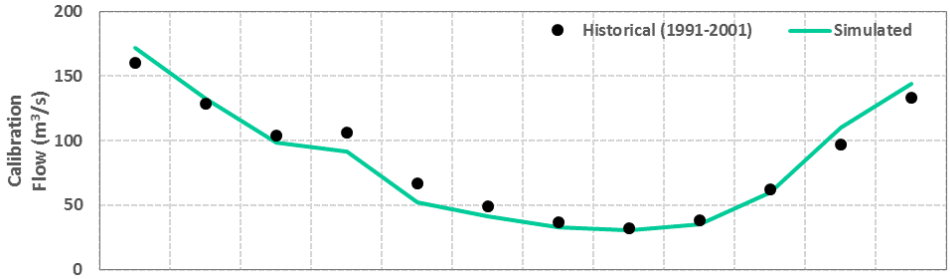

(a)

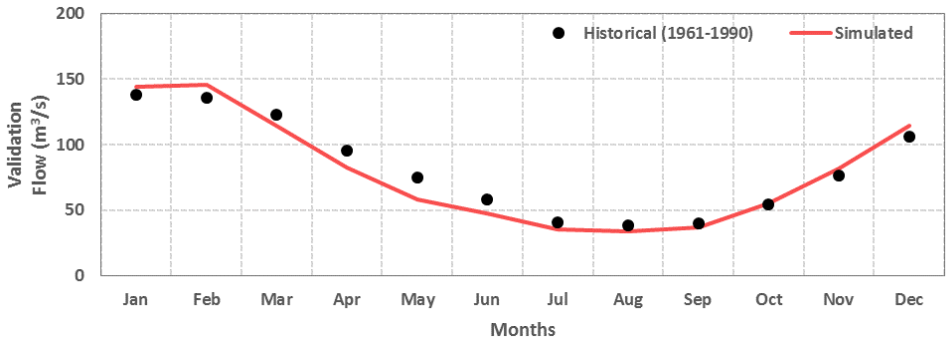

(b)

Figure 3.20: Mean flow comparison between historical and simulated values for calibration and validation period, Kingston sub-catchment.

Figure 3.20 shows the historical and simulated mean flow in each month, for calibration and validation period. The comparison between observed and simulated flows shows that, for both calibration and validation period, the spring flows simulated by SHETRAN are lower than the historical flows. The possible reason for this underestimation is due to the nature of the chalk. Chalk and limestone cover 43.2% of the Kingston catchment (NRFA 2012). During spring (March-June) the discharge is mainly fed from stored water in the chalk aquifers (the flows often exceeds the rainfall). Compared to conceptual hydrological models, the chalk aquifer is explicitly included in SHETRAN. Chalk is a dual porosity medium-matrix and significant fractures. To reflect this the SHETRAN parameters used had a high conductivity and a small difference between the residual moisture content and the porosity. Although

a simplified representation, SHETRAN does allow spatial variations on recharge and the effect of overlaying vegetation and soil.

Table A.5 compares the mean flow, errors and % change between observed and simulated discharge, for calibration and validation periods. Results show underestimation in mean annual flow in both time periods. For validation period the % of error between observed and simulated, ranges between -22.2% to +8.2%. In March with 22.2% underestimation, the difference between observed and simulated flows is greater than the other months. The maximum overestimation, with +8.2%, happens in December.

For calibration period in most of the months (March to October) there is an underestimation, ranges between -21.0% and -4.6%. Same as validation period, the difference between observed and simulated flow in March is at maximum level (-21.4%), while December with 14.8% has the greatest overestimation in simulated flow.

3.5.3.2 Calibration and validation analysis for Lee at Feildes Weir

The simulated discharge from SHETRAN in Lee sub-catchment is calibrated and validated for 1991-2001 and 1961-1990 respectively. Because there is a gap in discharge records from 1.6.1976 to 30.4.1978, the time series from 1.1.1976 to 31.12.1978 are excluded from the analysis.

The daily comparison between simulated and observed values for validation and calibration period are plotted in Figure 3.21. From the figure, it can be seen that in both the calibration and validation periods the simulated flow mimics a similar trend as observed flows. Also, the low flows are reasonably well captured by the model. Interesting to note that, despite the gap in the observed records (between years 1976-1978), the drought of 1976-77 well captured by simulation.

Table 3.5 shows the metrics used for evaluation the performance of SHETRAN in this catchment. As it can be seen, in calibration period (1991-2001) the comparison between daily observed and simulated discharge gives NSE of 0.67, Modified NSE of 0.56 and RMSE of 0.66 which are all in the acceptable range.

	Time period	NSE	Modified NSE	RMSE
Calibration	1.1.1991-31.12.2001	0.67	0.56	0.66 ($<2.09/2$)
Validation	1.1.1961-31.12.1990	0.65	0.49	0.68 ($<1.86/2$)

Table 3.5: Calibration and validation for Lee sub-catchment

As it can be seen in Table 3.5, the validation for 1961-1990 gives NSE of 0.65, modified NSE of 0.49 and RMSE of 0.68. So, similar to Kingston, in this catchment the NSE for the calibration period is higher than the validation period. More investigations show that in calibration period, the winter was wetter than validation period (except of December) and also there is more rainfall during April and June compared to the validation period. In addition, the mean PET for 1990-2001 is more than baseline,

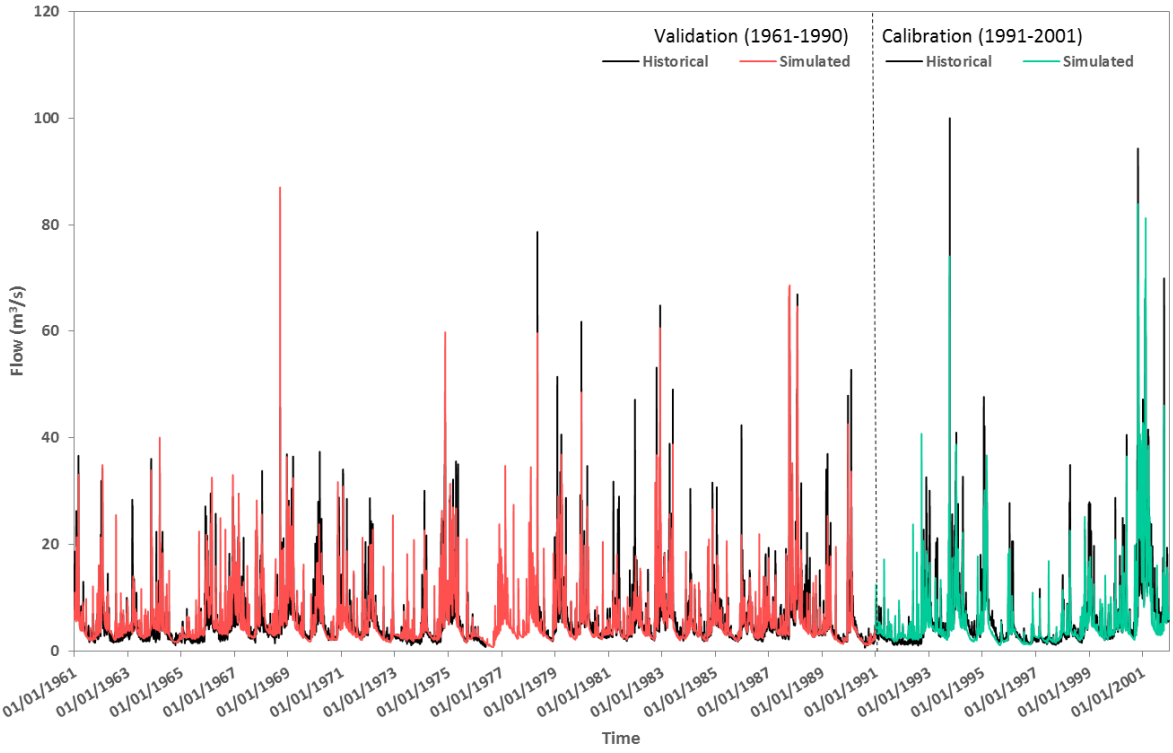

Figure 3.21: Calibration and validation for Lee sub-catchment.

which shows that it was warmer in 1990-2001 compared to validation period. Mean monthly flow has similar trend as rainfall and as it is expected during the winter, with more rainfall and less PET, the flow in calibration period is less than validation period. During warm months (from June to September) the measured flow for both time periods are similar. The annual mean total rainfall, PET and runoff for validation and calibration period are listed in Table 3.6.

	Rainfall (mm)	PET (mm)	Runoff (mm)
1961-1990 (excluding 1976-1978)	630.85	597.53	156.90
1991-2001	668.35	650.04	172.86

Table 3.6: Annual mean total rainfall, PET and run-off in Lee sub-catchment

Figure 3.22 compares the historical and simulated mean flow in each month, for calibration and validation period. The comparison between observed and simulated flows shows that, for calibration period, in March, September and October the flows simulated by SHETRAN are perfectly match the historical values. While from April to August the simulated discharge is slightly underestimated. In validation period, the underestimation in simulated flow is limited in 3 months of April, May and June. While the simulated flow is overestimated for the rest of the months. Overall, the mean simulated flow for validation period is overestimated (+4.8%) and for calibration period is underestimated (-4.0%). More details about the monthly comparison between observed and simulated flows are listed in Table A.6.

As previously mentioned, the reason for the underestimation of simulated values in spring is due to the nature of the chalk (covers 71.5% of the Lee sub-catchment) and inability of SHETRAN to adequately model the dual porosity mediummatrix in Chalk aquifers.

For the validation period the percentage of error between observed and simulated, ranges between -17.6% to +19.5%. The maximum overestimation, with +19.5%, happens in December, while May with -17.6% has the highest underestimation. For the calibration period, percentage of difference between simulated and observed flow ranges between -18.4% and 19.7%. In this period, June with -18.4% and November with +19.7% have the greatest under and overestimation respectively.

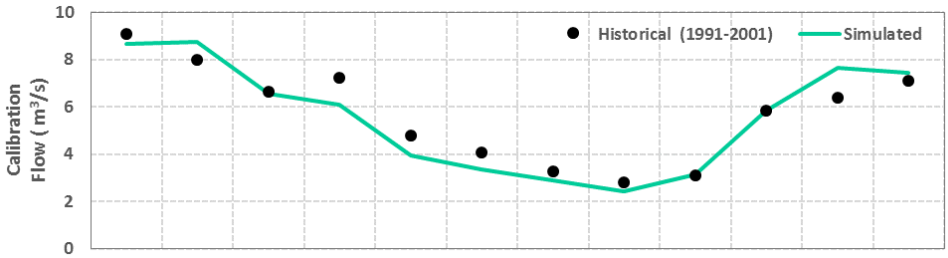

(a)

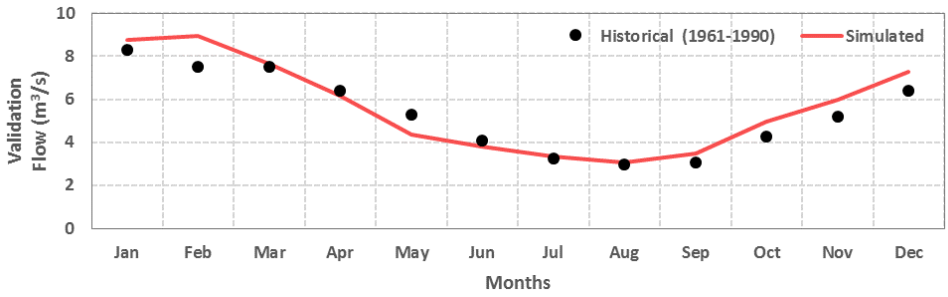

(b)

Figure 3.22: Mean flow comparison between historical and simulated values for calibration and validation period, Lee sub-catchment.

3.5.4 Integrating SHETRAN with spatial UKCP09 WG

In this section, the outputs of SWG are integrated using hydrological model of SHETRAN. The climate outputs from SWG are 100 runs with 100-year-long time series for control scenario (1961-1990). Hence, simulated flows given are generated for 100 runs of SHETRAN for Kingston and compared with the historical flows for 1961-1990.

Figure 3.23 compares the observed discharge (Q_{Obs}), simulated discharge with observed meteorological inputs (Q_S^{Obs}) and the average of simulated discharge with SWG meteorological inputs (Q_S^{SWG}) for Kingston. Although, there is a similar trends in simulated flows, underestimation in spring flows simulated by SHETRAN with SWG is slightly more than Q_S^{Obs}. This underestimation eventually leads to a lower annual average in simulated discharge in the Kingston sub-catchment.

The comparison between Q_S^{Obs} and Q_{Obs}, shows the uncertainty caused either by hydrological model of SHETRAN or uncertainty in observed data measurements. While, comparing Q_S^{Obs} and Q_S^{SWG}, shows the errors caused by SWG simulations. Finally, comparison between Q_S^{SWG} and Q_{Obs}, shows the accumulated uncertainty from SWG modelling and SHETRAN together and observed data. For the Kingston sub-catchment, the annual mean flow given from SHETRAN with observed input data (Q_S^{SWG}), is 5.6% less than historical flow (Q_{Obs}). This comparison quantifies the uncertainty caused by either SHETRAN or error in historical data measurement (including measuring rainfall, flow and PET calculation- individually or combination). Mean annual flow given by SHETRAN with simulated input (Q_S^{SWG}) is 5.9% lower than mean annual flow given from SHETRAN with observed input (Q_S^{Obs}) which shows the overall tolerance of hydrological modelling. While the simulated flow driven with synthetic meteorological data (Q_S^{SWG}) is 10.7% lower than historical value (Q_{Obs}) which in fact shows the combined uncertainty caused by SWG and SHETRAN hydrological model together. This shows that the overall tolerance of the integrated modelling is nearly 11.0% of observed annual flow which is nearly twice the uncertainty from UKCP09 SWG or SHETRAN hydrological modelling.

As it can be seen in Figure 3.23, in winter, summer and autumn Q_S^{SWG} better simulated the observed data. Even in February, there is less difference between Q_S^{SWG} and Q_S^{Obs}. More details about the comparison between simulated and observed flows are listed in Table A.7.

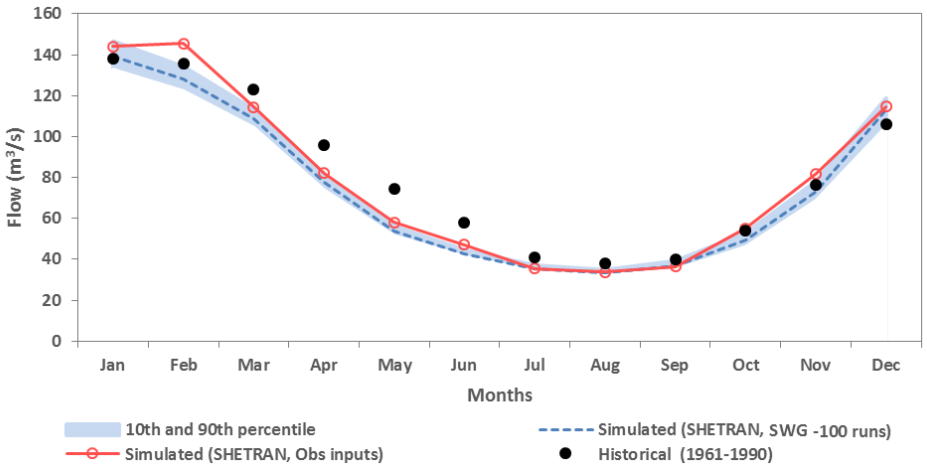

Figure 3.23: Mean flow comparison between observed historical and simulated flow with observed and modelled (SWG) input data, in Kingston sub-catchment.

Figure 3.24 illustrates the seasonal histograms of the 100 runs of SHETRAN for 1961-1990 against historical discharge in Kingston. As it can be seen, in winter (DJF), summer (JJA) and autumn (SON), the histogram of measured flow fall within the range of histograms of simulated flows. But for spring (MAM), the graph shows that the simulated flows are skewed to the lower values, which means that most of the simulated discharges are clustered towards the lower flows than observed values. This

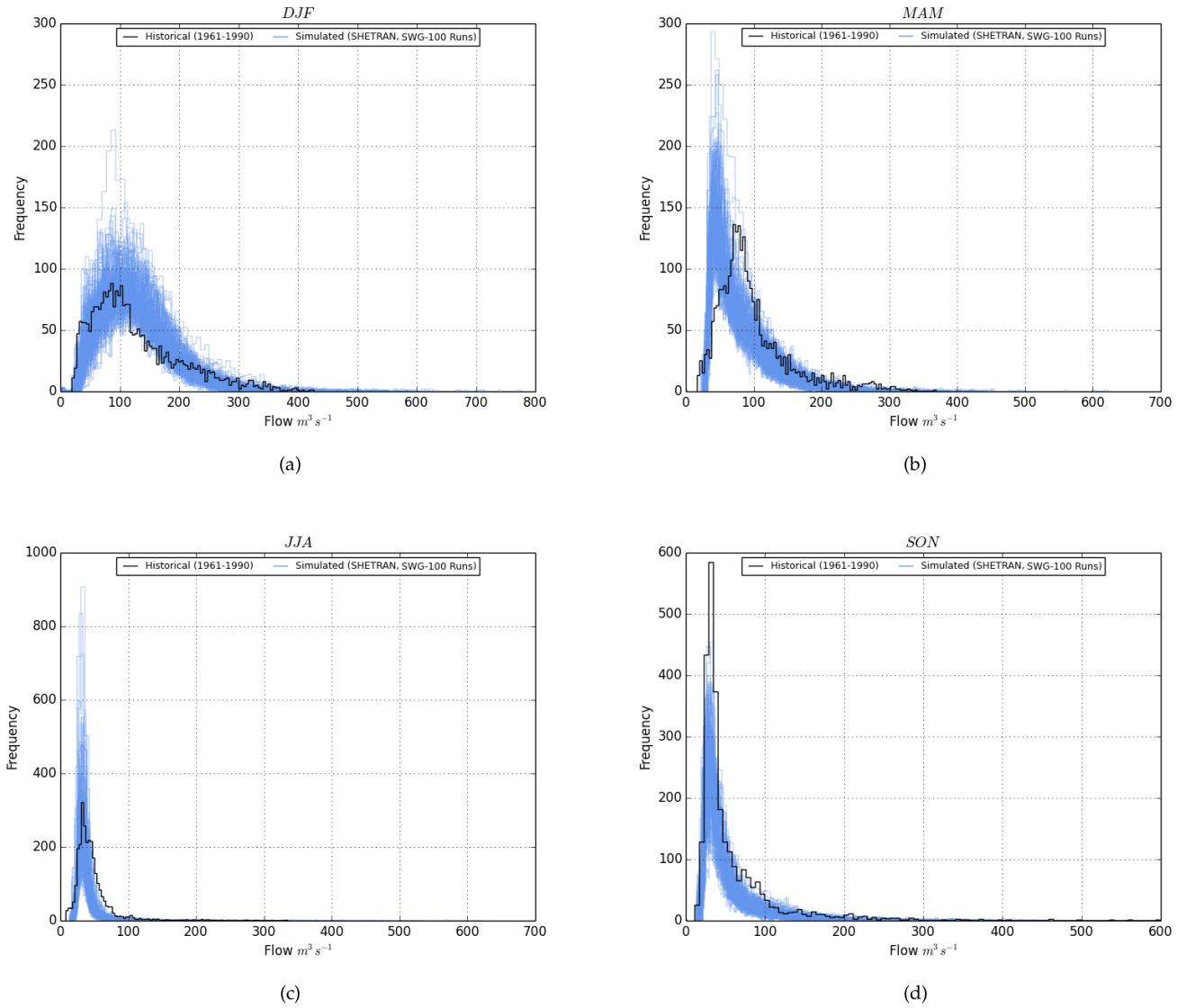

Figure 3.24: Histograms of historical and simulated flow, Kingston sub-catchment.

is the reason that the average of simulated flows are less than the measured.

The comparison between monthly average observed discharge (Q_{Obs}) against simulated discharge with observed inputs (Q_S^{Obs}) and the average of simulated discharge with SWG inputs (Q_S^{SWG}) for Lee is illustrated in Figure 3.25. As it can be seen, in contrast with the Q_S^{Obs}, the simulated flow by SHETRAN with SWG input (Q_S^{SWG}) either matches or underestimates the observed values.

In July, August, September and December, the simulated flows of Q_S^{SWG}, better match the observed values. In winter and autumn Q_S^{SWG} better simulates the observed data. However, underestimation in spring flows simulated by SHETRAN with SWG is slightly more than Q_S^{SWG}. This underestimation eventually leads to a lower annual average (-10.0%) in simulated discharge in Lee sub-catchment. More details about the comparison between simulated and observed flows are listed in Table A.8.

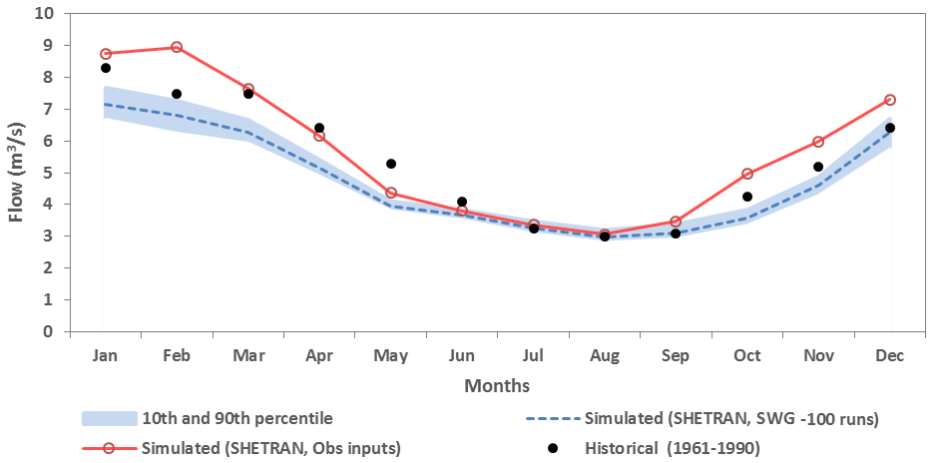

Figure 3.25: Comparison between mean flow of simulated and historical flow in Lee sub-catchment.

Figure 3.26 shows the seasonal histograms of 100 runs of simulated flow by SHETRAN against historical discharge in Lee, for 1961-1990. As it can be seen, similar to Kingston, the histogram of measured flow falls within the range of histograms of simulated flows in winter (DJF), summer (JJA) and autumn (SON). However, for spring (MAM) the graph shows that the simulated flows are skewed to the lower values, which means that most of the simulated discharges are clustered towards the lower flows than observed values. This results in the average of simulated flows being less than the measured.

3.5.5 Sensitivity of SHETRAN to meteorological input data

To assess the sensitivity of SHETRAN to meteorological input data, SHETRAN is run for control scenario (1961-1990) with rainfall and PET inputs from following approaches:

1. SWG-mean: in this approach, first the daily time series of rainfall and PET given from SWG (discussed in section 3.4.1) are averaged over each sub-catchment and

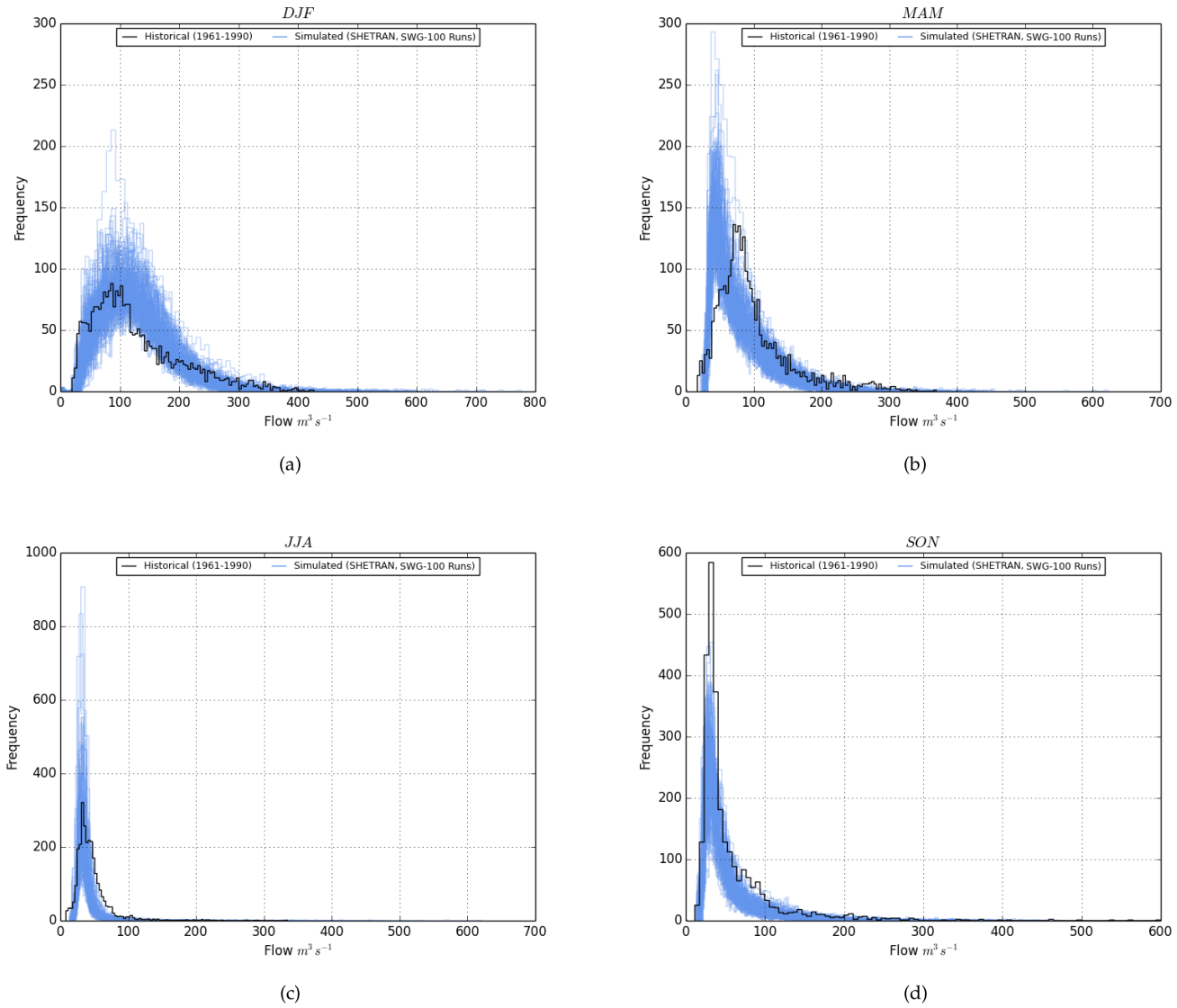

Figure 3.26: Histogram of simulated and historical flow, Lee sub-catchment.

then used uniformly as a daily time series in all the grids over that sub-catchment.

2. SSWG: in this approach, the rainfall and PET time series given from SSWG (discussed in section 3.4.1) are used as input to SHETRAN. (It is assumed that whole catchment has an equal amount of evapotranspiration and rainfall as the centroid grid in the catchment.)

In reality the distribution of rainfall varies spatially in the catchment depending on underlying mechanisms but in both of these approaches the assumption is that the daily rainfall distributed equally over the catchment to investigate the impacts of different type of precipitation distributions on catchment response. After running SHETRAN with these two approaches, the simulated discharges are compared with simulated flow by SHETRAN with spatial temporal distributed (SWG) PET and rainfall discussed in section 3.4.1 and historical discharge for 1961-1990.

Figure 3.27 shows boxplots of historical and simulated flows for Kingston sub-catchment. As it can be seen, SHETRAN with SWG input data gives the better simulation. Although, SHETRAN with SWG-mean input data gives a better simulations for February and November, the overall simulation is not as good as SWG. The simulated flow by SHETRAN with input data from SSWG is very biased and the values of discharge are considerably different from historical values. For SWG, the range of difference between the observed and simulated monthly flows ranges from -27.7% to -6.6%. For SWG-mean, this difference ranges between -33.1 to 14.3% while for SSWG ranges between -43.9% and -8.8%.

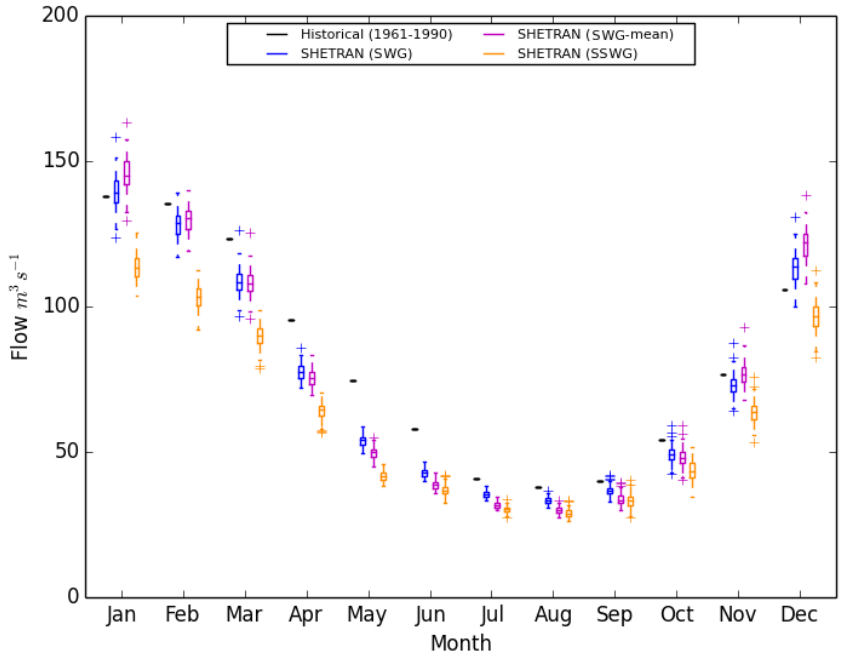

Figure 3.27: Boxplots of historical flow with simulated flow using SWG, SWG-mean and SSWG, Kingston sub-catchment.

Figure 3.28 compares the daily average of the historical and simulated flows for each month. The detailed comparison are listed in Table A.9. Table 3.7 also shows the daily average of flows in different seasons. As it can be seen, SHETRAN with SWG, gives the best simulation for winter, autumn and summer. However, SHETRAN with SWG-mean inputs, slightly better simulates the spring flows, while overestimates the winter flows. Finally, the SHETRAN with inputs from SSWG underestimates the flow almost in all of the seasons, for instance the simulated flow for summer is 37.3 % underestimated compared to the measured historical values. Based on the results, the SSWG causes the greatest underestimation in average of annual flow 23.8%, while with the SWG-mean and SWG the underestimation is 9.3% and 9.0% respectively. The comparison show that in overall SSWG better simulates the flow in Lee sub catchment. Moreover, in overall, the simulated flow with the SWG weather variables better represents the hydrological characteristics of the Kingston sub-catchment.

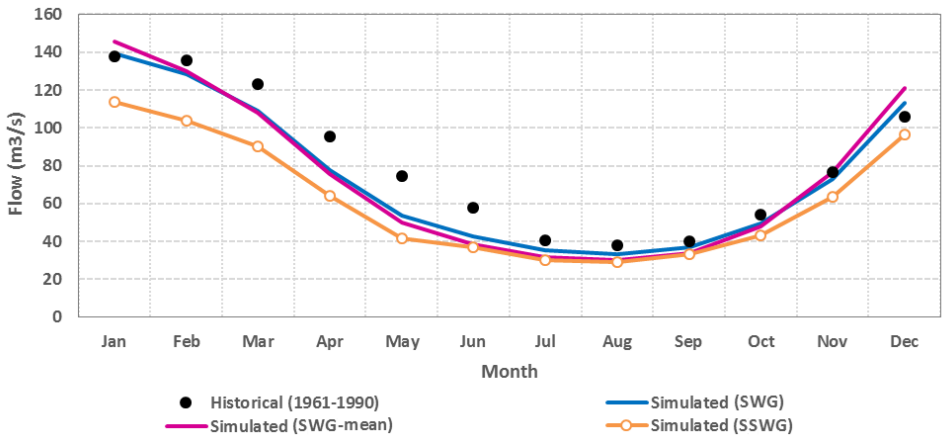

Figure 3.28: Mean flow comparison between historical and simulated with SWG, SWG-mean and SSWG, Kingston sub-catchment.

The boxplots of historical and simulated flows for Lee sub-catchment are illustrated in Figure 3.29. As it can be seen, in December, January, February and March, SHETRAN with SWG-mean input data better simulates the flow. From April to December, the average of simulated flow with SWG and SWG-mean are very similar. SHETRAN with SSWG input mostly overestimates the flow, except for April, July, October and November which gives the best fit between simulated and historical values. The daily average of the historical and simulated flows for each month, are illustrated in Figure 3.30 and listed in Table A.10.

The seasonal values of the daily mean flows in the Lee sub-catchment are listed in Table 3.8. The seasonal comparison shows that SHETRAN integrated with SWG better simulates the autumn flows, while SHETRAN with the SWG-mean input better simulates the flows in spring and winter. The summer flows simulated by SHETRAN with SSWG better match the historical values. Annually, the difference between average of historical and the simulated flows for SWG and SWG-mean is -11.5% and

Seasons	Flow (m^3/s)				Rainfall (mm)			PET (mm)		
	Historical (1961-1990)	SWG	SWG-mean	SSWG	Historical (1961-1990)	SWG	SSWG	Historical (1961-1990)	SWG	SSWG
Spring	132.26	125.49	127.87	102.45	1.93	1.94	1.72	0.76	0.83	0.82
Summer	75.99	58.14	54.65	47.66	1.80	1.77	1.70	2.60	2.51	2.46
Autumn	39.60	35.23	31.89	30.90	1.85	1.77	1.66	2.66	2.61	2.59
Winter	78.94	78.46	82.01	67.85	2.23	2.27	2.01	0.62	0.71	0.70
Annual	81.70	74.33	74.10	62.21	1.95	1.94	1.77	1.66	1.67	1.64

Table 3.7: Seasonal mean flow, rainfall and PET for historical and simulated with SWG, SWG-mean and SSWG, Kingston sub-catchment.

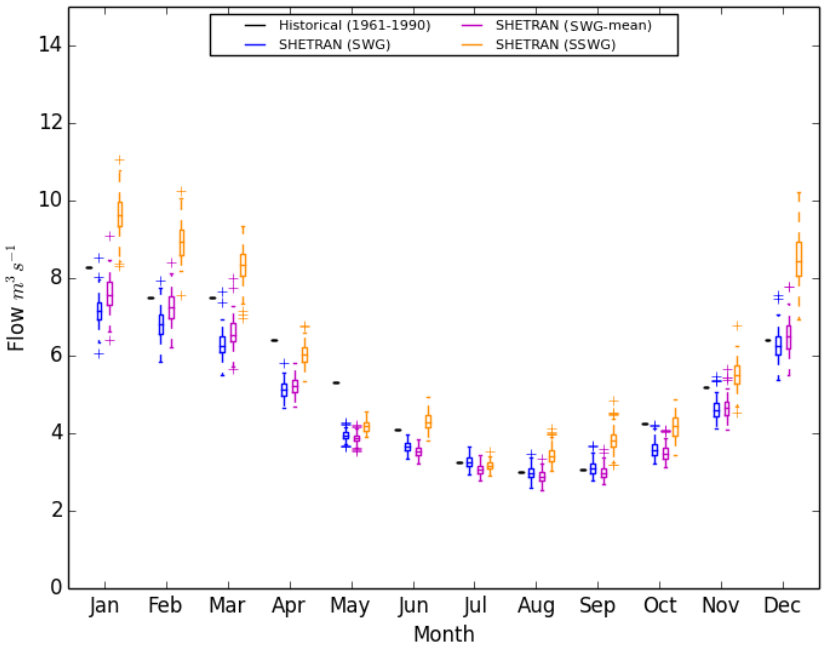

Figure 3.29: Boxplots of historical flow with simulated flow using SWG, SWG-mean and SSWG, Lee sub-catchment.

-10.2% respectively. While SSWG overestimate the annual average by 9.2%. The results show that in Lee sub-catchment, the SHETRAN with SSWG input weather variables, slightly better simulates the hydrological characteristics of the basin. It is important for this study to use SWG, given the scenarios included the spatial changes in land cover in the SHETRAN model.

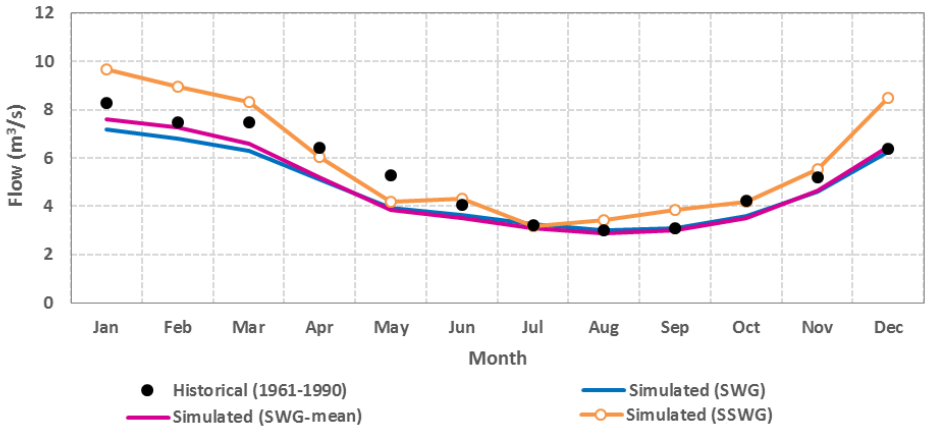

Figure 3.30: Mean flow comparison between historical and simulated with SWG, SWG-mean and SSWG, Lee sub-catchment.

Seasons	Flow (m^3/s)				Rainfall (mm)			PET (mm)		
	Historical (1961-1990)	SWG	SWG-mean	SSWG	Historical (1961-1990)	SWG	SSWG	Historical (1961-1990)	SWG	SSWG
spring	7.76	6.75	7.15	8.98	1.59	1.60	1.72	0.73	0.84	0.82
summer	5.26	4.24	4.20	4.84	1.65	1.63	1.70	2.56	2.54	2.46
Autumn	3.10	3.12	2.99	3.48	1.73	1.65	1.66	2.65	2.67	2.59
winter	5.28	4.82	4.88	6.06	1.90	1.93	2.01	0.59	0.72	0.70
Annual	5.35	4.74	4.81	5.84	1.72	1.70	1.77	1.63	1.69	1.64

Table 3.8: Seasonal mean flow, rainfall and PET for historical and simulate with SWG, SWG-mean and SSWG, Lee sub-catchment.

3.6 Water resources management model

In order to predict the availability of water in the catchment and also estimate the uncertainty distributions for water resources management options, the time series of river flows (simulated by hydrological model) are used to drive a water resources management model. In this project, the water resources model of London Area Rapid Water Resources Model (LARaWaRM) are used to simulate water resources system for the Thames catchment.

3.6.1 The London Area Rapid Water Resources Model (LARaWaRM)

To enable rapid analysis of climate and socio-economic scenarios a rule-based water resources management model of The London Area Rapid Water Resources Model (LARaWaRM) was developed in the MATLAB programming language. This water resources management model simulates water flow, water consumption, water storages, single and joint reservoir releases in surface and ground water in the Thames basin water system.

The model simulates the basin as a network consist of nodes and links. Lakes, reservoirs, aquifers, inflow gauge sites are represented by nodes in this model. The surface and groundwater conveyance between the nodes are represented by links which can be unidirectional or bidirectional. The requested water, in each demand node, are provided by either reservoir (surface storage) or inflow points.

The release from reservoirs can be either demand driven or can be based on reservoir rules and storage control curves which regulate release of reservoirs based on its storage volume. This storage volume can be based on an individual or a group of reservoirs. Water release from reservoirs and aquifers is calculated as a function of current capacity, available river flow and time of year:

$$\Delta ReservoirVolume = \Sigma Inflows - \Sigma Demands \tag{3.4}$$

The model simulates a 100-year time series of inflow in approximately 1 second on a PC with an Intel Core2. By using this model, probabilistic climate change scenarios and different population demand assumptions can be analysed and also the benefits of different decision adaptation options such as no adaptation, new reservoir, desalination plant, demand management and reducing leakage are quantified. Schematic of the LARaWaRM water resources model for Thames catchment is displayed in Figure 3.31.

In the Thames catchment, approximately 80% of water is supplied from surface water and the remaining 20% is abstracted from groundwater (Thames Water 2013). Surface water enters the system at Days Weir and the Lower Thames for the River Thames and at Feildes Weir on the River Lee. During droughts, when the surface water is limited, groundwater aquifers in this area have an important role in supplying water. The groundwater in this area yields from boreholes distributed over the basin.

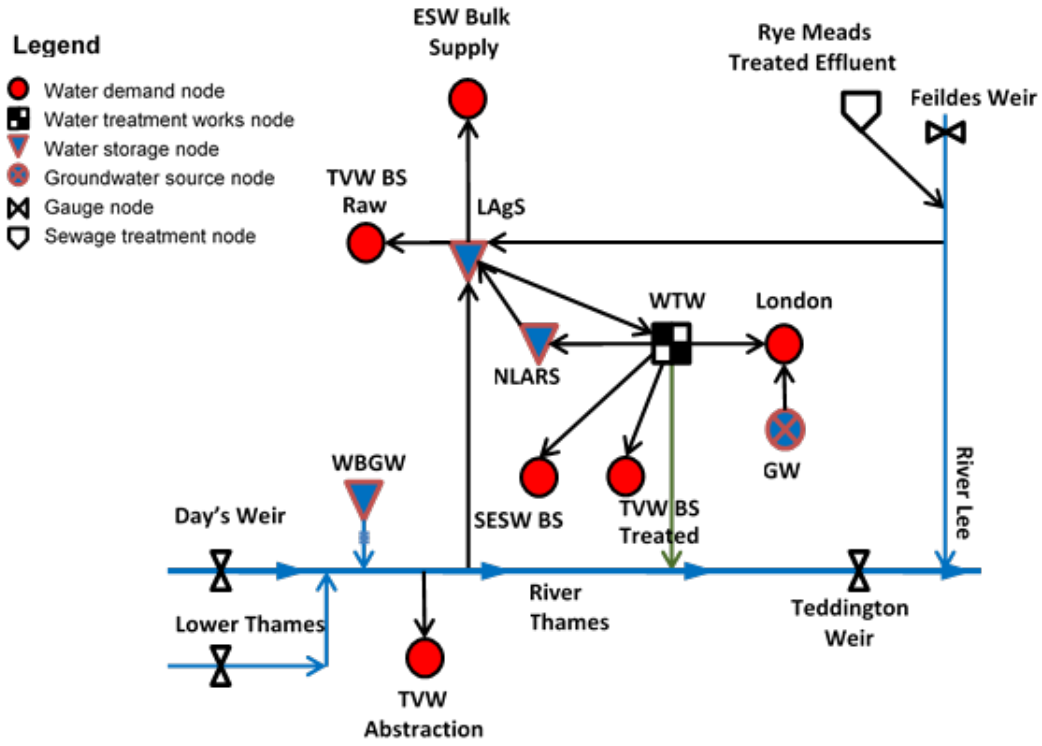

Figure 3.31: Schematic of water resources model (LARaWaRM).

This groundwater is modelled as an inflow of 467.4 Ml/day which contributes to meet the water demand.

Demand nodes are water consumption points that represent urban demand regions or bulk supply transfer that calls for allocation of water to meet their demand. The demand nodes for Thames catchment are listed in Table 3.9. Input data used in LARaWaRM are taken from Thames water reports (Thames Water 2013). The allocation for demand is also reduced to account for demand saving measures put in place by utility companies when reservoir levels pass certain capacity thresholds.

Demand Nodes	Ml/day
London	2000.00
Three Valleys Water Abstraction	414.00
Essex and Suffolk Water (ESW Bulk Supply)	91.00
Veolia Three Valleys Bulk Supply (TVW raw)	2.00
Veolia Three Valleys Bulk Supply (TVW treated)	12.00
Sutton and East Surrey Water (SESW BS)	5.00

Table 3.9: Demand nodes in the Thames catchment.

The London Aggregate storage (LAgS) used in LARaWaRM, represents the total storage capacity of the Thames and Lee reservoirs which provides just over 208 Mm^3 storage capacity. In LARaWaRM, the water is pumped first from River Lee and then from lower River Thames and diverted to LAgS. This diversion is subject to meet the minimum environmental flows and maximum daily abstraction in the river. Reservoir

trigger thresholds used in LTCD for demand saving measures are dynamic and vary monthly (see Figure 3.3). Table 3.10 lists the thresholds used by LARaWaRM to invoke the different levels of restriction (Levels of services and water use restrictions have been listed in Table 3.1).

Level of services	Month											
	Jan	Feb	Mar	Apr	May	Jun	Jul	Aug	Sep	Oct	Nov	Dec
level 1	69.5	82	89.5	92.1	92.1	90.9	86	74.9	64.8	61	59.8	61
level 2	42.2	47.8	55.3	65.2	74	76.5	74.7	67.7	55.7	46.2	41.1	40
level 3	33.6	37.3	43.4	52.1	60.9	65.9	67.2	62.4	51.2	41.2	34.9	32
level 4	17.4	19.8	24.8	29.8	34.8	38.6	39.8	39.8	37.4	31.2	25	20

Table 3.10: Percentage of reservoir total storage capacity that invokes the different levels of restrictions (Thames Water 2013).

In the Thames basin, there are backup storages used when flow crosses certain thresholds, during dry periods. These backup storages include North London Artificial Recharge Scheme (NLARS) and the West Berkshire Ground Water Scheme (WBGW). The NLARS is an aquifer storage which has a capacity of 64.4 Mm^3 and refilled when LAgS is full, and by excess treated water that is pumped to the ground in north London (at the rate of 35 to 40 Ml/d). The WBGW with a capacity of 40.7 Mm^3 is another aquifer storage which is only available during extreme droughts. The WBGW is refilled by small daily inflows but cannot be counted as an unlimited sources of water. Both of these aquifer storages are modelled as storage nodes in LARaWaRM. Flow from NLARS goes directly to main LAgS reservoir whilst WBGW is added onto available flow. These backup storages are activated when reservoir storage drops below Level 4 of the control diagram threshold and target flow reaches below 400 Ml/d.

There is a Water Treatment Work (WTW) in the Thames basin that supplies treated water for London and other utility companies (TVW BS and SESW BS). A part of the inflow into the WTWs leaks out and because many WTWs are located near the river, most of the leakage (equivalent to 12% of demand) returns to the Thames and is modelled as a contribution to the minimum environmental flow.

Total demand is a function of population, residential and non-residential consumption and leakage. In LARaWaRM, based on 2010 data, it has been assumed that per person residential demand is 168 l/person/day, non-residential demand is 370 Ml/day and leakage is 670 Ml/d (425 Ml/d for distribution loss and 165 Ml/d for other losses).

By running LARaWaRM, at each time step (daily), water moves in the system according to the input data and connectivity between components. In fact, there are five calculation steps in the model:

1. Catchment add water to river flows. In this case the model reads in river flows directly from observed data (naturalised flow 1889-2005) (for the validation

process) or SHETRAN hydrological model simulations for scenario testing.

2. Environmental flow regulation is tested according to LTCD which may dictate augmenting river flows, or limiting abstractions.

3. Demand for water is satisfied by drawing water from any or all available supplies, such as river abstractions, groundwater abstractions and reservoirs, etc.

4. Reservoirs refill as necessary from their available supplies according to abstraction limits and refill rate rules.

5. At the end of the day, any reservoir which has had excess water pushed into it will spill into its attached river spillway, or another reservoir.

3.6.2 Validation of water resources management model

For validation, LARaWaRM was run with observed input data, naturalised inflows from Kingston and Lee sub-catchments for period between 1989 and 2005. In order to check how good the water resources model simulates the water system, the results given from LARaWaRM are compared with the daily total measured reservoir levels in the Thames catchment.

In previous studies in Thames catchment (e.g. Matrosov & Harou 2010), the validation was conducted with comparing the modelled results with EA Thames water resources system model of AQUATOR. But in this study, the results of LARaWaRM water resources model are compared with actual reservoir levels reported by Thames Water for the Thames catchment. For this aim, the daily Reservoir levels in the Thames catchment are obtained from Thames Water website [3]. The Thames Water reports daily reservoir levels since 1889 as percentage of usable or deployable capacity in the Lower Lee Group and Lower Thames Group reservoirs. For validation the total reservoir level was required. For this aim, the total reservoir level in London is calculated manually by aggregating the measured levels from Thames group and Lee group reservoirs, with the assumption that the contribution of Thames Group reservoirs and Lee group reservoir are 80% and 20% respectively. Figure 3.32 compares the total measured and simulated reservoir level in Thames catchment, and also shows the observed flow in Kingston and Lee for validation period (1889-2005).

As it can be seen from Figure 3.32, LARaWaRM correctly simulates reservoir level for Thames catchment, especially during the droughts. Based on this figure, the major droughts of 1990-92, 1995-97 and 2003-05 are well captured by the model. Based on the given results, the difference between measured and simulated reservoir level are smaller in drought events. The Water resources model simulates the reservoir full when the measured storage is higher than 90%. This difference can be due to uncertainty in measured data as well as manually calculating the total reservoir level from the measured levels taken from the Thames Water. Moreover, number

[3] https://data.london.gov.uk/dataset/london-reservoir-levels/

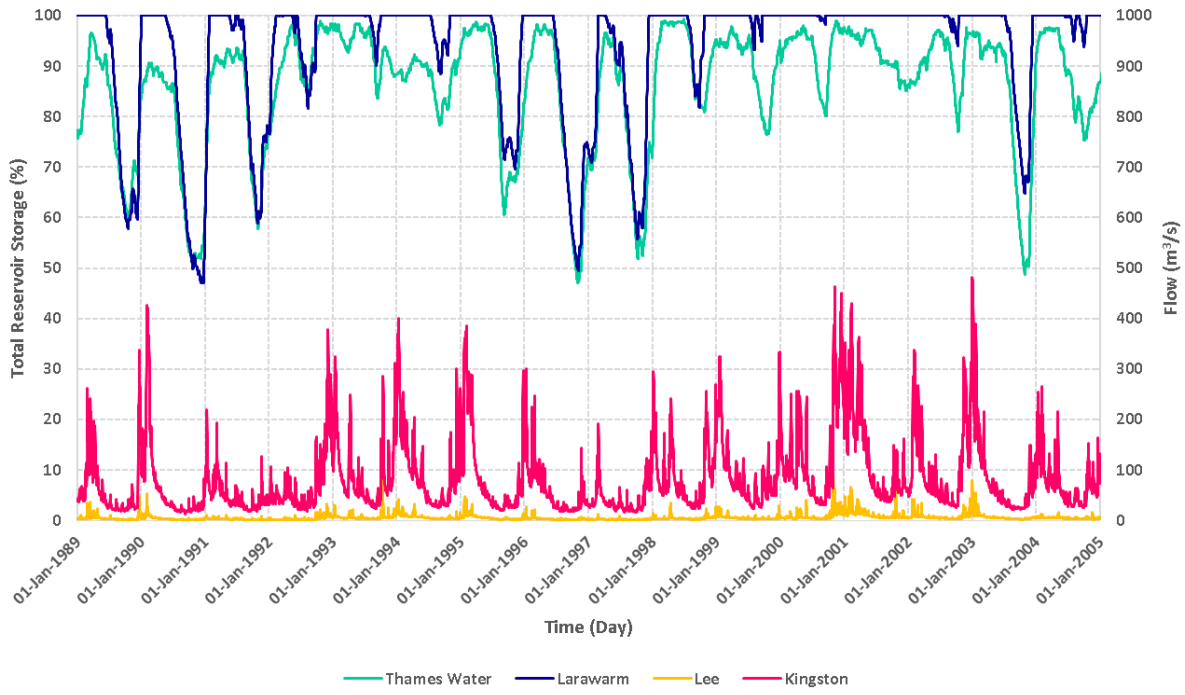

Figure 3.32: Details of the model validation, total reservoir level and observed flow data from 1989-2005.

of population and the water regulation used at the time in Thames catchment can contribute to this difference.

Figure 3.33 illustrates the total simulated and measured reservoir level and simulated NLARS storage for the period of 1989-2005. As it has been mentioned before, NLARS is a backup storage used in case of drought and then recharged with excess treated water. The plot shows that, in case of drought the NLARS level drops and by the end of droughts it starts to recover. For period between 1997 and 1998, the NLARS level drops to the minimum level and remained empty for a while. This is consistent with the NLARS recharge scheme operation reported by Environment Agency (EA 2016) which shows that in 1997 the abstraction from NLARS was very high, and the recharge was very small. After 1998, there was not any abstraction from NLARS and the backup storage recharged to its maximum level. As it can be seen, NLARS storage modelled by LARaWaRM (see Figure 3.33), in 1997 is almost empty for nearly 220 days, and then by increasing the reservoir level, it starts to recover and reaches to the maximum level. These show that the modelled storage perfectly matches the historical evidence.

To measure the correlation between measured and simulated reservoir levels, two metrics of Spearman's Rank Correlation and Pearson's Correlation Coefficient are used (Naghettini 2016). The Spearman correlation is a non parametric measure which evaluate the monotonic relationship (linear or non linear) between the ranking of two variables (continues or ordinal). In a monotonic relationship the variables change together, whether with a constant rate or not. The Spearman Rank Correlation is

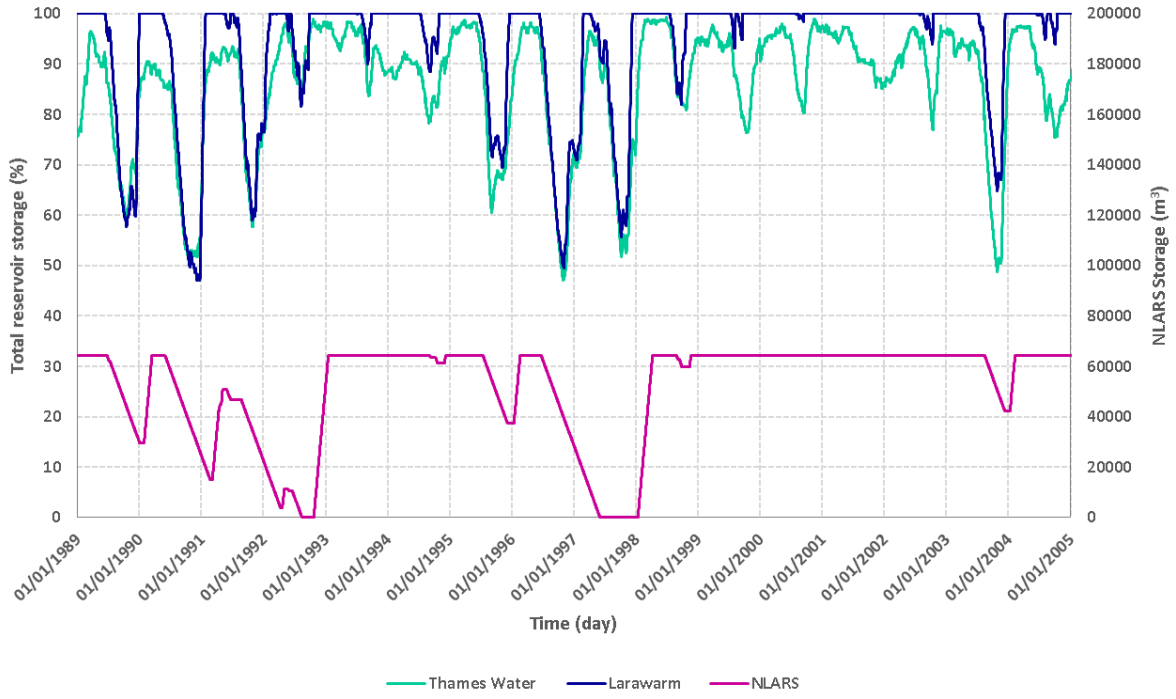

Figure 3.33: Details of the model validation, total observed and simulated reservoir and NLARS level for 1989-2005.

calculated with the following equation (Spearman 1904):

$$\rho = 1 - \frac{6\sum d_i^2}{n(n^2-1)} \tag{3.5}$$

Where ρ is Spearman Rank Correlation, d_i is the difference between the ranks of corresponding values x_i and y_i and n is number of value in each dataset. The Spearman correlation lies between -1 and 1. The correlation of 1 indicates that there is a perfect correlation between simulated and measured values, while the correlation coefficient of zero shows that there is no relationship between the values.

Pearson Correlation coefficient is another non parametric measure that provides a measure for the linear relationship between two continuous variables. In a linear relationships, a change in one variable is correlated with a proportional change in other variable. In contrast with Spearman, the Pearson evaluates the correlations between the raw values, not the ranks. The Pearson correlation Coefficient is calculated as:

$$r = \frac{\sum_{i=1}^{n}(x_i - \bar{x})(y_i - \bar{y})}{\sqrt{\sum_{i=1}^{n}(x_i - \bar{x})^2}\sqrt{\sum_{i=1}^{n}(y_i - \bar{y})^2}} \tag{3.6}$$

Where r is the Pearson Correlation Coefficient, n is the number of values, x_i and y_i are datasets and $\bar{x}$ and $\bar{y}$ are the means. The Pearson correlation coefficient ranges between -1 and 1 where correlation coefficient of 1 indicates that there is a perfect linear relationship between the datasets values while zero implies that there is no linear correlation.

Coefficient of Determination (R^2) is another metric to measure the correlation between simulated and measured datasets. The R^2 ranges between 0 and 1, when values greater than 0.5 implies strong correlation between the values (Moriasi et al. 2007). Figure 3.34 shows the correlation between mean monthly reservoir levels, measured and simulated, for Thames catchment. The values given for Pearson Coefficient, Spearman Rank Coefficient and R^2 are 0.9, 0.97 and 0.82 respectively. All of these measures prove that there is a very strong correlation between measured and simulated reservoir level in the Thames catchment. Not to mention that the high value given from Pearson implies the linear relationships between the values.

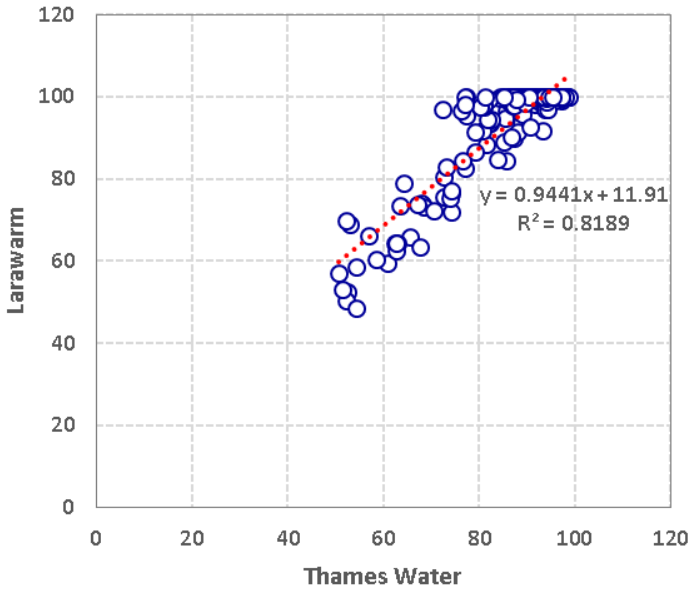

Figure 3.34: Mean monthly observed and modelled total reservoir storage for 1998-2005.

3.7 Summary

This chapter presented the novel integrated systems framework developed in this study to assess the implications of long-term uncertainties in water resources management. This chapter also outlined the characteristics of the Thames catchment, which was used as a real world case study. The proposed integrated system model was constructed for the Thames catchment. In this study the latest version of spatial UKCP09 WG has been used which unlike its previous version, is fully consistent with national gridded rainfall data set from the Met Office. In order to provide a wider range of information about possible range of climate and their impacts, 100 ensembles of 100-year long future climate scenarios were used. In addition, for the first time in Thames catchment impact studies, the physically based hydrological model of SHETRAN was used to simulate the hydrological characteristics of the basin. A rule-based water resources model of LARaWaRM was also used to simulate the potential future water resources risks and possible demand and supply adaptation options to manage the

potential risks in Thames basin.

The given results for validation showed that in overall SWG reasonably well reproduced the observed rainfall and PET statistics across the Thames catchment. The given results for validation of SWG showed that, for both sub-catchments, there was a slightly underestimation (9.0%) in monthly mean rainfall in July and 5.0% overestimation in October, which may be due to exist of rare extreme total daily rainfalls in the basin. The SWG also well simulated the PET for the Thames catchment. The PET is slightly better simulated for larger catchment as for Kingston there is only 0.5% difference between annual mean of observed and simulated values, while this difference for Lee is around 3.5%. Therefore, SWG provides a suitable platform for uncertainty analysis and also coupling with physically based hydrological model.

To simulate the hydrological characteristics of this catchment, the SWG was integrated to physically-based spatially-distributed hydrological model of SHETRAN. The given results for calibration and validation showed that SHETRAN integrated with SWG, well simulated the historical discharges, especially the low flows during historical droughts were well captured. The NSE for calibration and validation of Kingston sub-catchment were 0.90 and 0.78 respectively, and for Lee they were around 0.67 and 0.65 respectively. For Kingston sub-catchment, the annual mean flow given from SHETRAN with observed input data, was 5.6% less than historical flow. This comparison quantifies the uncertainty caused by either SHETRAN or error in historical data measurement (including measuring rainfall, flow and PET calculation-individually or combination). Mean annual flow given by SHETRAN with simulated input is 5.9% less than mean annual flow given from SHETRAN with observed input which shows the uncertainty from hydrological modelling. The simulated flow driven with synthetic meteorological data is 10.7% less than historical value which is in fact the combined uncertainty caused by SWG and SHETRAN hydrological model together. For the Lee, similar to Kingston, the combined uncertainty is around -10.0%, while the uncertainty from SWG increased further to -16.0%, and also there was 5.3% overestimation caused by modelling with SHETRAN. Hence, the results show that the uncertainty from combination of SWG and SHETRAN leads to nearly 10.0% underestimation in the annual mean flows in the Thames catchment.

In order to investigate the sensitivity of the SHETRAN hydrological model to the meteorological variables, three different distributions of rainfall and PET (spatial (SWG), mean spatial (SWG-mean) and Single-site (SSWG)) were tested over the Thames catchment. The comparison between historical and simulated flows showed that SHETRAN with SWG input data better represents the hydrological characteristics of the catchment. Although, SHETRAN with SWG-mean input data gives a better simulations for some of the months (e.g. February and November), the overall simulation is not as good as SWG one. The simulated flow by SHETRAN with input data from SSWG are very biased and the values of discharge are considerably different from historical values.

To simulate the water storage and frequency of water shortage in Thames catchment, a rule-based water resources management model of LARaWaRM are used. For validation, LARaWaRM was run with observed input data, naturalised observed inflows from Kingston and Lee sub-catchments for period between 1989 and 2005. In order to check how good the water resources model simulates the water system, the results given from LARaWaRM are compared with the daily total measured reservoir levels in the Thames catchment. Based on the results, the LARaWaRM correctly simulates reservoir level for Thames catchment, especially during the droughts as the major droughts of 1990-92, 1995-97 and 2003-05 are well captured by the model. The difference between the simulated and observed data can be due to the uncertainty in measured data as well as manually calculating the total reservoir level from the measured levels taken from the Thames Water. Moreover, the size of population and the water regulation used at the time in Thames catchment can also contribute to this difference.

Chapter 4

Climate Change Impact Assessment

4.1 Overview

This chapter discusses the impacts of climate change on water resources availability in the Thames catchment. The analysis mainly compares the changes in rainfall, PET and flow and water storage between the control (1961-1990) and future climate scenarios (2020s, 2050s and 2080s). For both the Lee and Kingston sub-catchments, the spatial UKCP09 WG (SWG) at 5 km resolution and under medium emission scenario, is used to drive 100 runs for the control period and 100 runs for future time periods. This is followed by projecting the possible change in reservoir storage and frequency of drought days in four time slices of the control, 2020s, 2050s and 2080s and proposing different adaptation options to tackle the projected deficiency of water supplies.

4.2 Climate change impact assessment for Thames catchment

This section discusses the impacts of climate change on rainfall, PET and flow. For this aim, for each of the Lee and Kingston sub-catchments, 100 runs of 100 years daily synthetic time series for control (1961-1990) and future scenarios (2020s, 2050s and 2080s) are considered.

4.2.1 Climate change impacts on the Kingston sub-catchment

4.2.1.1 Rainfall

Figure 4.1 shows boxplots[1] of projected daily rainfalls in the Kingston sub-catchment. The boxplots show the changes in distribution of daily mean rainfall between control and future climates. Uncertainty in rainfall projections are larger for further future climate scenarios. For example, the longer boxes for 2080s implies that variation in

[1]Each of the boxplots indicates the median, 25th, and 75th percentile values. Whiskers show the 1.5 times of inter quartiles (IQRs), the difference between 25th and 75th percentile values. The small crosses are outliers, which are any points of data that lies below (25th percentile - 1.5 IQRs) or above (75th percentile + 1.5 IQRs).

daily rainfall in this time period is greater than the other time slices. Compared to the control scenario, there is less rainfall in spring and summer (from April to September) whilst in autumn and winter more rainfall is expected to occur. Based on the given results, in all future climates, August and February are expected to be the driest and wettest month respectively.

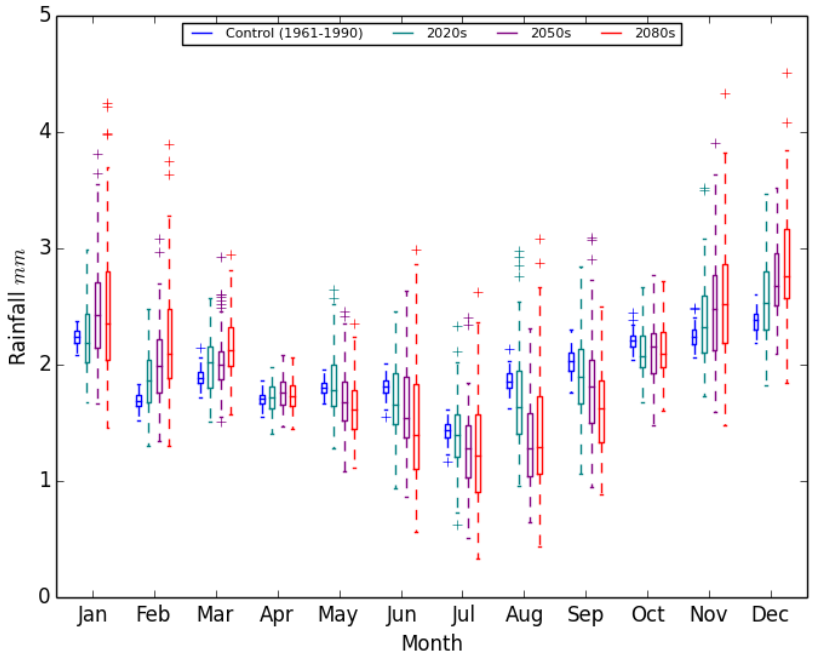

Figure 4.1: Boxplots of rainfall in Kingston sub-catchment.

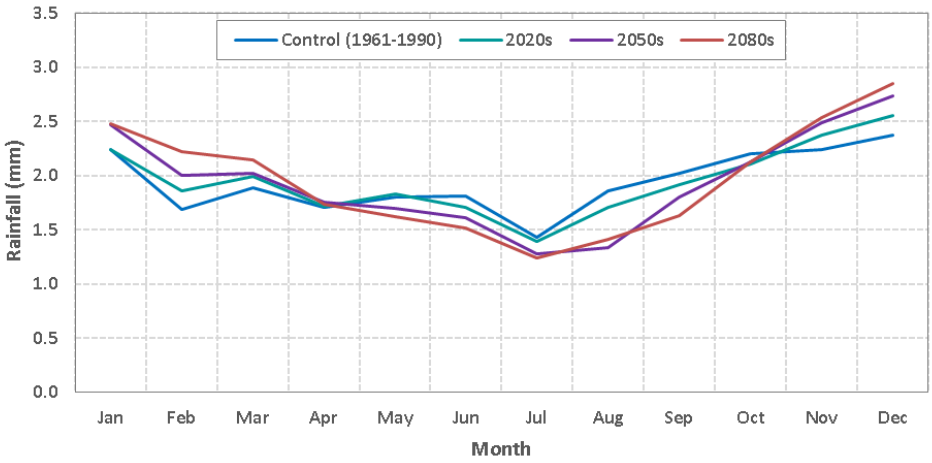

Figure 4.2: Mean rainfall in Kingston sub-catchment.

The percentage changes from mean daily rainfall in the control scenario are plotted in Figure 4.3. This figure highlights that all the time slices have a similar increasing trend from November to February and decreasing trend from May to October. The magnitude of change in 2080s is much greater than the other time slices, except for August 2050s in which the percentage of change in rainfall is the largest (-28.0%).

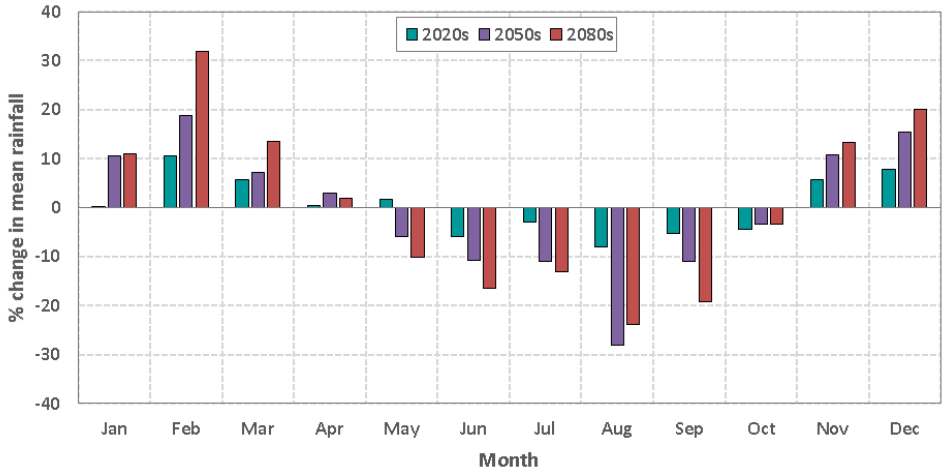

Figure 4.3: Change in mean rainfall relative to control period for the Kingston sub-catchment.

For 2080s, there is a decreasing trend in rainfall from May to October, ranging from -3.0% to -24.0%. From November mean rainfall increases until February, when the mean rainfall is 32.0% higher than the control scenario. In fact, May and November represent the turning points for rainfall trend in this catchment. Table B.2 lists the detailed change in the mean, 90th and 10th percentile of rainfall for future climate, compared to control scenario. As it is seen in this table, in February, there is a 64.0% increase in 90th percentile rainfall whiles 60.0% reduction in 10th percentile in August.

4.2.1.2 PET

Daily time series of potential evapotranspiration (PET) are generated by the spatial UKCP09 WG (SWG), with 5 km gridded climate variables using the FAO Penman-Monteith method. Figure 4.4 compares the boxplots of PET for control and future scenarios in the Kingston sub-catchment.

For all future climate scenarios, the PET is always higher than control scenario. The distribution of uncertainty in PET prediction is higher for 2080s. The range of uncertainty is expected to be higher during the summer (June, July and August) and lower during the winter. The results show that the average of projected PET are closer to the control scenario in winter.

Figure 4.6 reflects the percentage of change in PET for future scenarios compared to mean of 100 runs of control climate in Kingston catchment. The maximum difference from control scenario occurs in August 2080s, where there is 44.6% increase in PET compared to control scenario. Table B.4 lists the percentage of change in quantity of predicted PET from mean of 100 runs of control scenario. Based on the given results, by 2080s, between +24.5% and +73.8% in 90th percentile and -3.5% to 15.7% change in 10th percentile of PET are expected.

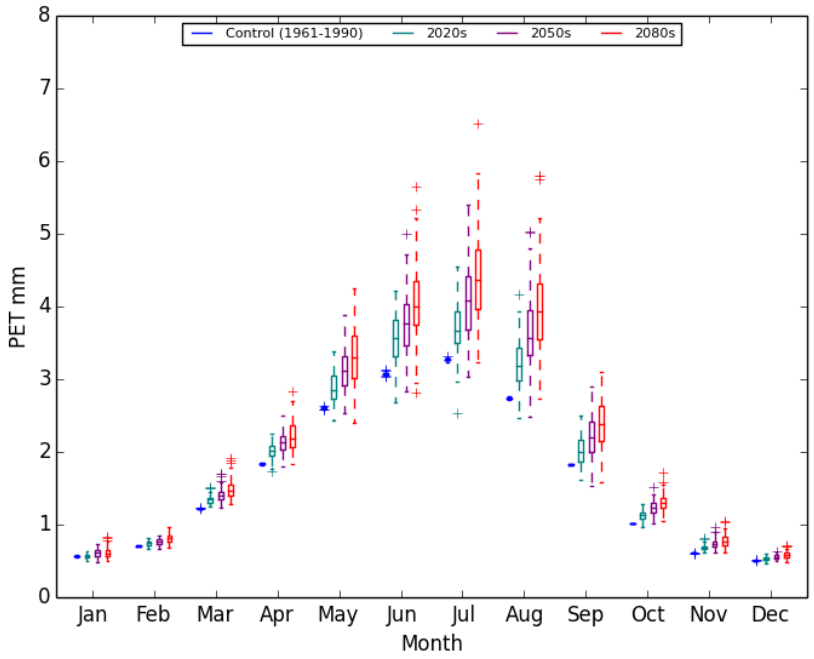

Figure 4.4: Boxplots of PET in Kingston sub-catchment.

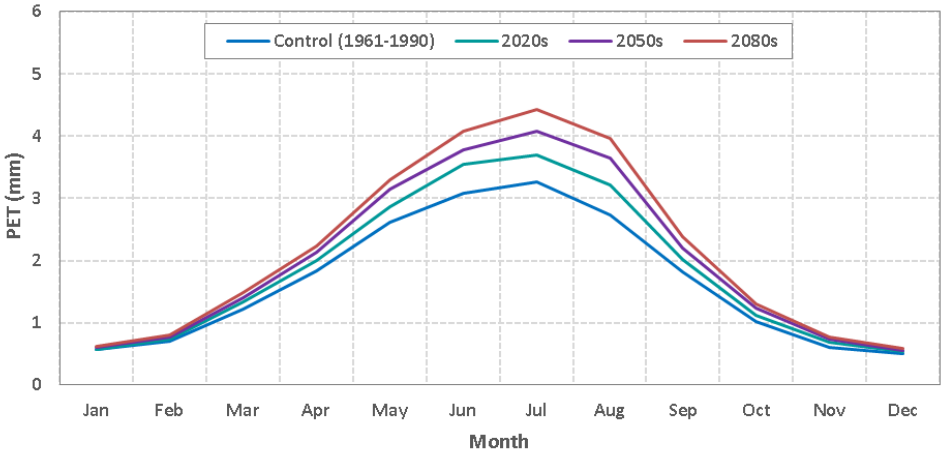

Figure 4.5: Mean PET from 100 runs of 100 years of control and future scenarios in Kingston sub-catchment.

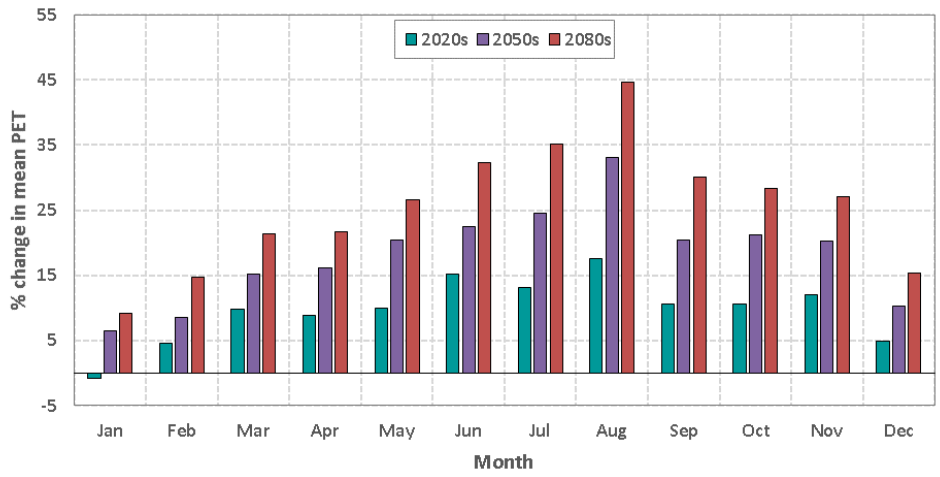

Figure 4.6: % change in man PET relative to control period in Kingston sub-catchment.

4.2.1.3 River flows

Boxplots of mean discharge in the Kingston sub-catchment are shown in Figure 4.7. This figure highlights that in all the months, the mean projected flow for future scenarios are less than control scenario. Figure 4.8 compares the daily average of flow in the control and future scenarios in all months. The control scenario has a decreasing trend from January to August, and increasing trend from September to December. Flows in January and August is maximum and minimum respectively.

In all the future scenarios, flows have a similar increasing trend from November to February and decreasing trend from March to August. Therefore, the maximum flow in future scenarios occurs in February while in control scenario this occurs in January. But similar to control scenario, the minimum flow is expected to be in August. This trend in flow projections is consistent with the previous section. As described before, the projected decrease in rainfall and increase in PET lead to lower flows in spring and summer.

The percentage change from mean of 100 runs for future and control scenarios are plotted in Figure 4.9. It can be seen that projected flows for 2080s are smaller than the other time slices. Based on the given results, this reduction in mean flow is much higher in 2080s, ranging from -3.6% in March and 44.5% in November. Further monthly statistics for percentage change from mean of 100 runs of control scenario are given in Table B.6.

In this table, Q10 (90^{th} percentile) represents the high flow, which means only 10% of the time, the flow is equal or greater than this value. Also, Q90 (10^{th} percentile) represents the low flow, which means 90% of the time, the flow is equals or greater than this value.

Based on the results of high flow (Q10) illustrated in Table B.6, in 2020s, there is an increase in high flows from January to December. There is an exception for October that the reduction of 4.8% is projected to occur. In 2050s, between 8.1% and 9.5% increase in

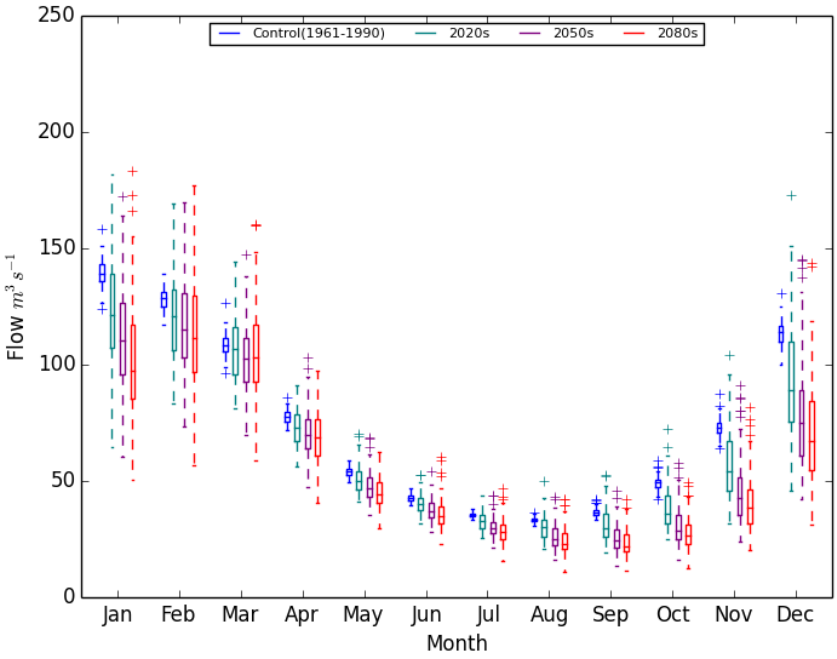

Figure 4.7: Boxplots of flow in Kingston sub-catchment.

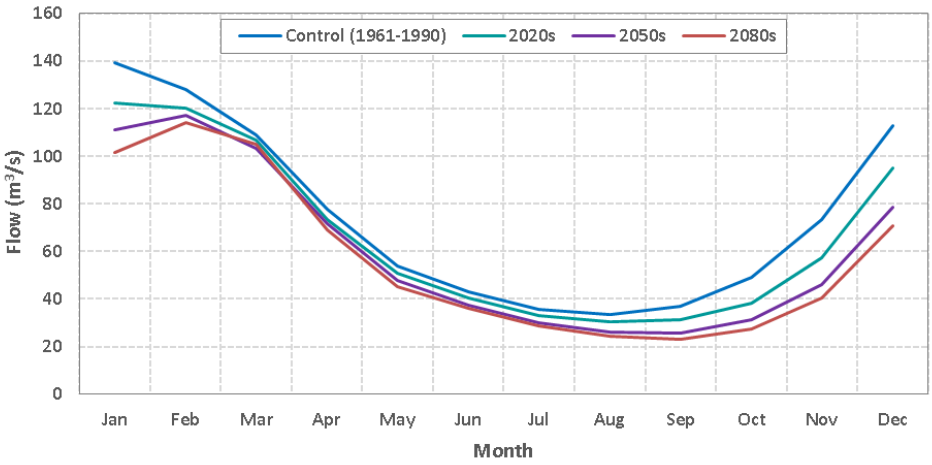

Figure 4.8: Mean flow in Kingston sub-catchment.

high flow in February, March and April are projected, while between 14.3% and 1.6% reduction in high flow occurs for the remaining months. Maximum changes in high flow (Q10) is expected to occur by 2080s, which ranges from -29.2% in November to +19.6% in February.

Based on the given results, the low flow (Q90) is projected to reduce in all future scenarios. The low flow reduces to its minimum level by September, in all future scenarios. These reductions in Q90 is higher for 2080s, ranging from -22.4% in March to -60.1% in November.

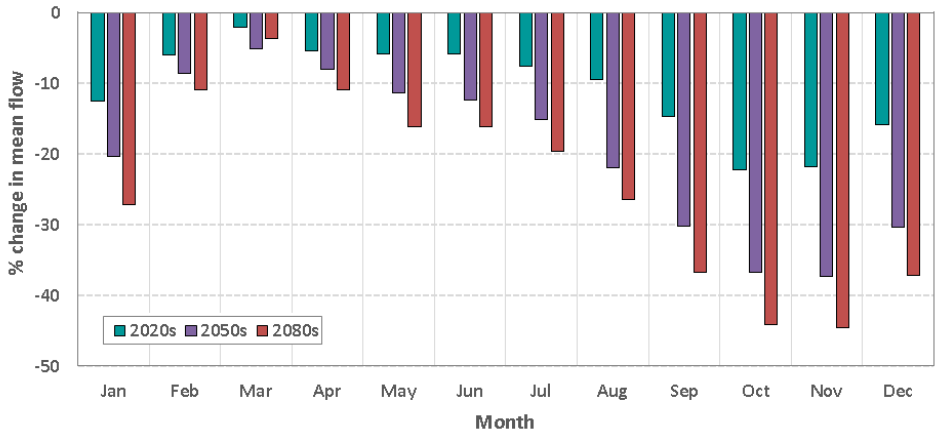

Figure 4.9: Change in mean flow relative to control period in Kingston sub-catchment.

To assess the range of possible changes in flow in Kingston catchment a range of flow duration curves for control and future scenarios are plotted. The flow duration curves for 100 runs of 100 years of control and future scenarios in Kingston are presented in Figure 4.10. In each of the plots in this figure, the comparison between control and future projections shows that the frequency of occurrence of all the possible range of flow increases for future scenarios. This wider range of possible frequencies, indicates that the uncertainty in projected flows in future scenarios, spatially for 2080s, are higher relative to the control. This is in consistent with the results showed in previous section about projected drier summers and wetter winters for Kingston sub-catchment. For flows lower than Q50, there is a reduction in projected flow which is a function of reduced summer and spring rainfall. There is a slight projected increase in flows higher than Q10 which is a consequence of increase rainfall in winter. The percentage change in flow quantiles from mean control to mean future are summarised in Table 4.1. As it can be seen, on average, in all of the future scenarios there is a reduction in flow relative to the control scenario.

4.2.1.4 Subsurface storage

Based on the results so far, climate change is likely to change precipitation and PET regimes and consequently alter flow distribution in the Kingston sub-catchment. Considering the importance of the knowledge about the future potential changes for

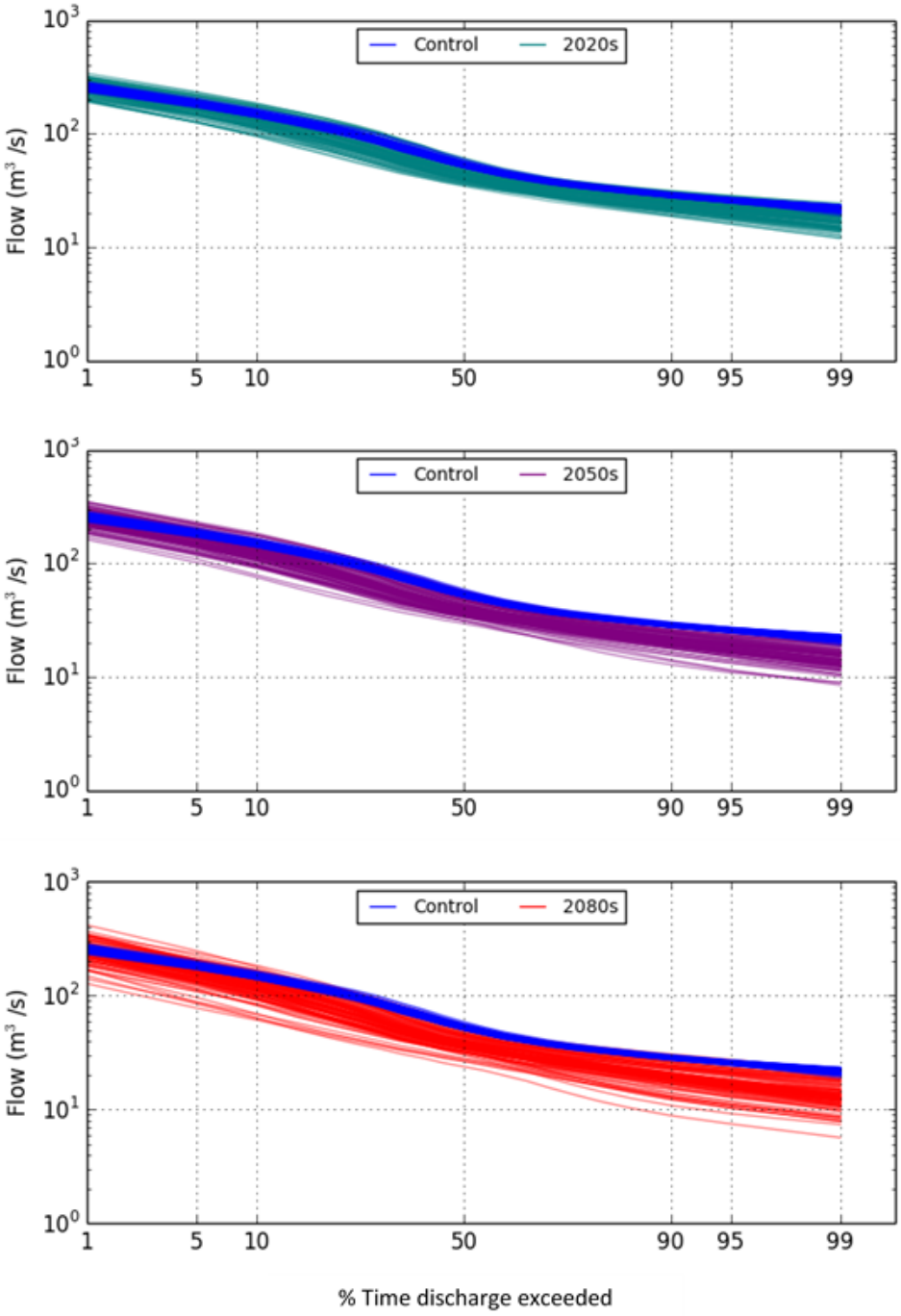

Figure 4.10: Range of flow duration curves for 100 runs of 100 years of control and future scenarios in Kingston sub-catchment.

Flow Quantiles	2020s	2050s	2080s
Q1	-0.08	-3.27	-2.72
Q5	-5.46	-10.87	-13.87
Q10	-8.50	-15.53	-20.09
Q50	-13.64	-23.00	-27.69
Q90	-12.65	-24.00	-30.42
Q95	-13.95	-26.21	-33.19
Q99	-16.90	-30.26	-37.64

Table 4.1: % change in mean flow quantiles from control to future scenarios, Kingston sub-catchment.

decision makers and water resources managers, it is therefore of interest to assess potential changes in subsurface storage in this sub-catchment.

The projected subsurface storage in the Kingston sub-catchment are presented in Figure 4.11. Analysing the 100 runs of 100 years simulated flow in Kingston, shows that in future there is a decreasing trend in projected subsurface storage relative to control. The size of the boxplots gets larger for further time slices. As for 2080s, the boxplots are the largest amongst the other future time slices, which indicates that the uncertainty in projecting the subsurface is the greatest in 2080s.

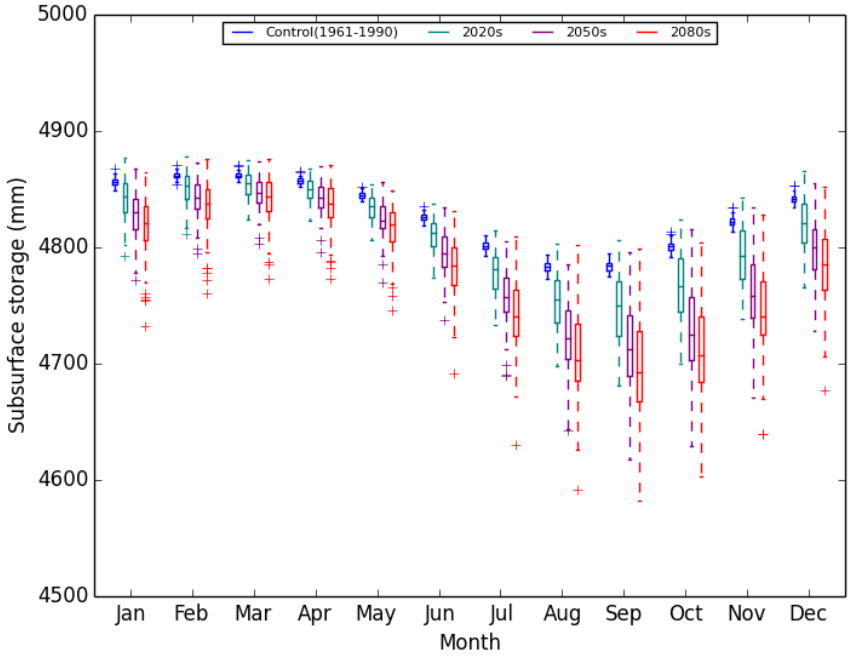

Figure 4.11: Boxplots of subsurface storage in Kingston sub-catchment.

Figure 4.12 shows a comparison of mean subsurface storage between control and the future scenarios. The curves illustrate that in future the mean projected subsurface storage is always lower than the control scenario. During winter, because of a higher amount of rainfall and lower PET, the subsurface storage is at its highest level.

While by reducing rainfall, increasing the temperature, and consequently increase of PET during spring and summer, the subsurface storage drops to its lowest level by September. The percentage of change in mean subsurface storage from control scenario are plotted in Figure 4.13. More details about mean, 90th and 10th percentiles of subsurface projections from control in the Kingston sub-catchment are listed in Table B.7 and Table B.8. By 2080s subsurface storage is projected to be between 0.41% and 1.9% less than control scenario. Overall, a 1.1% reduction in mean subsurface storage is expected to occur by 2080s. While the projected difference between 2020s and 2050s and control are expected to be around -0.42% and -0.82% respectively.

Seasonal comparison between subsurface values are listed in Table 4.2. The subsurface storage in summer and winter are at the lowest and highest level respectively. The percentage of difference between future and control in winter and autumn are the greatest. The given results show that in spite of projected rainfall increase in winter and spring, the flow is always lower than the control scenario. This shows that in future, as a result of higher temperature and consequently higher PET, the soil is always very dry and never get saturated enough to create surface run-off. The subsurface storage reduces the most by 2080s, which is in consistent with the projected rainfall, PET and flow presented in the previous sections.

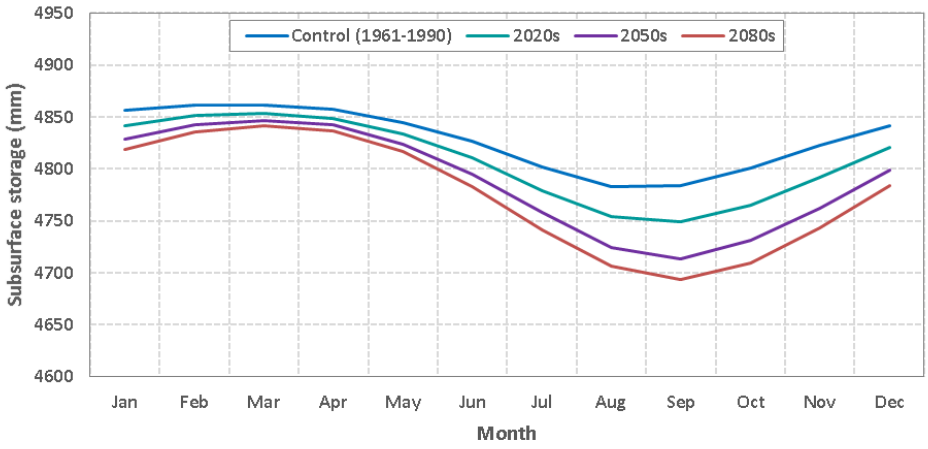

Figure 4.12: Subsurface storage in the Kingston sub-catchment.

4.2.2 Climate change impacts on the Lee sub-catchment

4.2.2.1 Rainfall

Figure 4.14 shows boxplots of rainfall in the Lee catchment. Rainfall has an increasing trend from September to January and decreasing trend from March to August. The given results show that, for all time slices the projected rainfall in April and October are similar to the control scenario. Generally, the distribution of uncertainty in 2080s is considerably larger than the other climate scenarios.

Figure 4.15 compares the mean rainfall in control and future scenarios. This plot

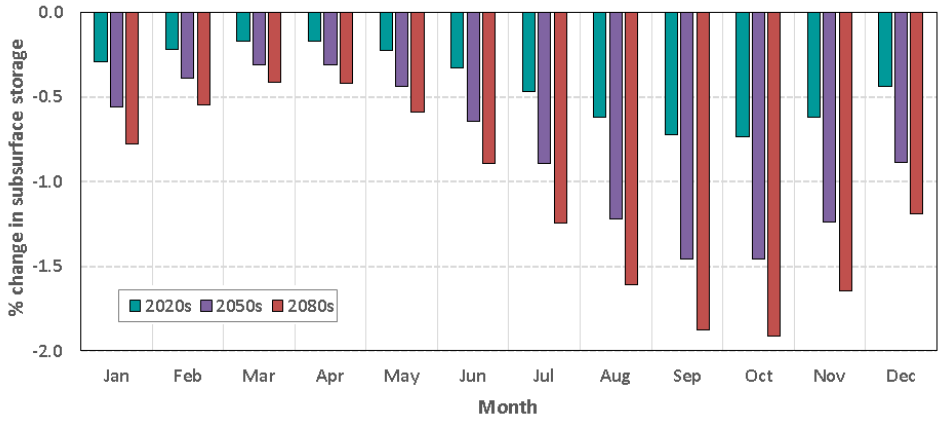

Figure 4.13: % change in mean subsurface storage relative to control period in the Kingston sub-catchment.

Season	Average (mm)				Change (%)			
	Control (1961-190)	2020s	2050s	2080s	Control (1961-190)	2020s	2050s	2080s
Spring	4859.88	4848.86	4839.56	4831.78	-	-0.23	-0.42	-0.58
Summer	4842.76	4831.05	4820.34	4812.08	-	-0.24	-0.46	-0.63
Fall	4789.38	4760.56	4732.28	4713.88	-	-0.60	-1.19	-1.58
Winter	4821.66	4792.91	4764.13	4745.37	-	-0.60	-1.19	-1.58
Annual	4828.42	4808.34	4789.08	4775.78	-	-0.42	-0.82	-1.09

Table 4.2: Seasonal subsurface storage in Kingston sub-catchment

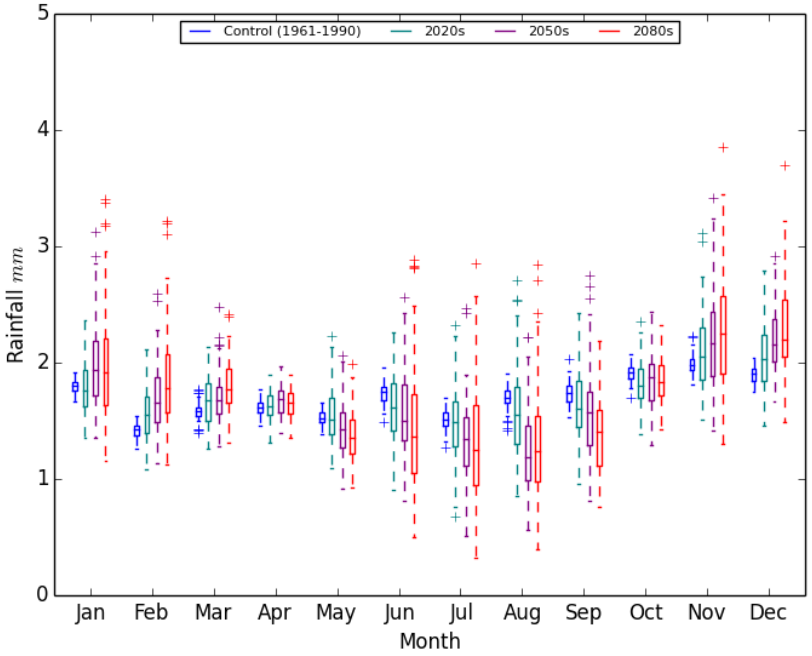

Figure 4.14: Boxplots of rainfall in the Lee sub-catchment.

highlights that from November to March, the projected rainfall for the future climates are higher than control scenario, while from April to October rainfall is lower than the control scenario. This implies wetter winter and drier spring, summer and autumn in future. Details about the values of mean rainfall in control and future scenarios are shown in Table B.9.

The percentage of change in rainfall from the mean of 100 runs for control scenario are plotted in Figure 4.16. The maximum growth in the increase of rainfall are expected to occur in February. More detailed results about the percentage changes from mean of 100 runs of control scenarios are shown in Table B.10. In 2080s, in February, the 90th percentile of rainfall is expected to increase by 64.0% compared to the control scenario. August with 23.6% decrease in mean rainfall and 58.3% reduction in 10th percentile, is the driest month.

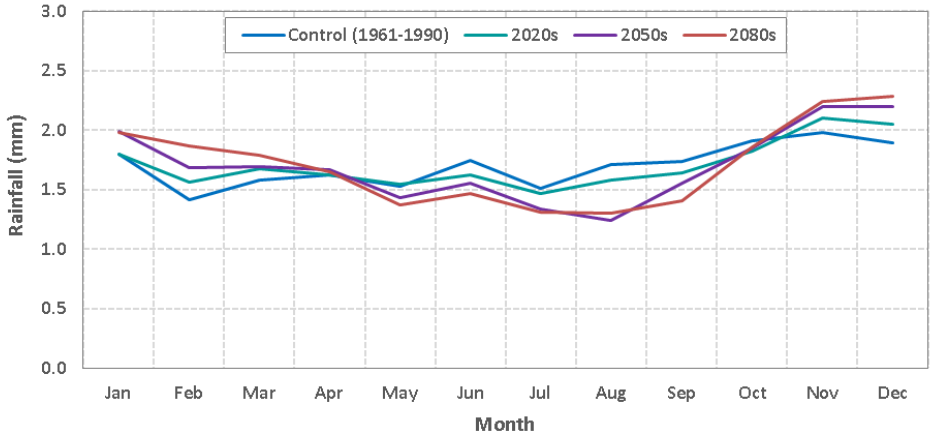

Figure 4.15: Mean rainfall in the Lee sub-catchment.

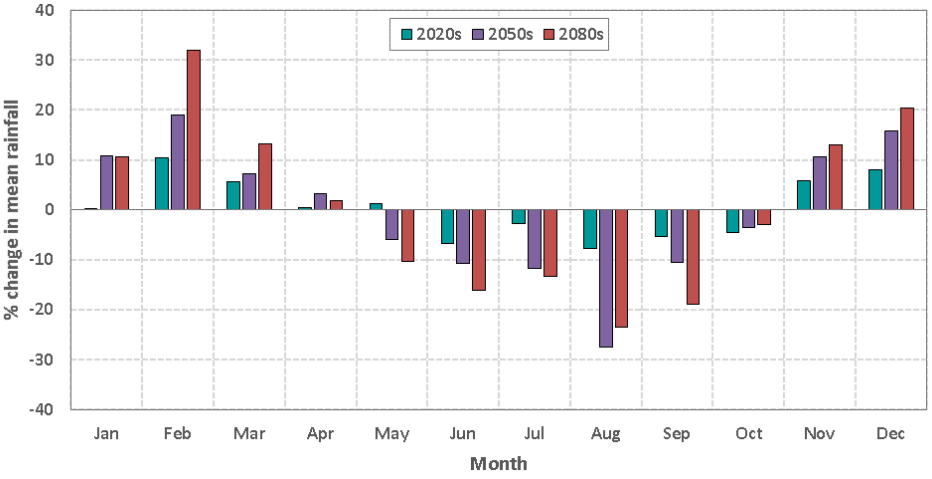

Figure 4.16: Change in mean rainfall relative to control period in Lee sub-catchment.

4.2.2.2 PET

Figure 4.17 illustrates the boxplots of daily PET in the Lee sub-catchment. Similar to the Kingston sub-catchment, there is an increasing trend in PET projections. From September to December there is a decreasing trend in PET. The minimum change in PET is expected to occur in January while the maximum change occurs in August. This figure shows a wider range of uncertainty in projected PET for future scenarios, especially in the2080s. Figure 4.18 compares mean PET for control and future scenarios. The quantity of mean, 10th and 90th percentile PET for control and future climates are tabulated in Table B.11.

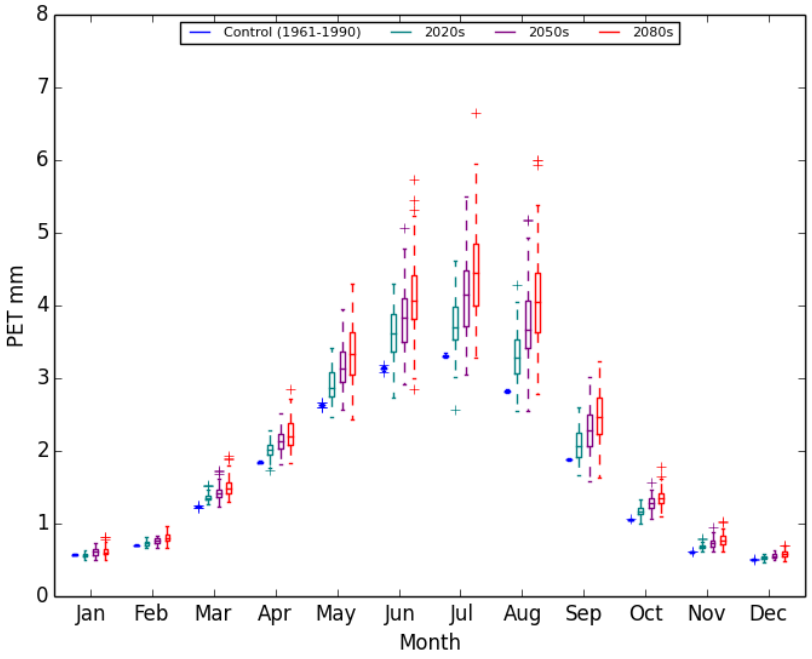

Figure 4.17: Boxplots of PET in the Lee sub-catchment.

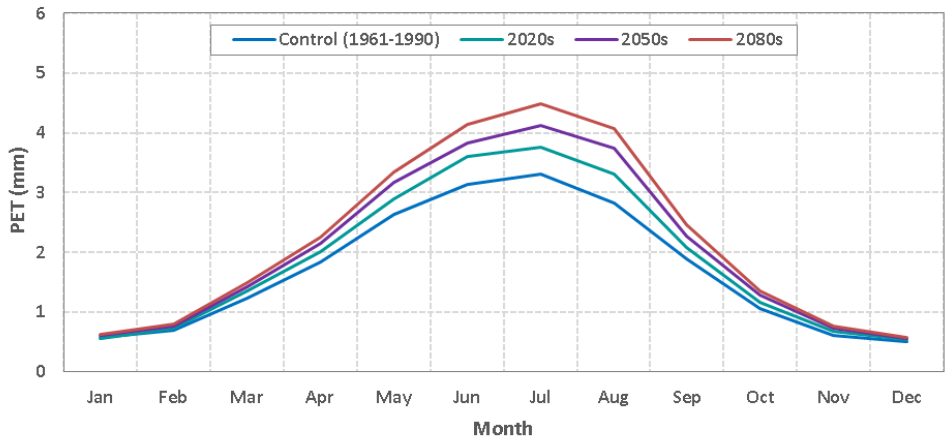

Figure 4.18: Mean PET in the Lee sub-catchment.

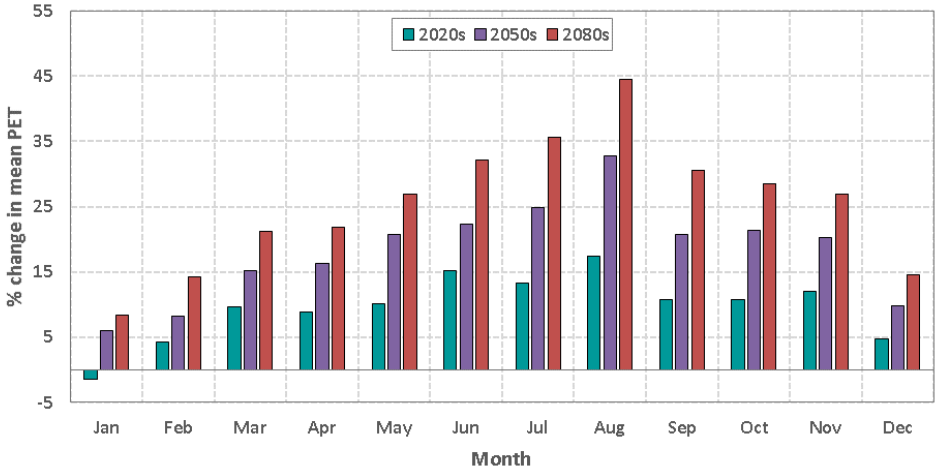

Figure 4.19: Change in mean PET relative to control period in Lee sub-catchment.

Figure 4.19 and Table B.12 also provide further details about percentage of change in mean PET of future scenarios from mean of 100 runs for control scenario. Based on the given results, in 2020s, there is a slight decrease (-1.4%) in PET in January, relative to control scenario.

There is an increase in PET in all future scenarios, except for 2020s in which the PET decreases by 1.4% relative to the control scenario. The range of increase in PET is greater for 2080s, which is between 8.3% in January and 44.5% in August. In addition, for 2080s, between 23.1% and 73.9% increase in 90th percentile and between 3.9% and 15.7% reduction in 10th percentile are expected to occur.

4.2.2.3 River flows

Figure 4.20 shows the boxplots of flow for control and future scenarios. The projected flow is always lower than the control scenario. It also illustrates that the spread of uncertainty in flow projections for future scenarios, especially 2080s, is higher than the control scenario. This uncertainty in winter and autumn is greater than in other seasons, which is consistent with the higher uncertainty in rainfall projections in these seasons (explained in previous section). The quantity of mean, 10th and 90th percentile flows are listed in Table B.13.

Figure 4.21 compares the mean of 100 runs of simulated flows of control and future scenarios. In all future scenarios, February has the highest flow, while in control scenario flow in January is higher than the other months. It can also be seen that in May, the difference between mean flows are minimum. In February and March the projected mean flow for 2050s and 2080s are very similar.

Figure 4.22 and Table B.14 also provide more details on percentage of change in mean flow from mean of 100 runs of control scenarios. Based on this figure, in all the future climate scenarios, the projected flow is always lower than the control scenario. This reduction is higher for 2080s, which ranges from 11.9% in May to 37.3%

in September. For 2050s and 2020s, the maximum reduction in flow occurs in October by 19.2% and 30.8% respectively. In 2080s, between -24.7% and 9.2% change in Q10 and between 19.2% and 53.4% reduction in Q90 is expected to occur.

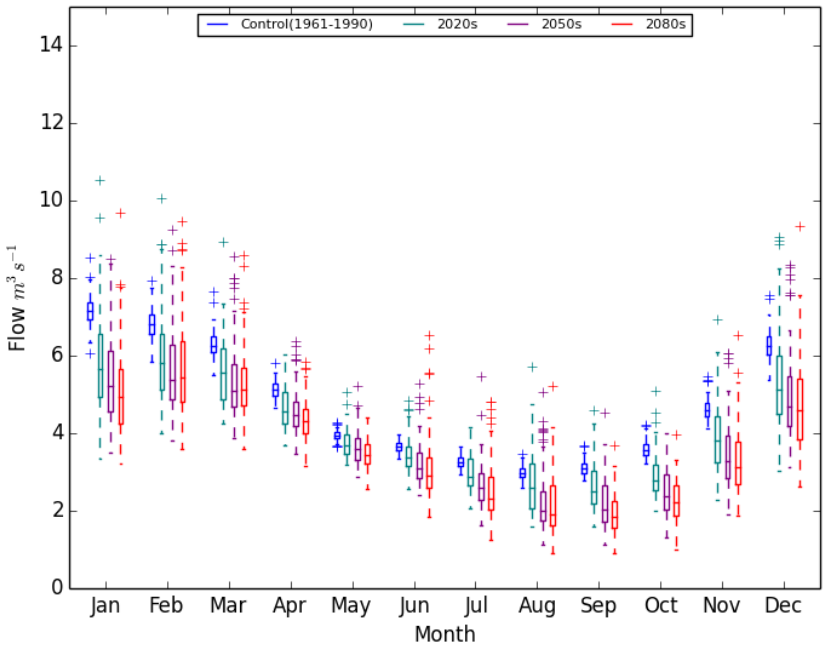

Figure 4.20: Boxplots of flow in Lee sub-catchment.

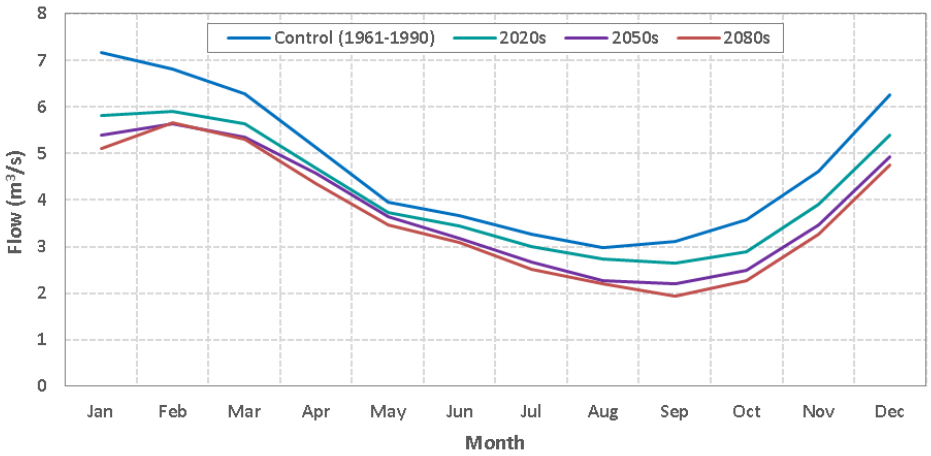

Figure 4.21: Mean flow in Lee sub-catchment.

Flow duration curves for 100 runs of 100 years of control and future scenarios are plotted in Figure 4.23. This is to assess the range of possible changes in future flow in the Lee sub-catchment. The plotted flow duration curves show that the frequency of occurrence of all the possible ranges of flows increases for future scenarios. Similar to the Kingston sub-catchment, the range of possible frequencies for future scenarios gets wider which shows that the range of uncertainty in projected flows in future scenarios, spatially for 2080s, are higher relative to the control scenario. This is consistent with the

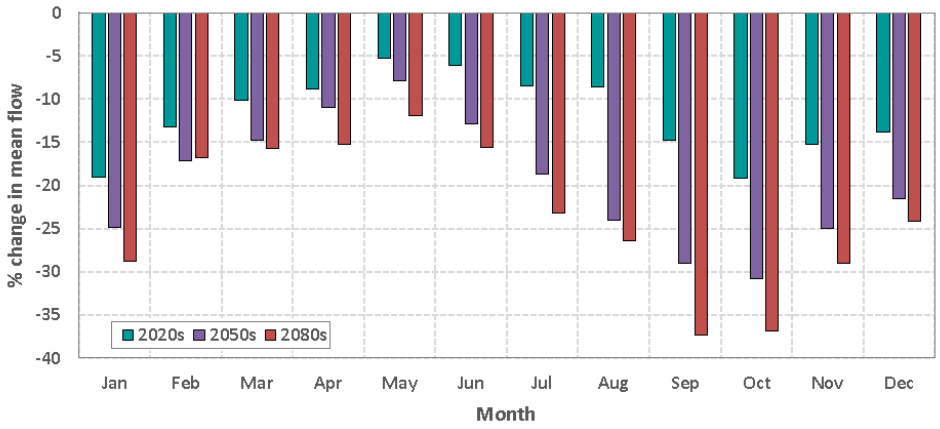

Figure 4.22: Change in mean flow relative to control periods in Lee sub-catchment.

Quantiles	2020s	2050s	2080s
Q1	-6.65	-11.40	-11.32
Q5	-15.53	-23.11	-25.75
Q10	-17.38	-25.65	-29.27
Q50	-9.54	-15.61	-19.13
Q90	-15.59	-27.48	-33.67
Q95	-16.76	-29.03	-35.34
Q99	-17.46	-30.13	-36.97

Table 4.3: % change in mean flow quantiles from control to future scenarios in Lee sub-catchment.

results showed in previous section about predicting drier summers and wetter winters in Lee basin.

Similar to Kingston, there is a reduction in projected flow lower than Q50. This reduction is a result of a decrease of the amount of precipitation in summer and spring. For flows higher than Q10, a slight increase is predicted. The wider range of frequencies in higher flows is a consequence of increased winter rainfalls. Table 4.3 shows the percentage change in mean flow quantiles from control to future scenarios. As it can be seen, flow quantiles of future scenarios are always lower than control period. This reduction is greater for low flows. The prediction shows that by 2080s, in average, between 33.7% and 37.0% reduction in low flows (Q90, Q95 and Q99) are expected to occur (35.3% reduction in Q95).

4.2.2.4 Subsurface storage

The boxplots of subsurface storage for control and future scenarios of the Lee sub-catchment are presented in Figure 4.24. Analysing the 100 runs of 100 years of simulated subsurface storage, shows a decreasing trend in projected future subsurface storage relative to the control scenario. As it can be seen in Figure 4.24, size of the boxplots gets larger for further time slices, especially for 2080s.

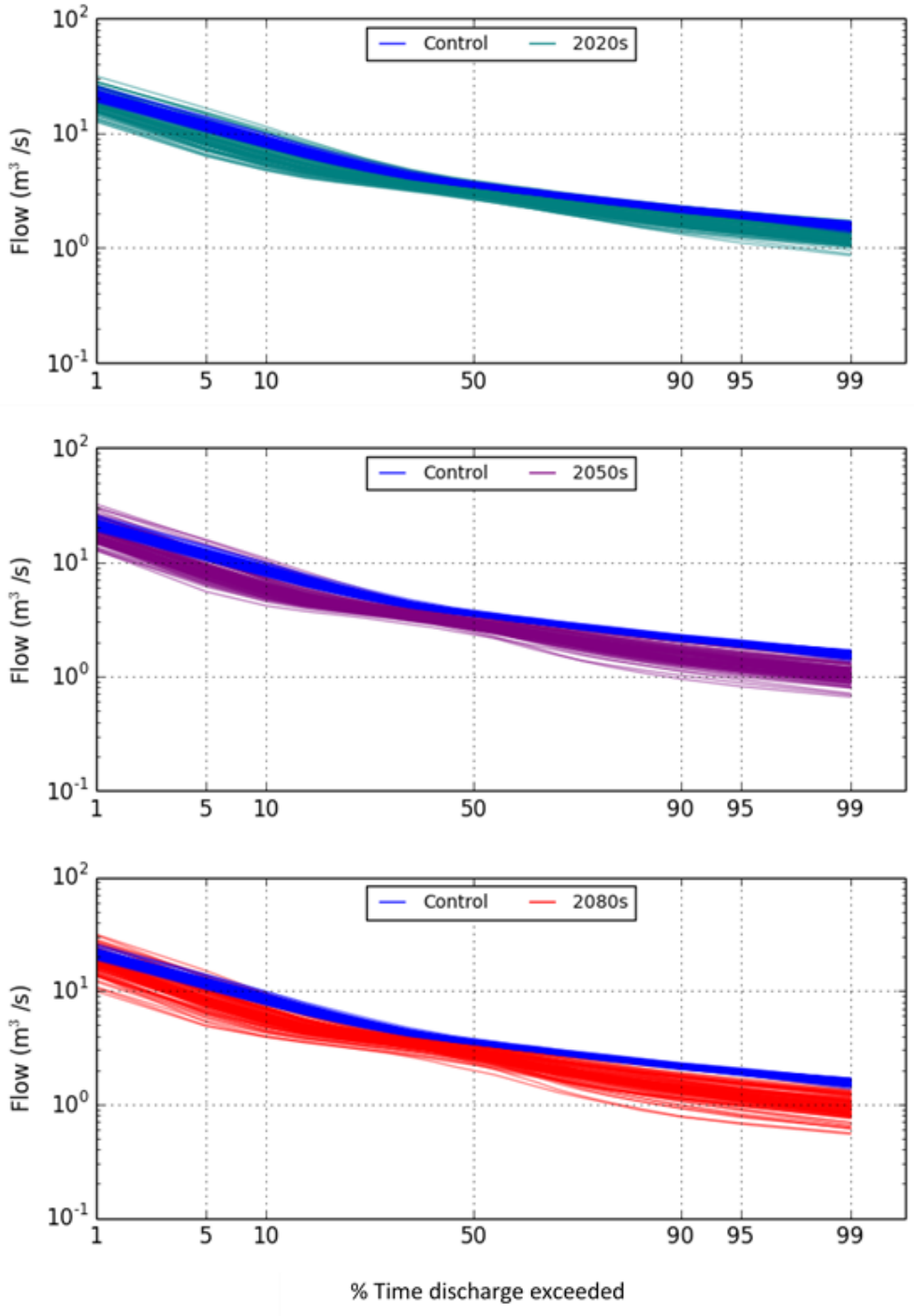

Figure 4.23: Range of flow duration curves for 100 runs of 100 years of control and future scenarios, Lee sub-catchment.

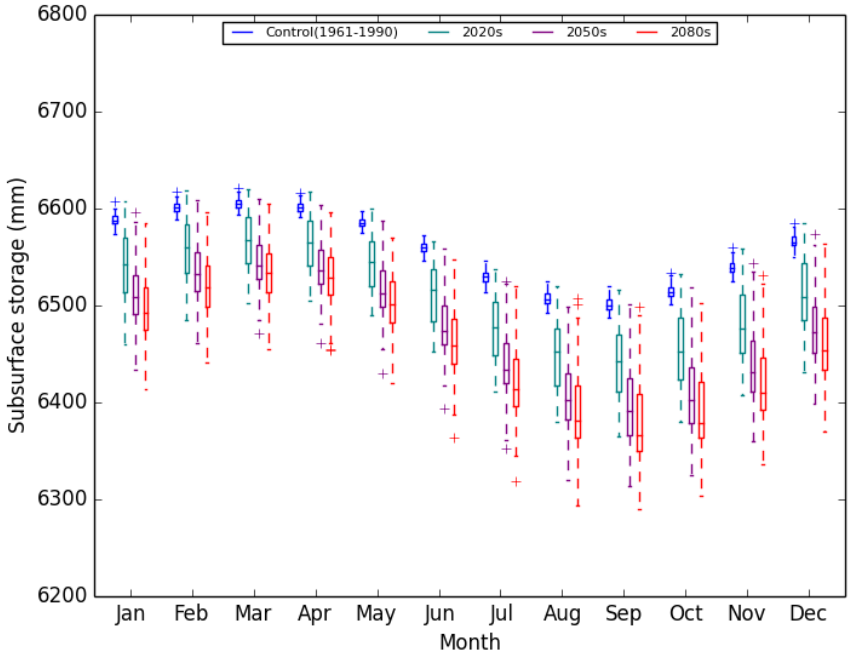

Figure 4.24: Boxplots of subsurface storage in Lee sub-catchment.

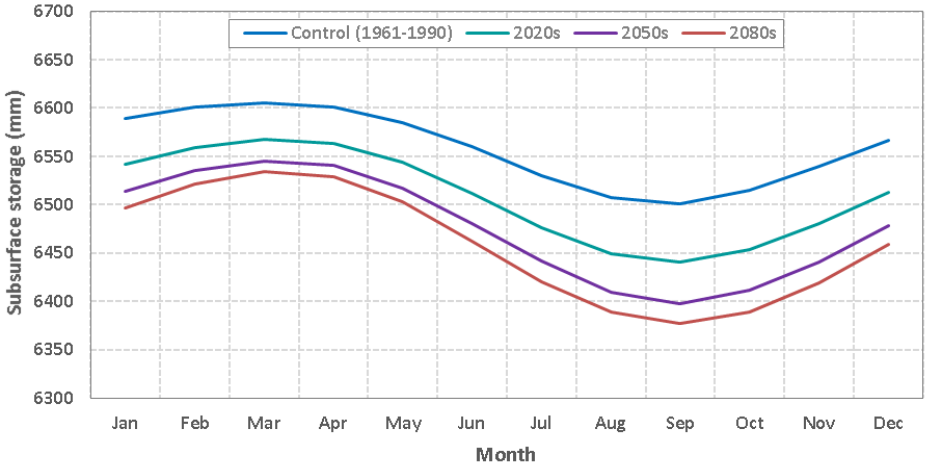

Figure 4.25: Mean subsurface storage in Lee sub-catchment.

Plots of mean subsurface storage of the control and the future scenarios are presented in Figure 4.25. Based on this figure, in future, the mean projected subsurface storage is always lower than the control scenario. Due to the increase in projected winter rainfall, the subsurface storage is at the highest level in this season. In line with projected rainfall, the subsurface storage drops to the lowest level by September. All of these results for Lee sub-catchment are in consistent with the change in projected rainfall, PET and flow which were discussed earlier. Figure 4.26 illustrates the change in mean subsurface storage from the control scenario.

More details about mean, 90th and 10th percentiles of subsurface projections and percentage of changes from control scenario are listed in Table B.15 and Table B.16 respectively. Based on the results presented in these tables, for all future scenarios, the maximum and minimum change in subsurface storage is expected to occur by March and October respectively.

Seasonal comparison between subsurface values are listed in Table 4.4. As it can be seen, among the studied future time slices, the maximum reduction in annual mean subsurface storage is expected to occur by 2080s (-1.5%). In future scenarios, the average of subsurface storage is expected to be lower than the control scenario in all seasons. The minimum change in subsurface storage occurs in spring, while the percentage of change from control scenario is the greatest in winter, especially by 2080s which the mean subsurface storage is expected to be 1.8% lower than control scenario.

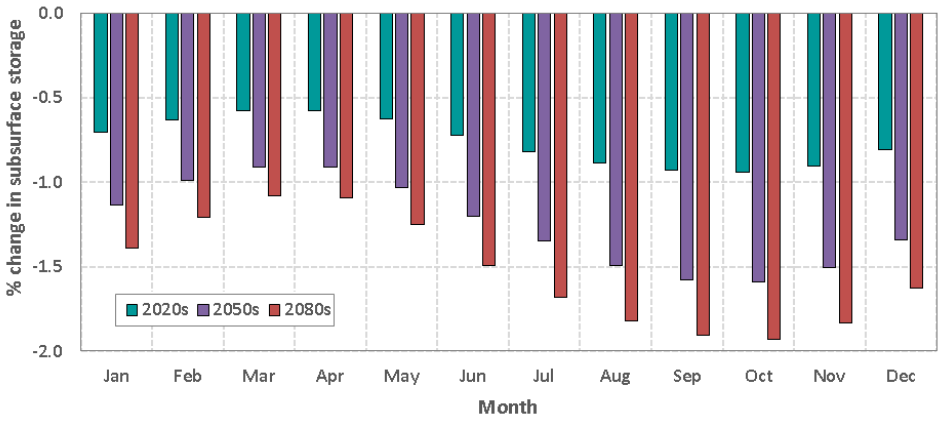

Figure 4.26: Change in future subsurface storage relative to control period in Lee sub-catchment.

4.2.3 Summary of the results for climate change impact assessment of flow for the Thames catchment

The 2080s is the most uncertain time slice, and the projection for 2080s represents the most severe possible impacts of climate change in the future. Hence, this time slice is used as a representative of the future impacts scenarios to summarize the impacts of climate change in the Thames catchment. Table 4.5 and Table 4.6 summarise the

Season	Average (mm)				Change (%)			
	Control (1961-190)	2020s	2050s	2080s	Control (1961-190)	2020s	2050s	2080s
Spring	6598.44	6556.27	6531.61	6517.48	0.00	-0.64	-1.01	-1.23
Summer	6582.15	6539.81	6513.18	6498.03	0.00	-0.64	-1.05	-1.28
Fall	6512.72	6455.70	6416.76	6395.31	0.00	-0.88	-1.47	-1.80
Winter	6540.14	6482.28	6443.45	6422.60	0.00	-0.88	-1.48	-1.80
Annual	6558.36	6508.51	6476.25	6458.35	0.00	-0.76	-1.25	-1.53

Table 4.4: Seasonal subsurface storage in Lee sub-catchment.

ranges of changes in mean rainfall, PET, flow and subsurface storage in Kingston, for each season by 2080s relative to the control scenario. Rainfall is projected to increase in spring and winter. The annual mean daily rainfall is projected to have a slight increase (+0.09%) by 2080s, which shows that total amount of rainfall is almost the same as the control scenario.

For the Kingston catchment, the given results from simulations show that by 2080s, PET is expected to increase in all the seasons and the annual mean daily PET is projected to increase by 26.6%. Because PET is more affected by the temperature, it can be concluded that by 2080s the overall temperature is expected to increase in all of the seasons. Another interesting results given from this study is that there is a reduction in flow and subsurface storage in all the seasons, which indicates that they are more influenced by temperature and consequently the PET. The given results show that, 24.1% and 1.1% reduction in annual mean daily flow and subsurface storage is projected to occur respectively.

	Seasonal				Annual
	Spring Mar Apr May	Summer Jun Jul Aug	Autumn Sep Oct Nov	Winter Dec Jan Feb	
Rainfall (mm)	2.28	1.62	1.43	2.51	1.96
PET (mm)	0.97	3.20	3.59	0.89	2.16
Flow (m^3/s)	73.11	29.69	30.46	95.62	57.22
Subsurface storage (mm)	4831.78	4812.08	4713.88	4745.37	4775.78

Table 4.5: Summary table of mean seasonal rainfall, PET flow and subsurface storage for 2080s, Kingston sub-catchment.

The given results for Lee sub-catchment are summarised in Table 4.7 and Table 4.8. These tables show the range of changes in mean rainfall, PET, flow and subsurface storage for each season by 2080s relative to the control scenarios. The analysed results show that, similar to Kingston, there is an increase in spring and winter and a decrease in summer and autumn rainfalls in the Lee sub-catchment. The annual mean daily

	Seasonal				Annual
	Spring	Summer	Autumn	Winter	
	Mar Apr May	Jun Jul Aug	Sep Oct Nov	Dec Jan Feb	
Rainfall	+17.8%	-8.44%	-19.22%	+10.23%	+0.09%
PET	+16.72%	+27.68%	+37.29%	+24.86%	+26.64%
Flow	-8.76%	-20.31%	-42.60%	-24.63%	-24.08%
Subsurface storage	-0.58%	-0.63%	-1.58%	-1.58%	-1.09%

Table 4.6: Summary table of % change in mean seasonal rainfall, PET, flow and subsurface storage from control to 2080s, Kingston sub-catchment.

rainfall is projected to have slight increase (0.19%) by 2080s.

For Lee sub-catchment, the results from simulations illustrate that by 2080s, the PET is expected to increase in all the seasons and the annual mean daily PET is projected to increase by 26.6% (higher than Kingston sub-catchment). Another interesting result given from this study is that despite of increasing rainfall, flow and subsurface storage are predicted to reduce in all the seasons. This reduction indicates that both flow and subsurface storage are more affected by temperature and consequently the PET. Based on the results, the annual mean daily flow and subsurface storage are projected to drop by 23.2% and 1.5% by 2080s respectively.

	Seasonal				Annual
	Spring	Summer	Autumn	Winter	
	Mar Apr May	Jun Jul Aug	Sep Oct Nov	Dec Jan Feb	
Rainfall (mm)	1.88	1.49	1.34	2.13	1.71
PET (mm)	0.97	3.24	3.67	0.90	2.20
Flow (m^3/s)	5.36	3.64	2.22	3.43	3.66
Subsurface storage (mm)	6517.48	6498.03	6395.31	6422.60	6458.35

Table 4.7: Summary table of mean seasonal rainfall, PET for 2080s, Lee sub-catchment.

	Seasonal				Annual
	Spring	Summer	Autumn	Winter	
	Mar Apr May	Jun Jul Aug	Sep Oct Nov	Dec Jan Feb	
Rainfall	+17.8%	-8.36%	-18.82%	+10.13%	+0.19%
PET	+16.31%	+27.79%	+37.52%	+24.78%	+26.60%
Flow	-20.71%	-14.33%	-28.92%	-28.82%	-23.19%
Subsurface storage	-1.23%	-1.28%	-1.80%	-1.80%	-1.53%

Table 4.8: Summary table of % change in mean seasonal rainfall, PET and flow from control to 2080s, Lee sub-catchment.

4.3 Water resources availability in Thames catchment

LARaWaRM was used in this study to discover the potential impacts of climate change, socio economic drivers and supply and demand changes on the availability of water resources in Thames catchment. To assess the impact of climate change on availability of water resources, the 100 runs of 100 years simulated river flows generated by SHETRAN for the four time slices of control (1961-1990), 2020s, 2050s and 2080s are input into LARaWaRM.

To investigate the impacts of population growth on water resources, population and employment growth has been used to estimate the demand for water in the future. The population projections are based on Greater London Authoritys strategic plan for London (GLA 2014*a*). The population growth of London are projected up to 2040, which is expected to be around 10.0 to 10.7 million. Therefore, the population projections for 2050s and 2080s are calculated by an extrapolation technique and listed in Table 4.9.

The projections for employment growth in Thames catchment is based on GLA economics which is based on ONS data (GLA 2014*b*). Five different main employment sectors are considered in LARaWaRM: Primary and Industry, services, Construction, Finance and Professional, public and other. The employment growth projection by GLA is only up to 2036, therefore the projections for 2050s and 2080s are calculated by extrapolation. The actual and projected populations works in different employment sectors, for years between 2010 and 2080s are listed in Table 4.9.

Year	Population	Employment				
		Primary & Industry	Services	Construction	Finance & Professional	Public & others
2010	8,107,073	411,000	1,030,000	238,000	1,854,000	1,211,000
2020	9,127,567	346,499	1,178,973	255,516	2,125,988	1,283,002
2050	10,776,890	171,492	1,355,850	239,840	3,104,601	1,397,247
2080	12,183,948	82,000	1,532,000	221,000	4,102,000	1,503,000

Table 4.9: Population and employment projections for London

4.3.1 Impacts of climate and population change on total reservoir storage

By using synthetic flow time series, generated by SHETRAN, as input to drive LARaWaRM the total reservoir storage in Thames catchment are generated. Figure 4.27 shows boxplots of daily mean total reservoir storage, for 100 runs of 100 years, simulated for different climate and population projections. In each of these four sub-figures, it has been assumed that population is constant over the time and only climate scenarios are changed. By comparing these sub-figures, the impact of population change on total reservoir storage in Thames catchment are analysed.

Figure 4.27(a) illustrates the impact of climate change on reservoir level if the population remains constant at its current number. Results given by water resources model shows that for control scenario, there is substantial amount of water in the reservoir throughout the year. Even by the end of the summer, when the storage in reservoir is normally low, there is nearly 90.0% water in the reservoir. While, as it can be seen, the total reservoir level drops for all future climate scenarios, as for 2080s the reservoir is much lower than the one for control scenario. Comparing all four population projections show that by increasing the population, as the demand for water increases, the reservoir level reduces. More details about the mean reservoir levels for all these population and climate change scenarios are listed in Table B.17 and Table B.18.

For each population projection, the uncertainty in reservoir storage estimation is getting larger for further future climate scenarios. For example, the longer boxes for 2080s implies that variation in mean reservoir level in this time period is greater than the other time slices. Moreover, the figure compares the distribution of change in total reservoir levels in each month. From March to June the uncertainty in projections of reservoir level is smaller than other months. For instance, for current population, by 2080s, in May between 80.0% and 100% water is expected to be in the reservoir, while the total reservoir level in November can range between 98.0% to 18.0%. Therefore, especially during autumn and winter, there is a larger range of possibility in reservoir storage, which indicates that uncertainty in prediction of water storage is very large. By keeping the population at current level, in 2080s there is 14.0% reduction in annual mean reservoir level compared to the control climate. If population changes to 2080s, for control climate the annual mean reservoir is 12.0% less than that from control climate with current population.

In all population scenarios, compared to control scenario there is always less water in the reservoir in future time slices. Based on the given results, in all future climates, in April and October the reservoirs is expected to be at the highest and lowest level respectively. For all climate scenarios, from beginning of summer (June) the reservoir storage reduces until October which it reaches to its minimum level. From October, by start of the rainy seasons, the reservoir level increases. For the control scenario, the reservoir storage fully recovers by January and stays full until June. While for future climate projections, compared to control scenario the recovery process takes longer and the full reservoir lasts for fewer months.

If population grows and climate changes as they are projected for 2080s (see Figure 4.27(d)), the water storage in reservoir is expected to be nearly 26.0% in October. This shows that by 2080s, the projected minimum reservoir storage in Thames catchment is expected to be 70.0% lower than the reservoir level for current population with control climate. This minimum reservoir storage is also 54.0% less than current population with 2080s climate and 57.0% lower than reservoir level with 2080s population and control climate. These are all show that in future as a result of population growth and

climate change, water resources in the study area could be under greater pressure.

If the population remained as it is projected for 2080s, the annual mean water storage for climate of 2080s, is 24.0% less than control climate with same population. Which is also 22.0% lower than 2080s climate with current population, and 33.0% lower than control climate with current population. Despite previous studies (Walsh et al. 2016, Borgomeo et al. 2014), these results indicate that by 2080s, the climate could have a greater impact on water supply security than population. The combination of population and climate change could have a greater impact on water supply security than each of them as individual drivers.

4.3.2 Impacts of climate and population change on number of drought days

Number of drought days is the frequency of the days that the demand saving restrictions are imposed on water use. The level of services and their Demand saving (DS) restrictions are listed in Table 3.1 and has been described in details in section 3.3. In this section, the projected number of drought days in Thames catchment, for different population and climate change scenarios, are presented and analysed. These numbers are from 100 years of 100 runs given by LARaWaRM.

Figure 4.28 illustrates the number of days that DS restrictions were applied for climate change projections runs (control, 2020s, 2050s and 2080s) with four population growth scenarios (current , 2020s, 2050s and 2080s). More details about the impact of climate change on number of drought days, for different population and also their % of change compared to their control scenario are listed in Table B.19.

From the given results shown in Figure 4.28 and Table B.19, it can be seen that the minimum total number of drought days is for control scenarios with current population. The number of drought days increases for future climate projections. In fact, future climate projections implies a greater range of uncertainty in the estimation of drought days, especially for level 4 as the size of boxplots are larger for 2080s compared to other climate scenarios.

For all population growth, there is an increasing trend in number of drought days for future climate scenarios, as the number of drought days for climate scenario of 2080s is always greater than the others. For the current population, the total number of drought days for climate projection of 2080s is 541.0% greater than that from control scenario. By increasing the population, the range of uncertainty and variability in number of drought days gets larger. For a single climate scenario of 2080s, by comparing the total number of drought days for the current population with that from population growth of 2080s, it can be seen that for population growth of 2080s the total number of drought days is 84.0% greater than current population. This shows the contribution of population growth in number of drought days.

Moreover, contribution of combination of population growth and climate projection is much higher than that from climate or population scenarios alone. Combination of

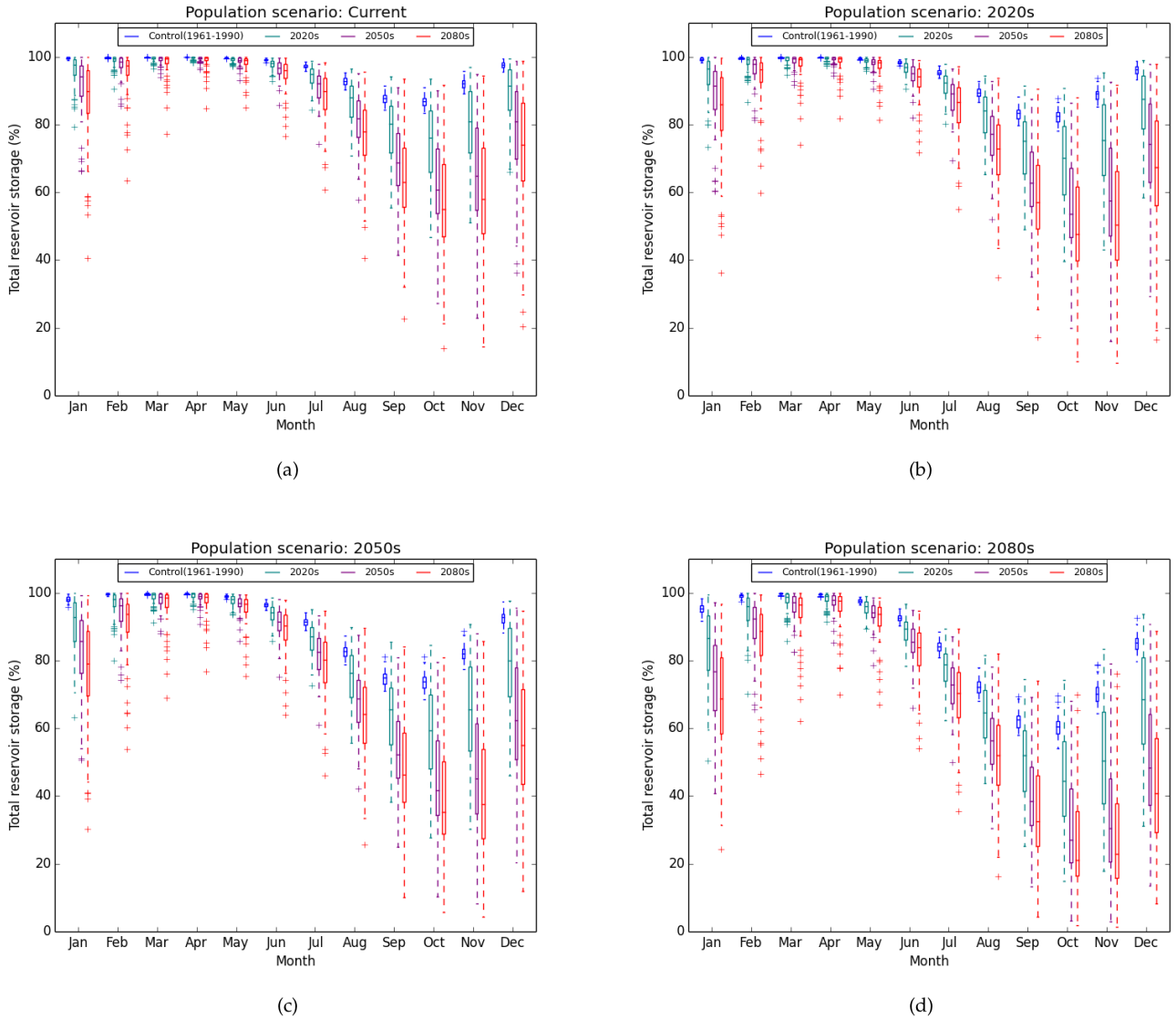

Figure 4.27: Boxplots of total reservoir storage for different climate and population scenarios a) Current population (2010) b) population scenario for 2020s c) population scenario for 2050s d) population scenario for 2080s, for the Thames catchment.

climate and population growth scenarios show that, for example, if both the climate change and population growth are as expected for 2080s, there is 1083.0% increase in total number of drought days compared to current population with control climate.

4.3.3 Adaptation options

The computational efficiency of water resources management model of LARaWaRM is very advantageous to enable a range of different adaptation options to be tested. For this aim, by altering the existing properties of models and also adding new links and nodes, different adaptation options are tested for different climate and population scenarios (from 2020s onward). The adaptation options considered are as follows:

- Desalination plant (D): represents the Thames Water desalination plant in Beckton which supplies capacity of 150 Ml of drinking water per day.
- Leakage reduction (L): represents the linear reduction in leakage (8.5% by 2020s, 23.0% by 2050s, 40.0% by 2080s). As it is noted by Thames Water (2013) compared to 2010, there could be 17.0% reduction in leakage by 2040s (Leakage is expected to be around 556 Ml/d by 2040s).
- New reservoir (R): is another supply option to construct a new reservoir with 100 million m^3 capacity which only applies for 2050s onward as it would take 30 years to construct such a reservoir.
- Different combinations of supply options such as Desalination and Reduced leakage (D+L); Desalination and New reservoir (D+R), Reduced leakage and New reservoir (L+R), Desalination and Reduced leakage and New reservoir (D+L+R).
- Demand reduction: represents reducing per person water demand from 168 l/p/d to 125 l/p/d, which is the target water consumption for all new properties in Thames area (Thames Water 2013).

The number of drought days given from different supply adaptation options, without demand reduction, are compared in Figure 4.29. More details about mean number of drought days and also % change compared to No adaptation scenario are presented in Table B.20 and Table B.21.

As it can be seen, the overall reduction in number of drought days shows the benefits of these adaptation options on managing water resources in Thames area. When both climate and population projections are for 2020s, three adaptation options of Desalination plant, Reduced leakage and Desalination and leakage are tested. Based on the given results, by using these adaptation options, the number of drought restrictions, Level 1 to Level 4, are reduced.

In 2020s, combination of desalination plant and reduced leakage has a greater impact than the desalination plant or reduced leakage. Combination of desalination plant and reduced leakage is the most effective adaptation option in the 2020s, which

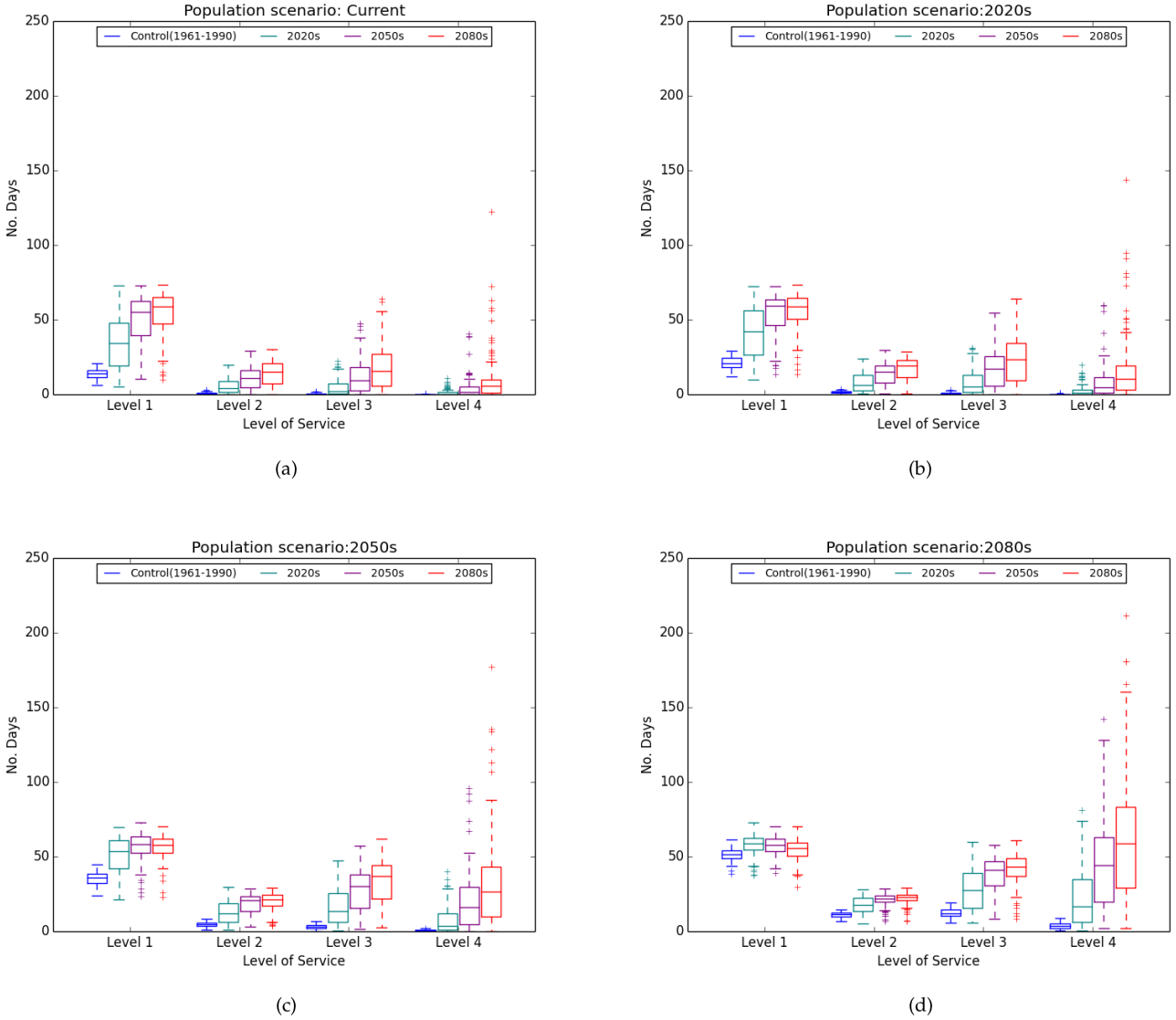

Figure 4.28: Number of demand saving days in 100 years for different population scenarios and climate change scenario in the Thames catchment.

leads to 56.7% reduction in number of drought Level 4. Desalination plant alone with 48.0%, and reduced leakage with 15.0% drop in number of drought Level 4, are ranked as second and third best options.

For 2050s, increasing the storage capacity of London by 100 million m^3 has the greatest impact on reducing the frequency of drought Level 1 and 2. Based on the results, adding the new reservoir reduces the drought Level 1 and 2 by 53.0% and 34.0% respectively. While, combined contribution from desalination plant, leakage reduction and new reservoir with 88.0% reduction is the most effective option on reducing the frequency of drought Level 4. In 2050s, combination of Leakage and reservoir as well as desalination and new reservoir can be categorised as second and third most effective options for drought Level 4. Interestingly, combination of desalination plant and reduced leakage, which was the most effective option in 2020s, is less effective in 2050s as it only reduces the number of drought Level 4 by 58.0%.

In 2080s, same as 2050s, although all adaptation options have substantially contributed in reducing the number of drought days, still the combination of three adaptation options of desalination, leakage and new reservoir with 74.0% reduction is the most effective option to reduce frequency of drought Level 4. Interesting to note that, although this combination effectively reduces the frequency of drought Level 4, it also increases the frequency of drought Level 1 by 26.0%. This shows that by using this combination, the supplied water in the system contributes to avoid the occurrence of Level 4 but still reservoir is not full enough to prevent the drought Level 1.

In addition to supply adaptation options, a demand option was also tested in this study. The proposed demand saving option is to reduce the per person demand by 25.0% from 168 l/p/d (current) to 125 l/p/d. Figure 4.30 shows the impact of 25.0% reduction in per person water consumption in number of drought days in Thames catchment. In this figure, the No adaptation option illustrates the impact of demand reduction itself and the others show the impact of combination of demand and supply options on water shortage in the Thames catchment. More details about mean number of drought days, after 25.0% reduction in per person demand, are presented in Table B.22 and % change compared to No adaptation scenario are listed in Table B.23.

As it can be seen in this figure, by reducing the demand to 125 l/p/d, the chance of having DS restrictions for 2020s and 2050s is zero. For 2080s, the demand reduction itself, without considering any supply adaptation options, reduces the number of drought days at Level 4 by 64.0% compared to no demand reduction (presented as no adaptation option in Figure 4.29). In fact, the given results show that a 25.0% reduction in demand has the greatest contribution in reducing the number of drought days compared to any of the individual or combined adaptation options with no demand reduction.

Moreover, as it can be seen, all supply options have a positive impact in reducing number of drought days at Level 4. A combined contribution of construction new reservoir, leakage reduction and desalination plant with 91.5% reduction compared to

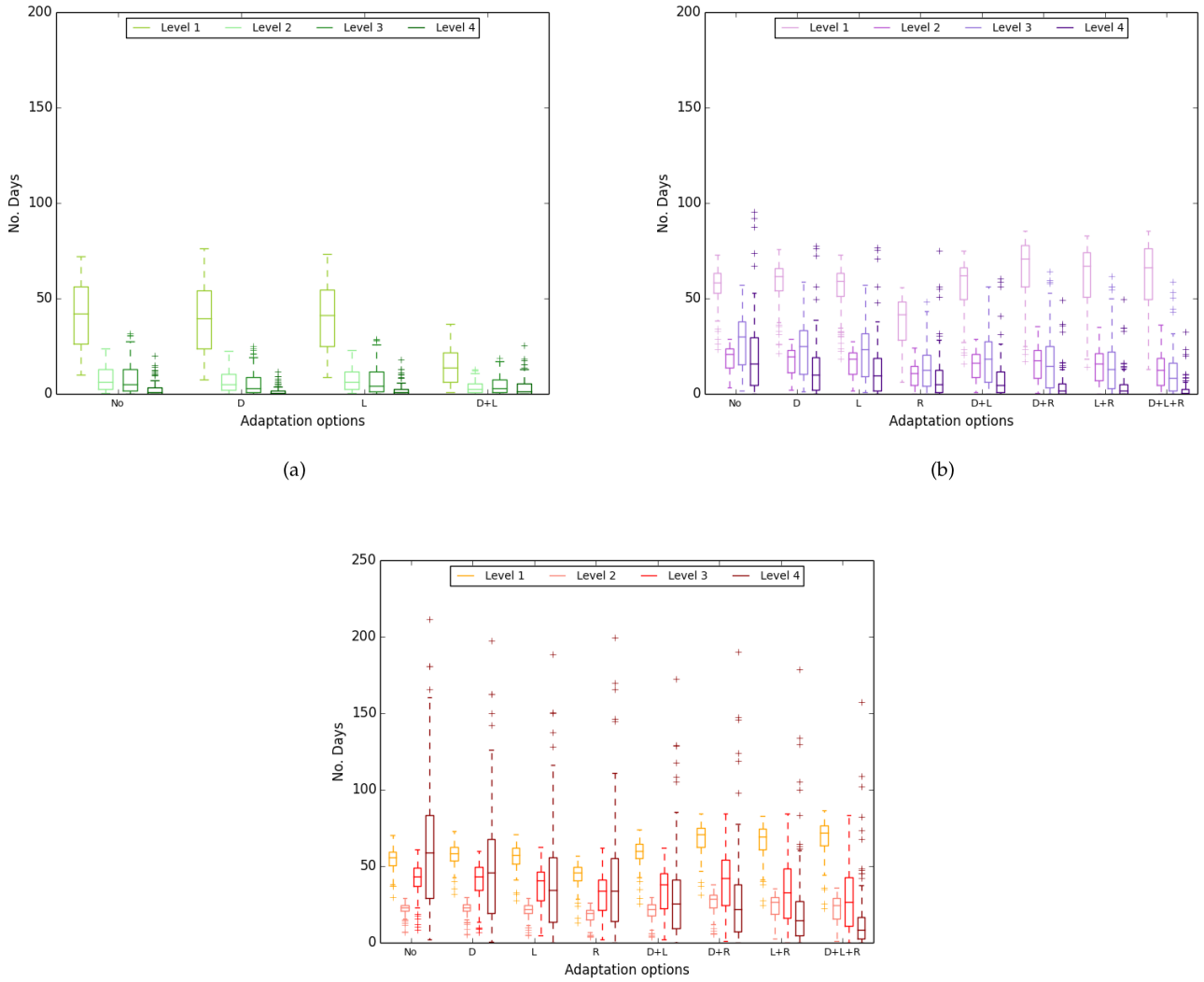

Figure 4.29: Boxplots of number of demand saving days in 100 years for different adaptation options (without demand reduction), under climate and population scenarios of (a) 2020s, (b) 2050s, (c) 2080s, for the Thames catchment.

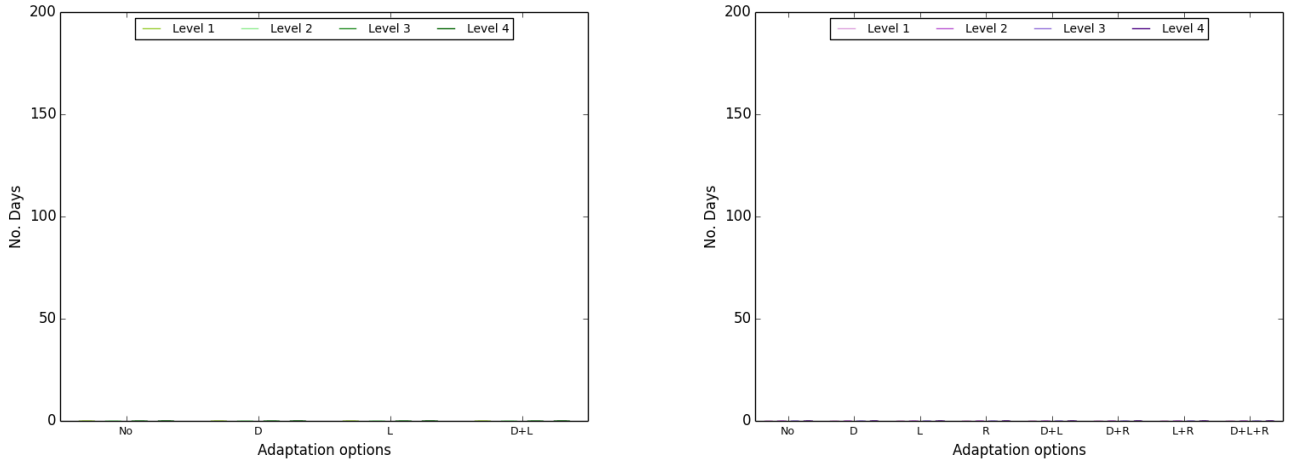

(a)

(b)

(c)

Figure 4.30: Boxplots of number of demand saving days in 100 years for different adaptation options (after 25.0% reduction in per person demand), under climate and population scenarios of (a) 2020s, (b) 2050s, (c) 2080s, for the Thames catchment.

no adaptation option is the most effective. In fact, based on the given results, using these combined contributions in conjunction with 25.0% demand reduction is the most effective adaptation option to tackle the negative impacts of climate and population change in the Thames catchment.

4.4 New insights gained from this study

It was stated previously that in this study the newly updated version of the spatial UKCP09 weather generator (discussed in section 3.4), and the hydrological model of SHETRAN are used. Hence, comparing the findings of the present research with results obtained previously for the Thames catchment show how using different versions of UKCP09 and different hydrological models can affect the research outcomes. For instance, in the studies demonstrated by Walsh et al. (2016) and Borgomeo et al. (2014) for the Thames Catchment, the previous version of spatial UKCP09 weather generator and the conceptual hydrological model CATCHMOD were adopted. The overall conclusion from both of these studies was that population growth has a greater impact on future drought risk than climate projections. While in contrast, the findings of the present research indicate that climate change has a greater contribution to drought risk and water supply security than the population growth. This significant difference in the results is not surprising, given that the previous version of UKCP09 overestimated the baseline rainfall.

In addition, Walsh et al. (2016) noted that an extreme reduction of 35.0% in daily per capita demand by 2020s could eliminate the risk of drought level 4, and by 2050s a combination of demand and supply adaptation options need to be considered. While, in the present study, the results show that only 25.0% reduction in per person water demand could offset the risk of having drought orders by 2020s and 2050s, and lead to a 64.0% drop in number of drought Level 4 by 2080s. This study also shows that by 2080s, using combined contribution of D+L+R in conjunction with 25.0% demand reduction, contributes to 91.5% reduction in number of drought days Level 4, and is the most effective adaptation option to tackle the negative impacts of climate and population change in the Thames catchment.

4.5 Summary

This chapter presented future impacts of climate change on Thames catchment for four representative time slices Control (1961-1990), 2020s, 2050s and 2080s. The given results indicated that proportion of uncertainty in projected rainfall, PET and discharge in 2080s is much greater than the other time slices. The comparison between projected values with the control scenario showed that the maximum changes are expected to occur by 2080s. Based on the results, by 2080s, rainfall is projected to increase in spring and winter and decrease during summer and autumn. However, a very small

projected increase in annual mean rainfall (+0.09% and +0.19% for Kingston and Lee respectively) shows that in overall, there could not be a considerable change in total amount of rainfall compared to control scenario (modelled). While, for both Kingston and Lee sub-catchments, the given results from simulations show that by 2080s, the PET is expected to increase in all the seasons and the annual mean daily PET is projected to increase by 26.6%. Because PET is more affected by the temperature, it can be concluded that by 2080s the overall temperature is expected to increase in all the seasons. Moreover, based on the given results, there is a reduction in flow and subsurface storage in all the seasons in both sub-catchments. The results also showed 24.0% and 1.3% reduction in annual mean daily flow and subsurface storage in the Thames catchment respectively. This indicates that flow and subsurface storage in the Thames catchment are more influenced by temperature and consequently the PET, rather than rainfall.

In this chapter, by running water resources management model of LARaWaRM, the impacts of different climate change scenarios and different population and demand projections for four representative decades of 2010s (current), 2020s, 2050s and 2080s, on total reservoir level and drought frequencies in Thames catchment have been simulated. For this aim, the synthetic input flows (generated by SHETRAN) are used as input to LARaWaRM. This is to simulate the water storage and frequency of water shortage in Thames catchment. Despite the limitation in projecting the size of populations and climate projections which lead to a large uncertainty in estimating the reservoir storage in future, using water resources model of LARaWaRM made it possible for the decision makers to have a broader understanding of sensitivity of water resources in Thames basin. The given results indicate that the general trend in water storage is a continual decrease. This is a consequence of increase in demand for water which is due to the climate change, growth in population, and increase of living standards. It is also illustrated that by 2080s, the climate could have a greater impact on water supply security than population. Moreover, the combination of population and climate change projections have a greatest impact on reducing the water storage and increasing the frequency of drought incidents than climate change only or population change only scenarios.

Testing different decision adaptation options such as new reservoir, desalination plant, leakage reduction and multiple combinations of them shows that without further demand and supply adaptation options, the available water resources cannot meet the customers water demand in the area. Based on the given results, with no demand reduction, the combination of constructing new reservoir, desalination plant and leakage reduction is the most effective adaptation option which can contribute to reduce the number of drought days Level 4 in 2080s by 74.0%. While a 25.0% reduction in demand reduces the number of drought by 100% in 2020s and 2050s and leads to -64.0% drop in number of drought days Level 4 by 2080s. This shows that by 2050s, a 25.0% reduction in demand has the greatest contribution in reducing the number of

drought days compared to any of the individual or combined adaptation options with no demand reduction. In 2080s, using combined contribution of D+L+R in conjunction with 25.0% demand reduction, contributes to 91.5% reduction in number of drought days Level 4, and is the most effective adaptation option to tackle the negative impacts of climate and population change in the Thames catchment.

Chapter 5

Structured Uncertainty Analysis

5.1 Overview

This chapter presents structured uncertainty analysis conducted to assess the sensitivities of water resources in the Thames catchment. Impacts of uncertainties caused by socio economic drivers such as land cover, population change, per capita consumption and leakage on availability of water resources, in the 3 time slices of 2020s, 2050s and 2080s, are discussed.

5.2 Uncertainty analysis for Thames catchment

For uncertainty analysis socio economic parameters such as land use, population, per person demand (PCC) and leakage have been chosen to be analysed. For this aim, two scenarios for land use, nine scenarios for population, 15 scenarios for PCC and ten scenarios for leakage have been considered. Considering 4 different time slices (control, 2020s, 2050s and 2080s) for each of these possibilities, there are 10800 different combinations to be analysed. Since analysing this amount of data in terms of simulation time, is extremely expensive, only a few critical combinations are discussed here. For understanding the impacts of these parameters, each time only one of them is changed while the other parameters are kept constant. All the abbreviations used in following sections are described in Table 5.1.

5.3 Uncertainty in land use change

Based on GLA (2014*a*), under medium growth scenario, population in London is expected to be around 12 million by 2080s which shows 50.0% growth in population compare to 2010. This population growth may lead to an increase the need for housing and urbanization development in the area. So it would be of interest to understand how urbanization growth would affect the water availability in the Thames catchment.

Uncertainty Scenarios	Adaptation Options (A)	Population (P)	Per Person Demand (D) (l/p/d)	Leakage (L) (Ml/d)	Land Cover (U)
A1-P (0%)-D (0%)-L (0%)-U1	No adaptation	8,107,073	168	670	Current
A1-P (All)-D (0%)-L (0%)-U1	No adaptation	All population scenarios	168	670	Current
A1-P (0%)-D (All)-L (0%)-U1	No adaptation	8,107,073	All demand scenarios	670	Current
A1- P (0%)-D (0%)- L(All)-U1	No adaptation	8,107,073	168	All leakage scenarios	Current
A1-P (0%)-D (0%)-L (0%)-U2	No adaptation	8,107,073	168	670	New

Table 5.1: Abbreviation description for uncertainty analysis scenarios.

Current land cover map with 1 km (provided by LCM2007) and 5 km resolutions are illustrated in Figure 5.1.

For uncertainty analysis it was decided to explore the impact of urbanisation in Thames catchment but unfortunately there is no clear information about future expansion of urban area. In order to understand the impact of urban expansion in this catchment, it is assumed that number of grid cells with urban land cover doubles. Also there is an assumption that this urbanisation expansion is mostly take place around the current areas with urban land cover. Therefore, at first the number of urban grids with 1 km resolution are doubled, by converting the land cover of non-urban grids to urban land cover. Then new land cover map (with 1 km resolutions) is aggregated to 5 km resolution.

For increasing the urbanized area, it is assumed that first grids with the shrubs, then bare grounds and finally arable areas are converted to urban areas. In converting the land cover of the grids, from non-urban to urban, based on screen belt policy preserving green areas such as grass, deciduous forests and evergreen forests is of the essence. However, in some of the areas within the Thames catchment changing grass cells to urban is inevitable, but is tried to preserve them as much as possible. By increasing the urban developments (in 1km map) and reducing the resolution to 5 km, the number of urban cells in Kingston is increased from 30 to 87, and in Lee catchment increased from 10 to 15 cells. Figure 5.2 show the land cover maps for 1 km and 5 km resolutions after increasing the urban areas. Table 5.2 summarizes the number of cells with different land covers for current and increased urban developments in the Lee and Kingston sub-catchments, with 5 km resolution.

Vegitation type	Lee		Kingston	
	Current	New land cover	Current	New land cover
1. Arable	29	24	247	222
2. Bare	0	0	1	0
3. Grass	1	1	101	71
4. Deciduous Forest	0	0	14	14
5. Evergreen Forest	0	0	3	3
6. Shrub	0	0	1	0
7. Urban	10	15	30	87
Total number of cells	40		397	

Table 5.2: Number of cells for different land cover, in Lee and Kingston sub-catchments with 5 km resolution.

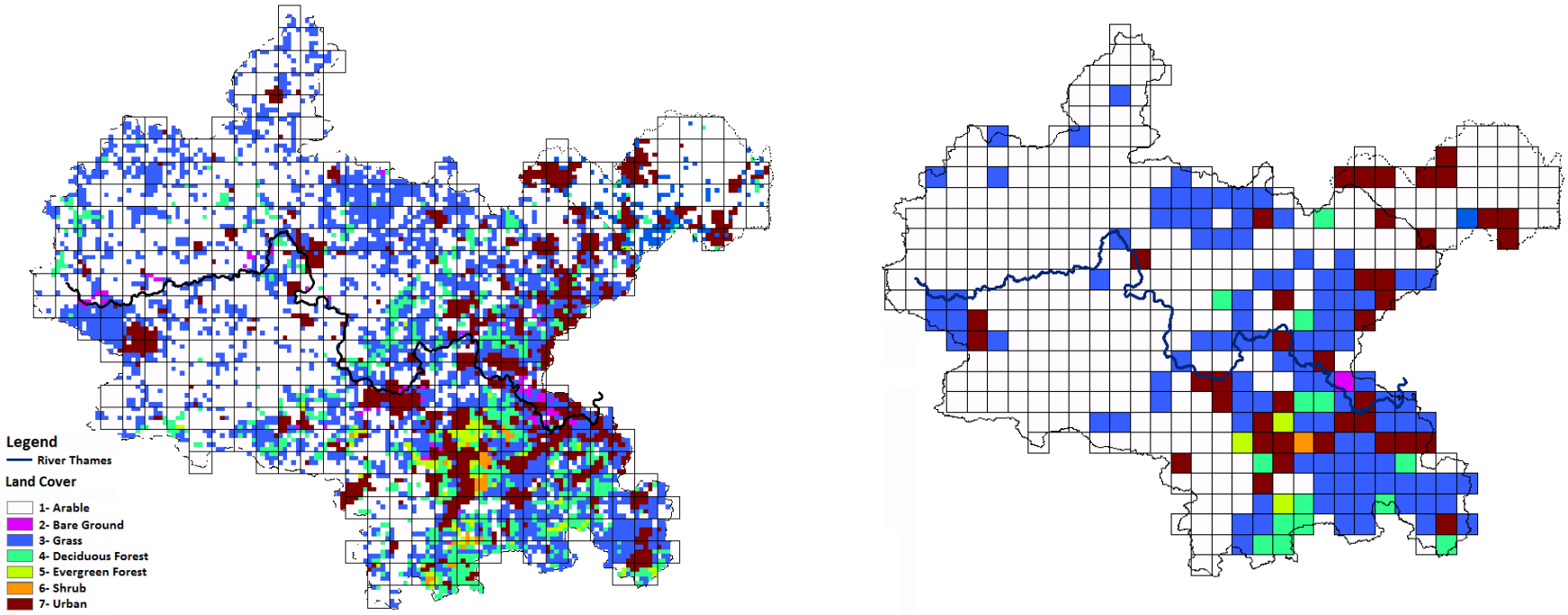

(a) (b)

Figure 5.1: Thames catchment current land cover map a) 1 km b) 5 km

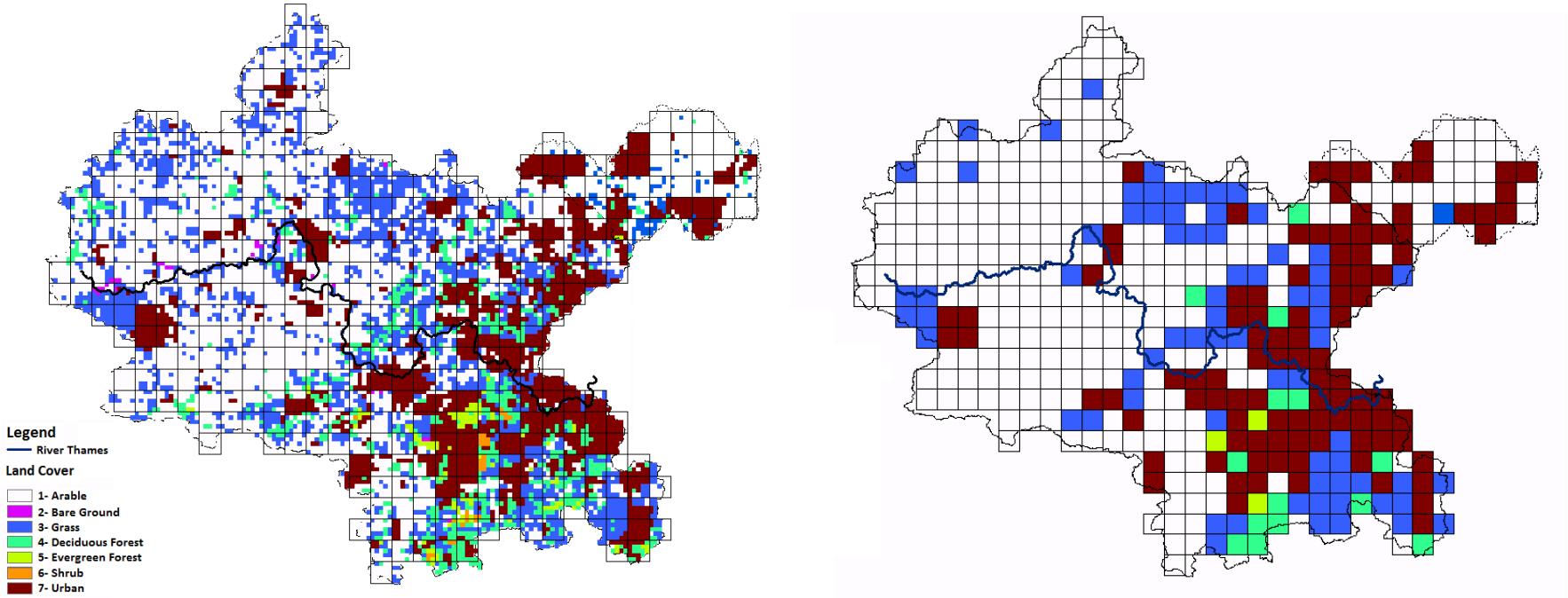

(a) (b)

Figure 5.2: Thames catchment land cover map with increased urban developments a) 1 km b) 5 km

5.3.1 Land cover change and flow

5.3.1.1 Thames sub-catchment

The increase of urbanization in 1 km land cover map in Kingston sub-catchment, led to a 190.0% rise in number of the urban cells with 5 km resolution. In order to investigate the impacts of urbanisation expansion in this catchment, SHETRAN was run with the new land cover map at 5 km resolution. Figure 5.3 illustrates total annual flow in the Kingston sub-catchment before and after increasing urbanization in the area for years between 1991 and 2002 (the calibration period). The results show that due to the urbanisation, the annual discharge in Kingston increases. This increase in discharge show that, although the majority of Kingston catchment is arable, as a result of urbanisation, there are more impermeable areas in this catchment which leads to an increase in surface water run-off. The detailed percentage of changes in the annual flow are shown in Table C.1. Based on the results, a 190.0% increase in urban area in Kingston catchment raises the annual discharge by 3.4% to 20.1%.

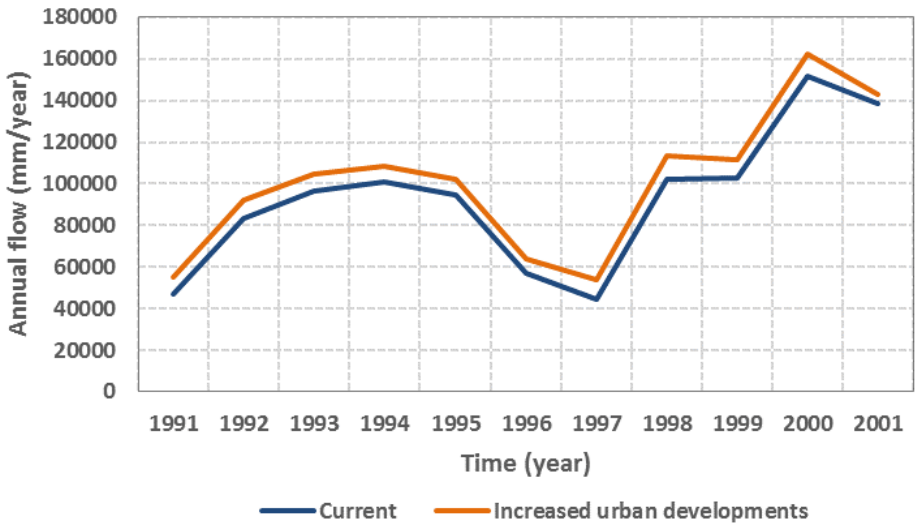

Figure 5.3: Impacts of increasing urban area on total annual flow in Kingston sub-catchment (1991-2001).

SHETRAN was run for control and future scenarios with new land cover grids. Figure 5.4 illustrates the boxplots[1] of mean flow at Kingston after increasing the urbanization and the results are compared with the current land cover in Table 5.3. In all of the time slices, the projected flow with new land cover is more than the current one. Urbanization expansion in this area, led to increase the mean flow by 4.5% to 24.0% in 2020s, and 5.9% to 29.4% in 2050s. This increase is projected to be greater by 2080s, as between 6.4% to 31.0% increase in mean flow is expected to happen. In all of the future time slices, the minimum increase in mean flow occurs during spring,

[1]Each of the boxplots indicates the median, 25th, and 75th percentile values. Whiskers show the 1.5 times of inter quartiles (IQRs), the difference between 25th and 75th percentile values. The small crosses are outliers, which are any points of data that lies below (25th percentile - 1.5 IQRs) or above (75th percentile + 1.5 IQRs).

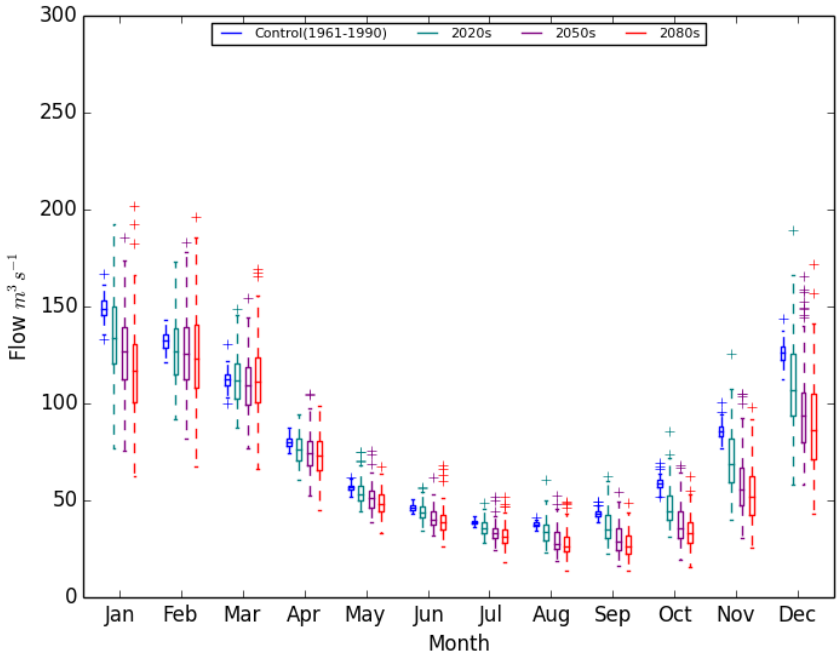

Figure 5.4: Boxplots of mean flow in Kingston sub-catchment after increasing urban area.

especially in April. The maximum increase in mean flow occur during autumn and winter, when there is more precipitation and the soil, as a result of urbanization, is less permeable.

5.3.1.2 Lee sub-catchment

The Lee catchment is mostly, regarded as an arable area. By increasing the urban cells and running SHETRAN for the calibration period an increase in peak flows and annual discharges is observed. Figure 5.5 compares the total annual flow in Lee catchment before and after increasing urbanization in the area. The detailed percentage of annual changes are shown in Table C.2. As a result of urbanisation, there is more impermeable area in the catchment which also lead to an increase in surface water in case of rainfall. Based on the results, a 50.0% increase of urban area in the Lee catchment increasing the annual discharge by 2.9% to 25.0%.

For control and future scenarios, the mean flow in each months are illustrated in Figure 5.6 and Table 5.4. As it can be seen, similar to the Kingston sub-catchment, in all of the time slices, the projected flow with new land cover is greater than the current. The urbanization expansion in this area, led to an increase in the mean flow by 4.3% to 25.2% in 2020s, by 3.3% to 22.3% in 2050s and by 3.3% to 19.8% in 2080s, compared to the current land cover. However, unlike Kingston, for Lee the range of projected change in mean flow is greater for 2020s. In all of the future time slices, the rate of change in mean flow during spring and summer is less than autumn and winter, when there is more precipitation and the soil, as a result of the urbanization is less permeable.

Month	Flow (m^3/s)								Change (%)			
	Current land cover				Increased urban developments							
	Control (1961-1990)	2020s	2050s	2080s	Control (1961-1990)	2020s	2050s	2080s	Control (1961-1990)	2020s	2050s	2080s
Jan	139.51	122.17	111.16	101.70	148.84	134.46	126.83	118.19	6.69	10.06	14.09	16.21
Feb	128.12	120.43	117.06	114.18	132.33	127.74	127.03	126.27	3.29	6.07	8.52	10.59
Mar	108.83	106.59	103.27	104.92	112.64	112.31	110.29	113.09	3.50	5.37	6.79	7.79
Apr	77.66	73.53	71.46	69.22	80.08	76.85	75.66	73.65	3.11	4.51	5.88	6.40
May	53.90	50.74	47.76	45.18	56.68	54.28	51.57	49.02	5.16	6.96	7.97	8.51
Jun	42.87	40.39	37.57	35.95	46.39	44.24	41.34	39.80	8.20	9.54	10.03	10.72
Jul	35.53	32.87	30.16	28.55	38.86	36.21	33.37	31.77	9.36	10.14	10.63	11.27
Aug	33.37	30.22	26.08	24.58	37.61	34.22	29.54	28.18	12.69	13.23	13.27	14.67
Sep	36.78	31.37	25.67	23.27	43.26	36.90	30.21	27.28	17.62	17.62	17.68	17.23
Oct	49.24	38.32	31.17	27.51	59.07	46.88	38.55	34.10	19.97	22.32	23.66	23.96
Nov	73.18	57.28	45.91	40.61	85.92	71.02	59.39	53.45	17.40	23.98	29.38	31.62
Dec	112.96	95.03	78.77	70.96	125.78	111.08	96.90	89.80	11.35	16.89	23.02	26.54

Table 5.3: Comparing mean flow in Kingston sub-catchment before and after increasing urban area, and % change relative to the current land cover.

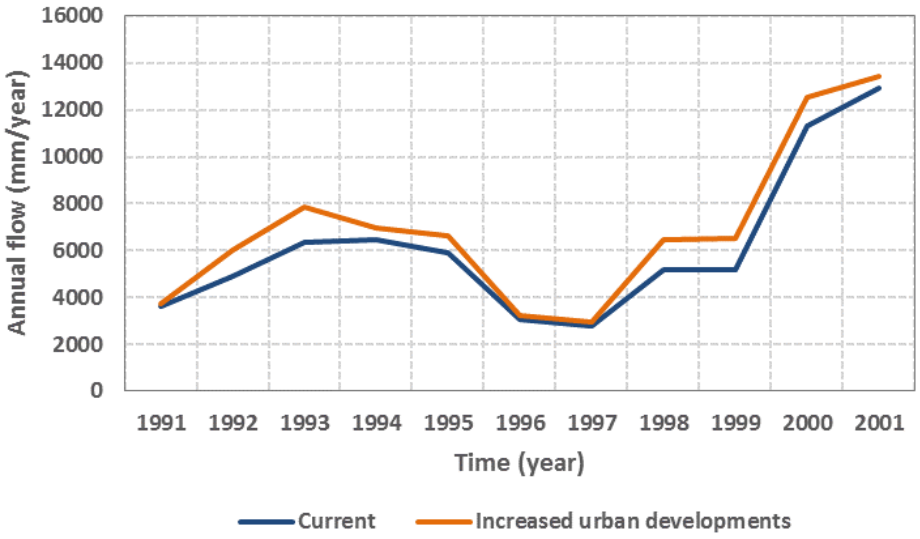

Figure 5.5: Impact of increasing urban area on total annual flow in Lee sub-catchment (1991-2001).

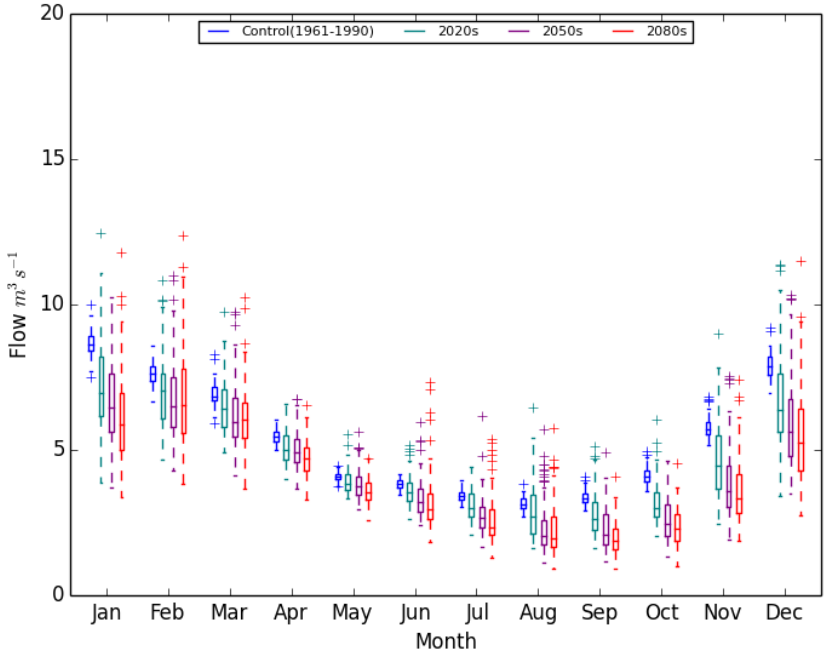

Figure 5.6: Mean flow in Lee sub-catchment after increasing urban area.

For the Lee sub-catchment, it is expected to have more than 25.0% increase in discharge by December in control and 2020s, while in 2050s the maximum increase is expected to occur in January (22.2%). By 2080s the maximum rise in mean flow occurs in February by 19.8%, compared to the current land cover.

5.3.2 Land cover change and water resources availability

After running SHETRAN for the new land cover, the water resources model of LARaWaRM was run with new sets of inflow modelled by SHETRAN for the Thames catchment. Figure 5.7 shows the impact of urbanization growth on number of demand saving days (demand saving days have been discussed in section 3.3 and Figure 3.3) for control, 2020s, 2050s and 2080s in the Thames catchment. This figure compares the number of drought days before and after increasing the urban area. The mean number of demand saving days and the percentage of change compared to the current land cover are listed in Table C.3.

The results show that after increasing urbanisation, in all of the time slices there is a decreasing trend in number of the drought days. In control scenario, the urbanization expansion reduces the number of days with demand saving Level 4 by 100%. This is also leads to a significant reduction in number of days with demand saving Level 1, 2 and 3. In 2020s, the number of drought days at Level 1 reduces by 42.5%. Also, compared to the current land cover, there is an 81.0% reduction in mean number of drought days at Level 4. In 2050s, the number of drought days at Level 3 and 4 are reduced by 62.0% and 75.0% respectively.

By 2080s, as a result of increasing the urbanization, similar to other time slices, number of days in Level 1 has the maximum reduction. Level 2 and 3 are reduced by 42.0% and 52% respectively. The results also show that the mean number of Level 4 drought days are expected to reduce by 66.0%.

Figure 5.8 presents the total reservoir storage in Thames catchment after increasing the urbanization in this area. The monthly boxplots illustrate an increase of uncertainty in variation of reservoir level during summer, fall and especially winter. Table C.4 compares the total reservoir level before and after increasing the urbanized area. The comparison shows that urbanization development increases the total reservoir storage in all of the time slices and reduces the size of the boxplots and distributions in range of the uncertainty in reservoir storage projection compared to the current land cover (see Figure 4.27 (a)).

In the control scenario, the total reservoir storage is estimated to increase by 0.01% to 6.5%. The maximum rise of 6.5% is expected to occur in October. While in 2020s the percentage of changes range from 0.30% to 11.0%, maximum rise in reservoir storage is expected to occur in November and December. Also in 2050s, the total reservoir storage is expected to have the minimum raise of 0.30% in March and the maximum raise of 17.9% in November. Likewise, these changes are estimated to be even greater

Month	Flow (m^3/s)								Change (%)			
	Current land cover				Increased urban developments							
	Control (1961-1990)	2020s	2050s	2080s	Control (1961-1990)	2020s	2050s	2080s	Control (1961-1990)	2020s	2050s	2080s
Jan	7.17	5.81	5.39	5.10	8.66	7.20	6.59	6.07	20.75	23.98	22.33	18.97
Feb	6.81	5.91	5.64	5.67	7.64	7.02	6.78	6.79	12.20	18.94	20.13	19.83
Mar	6.29	5.65	5.36	5.30	6.89	6.51	6.21	6.14	9.59	15.19	15.85	15.81
Apr	5.13	4.68	4.56	4.35	5.48	5.11	5.01	4.72	6.87	9.13	9.78	8.67
May	3.95	3.74	3.64	3.47	4.09	3.91	3.80	3.60	3.75	4.66	4.51	3.62
Jun	3.66	3.43	3.19	3.09	3.83	3.60	3.31	3.21	4.82	4.77	3.89	3.96
Jul	3.27	2.99	2.66	2.51	3.42	3.12	2.75	2.59	4.75	4.32	3.35	3.30
Aug	2.98	2.73	2.27	2.20	3.17	2.88	2.36	2.28	6.13	5.37	4.06	3.54
Sep	3.11	2.65	2.21	1.95	3.36	2.80	2.29	2.00	8.25	5.63	3.79	2.74
Oct	3.59	2.90	2.48	2.27	4.10	3.16	2.62	2.36	14.28	9.03	5.68	4.08
Nov	4.61	3.91	3.46	3.27	5.74	4.66	3.89	3.59	24.60	19.22	12.64	9.64
Dec	6.27	5.40	4.92	4.76	7.89	6.76	5.91	5.54	25.92	25.16	20.26	16.42

Table 5.4: Comparing mean flow in Lee sub-catchment before and after increasing urban area, and % change relative to the current land cover.

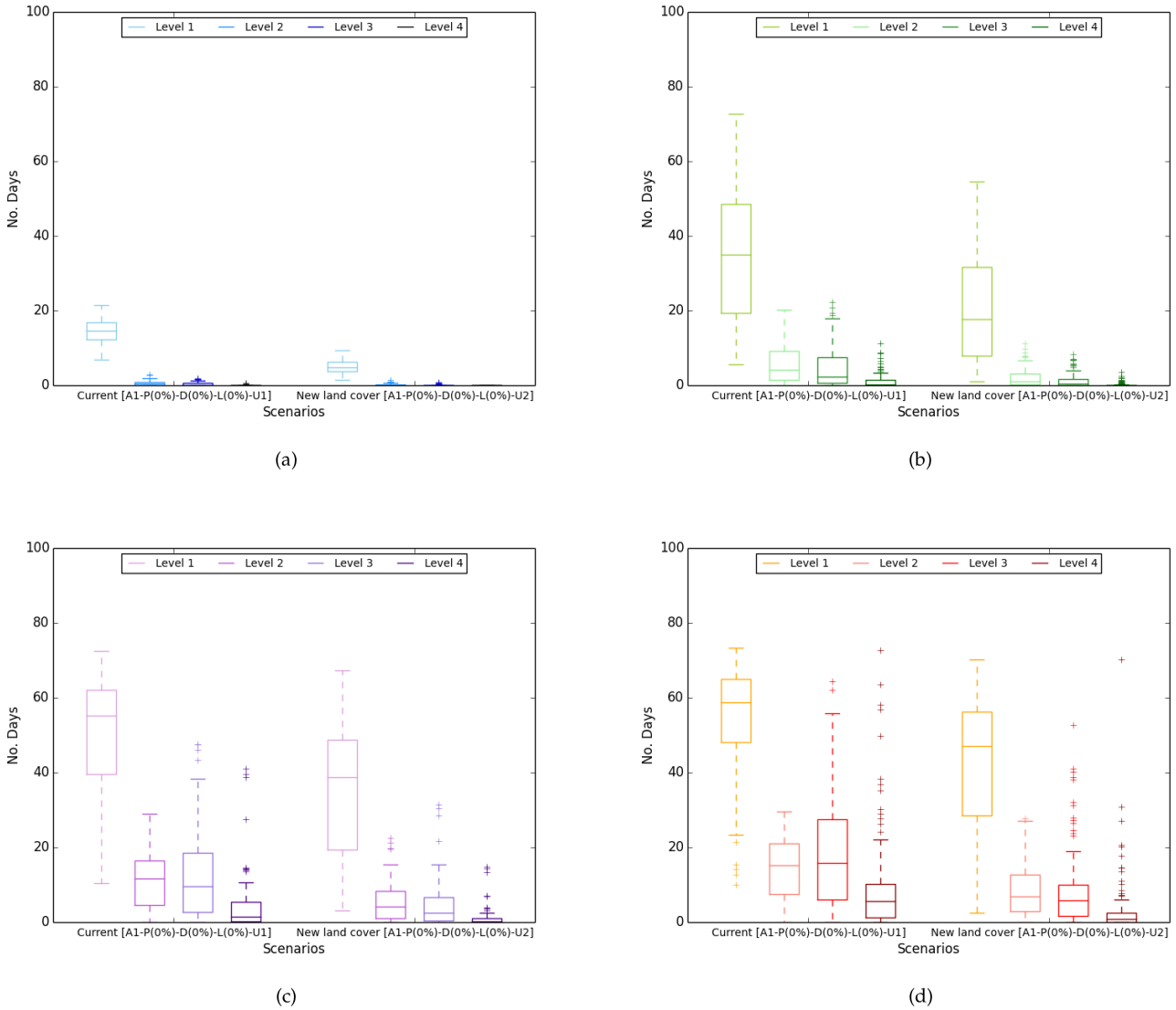

Figure 5.7: Impacts of land cover change on number of drought days in 100 years, when population, demand and leakage remain at their current level (A1- P (0%)- D (0%) - L (0%)- U1) vs (A1- P (0%)- D (0%) - L (0%)- U2): (a) Control, (b) 2020s, (c) 2050s, (d) 2080s

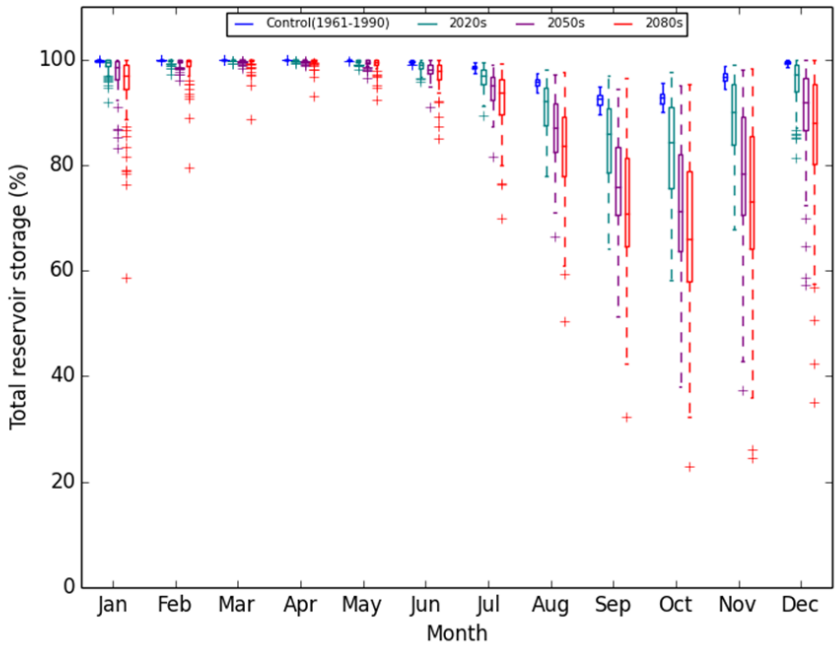

Figure 5.8: Boxplots of the total reservoir storage in Thames catchment after increasing the urbanization in this area (A1-P (0%)-D (0%)-L (0%)-U2).

in 2080s, as the reservoir storage is expected to increase by 0.68% to 22.0%, compared to the current land cover. Except the control scenarios, in all other future time slices, as a result of increasing the urbanized area, October, November and December are expected to have the highest rise in total reservoir storage compared to the current conditions while March is predicted to be the least impacted month.

5.4 Uncertainty in population change

Based on GLA (2014*a*), the population of London is expected to reach to 10.0 to 10.7 million by 2041. The London population projections for low, medium and high scenarios are illustrated in Figure 5.9. Table C.5 lists the actual and projected population between 2010 and 2080s. After 2040, the population projections are calculated by an interpolation technique. Note that, year 2010 has been chosen as a base scenario to make the comparison in this chapter. Figure 5.10 shows the percentage of change in London population relative to 2010.

Based on Figure 5.10, the London population is expected to rise by 41.0 to 60.0% by 2080s, compared to 2010 population. For uncertainty analysis, in order to cover all the possibilities, a wider range of changes in population is considered. Table 5.5 shows the range of change in population (between -15.0% and +75.0%) considered for this study. The Population (0.0%) indicates the population in year 2010.

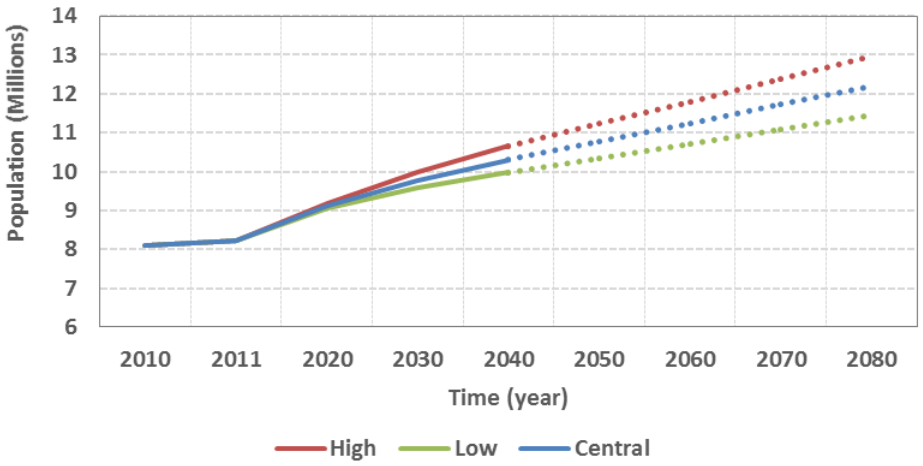

Figure 5.9: London population projections based on GLA (2013).

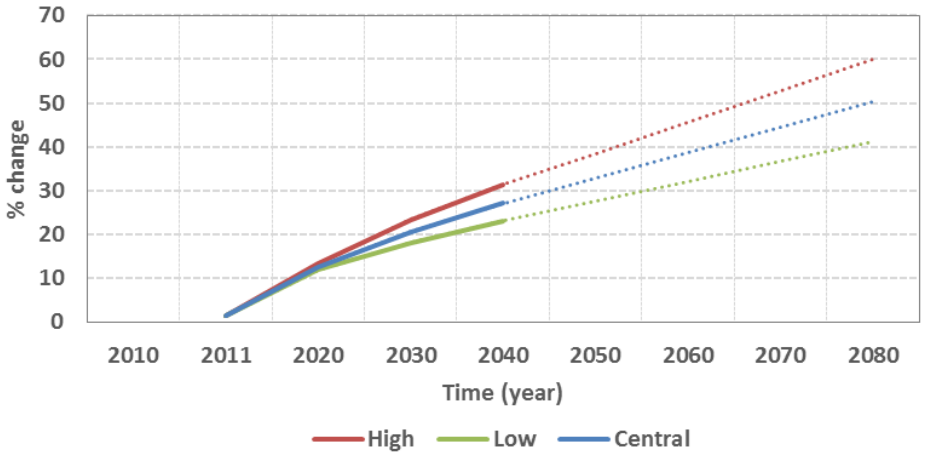

Figure 5.10: Percentage of change in population projections compared to 2010.

	Percentage of change								
	-15%	-10%	-5%	0%	5%	10%	25%	50%	75%
Population	6,891,012	7,296,366	7,701,719	8,107,073	8,512,427	8,917,780	8,613,765	12,160,610	14,187,378

Table 5.5: Percentage of change in population for uncertainty analysis (relative to 2010).

5.4.1 Population change and drought frequency

In this section, to understand the impacts of population change on water resources in the Thames catchment, the leakage and demand are considered constant at their current level and water resources model of LARaWaRM is run for nine different population scenarios (see Table 5.5). Figure 5.11 presents the number of demand saving days for each population change scenario, for control, 2020s, 2050s and 2080s. In this figure, population changes by -15.0% to +75.0% relative to the population of London in 2010 (P (0.0%)). The mean number of demand saving days are shown in Table C.6.

As it is shown in Figure 5.11, for all of the climate projections, change in population clearly affects the number of demand saving days. Based on the results, a 15.0% reduction in population of the Thames catchment, reduces the mean number of days with demand saving Level 4 by 72.0% by 2050s, and 61.0% by 2080s. On the other hand, increasing population significantly increases the demand saving Level 4 days. For instance, given a 5.0% increase in population, the number of Level 4 demand saving days increases by 50.0% in 2020s and if the population growth raised by 75.0%, the mean number of Level 4 demand saving days is 43 times more than that with P(0.0%).

Similarly, in 2080s, a decrease of 15.0% in population reduces the mean number of Level 1 demand saving days by 11.0%, Level 2 by 30.0%, Level 3 by 42.0% and more importantly Level 4 by 61.0%. In addition, if the population growth continued by 75.0%, in 2080s, the number of Level 4 drought days is expected to be 10 times more than the number of drought Level 4 of 0.0%. This means that impact of population change on Level 4 demand saving days is more significant than the other demand saving levels. Table C.7 shows percentage of change in mean number of drought days compared to current population (P (0.0%)).

Based on the results, for each of the time slices, there is a clear relationship between population change and number of demand saving days. Both population growth and climate projections increase the number of drought saving days in Thames catchment. These impacts are more significant in 2080s than the other time slices. In fact, if demand and leakage remain at their current level, by reducing the population, there is a decreasing trend on the number of demand saving days. On the other hand, increasing the population led to higher number of drought days. Therefore, when the growth of population and climate scenarios align together, they lead to a bigger variation and uncertainty on demand saving levels, especially at Level 4.

5.5 Uncertainty in per capita demand

Despite the growing population, there has always been an attempt to reduce the demand for water. To achieve that, water companies try to increase peoples awareness about the importance and limitation of natural water resources. This reduction can be gained by reducing per capita consumption (PCC), through promoting use of water

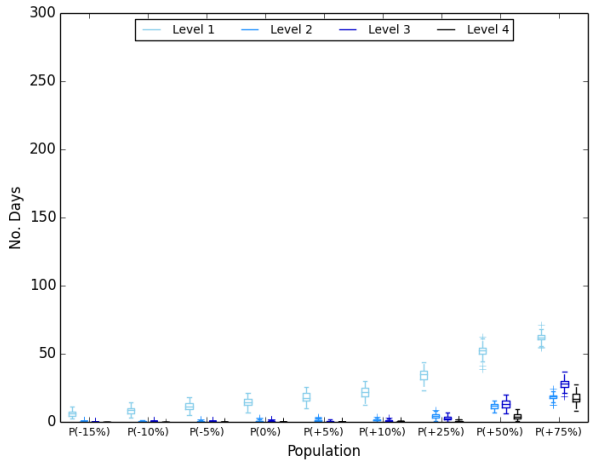

(a)

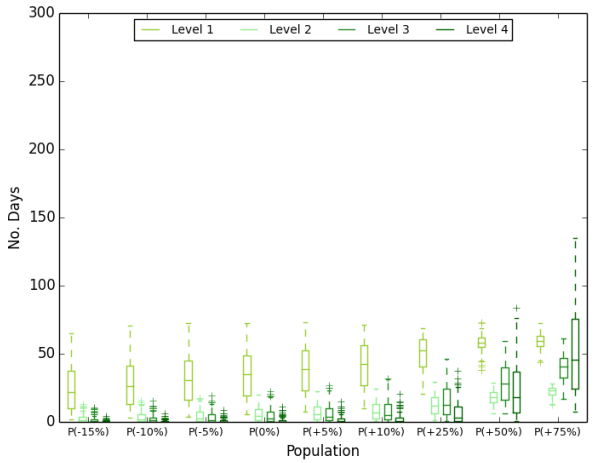

(b)

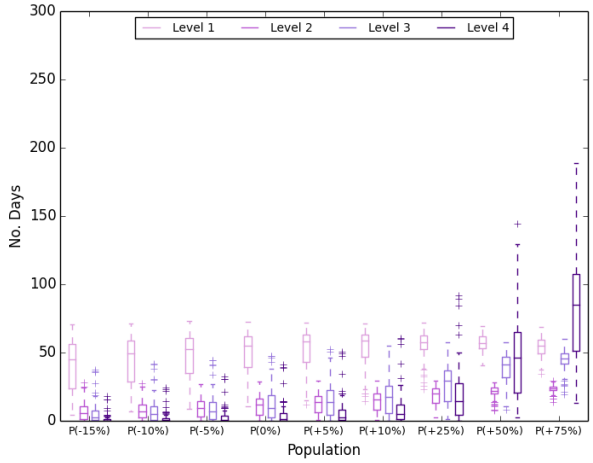

(c)

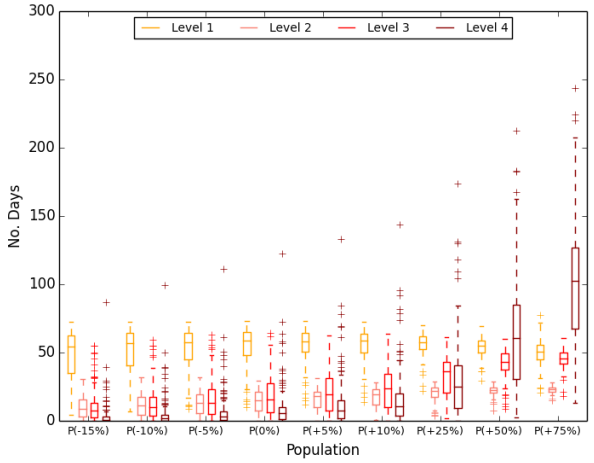

(d)

Figure 5.11: Boxplots of demand saving days (in 100 years), when only population is changed and demand and leakage are constant at their current level [A1-P (All)-D (0%)-L (0%)-U1]: (a) Control, (b) 2020s, (c) 2050s), (d) 2080s

efficient appliance as well as technological advances, installing meters and reduction in leakage. The annual average of household demand reported by Thames Water (2013) are shown in Table 5.6.

	2011/12			2039/40		
	Measured	Unmeasured	Average	Measured	Unmeasured	Average
PCC (l/p/d)	139.78	171.07	164	141.16	174.21	165.95

Table 5.6: Annual average per person demand for London (Thames Water, 2013).

As shown in Table 5.6, in 2011/12 the annual average per person demand for London was 164 l/p/d which based on Thames Water prediction, will rise to nearly 166 l/p/d by 2040. On the other hand, the standard per head water consumption for new built houses in this area, subject to the Building Regulations Part G, are expected to be 125 l/p/d (Defra 2008). Based on a code for sustainable homes level 5, this even can be reduced to 105 and 80 l/p/d. It has also noted by Thames Water that with effective measures and development of new technologies PCC in this area can drop to average 130 l/p/d by 2030 and remains at 125 l/p/d by 2040. There is also another possibility that PCC reduces to 120 l/p/d but as Thames Water noted there is still not enough evidence available to set the target demand on a lower level as 125 l/p/d in this area (Thames Water 2012).

Therefore, according to Thames Water (2013) PCC, in this area, is forecasted to range between 125 and 166 l/p/d by 2040s. Compared to 2011/12 (164 l/p/d), -24.0% to +1.2% changes in PCC might happen by 2040s. Consequently, compared to 2010 (168 l/p/d), there could be -25.6% to +2.8% changes in PCC by 2080s.

The aim of uncertainty analysis in this chapter is to test a rigorous range of possible changes that might occur in demand by 2080s. As a result, to cover all the possible ranges, it has been decided to extend the range of per capita demand from -50.0% to +20.0%. Percentage of changes and range of the predicted demands are illustrated in Table 5.7. In this table, PCC (0.0%) is the per person demand of water in 2010 which has been chosen as a baseline to make the comparison.

	Percentage of change														
	-50%	-40%	-38%	-30%	-25%	-20%	-15%	-10%	-5%	0%	0.50%	5%	10%	15%	20%
PCC (l/p/d)	84	101	105	118	126	134	143	151	160	168	169	176	185	193	202

Table 5.7: Percentage of change in per person consumption for uncertainty analysis (relative to 2010).

5.5.1 Demand change and drought frequency

In this section the impacts of household demand change on water resources are discussed. To achieve that, the water resources model of the Thames catchment has been run for 15 different PCC scenarios while leakage and population have remained

constant at their current level. Figure 5.12 illustrates the impact of PCC change on number of demand saving days for control, 2020s, 2050s and 2080s. In this figure, PCC changes between -50.0% to +20.0% relative to PCC in 2010 (D (0.0%)). The mean number of demand saving levels are demonstrated in Table C.8.

The boxplots in Figure 5.12, indicate that in each of the time slices, there is a direct link between the PCC and the number of demand saving days. In the control scenario, any change in PCC mostly affects the drought level 1, while in other climate projections, the PCC changes affect almost all of the drought levels. As it can be seen, increasing the PCC not only increases the median number of the drought days but also it leads to a larger variability and uncertainty in estimating the number of demand saving days.

By reducing the demand by 50.0%, there could be a 98.0% reduction in mean number of demand saving Level 4 in 2080s. On the other hand, by increasing the PCC by 20.0% there could be a significant rise in all demand saving days, especially in mean number of drought Level 4 which is estimated to increase by 147.0%.

Comparing different time slices shows that the impacts of PCC change in 2080s is more significant than the 2020s and 2050s. As Figure 5.12 indicates, the uncertainty in estimating number of Level 4 drought days in 2080s is much larger than control, 2020s and 2050s. Based on the data given in Table C.8, this happens because the impacts of increasing demand magnified more severely by climate projection in 2080s. Table C.9 shows percentage of change in mean number of drought days compared to the current demand (D (0.0%)).

5.6 Uncertainty in leakage trends

The growth of population and impacts of climate change on water resources urge the need to save water and reduce the wastage as much as possible. The Office of Water Services (Ofwat) set out targets for water utility companies to reduce leakage and wastage of water in their supplying area. For this aim, Ofwat monitors the companies to quantify their performance in reducing leakage to a sustainable level and achieving water efficiency target to save 1 litter per property per day (Ofwat 2009).

In the Thames Water supply area, 72.0% of leakage are from distribution loss which is happening in Thames Water distribution network and other 28.0% loss is happening in customers pipes which are the customers responsibility to fix them (Thames Water 2012). Thames Water supply infrastructure dates back to Victorian time, therefore age more than 100 years old (33.0% of them are more than 150 years old). Annual average leakage in Thames catchment which are reported by Thames Water, are tabulated in Table 5.8 (Thames Water 2017).

As illustrated in Table 5.8, the annual average leakage for 2010 was 670 Ml/d while the target leakage was set by Ofwat to be 685 Ml/d. Thames Water reduced the leakage by managing pressure in older water networks, detecting leaks, fixing and replacing

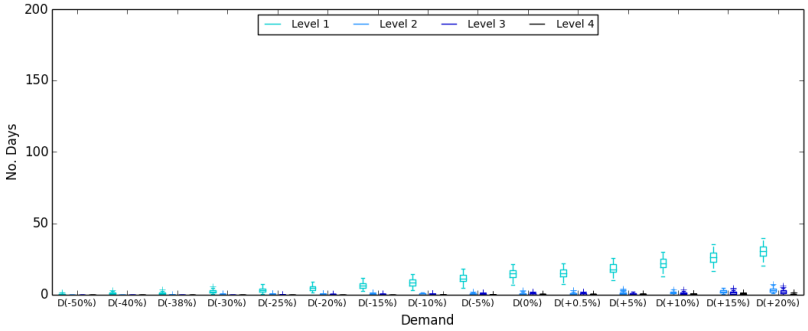

(a)

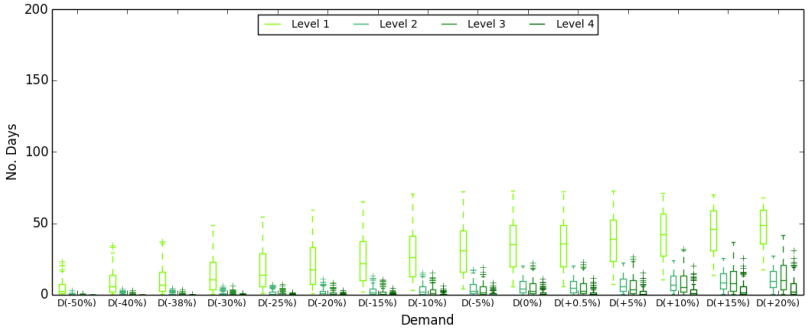

(b)

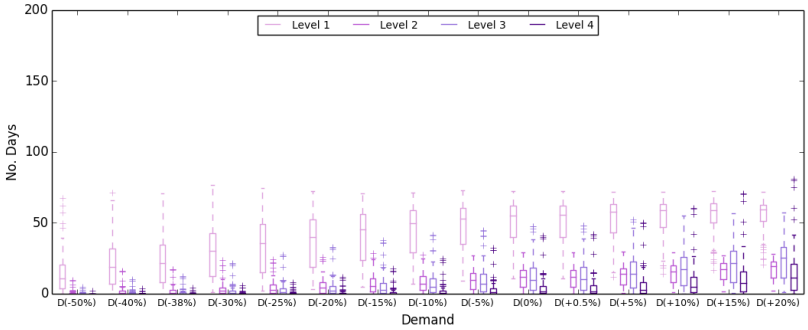

(c)

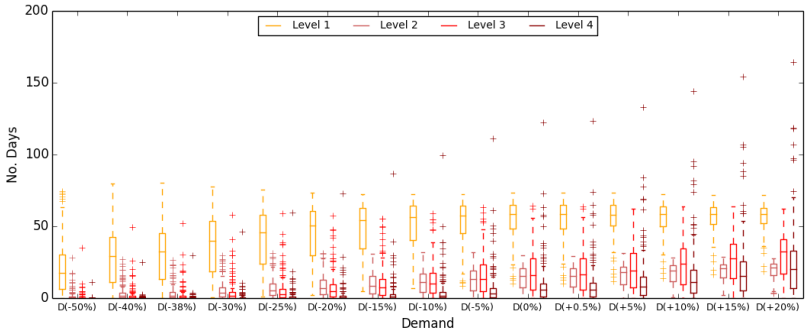

(d)

Figure 5.12: Boxplots of demand saving days (in 100 years), when only PCC is changed and population and leakage are constant at their current level (A1- P (0%)-D (All)- L (0%)- U1) : (a) Control, (b) 2020s, (c) 2050s), (d) 2080s.

old leaky water pipes. In 2013, the leakage rate in this area was reduced to 644 Ml/d (about 25.8% of supply) (Thames Water 2017).

It has also been noted in the Thames Water Annual Report (for 2014/15) (Thames Water 2017) that in 2015, due to the colder winter and higher rate of pipe burst, the annual average leakage in Thames catchment increased to 665 Ml/d. Although the leakage increased in this year, it was still below the target of 673 Ml/d set by Ofwat.

	Year				
	2010/11	2011/2012	2012/2013	2013/14	2014/15
Leakage target (Ml/d)	685	673	673	673	673
Annual average Leakage (Ml/d)	670	639	646	644	665

Table 5.8: Annual Average leakage reported by Thames Water (2013).

It is also highlighted by the Thames Water that the leakage in the Thames catchment is projected to reduce by 10.0% (59Ml/d) between 2015-20 (Thames Water 2012). Moreover, the target leakage for Thames Water is to reduce the leakage to 556 Ml/d by 2040s. Therefore, compared to 2010 it is expected to reduce the leakage by 17.0% by 2040s (3.8 Ml reduction each year). After the 2040s, the leakage might be maintained at this level, increase or reduce. As a result, it has been decided to consider a wider range of possibilities in the amount of leakage by 2080s. Table 5.9 shows the percentage of changes in leakage used for uncertainty analysis in this chapter. Leakage (0.0%) indicates the leakage in 2010 reported by Thames Water (2013).

	Percentage of change									
	-40%	-20%	-17%	-15%	-10%	-5%	0%	5%	10%	15%
Leakage (Ml/d)	404	536	556	569	603	636	670	703	737	770

Table 5.9: Percentage of change in leakage for uncertainty analysis (relative to 2010).

5.6.1 Leakage change and drought frequency

This section shows how leakage changes may affect water resource availability in the Thames catchment. To analyse the impact of leakage change, water resources model of the Thames catchment has been run for 10 different leakage scenarios while PCC and population have remained constant at their current level. Figure 5.13 shows the impact of leakage change on number of demand saving days for control, 2020s, 2050s and 2080s. In this figure, leakage changes between -40.0% to +15.0% of the average leakage in London in 2010 (L (0.0%)). The mean number of demand saving levels are tabulated in Table C.10.

In all of the time slices, the median number of days with drought Level 1 are significantly higher than the other drought saving days. In the control scenario, number of the days with drought Level 2, 3 and 4 are very low. While in 2020s, in

addition to drought Level 1, higher number of drought Level 2, 3 and 4 are expected to occur. By increasing leakage, there is a slight increasing trend in all levels of demand saving days. This trend is the same in 2050s and 2080s as well. In 2080s, by increasing the leakage by 10.0%, there is nearly 35.0% increase in number of drought days Level 4, while by reducing the leakage to 5.0% and even 10.0% , only a 10.0% reduction in Level 4 demand saving days is expected. But when 40.0% leakage reduction happens, the mean number of drought Level 4 estimates to reduce by 38.0%.

In fact, the results show +34.5% and -20.0% difference regarding 15.0% positive and 15.0% negative uncertainties respectively. This indicates that the positive uncertainty manifest itself to a bigger rate difference compared to the negative one. Table C.11 shows percentage of change in mean number of drought days compared to the current leakage (L (0.0%)).

5.7 Summary

In this chapter, for uncertainty and sensitivity analysis, different range of possible changes in socio-economic drivers such as population, per capita consumption, leakage and land cover as well as their impacts on availability of water, for the 3 time slices of interest (2020s, 2050s and 2080s), in Thames catchment were tested. The analysis indicated that increase of population, PCC and leakage have direct impact on water availability which eventually lead to increase in number of Level 4 demand saving days.

Based on the results, in all of the future time slices, increasing the urban development in Thames area increases the flow in the catchment which eventually led to a reduction in number of demand saving days compared to the current land cover in this catchment. Based on the results, by 2080s, a 190.0% increase in urban area in the Kingston sub-catchment led to an increase in the mean flow by 6.4% to 31.0% and a 50.0% increase in urbanized area in Lee sub-catchment, increases the mean flow by 3.3% to 19.8%, compared to the current land cover. In all of the future projections, the rate of change in mean flow during spring and summer is less than autumn and winter, when there is more precipitation and the soil as a result of urbanization, is less permeable.

The results also show that the mean number of Level 4 drought days are expected to reduce by 65.0% compared to the current land cover. The comparison between total reservoir level before and after increasing the urbanized area, shows that urbanization development increases the total reservoir storage in all of the time slices. Also for the new land cover, the size of the boxplots and uncertainty, distributions in range of the reservoir storage projections, are smaller relative to the current land cover. In all of the future time slices, as a result of increasing the urbanized area, October, November and December are expected to have the highest raise in total reservoir storage compared to the current conditions while March is predicted to be the least impacted month. The

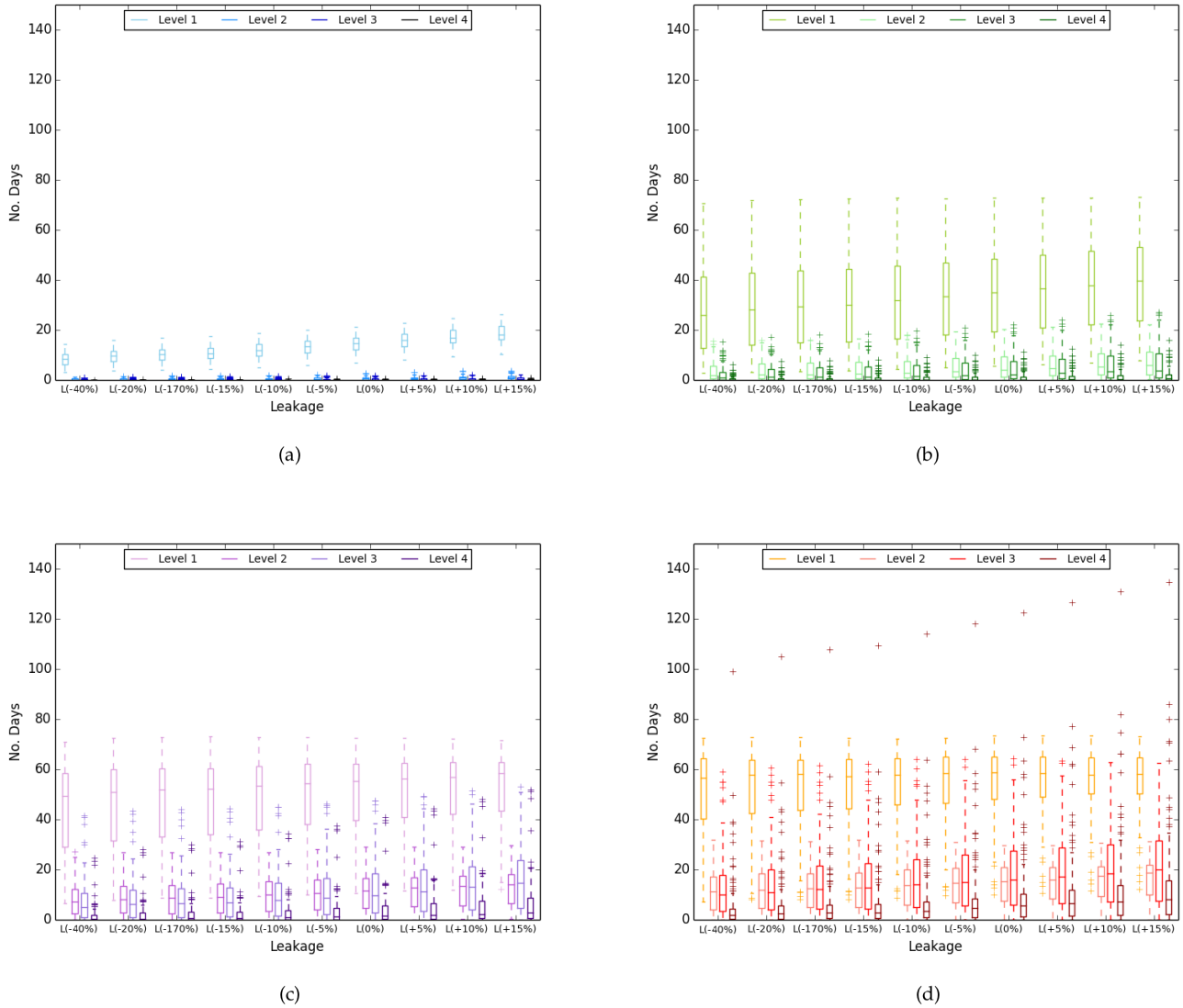

Figure 5.13: Boxplots of demand saving days in 100 years, when only leakage is changed and population and demand are constant at their current level (A1- P (0%)- D (0%) - L (All)- U1): (a) Control, (b) 2020s, (c) 2050s), (d) 2080s

range of changes in the reservoir storage by 2080s, is expected to be between 0.68% and 22.0%, compared to the current land cover.

The analysis show that, due to a linear relationship between population and PCC, once one of them is changed and the other one considered constant, the overall effects on number of demand saving days is the same. For instance, when demand and leakage are constant at their current level, -10.0% reduction in population leads to 44.6% drop in number of Level 4 demand saving days for 2080s, which is exactly the same as the time when there is 10.0% reduction in demand while population and leakage are kept at their current level. The results also show that change in PCC and population directly affects the number of drought days. In fact, by reducing the population and PCC, there is a decreasing trend on the number of demand saving days. On the other hand, increasing the population and PCC lead to increase the number of drought days. These impacts are more significant in 2080s than the other time slices. In fact, when the growth of population or demand, align with the climate scenarios, they lead to a greater variation and uncertainty on demand saving levels estimations, especially at Level 4.

The uncertainty analysis also indicated that the number of demand saving days are significantly affected by the amount of leakage in this catchment. When population and PCC are constant at their current level, by increasing the leakage, there is an increasing trend in number of demand saving days, and by decreasing the leakage there is a reduction in number of drought days. The impacts of leakage change on number of demand saving days are more significant for 2080s which shows that the impacts of change in leakage magnifies more severely by the climate projection for further time slices. In the 2080s, the results show +34.5% and -20.0% difference regarding 15.0% positive and 15.0% negative change in leakage respectively. This indicates that the 15.0% increase in leakage manifest itself to a bigger rate of change in number of demand days compared to the 15.0% reduction in leakage. The results also show that reducing leakage by 10.0% lead to 10.2% drop in number of drought days at Level 4 by 2080s, while a 10.0% reduction in population/PCC leads to 44.6% drop in number of Level 4 demand saving days. This comparison shows that for a similar amount of change, the impacts of population or PCC on number of demand saving days are more significant than the leakage.

Chapter 6

Reliability and Robustness Analysis

6.1 Overview

This chapter discusses the implications of the results presented in Chapter 5. This is presented by considering two combinations of uncertainties that are at the low and high plausible extremities of water availability. The robustness of different adaptation options, under current and future climate changes, against these extremities are considered. Sensitivity testing of the water resource model is used to help explain the results.

6.2 Analysis of combined uncertainties

In order to analyse the impacts of combined uncertainties, many different combination of population, demand (PCC) and leakage could be considered. Since analysing all of the possible combinations in terms of simulation runs, is computationally expensive, two water use scenarios are considered here. These two scenarios are constructed by taking the combination of uncertainties in population change, leakage and per person water demand (PCC), that give the lowest (Low Scenario) and highest (High Scenario) water use. The range of plausible changes in these parameters are discussed in Chapter 5. These two extreme water scenarios are illustrated in Figure 6.1 and the percentage changes in their components, relative to their current values, are listed in Table 6.1.

	Population	Demand (PCC)	Leakage
High scenario	+75%	+20%	+15%
Low scenario	-15%	-50%	-40%

Table 6.1: High and low water use scenarios

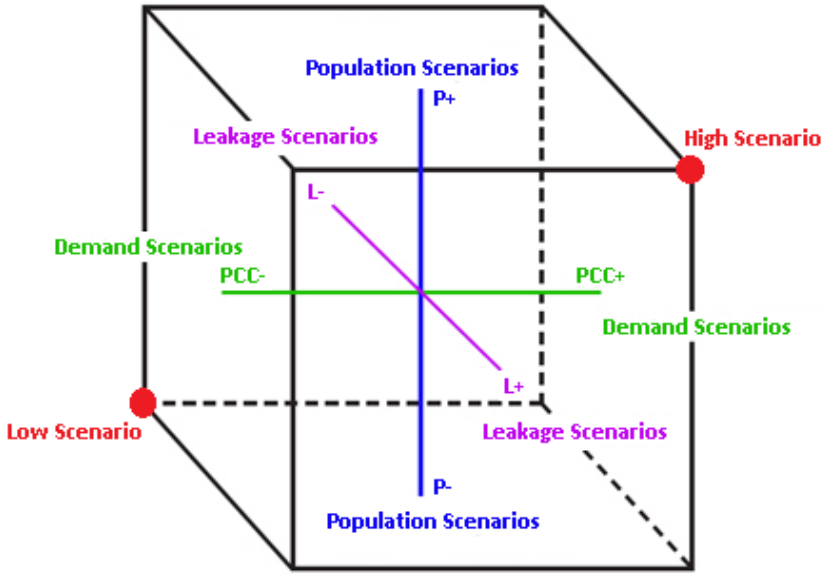

Figure 6.1: High and Low water use scenarios with no adaptation options

6.2.1 High Scenario: population, demand and leakage are at maximum levels

In this combination it is assumed that all of the parameters including population, demand and leakage are at their maximum possible levels. In fact, it is assumed that the population increases by 75.0% to 12.1 M, the PCC increases by 20.0% to 202 l/p/d, and at a same time, as a result of increasing the demand and ageing the water supply networks, the leakage increases by 15.0% to 770 Ml/d. Figure 6.2 shows how the number of drought days would be affected if the High water use scenario occur. The difference in mean number of drought days for current and the high scenario are tabulated in Table D.1.

Based on the boxplots[1] illustrated in Figure 6.2, by increasing the population, leakage and demand to their maximum levels, there would be a huge difference in number of drought days compared to the current situation. In all the time slices there is a significant increase in the number of droughts at Levels 2, 3 and 4. In 2050s and 2080s, there is a reduction in number of days with drought Level 1 while a considerable jump in number of droughts in Levels 2, 3 and especially 4 are predicted. Based on the given results, by 2080s, the number of Level 4 drought days is expected to be 14 times greater than current numbers. In other words, High water use scenario leads to 1318.0% increase in the number of days with drought. In all of the time slices, the variability in the number of Level 4 demand saving days is much larger than the other demand saving days. This indicates a higher uncertainty in prediction of long-term impacts of socio economic drivers in availability of water in Thames catchment.

[1]Each of the boxplots indicates the median, 25th, and 75th percentile values. Whiskers show the 1.5 times of inter quartiles (IQRs), the difference between 25th and 75th percentile values. The small crosses are outliers, which are any points of data that lies below (25th percentile - 1.5 IQRs) or above (75th percentile + 1.5 IQRs).

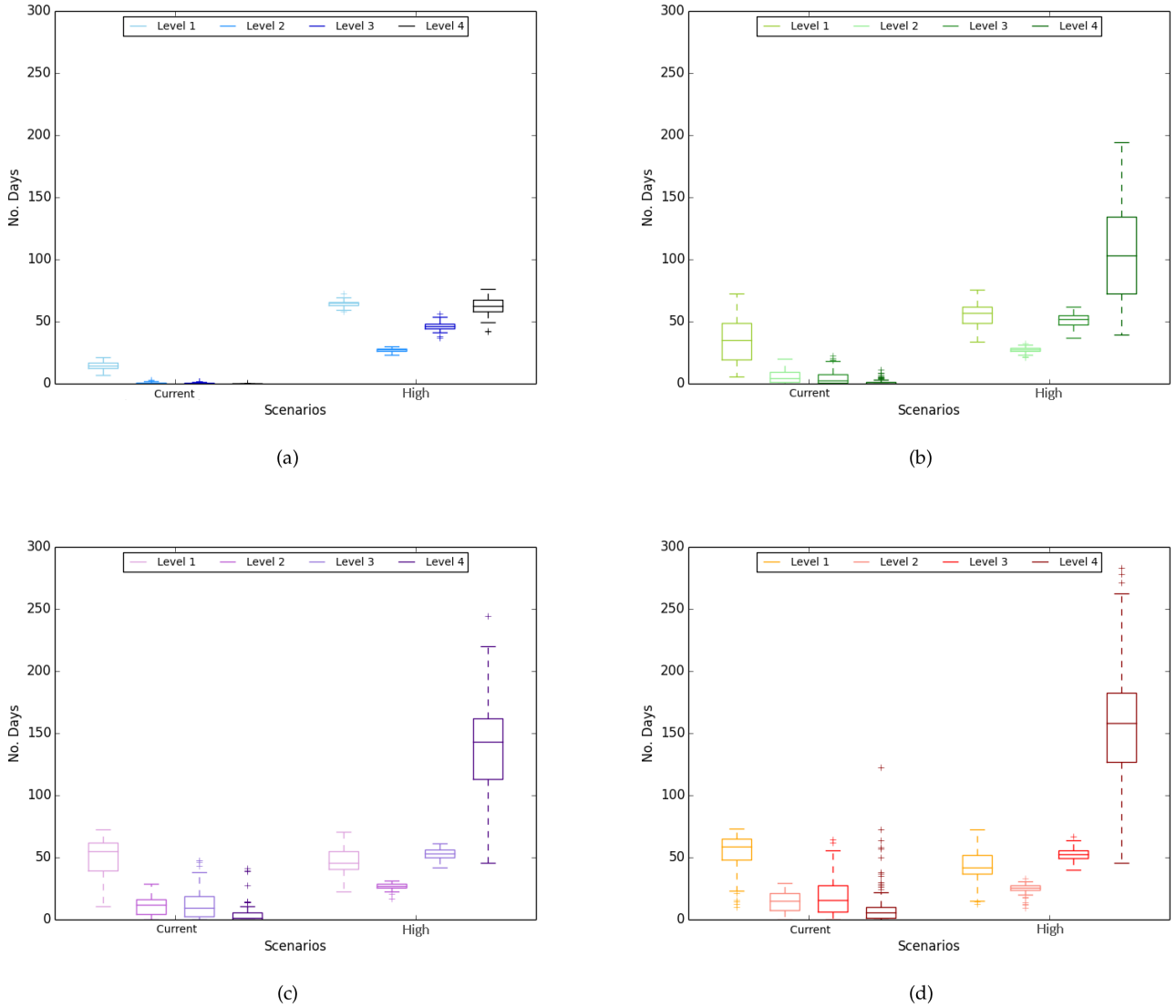

Figure 6.2: Impact of High water use scenario on mean number of drought days (current land cover) for: (a) Control, (b) 2020s, (c) 2050s, (d) 2080s

6.2.2 Low Scenario: population, demand and leakage are the minimum levels

This combination is one of the best case scenarios, that is within the range of plausible uncertainties, that could occur in Thames catchment for water demand. In this scenario, all of the parameters including population, demand and leakage would be at their minimum levels. It is assumed that population reduces by 15.0% to 6.8 M, PCC reduces by 50.0% to 84 l/p/d, and leakage decreases by 40.0% to 404 Ml/d. Figure 6.3 shows the impact of Low water use scenario on mean number of the drought days compared to current scenario. More details are listed in Table D.2.

Results in Figure 6.3 and Table D.2, show that by reducing the population, leakage and demand to their minimum levels, in all of the time slices there would be a significant drop in number of drought days compare to the current situation. In the control scenario, number of drought days are estimated to be almost zero and in 2020s there is 96.9% reduction in number of droughts at Level 1, while there is not any Level 2, 3 or 4. In the 2050s and 2080s, there is a huge reduction in number of drought days, especially Level 4 which has 100.0% reduction. In all of the time slices, the number of Level 4 drought days is zero which indicates the importance of these three socio economic drivers in availability of water in the Thames catchment.

The mean reservoir level for the Low, current and the High water use scenarios in Thames catchment are illustrated in Figure 6.4. In this figure, there is a plot for each of the water use scenarios, which presents the mean, 10th and 90th percentile of reservoir storage for each month. More details are listed in Table D.7. As it can be seen, for the Low case scenario, the reservoir is almost full at the beginning of each year and by the end of summer there is a drop in the reservoir level. Even in October of 2080s, when the storage of water is expected to be at its lowest level, the reservoir is almost 80.0% full. After October, the reservoir starts to recover until April when it gets to its fullest condition. In contrast, for the High water use scenario, the reservoir is never 100.0% full. By 2050s, when the water storage is normally at its minimum level in October, the reservoir storage is only 7.5%. This gets even worse for the 2080s as there is only 5.4% storage in October. Table D.8 shows the percentage of change in mean reservoir level in High and Low water use scenarios compared to current scenario for control, 2020s, 2050s and 2080s.

6.2.3 Effectiveness of supply adaptation options

In this section the impacts of different adaptation options on the frequency of drought days, under the High water use scenario (with current land cover and also increased urbanization scenarios) are presented. For this aim, different supply adaptation options such as a desalination plant (D) with the capacity of 150 Ml per day, New reservoir (R) with capacity of 100 million m^3, and a combination of desalination and new reservoir (D+R) are considered.

The impacts of different adaptation options on the frequency of demand saving

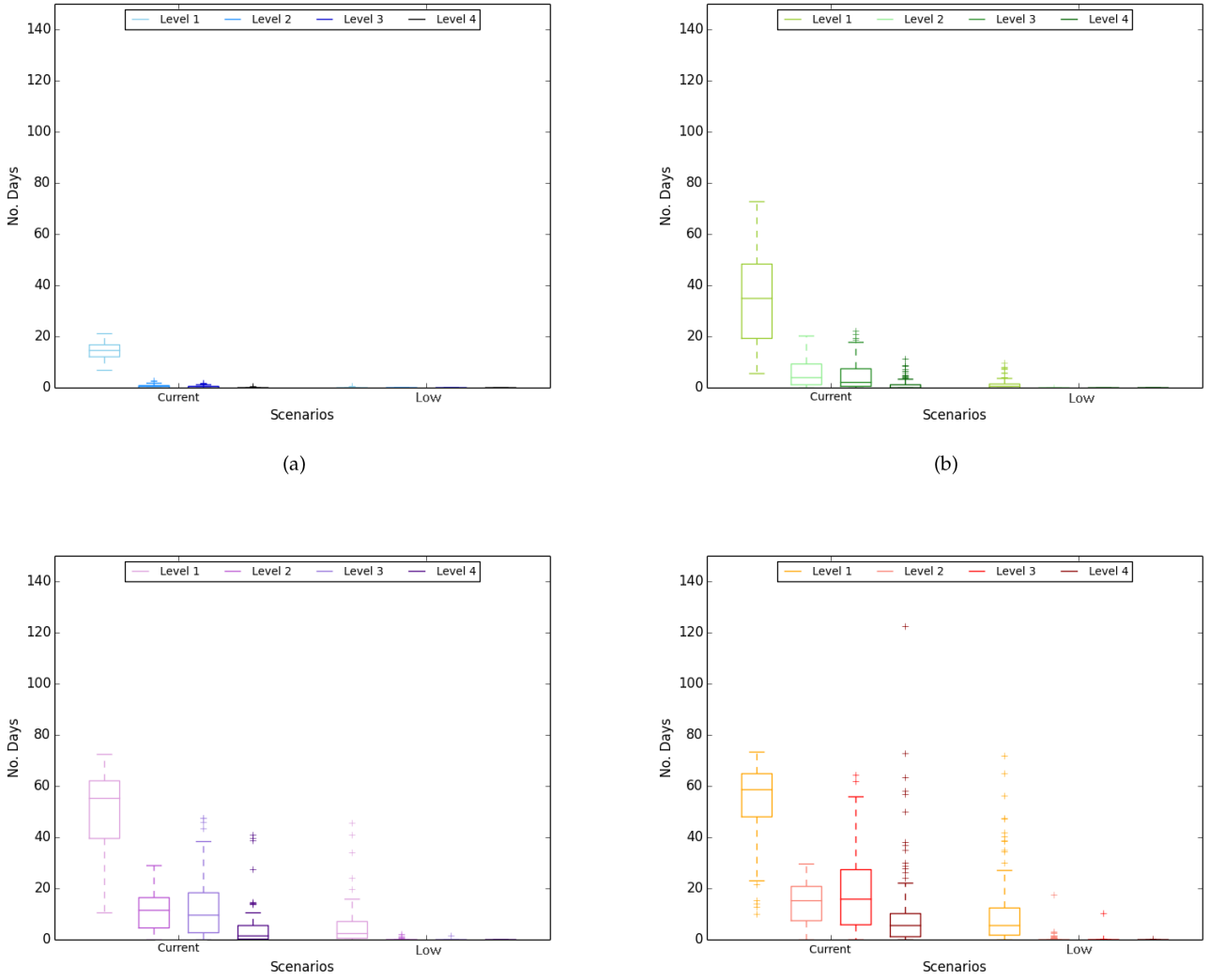

Figure 6.3: Impact of Low water use scenario on mean number of drought days (current land cover) for: (a) Control, (b) 2020s, (c) 2050s, (d) 2080s

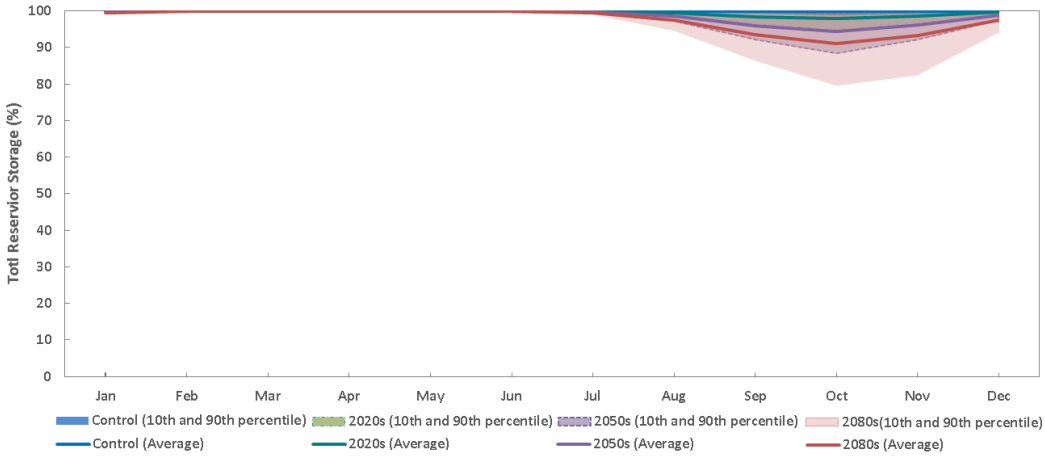

(a)

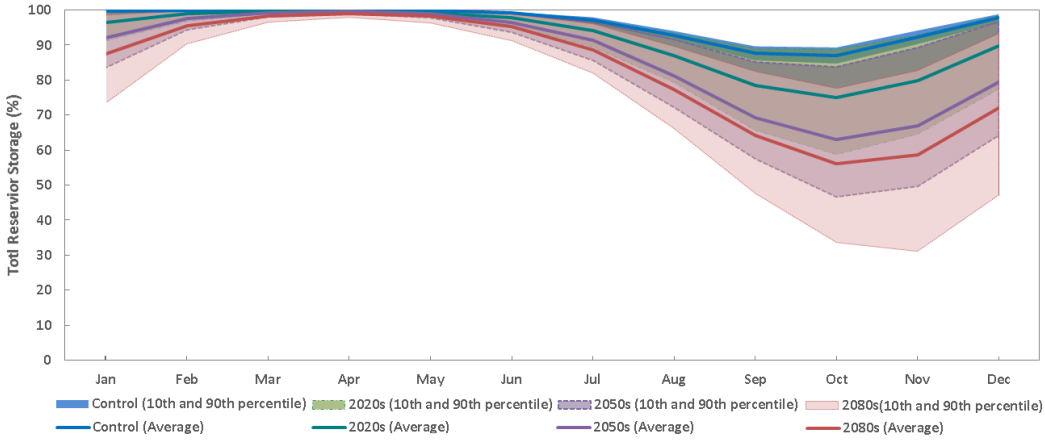

(b)

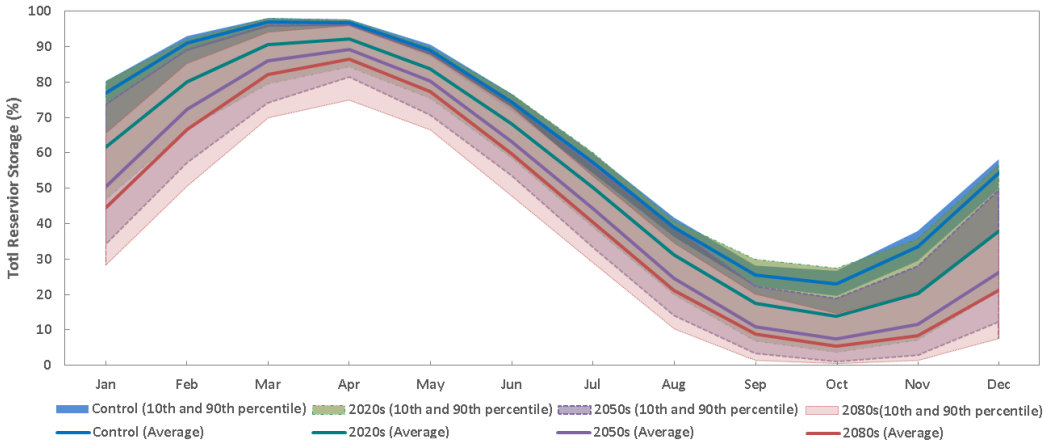

(c)

Figure 6.4: Mean total reservoir storage for: (a) Low water use scenario (b) current (1961-1990) (c) High water use scenarios.

days for High water use scenario with current land cover and increased urbanization scenarios, under different climate scenarios are illustrated in Figure 6.5. In this figure, each of the pie charts shows the proportion of mean number of days with drought Level 1, Level 2, Level 3 and Level 4. The diameter of the pie charts indicates the total number of the drought days. From this figure it is clear that the size of the pie charts increases for future time series which shows that there is an increasing trend in total number of drought days from current climate to 2080s. It is also seen that the number of drought Level 4 increases for further time slices.

It is also shown that for each climate scenario, the adaptation options reduce the number of Level 4 drought days. However, the change in total number of drought days is not significant. From the pie charts, it can be seen that for different adaptation options, the proportion of drought days Level 2 and 3 are similar. Also there is a reduction in number of drought days Level 4, while there is an increase in number of drought days Level 1. This shows that the amount of supplied water provided by adaptation options contribute in reducing the Level 4, but they are not sufficient to prevent incidence of drought. Based on the results, for High water use scenario, generally the combination of desalination and new reservoir is the most effective adaptation options in reducing the number of Level 4 drought days, while desalination can be categorised as the least effective options among the other levels.

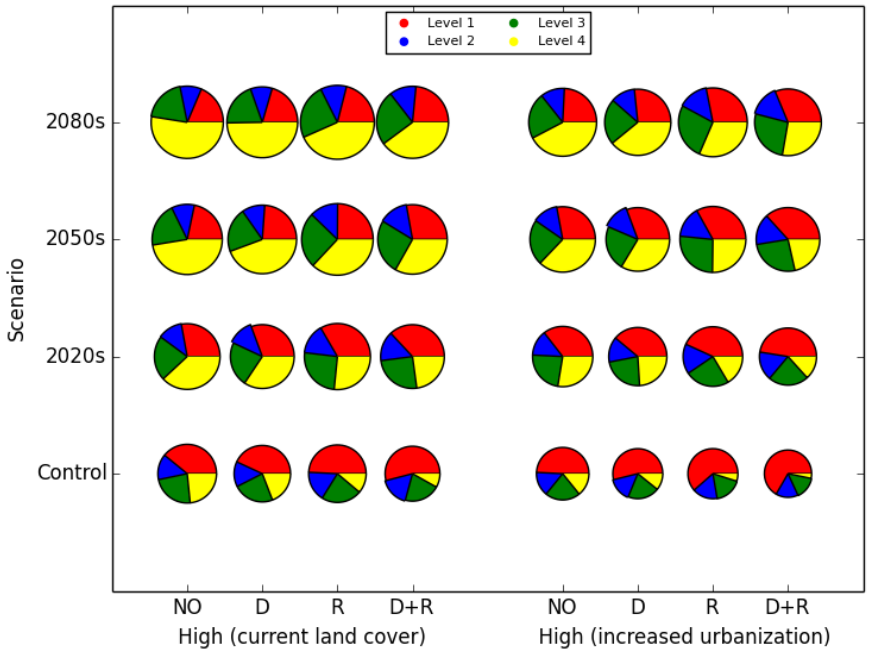

Figure 6.5: Mean number of drought days in 100 years, for different adaptation options, for High water use scenario with current land cover and increased urbanization. Each of the pie charts shows the proportion of mean number of Level 1, Level 2, Level 3 and Level 4 demand saving days. The diameter of pie charts indicates the total number of the demand saving days.

In addition, it can be seen that with current land cover, in 2020s, desalination plant and constructing a new reservoir reduces the mean number of drought Level 4 by 14.8% and 29.3% respectively. Consequently, combination of desalination plant and a new reservoir the number of drought Level 4 by 34.5%. However, this combination is less effective in 2050s as it only reduces the number of drought Level 4 by 31.0% but still is the most effective option in reducing the frequency of drought days. In 2080s, same as other time slices, although all adaptation options have substantially contributed to reducing the number of drought days, still the combination of desalination and new reservoir with 24.7% reduction in number of drought Level 4 is the most effective option.

Moreover, from comparing the pie charts for High scenario with current land cover and the increase urbanization scenario, it is explored that contribution of the adaptation options on reducing number of drought days with increased urbanisation is greater than the current land cover scenario. For example, in 2020s the combination of desalination and new reservoir may lead to 57.0% reduction in number of drought Level 4 while this reduction, for current land cover, was about 43.5%. Similarly for 2050s and 2080s, for combination of these adaptation options, the reduction in number of drought Level 4 are 45.3% and 36.7% respectively which are approximately 45.0% and 40.0% less than the number of the drought days for High scenario with current land cover for the similar time slices.

The spread and range of uncertainty in projecting the mean number of drought days for current and increased urbanization scenarios are presented in Figure 6.6 and Figure 6.7 respectively. The larger boxplots for 2080s indicates that the spread of uncertainty for further time slices, especially 2080s is greater than the others. As it can be seen the change in magnitudes of uncertainty through different time slices is non-linear which indicates that prediction for further time slices carry a higher rate of uncertainty.

More detailed results for the High water use scenario with current land cover are listed in Table D.3 and Table D.4. Results the for High scenario with increased urbanization are listed in Table D.5 and Table D.6.

6.3 Stress testing of water resources in London

The uncertainty analysis, one at a time and in combination, shows a non-linear system response. To understand this further, the water resources model (LARaWaRM) was stress-tested to explore how water resource responds to different long-term trends in flows. Two tests were undertaken, in both it has been assumed that input flows to the catchment were constant over 100 years. For the first test the LARaWaRM included the standard demand savings rules, the second removed demand savings from the system operation.

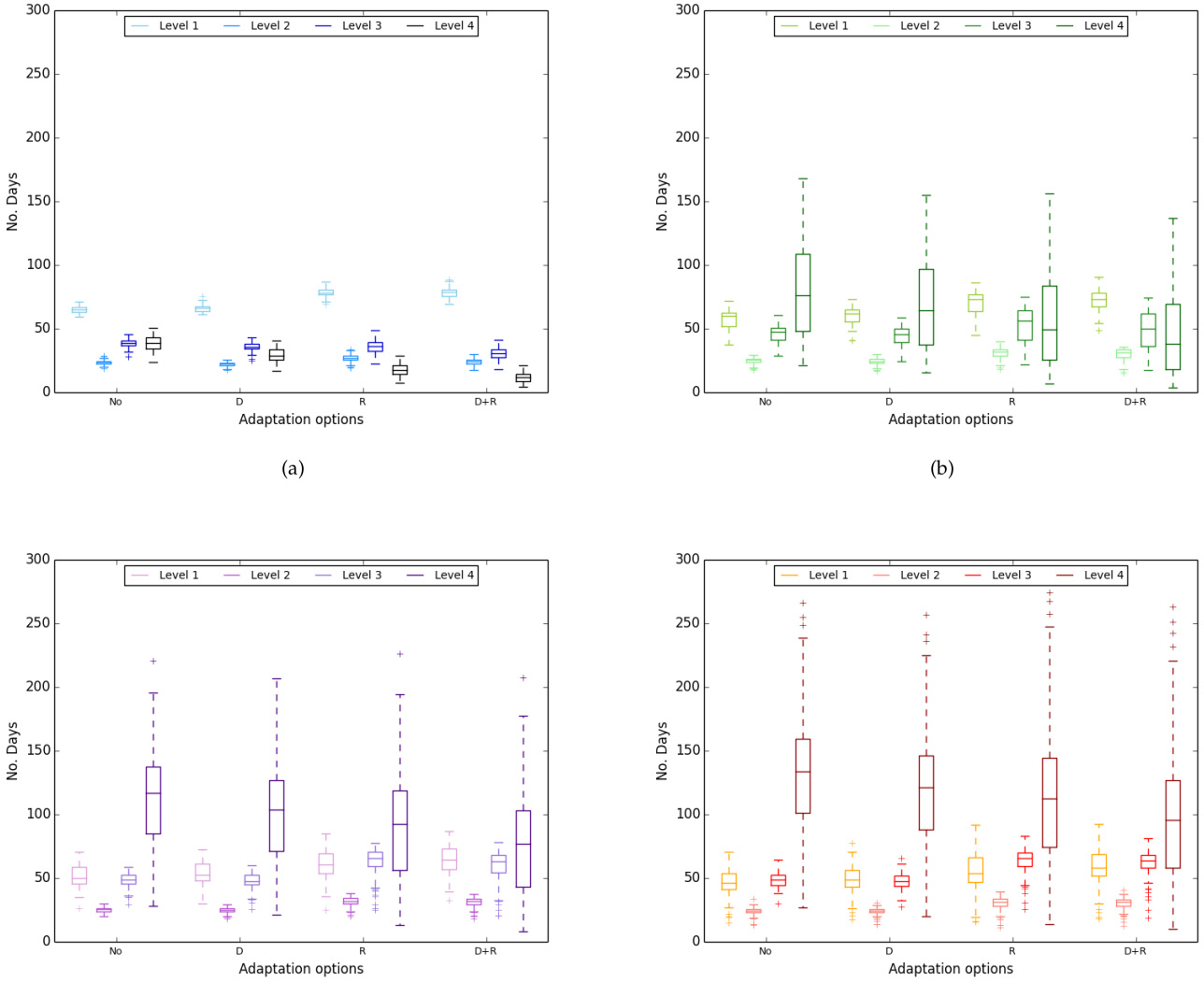

Figure 6.6: Adaptation options for High scenario with current land cover: (a) Control, (b) 2020s, (c) 2050s, (d) 2080s

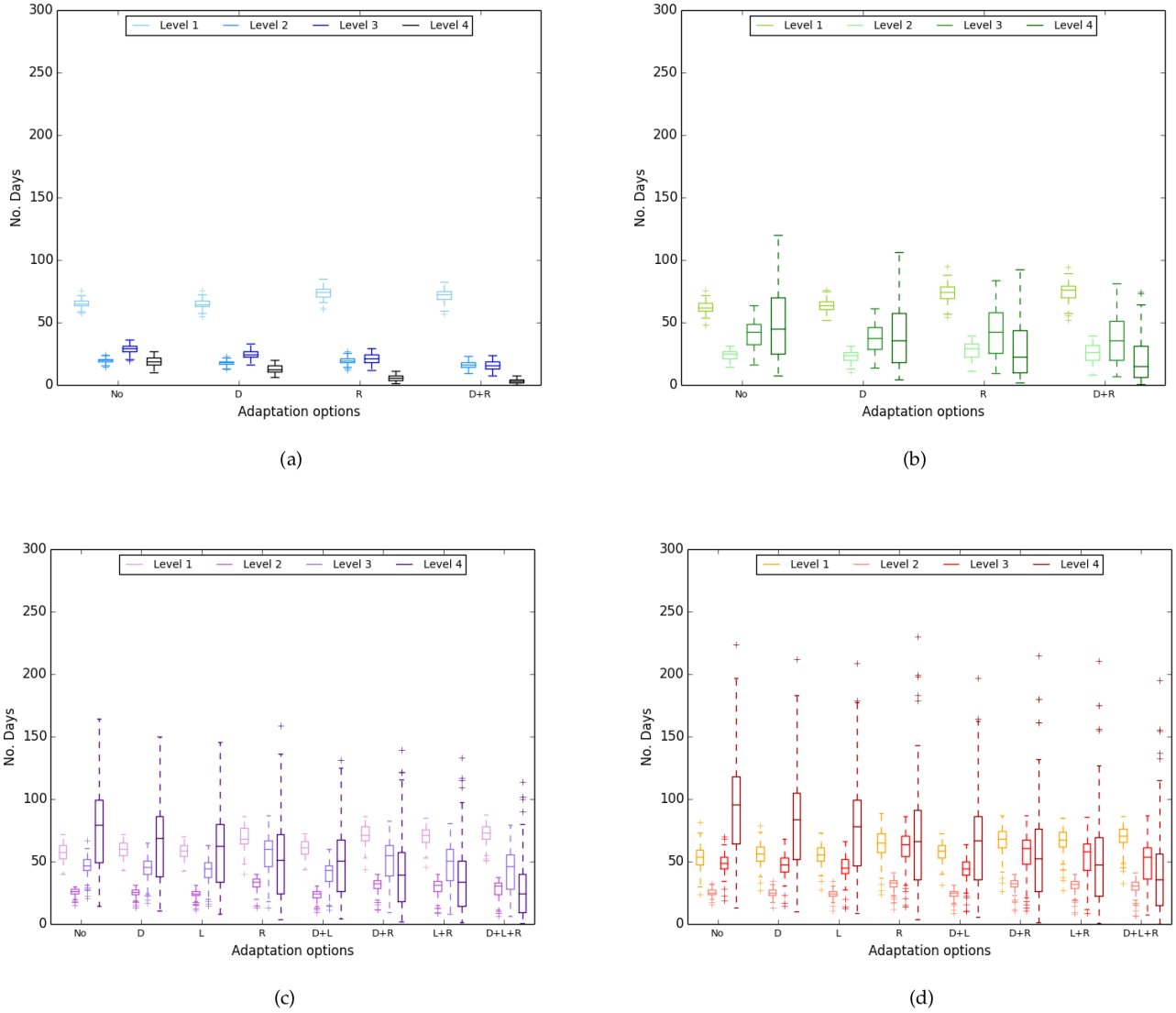

Figure 6.7: Adaptation options for High scenario with increased urbanization: (a) Control, (b) 2020s, (c) 2050s, (d) 2080s

6.3.1 Stress testing: current demand saving measures

In this stage it has been assumed that inflows from Kingston and Lee sub-catchments are constant every day, for 100 years and the demand saving levels are considered in the system. All other parameters such as population, demand and leakage are kept constant at their current levels. Just the response of the water resource system to different flows is considered. A range of possible input flows to the Thames catchment, at Kingston and for the River Lee for the minimum, mean, maximum and different quantiles (Q5, Q10, Q50, Q90, Q95) is calculated. The range of input flows from each sub-catchment, and also total flows to the Thames catchment are listed in Table 6.2. The input flows used for stress testing the Thames catchment in this study ranged between a minimum flow of 0 m^3/s and maximum flow of 633 m^3/s (Figure 6.8).

Statistics	Kingston	Lee	Total input flow (m^3/s)
Minimum	15.87	1.14	17.01
Q99	21.58	1.57	23.15
Q95	25.74	1.92	27.67
Q90	28.54	2.16	30.70
Q50	52.95	3.52	56.47
Average	74.11	4.73	78.84
Q10	149.99	8.48	158.47
Q5	183.59	11.76	195.34
Maximum	528.46	105.40	633.85

Table 6.2: Statistics of input flows in the Thames catchment.

Figure 6.10 shows the relationship between flow and mean reservoir level in the Thames catchment. As it can be seen, by increasing the long-term input flow, the reservoir level (averaged over the year) increases gradually. For flows less than 19.54 m^3/s the reservoir is almost empty, but by increasing the flow, the reservoir storage increases too. Based on the given results, for flows more than 39 m^3/s (Q70) the reservoir is always full.

Figure 6.11 shows how long takes for the water system to empty. According to the following graph, by increasing the input flow, it takes longer to empty. For instance, in worst situation when there is no rainfall and there are not any flows in Thames catchment (input flow= 0 m^3/s), it takes 88 days for the reservoir to reach the lowest level. By increasing the input flow to 19.5 m^3/s it takes nearly 2 years (663 days) for the system to empty and for flows bigger that 19.5 m^3/s the reservoir never empties.

Figure 6.12 shows the number of days that reservoir levels drop below service level thresholds over a 100 year time series. The results are also listed in Table D.9. According to the analysis, for low flows, the number of Level 4 demand saving days is very high. By increasing the input flow, the number of Level 4 demand saving days reduces and eventually, if the inputs flow reaches to 27.66 m^3/s, it drops to zero. As

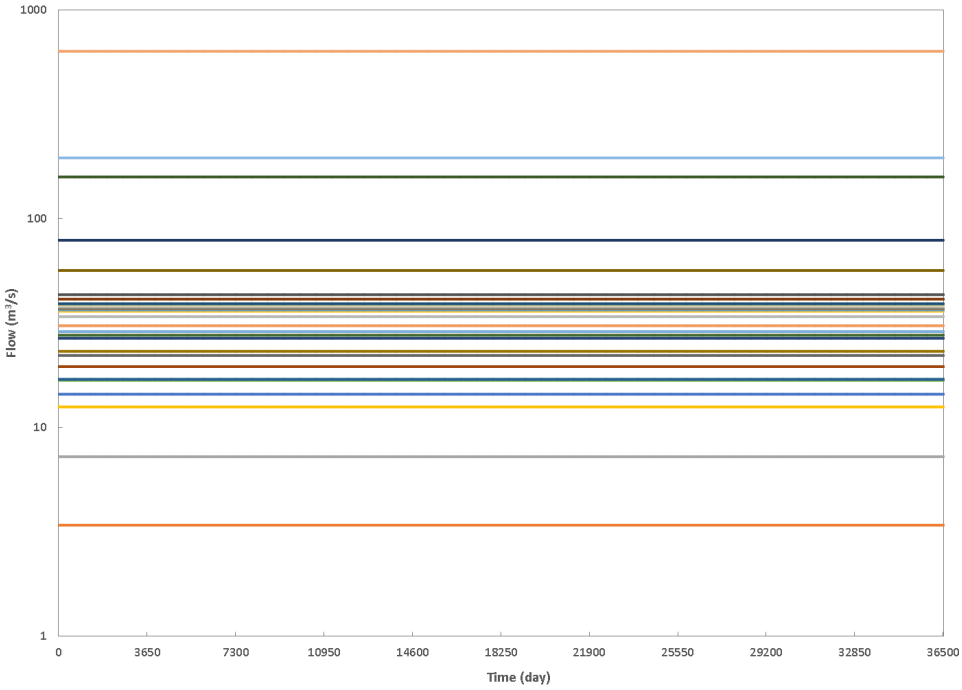

Figure 6.8: Input flows for stress testing the water resources system in Thames catchment.

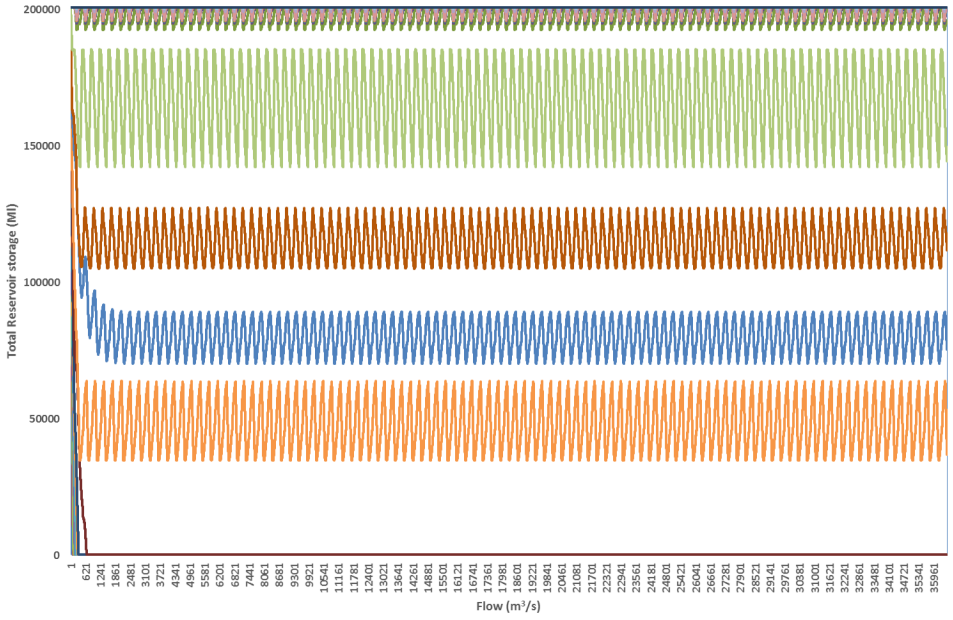

Figure 6.9: Total reservoir storage in the Thames catchment.

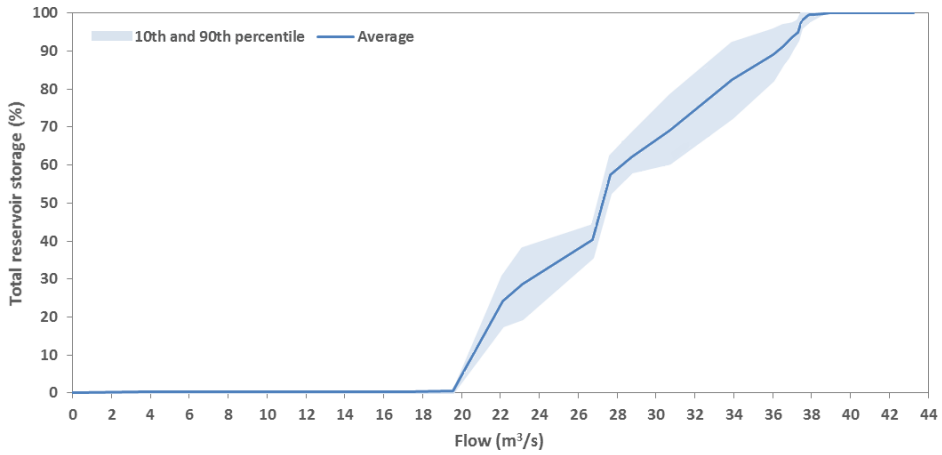

Figure 6.10: Relationship between flow and mean reservoir level.

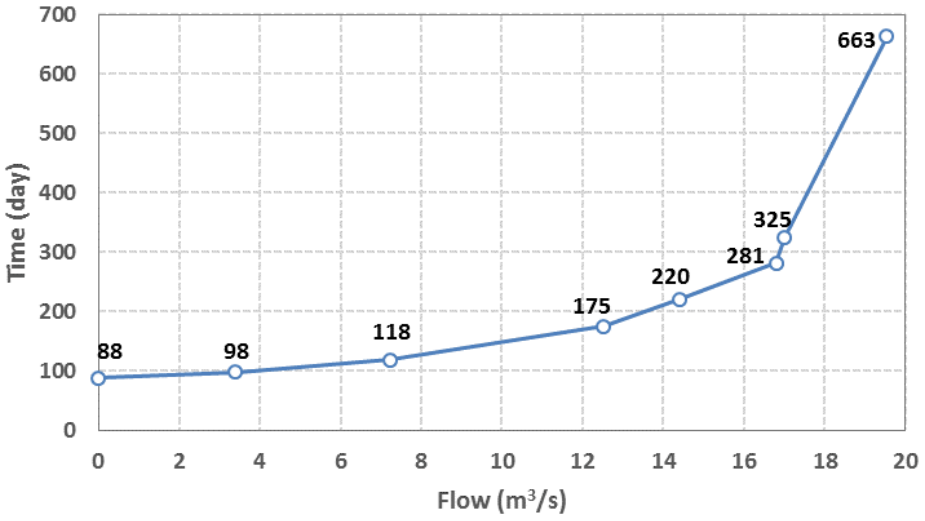

Figure 6.11: Time for the water system to empty.

a result of reduction in Level 4 demand saving days, number of the days for Level 1 to 3 demand saving increases. For flows more than 30.7 m^3/s the frequency of Level 4 demand saving days drops to zero and for flows greater than 33.94 m^3/s, Level 2 demand saving days reduces to zero. While, number of the Level 1 demand saving days increases by the time and reaches to the peak if the flow reaches to 30.70 m^3/s. After that, there is a negative slope in number of the demand saving days until it drops to zero for flows bigger that 36.78 m^3/s. It can be concluded that for flows bigger than 36.78 m^3/s there is no concern about the drought risk as reservoir contains enough water to meet all the demand.

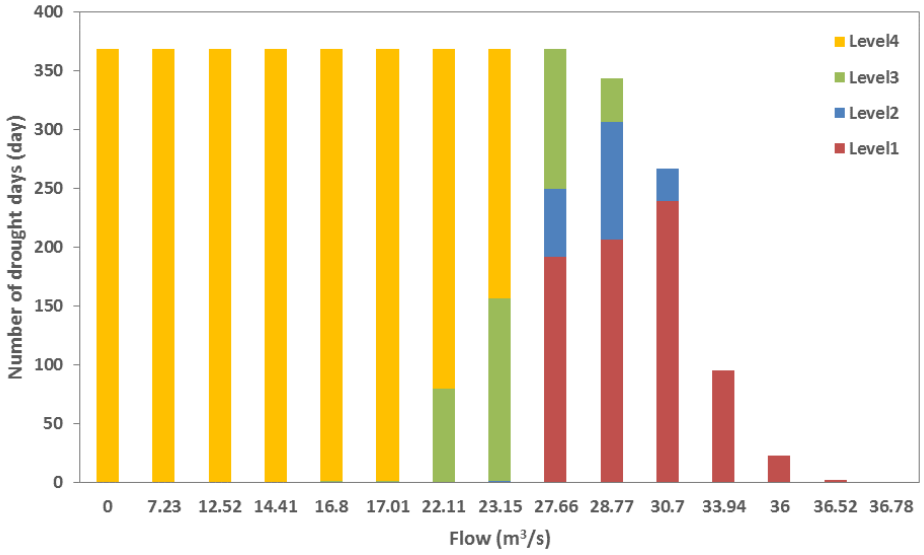

Figure 6.12: Number of drought days.

6.3.2 Stress testing: no demand saving measures

The analysis was repeated, but in this instance the demand saving levels have been removed from water resources model. The relationship between flow and mean reservoir level in the Thames catchment, after eliminating the level of services, is shown in Figure 6.13. As can be seen, by increasing the input flow, the average of reservoir level increased gradually. For flows less than 30.70 m^3/s the reservoir is almost empty, but by increasing the flow, the reservoir storage increases dramatically. For flows greater than 39.10 m^3/s the reservoir reaches its maximum level and remains 100.0% full. Removing the demand saving levels, higher flows are required to replenish the reservoir, showing the importance of considering demand saving measures in preserving water in the Thames catchment.

Figure 6.14 compares the time taken for the reservoir to empty, over 100 years, before and after eliminating the level of services. When there is no input flow, without demand saving measures it takes 68 days for the water system to empty, if river flow is 22.11 m^3/s it takes 6 months (183 days) for the reservoir to empty. When there are no demand savings levels, the flow needs to exceed 30.70 m^3/s to ensure the water

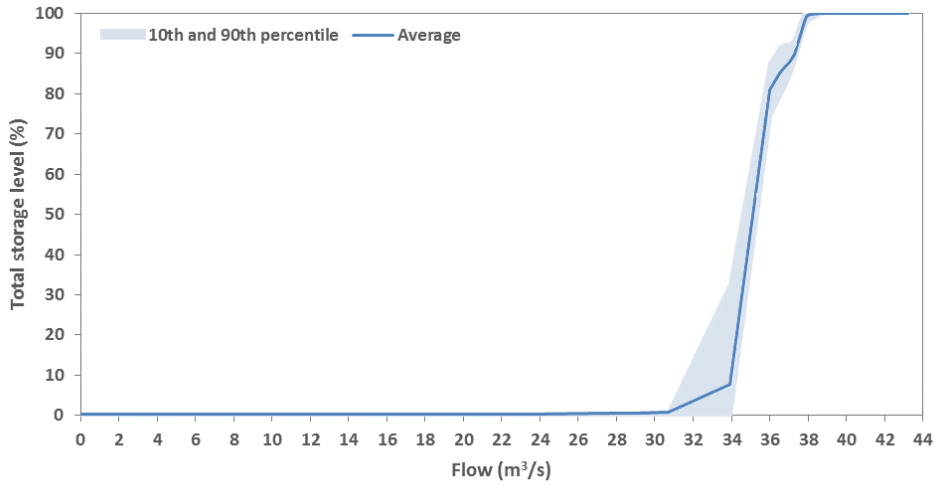

Figure 6.13: Relationship between flow and mean reservoir level (no demand saving measures)

system does not empty. Therefore by comparing the two analyses, it can be seen that the maximum flow that required for the system to never empty, is 57.00% higher when there are no demand savings measures, which shows the importance of demand management in the Thames catchment.

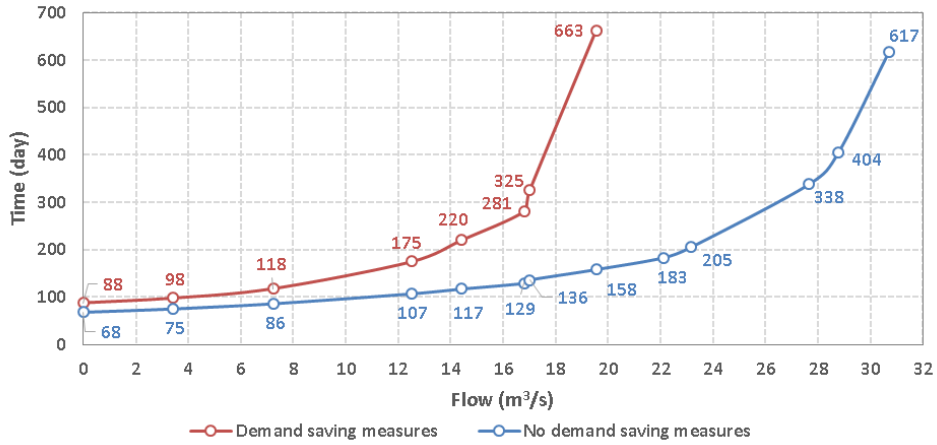

Figure 6.14: Time for the water system to get empty, before and after eliminating demand saving measures from the system

Based on Figure 6.15, there is a reverse relationship between inflow and number of drought days. By increasing the flow, the number of drought days Level 4 reduces, as for flows greater than 37.50 m^3/s there is no drought. This shows that the maximum flows required for the system to eliminate the drought is 2.0% higher when there are no demand saving measures.

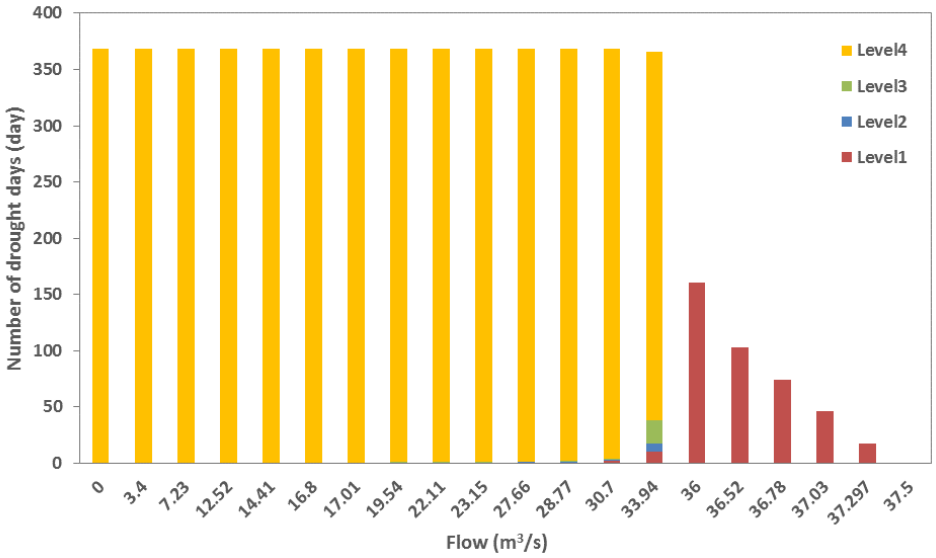

Figure 6.15: Number of drought days (no demand saving measures)

6.4 Summary

This chapter discussed the implications of the results presented in Chapter 5. There are many different combinations of water use scenarios to be tested. Two extreme, but plausible, scenarios of Low and High water consumption were considered. The High scenario incorporated a 75.0% increase in population, a 15.0% increase in leakage and a 20.0% increase in PCC. The results indicated that by 2080s the High water use scenario led to an increase in the number of drought Level 4 by 1318.0%, compared to the current scenario. While the Low scenario which represented 15.0% reduction in population, 40.0% reduction in leakage and 50.0% reduction in PCC, led to a reduction in the number of drought days by 100.0%. These results implied that availability of the water in the system is highly affected not only by the climatic drivers but also by the socio-economic drivers that influence demand for water. Moreover the variation in the range of possible drought incidence are larger for future time slices. Also, in all of the time slices variability in estimating the number of drought Level 4 is much bigger than the other demand saving days. This indicates a higher uncertainty in prediction of long-term impacts of climatic and non-climatic drivers in predicting the drought, especially Level 4 demand savings, and also availability of water resources in Thames catchment.

The robustness of different adaptation options, under current and future climate changes, against High water use scenario also showed that for all the time slices, a combination of a desalination plant and constructing a new reservoir, is the most effective option in reducing the number of Level 4 drought days. By 2080s, combination of desalination plant and constructing new reservoir, reduces the number of Level 4 demand saving by 24.7%. Moreover, for High scenario with current land cover and the increase urbanization scenario, it is explored that contribution of the

adaptation options on reducing number of drought days with increased urbanisation is greater than the current land cover scenario. Results for High water use with increased urbanisation show that by 2080s, the combination of desalination and new reservoir led to approximately 40.0% drop in Level 4 demand saving days relative to High scenario with current land cover for the similar time slice. It is worthy to note that, in order to to check the feasibility of these adaptation options and choose the most sustainable one, calculating the cost and also comprehensive research about other socio-economic aspects of the proposed options are necessary.

To understand further about the non-linear response of water system in Thames catchment, the water resources model (LARaWaRM) was stress-tested to explore how water resource was respond to different long-term trends in flows. For this aim, two analyses were undertaken. In both analyses, it was assumed that input flows to the catchment were constant over 100 years, in first stage the LARaWaRM was run including the current demand saving measures while in second one they were eliminated from the system. According to the results given from stress testing, by increasing the input flows (constant over the 100 years), the average reservoir level increases gradually. Based on this result, with considering the demand saving measures, there were thresholds for flows less than 19.54 m^3/s and greater than 39.00 m^3/s which means that for the input flows less than 19.54 m^3/s the reservoir is always empty while for flows greater than 39.00 m^3/s the reservoir is full over 100 years. While, after eliminating the demand saving measures from the model, the required flow for the system to never empty, is 39.10 m^3/s which is 57.0% greater than when having demand saving measures. From a drought risk point of view, when demand saving measures are considered, there is no drought risk for flows greater than 36.78 m^3/s. While after eliminating the demand saving measures, the maximum required flow for the system to eliminate the drought increases by 2.0% to 37.5 m^3/s. This shows the importance of considering demand saving measures for water supply security in Thames catchment.

Chapter 7

Conclusion

7.1 Review of key findings

Managing water resources under uncertainty is an ongoing challenge for water companies and decision makers. This research has provided insights into a number of uncertainties in the long-term management of water resources to aid more robust planning and decision making. These are reviewed against the original objectives set out in Chapter 1.

7.1.1 Objective 1: Develop a systems model that couples rainfall, catchment hydrology, water resources and consumption for the Thames catchment.

In order to achieve Objective 1, a novel integrated systems model has been developed. The constructed integrated systems model coupled simulations of weather under current and future climates, catchment hydrology, and the water resources system. These models can be implemented on any catchment, nationally and internationally, to assess the likelihood and magnitude of water scarcity. In addition, this integrated systems model can be adapted to incorporate other weather generators, hydrological and water resources models. More details about constructing this integrated systems model were presented in Chapter 3.

In this study, this integrated systems model was demonstrated on the Thames catchment, a region which is pressured by population growth, climate change and other socio economic drivers. In order to construct the integrated systems model for the Thames catchment, the latest version of spatial UKCP09 WG (SWG) was used which unlike its previous version, is fully consistent with national gridded rainfall data set from the Met Office. In addition, for the first time in the Thames catchment impact studies, the physically based hydrological model of SHETRAN was used to simulate the hydrological characteristics of the basin. This model was coupled with a rule-based water resources model of LARaWaRM to simulate the potential future water resources risks and possible demand and supply adaptation options to manage

the potential risks in the Thames catchment. In order to provide a wider range of information about possible range of climate impacts, 100 ensembles of 100-year long future climate scenarios simulated.

Through the validation it became apparent that SWG reasonably reproduced the observed rainfall and PET statistics across the Thames catchment and provides a suitable platform for uncertainty analysis in this study. To simulate the hydrological characteristics of this catchment, the SWG fed input to physically-based spatially distributed hydrological model, SHETRAN. Calibration and validation results showed that SHETRAN integrated with SWG, simulated the historical river flows, especially the low flows during historical droughts well. The comparison between historical flow, SHETRAN driven with observed rainfall and PET, and SHETRAN with synthetic time series of rainfall and PET simulated by SWG, showed the quantities of the uncertainty caused by the SWG or SHETRAN as well as the combined uncertainties from both . This comparison showed that the uncertainty from SWG aggregated with uncertainties from SHETRAN led to an approximately 10.0% underestimation in the annual mean flows in the Thames catchment (projected changes that are smaller than these error bounds are within the noise of model error). Through the sensitivity analysis of SHETRAN with the input meteorological variables, it was found that SHETRAN with SWG input data better represents the hydrological characteristics of the catchment. To simulate the water storage and frequency of water shortage in Thames catchment, a rule-based water resources management model of LARaWaRM was used. Based on the results given for validation, LARaWaRM with historical river flows, correctly simulated the total reservoir storage in the Thames catchment, particularly during the droughts, especially the major droughts of 1990-92, 1995-97 and 2003-05 which were well captured by the model.

Chapter 4 demonstrated how the proposed integrated systems model can be used for climate change impact studies, on the Thames catchment. Results were given for three representative future time slices of 2020s, 2050s and 2080. Results indicated that the proportion of uncertainty in projected rainfall, PET and discharge in 2080s is much greater than the other time slices. The comparison between projected values with the control scenario also showed that the maximum changes are expected to occur by 2080s. Results also indicated that by the 2080s, when accounting for all uncertainties considered here, there would not be a considerable change in total amount of rainfall relative to the control period (1961-1990). However as a result of an increase in temperature, the annual mean PET is expected to increase by 26.6%. The results also showed that the river flow and subsurface storage were more influenced by temperature and consequently the PET, rather than rainfall. Hence, based on the results, a 24.0% and 1.3% reduction in annual mean daily flow and subsurface storage are projected to occur in the Thames catchment respectively.

From a water resources management point of view, it is important to estimate the frequency of time that a system fails to meet the demand under climate change.

Therefore, it is interesting to discover how the number of system failures changes in future, compared to the control scenarios. To simulate the water storage and frequency of water shortage in Thames catchment, the synthetic time series of flows, simulated by SHETRAN for control and future time slices, were used as input to water resources management model of LARaWaRM. Limitations in projecting the size of populations and climate projections led to a large uncertainty in estimating the reservoir storage in future. In this study, use of the water resources model LARaWaRM, made it possible to have a broader understanding of sensitivity of water resources in the Thames catchment. The analysis showed that, as a consequence of an increase in demand for water (due to the climate change, growth in population, and increase of living standards), the general trend in future water storage is a continual decrease. Moreover, analysing the uncertainties caused by climate and population change scenarios on total reservoir level and drought frequencies in Thames catchment, illustrated that by 2080s, the climate change could have a greater impact on water supply security than population growth. The uncertainty from combination of population and climate change projections have a greatest impact on water scarcity in the Thames catchment, than climate change only or population change only scenarios. Based on the results, under current population and climate trends by 2080s, relative to the control period (1961-1990), a 1083.0% increase in the total number of drought days are expected to happen. Hence investment in monitoring to reduce these uncertainties would help improve the robustness of investment decisions.

7.1.2 Objective 2: Identify and quantify key uncertainties in long-term water resources management.

To address objective 2, a range of key uncertainties in long-term management of water resources have identified via an extensive literature review, conducted in the UK and globally. Based on the literature, natural variability in hydrological processes, as well as future changes in climate, land use, demography and other socio economic factors were highlighted as increasing pressure on water resources and posing a threat to water security. The potential approaches to handling these uncertainties were outlined in Chapter 2 and quantified through the modelling approach in the subsequent chapters.

7.1.3 Objective 3: Test a range of adaptation options and assess their robustness to these uncertainties.

In order to address Objective 3, the constructed integrated system's model was used to assess the effectiveness of different demand and supply decision adaptation options and their robustness on water security in the Thames catchment. These analysis were presented in Chapter 4. Analysing the impacts of climate change on water resources, indicated that without further demand and supply adaptation options, there

would not be enough water available to meet the customers demand in this area. Moreover, based on the results, in order to reduce the drought risks in this catchment, a portfolio of supply adaptation measures, that includes different combinations of desalination plant with capacity of 150 Ml, constructing a new reservoir with 100 Mm^3 capacity and linear reduction in leakage to 40.0% by 2080s, was tested. The sensitivity testing showed that measures taken to reduce per capita water demand by 25.0% was more robust to future uncertainties than any of the individual or combined supply adaptation options, especially for 2020s and 2050s as the risk for drought could be reduced to zero. However, for 2080s, a combined contribution of demand and supply adaptation options could reduce number of Level 4 demand saving days in this catchment by 97.0%. This shows that implementation of combined supply and demand management options, is the most effective adaptation option to reduce the risk of failures in meeting the future water demand in the Thames catchment. However, from a financial and environmental point of view, the combination of all adaptation options is not always the best option. For instance, demand saving options may be more flexible and less controversial than supply options such as constructing a new reservoir or desalination plant which are more costly than demand management options such as water meter installation, grey water recycling, rainwater collection and use of water efficient appliances. Hence, in order to check the feasibility of these adaptation options and choose the most sustainable one, calculating the cost and also comprehensive research about other socio-economic aspects of the proposed options are necessary.

7.1.4 Objective 4: Stress test the system model to analyse the impacts of uncertainties and sensitivities of water resources in Thames catchment.

The proposed integrated model and its ability for sensitivity analysis, led to improved understanding of the potential impacts of climactic and socio-economic changes, such as population, per capita water consumption (PCC), leakage and land use, on managing water resources in Thames catchment. This analysis addressed Objective 4 and was presented in Chapter 5. In this study, a different range of possible changes in socio-economic drivers such as population, per capita consumption, leakage and land cover for the 3 time slices of interest (2020s, 2050s and 2080s) as well as their impacts on availability of water in Thames catchment were tested. The analysis indicated that an increase of population, PCC and leakage have direct impact on water availability. In fact, the growth of these parameters, aligned with the climate scenarios, led to a greater variation and uncertainty on demand saving levels estimations, especially at Level 4. In contrast, based on the results, increase of urbanization led to a reduction in number of drought days and an increases in the total reservoir storage in all of the time slices. In all of the future projections, the rate of change in mean flow during spring and summer was lower than autumn and winter, when there is more precipitation and

the soil as a result of urbanization, is less permeable.

In this study, uncertainty and sensitivity analyses were undertaken to assess the implications of uncertainties on water scarcity, and to subsequently identify water resources management options that are robust to these uncertainties. This part of analysis also addressed Objective 4 and was presented in Chapter 6. In this study, two extreme, but plausible, scenarios of Low and High water consumption were considered. The High scenario incorporated a 75.0% increase in population, a 15.0% increase in leakage and a 20.0% increase in PCC, while the Low scenario which represented 15.0% reduction in population, 40.0% reduction in leakage and 50.0% reduction in PCC. The analysis of these two water consumption scenarios implied that availability of the water in this system is highly affected by not only the climatic drivers but also by the socio-economic drivers which affect demand for water. Moreover, the analysis showed that the variation in the range of possible drought incidence are larger for future time slices. Also, in all of the time slices, variability in estimating the number of drought Level 4 was much larger than the other demand saving days.

This indicated a higher uncertainty in the prediction of long-term impacts of climatic and non-climatic drivers in predicting the drought, especially Level 4 demand savings, and also availability of water resources in the Thames catchment. The robustness of different adaptation options, under current and future climate changes, against High water use scenario also showed that for all the time slices, a combination of a desalination plant and constructing a new reservoir, was the most effective option in reducing the number of Level 4 drought days. Moreover, for High scenario with current land cover and the increased urbanization scenario, the contribution of the adaptation options on reducing number of drought days with increased urbanisation was greater than the current land cover scenario. Results for High water use with increased urbanisation indicated that by 2080s, the combination of desalination and new reservoir led to approximately 40.0% drop in Level 4 demand saving days relative to High scenario with current land cover by the similar time slice.

In order to understand further about the non-linear response of water system in the Thames catchment, the integrated systems model constructed for the Thames catchment were stress-tested which showed how water resource responded to different long-term trends in the river flows. Based on these results, with considering the demand saving measures, for the input flows less than 19.54 m^3/s the reservoir is always empty while for flows greater than 39 m^3/s the reservoir is full over 100 years. While, after eliminating the demand saving measures from the model, the required flow for the system to never empty, is 39.10 m^3/s which is 57.0% greater than when having demand saving measures. From a drought risk point of view, when the demand saving measures are considered, there is no drought risk for flows greater than 36.78 m^3/s. While after eliminating the demand saving measures, the maximum required flow for the system to eliminate the drought increases by 2.0% to 37.5 m^3/s. This shows the importance of considering demand saving measures for water supply security in

the Thames catchment.

7.2 Future work

7.2.1 Further development of existing framework

The integrated systems' model developed in this study provides a practical insight into multiple sources of uncertainties in the simulation of the future impacts (e.g. model structure, inputs, outputs etc) which can be very beneficial for robust water resources management decision making. Demonstrating the proposed integrated systems model has provided a comprehensive understanding about uncertainties in long-term management of water resources in the Thames catchment, an area which is highly pressured to supply London's water demand. However, there are some future research directions to improve the current framework application.

The constructed integrated model can be used for any catchment, from across the UK and internationally, and also can be adapted to include any weather generator, hydrological and water resources model. In this study the most recent version of spatial UKCP09 WG was used to simulate the future climate projections for the Thames catchment. This version is not freely available. However, CEH GEAR (Tanguy et al 2014) is a 1 km gridded rainfall dataset released by CEH which unlike UKCP09 WG, is a freely available dataset. Hence, coupling the integrated model presented in this study with CEH GEAR, would also provide a valuable comparison for Thames catchment studies.

Although physically based hydrological models such as SHETRAN is very data intensive, it is more suitable for uncertainty analysis, as it better captures the spatial characteristics of the catchment compared to the conceptual models (Beven 2012). Moreover, SHETRAN hydrological model has the ability that it can to easily expand to the neighbour catchments, so expanding this study to the South East, or even whole UK which would be of value when considering supply options such as inter-basin transfers.

For simulating Thames catchment, first 1 km resolution was used, but because of very long run times, the resolution were decreased to 5 km. Therefore, running SHETRAN at a finer resolution (e.g. 1 km) would be of interest (in case of having time and access to high speed hardware/computers) to better capture the physical processes occurring in the catchment given for example land use change.

During this study, in simulating the hydrological characteristics of the Thames catchment, there was a limitation in representing the groundwater aquifers using SHETRAN. Providing more comprehensive groundwater studies and groundwater models for Thames catchment could help better representing the real subsurface mechanisms and improve the accuracy of the simulation in this area. This is important given groundwater contributes to 20.0% London's supply (Thames Water 2013).

In addition, for land cover sensitivity analysis there was a need to find areas most likely considered for land cover change for expanding the urbanization in future. But unfortunately there was not enough information available. The given information from local authority plans were mostly about the increasing housing but not specifically about the land cover changes. As new houses can be constructed either on brownfield or greenbelt, increasing the housing does not necessarily mean the converting non-urban land to urban area and expanding the extent of urbanization. Therefore, inevitably for sensitivity analysis in choice of areas for urbanization expansion an assumption had to be made.

As a result of inability to fully represent the real water system, the models are mostly based on assumptions and simplifications of the real world. For running LARaWaRM some assumptions were also made. For instance, in demonstrating the case study of the Thames catchment, there was not enough information available about the artificial influences of stakeholders on hydrological cycle in Thames catchment. Hence, it was not clear how much water is abstracted from the River Thames in reality. For better simulating the hydrological cycle of Thames catchment, more data about actual abstraction from River Thames is required. Moreover, there were some difficulties in finding the range of future forecast for leakage and demand as there were confusion about the projections of these parameters in reports related to Thames area (e.g. Thames Water (2013)).

7.2.2 Consideration of other hazards

The water resources model of LARaWaRM, simulates the water system based on a simple aggregated model. In case of using LARaWaRM for more complex projects, some other performance metrics such as flood risks management measures or hydro-electronic schemes could be included in the model. In this work, the integrated systems model was constructed for drought management study. This integrated systems model can also be developed to study other hazards such as heat waves and flooding. For instance, the simulated river flows from SHETRAN can be used for flood risk studies. LARaWaRM can also be adapted for flood risk by changing performance metrics (e.g. flood alteration).

7.2.3 Adaptation economics

In this study, different demand and supply adaptation options were tested. Analysing the cost of the proposed adaptation options are not in the scope of this research. So in order to find the most sustainable option, calculating the cost and also comprehensive research about other socio-economic aspects of the proposed adaptation options are necessary. In order to evaluate the cost and benefits of water resources management options in the catchment, the integrated systems' model could be coupled with hydro-economic models (Harou et al. 2009). In addition, testing other possible adaptation

options such as inter basin water transfer and also altering the demand saving curves would be of value.

7.2.4 Alternative approaches to uncertainty analysis

In order to analyse the uncertainty and sensitivity of the integrated systems' model, One-at-a-time and All-at-a-time methods (Pianosi et al. 2016, Hamby 1994) have been used during this study. However, other uncertainty and sensitivity methods e.g. Information-Gap (Info-Gap) (Hipel & Ben-Haim 1999) and Variance-Based Sensitivity Analysis (VBSA) can also be adapted (Saltelli et al. 2010, Hamm et al. 2006). Furthermore, since, during this study, more emphasis has been placed on uncertainty and sensitivity analysis of the integrated model, no formal decision making analysis has been conducted. Hence, more formal decision making approaches e.g. Robust Decision Making (RDM) (Lempert et al. 2006, Lempert & Groves 2010) and decision-scaling method (Brown et al. 2012) can be tailored to this approach.

7.2.5 Adaptation pathways

Given the difficulty of predicting the future climate conditions, and the fact that investing in supply adaptation options, such as constructing a new reservoir is costly, it becomes crucial for decision makers to consider the uncertainty in future changes, and evaluate their decisions over the time (Hallegatte 2009, Curry & Webster 2011). Hence, adapting the dynamic approaches such as those proposed by Haasnoot et al. (2013), and Ranger et al. (2013) could be of interest to provide a more robust decision making framework. This would involve dynamically identifying a wider range of uncertainties, and by the timing and sequencing of options as adaptation pathways, exploring more flexible and profitable short-term and long-term adapting plans for the Thames catchment.

7.3 Implications for decision makers

Drought can have significant environmental, agricultural, social and economic consequences that are of relevance to a wide range of stakeholders. The key implications of this work for a range of stakeholders are now summarised:

Consumers: The results indicate that reducing per person water demand by 25.0% could reduce the incidence of drought significantly. Changes in water consumption are therefore recommended. These could be stimulated by demand management approaches such as efficient appliances, rainwater collection and grey water recycling systems as well as educating people to monitor and report water leakage.

Utilities: Water utility companies play a key role in managing demand for water. This could be achieved by constructing new reservoir and desalination plant, monitoring and maintaining infrastructure to minimise network leakage, investment in smart

meters for households, implement demand management through mechanisms such as education and variable tariffs.

City planners: One of the key findings of this research is the inverse relationship between urbanization and drought frequency. This implies that city planners should adopt policies in which sustainable urbanization is considered to be the goal. One key challenge, however, is to keep the size of urbanization to an optimum level for which the risk of drought, as well as floods are minimized. Another key policy for city planners is to provide regulations for retrofitting of existing buildings to achieve higher energy efficiency, lower CO_2 emission and lower water consumption. In line with above policies, public engagement in order to increase the awareness regarding the condition of water resources is vital.

Environment Agency: According to this study, the volume of flow in the River Thames and its sub-catchments could reduce by up to roughly 24.0% by 2080. This, therefore, reduces the volume of water abstracted from River Thames in order to protect the environment. The EA need to pose strict regulations to reduce the amount of abstracted water from the River Thames.

Central Government: During the course of this study, it was found that the climate change and increase in population are threatening the water availability in Thames catchment. As mentioned by Arnell et al. (2014) the ultimate strategy for reducing uncertain impacts on water resources is to mitigate future climate change. In order to mitigate these threats, governments should adopt long-term policies to reduce carbon footprint by shifting the energy consumption from fossil fuel to renewable energy and distribute economic activities outside London.

References

Abbott, M. B., Bathurst, J. C., Cunge, J. A., O'Connell, P. E. & Rasmussen, J. (1986), 'An introduction to the european hydrological systemsysteme hydrologique europeen,she, 1: History and philosophy of a physically-based, distributed modelling system', *Journal of Hydrology* **87**(1), 45–59.

Alcamo, J., Florke, M. & Marker, M. (2007), 'Future long-term changes in global water resources driven by socio-economic and climatic changes', *Hydrological Sciences Journal* **52**(2), 247–275.

Allen, R. G., Pereira, L. S., Raes, D. & Smith, M. (1998), 'Crop evapotranspiration-guidelines for computing crop water requirements-fao irrigation and drainage paper 56', *FAO, Rome* **300**(9), D05109.

Anderson, E. C. (1999), 'Monte carlo methods and importance sampling', *Lecture Notes for Stat 578C Statistical Genetics* .

Andreu, J., Capilla, J. & Sanchs, E. (1996), 'Aquatool, a generalized decision-support system for water-resources planning and operational management', *Journal of Hydrology* **177**(3), 269–291.

Arnell, N. W., Charlton, M. B. & Lowe, J. A. (2014), 'The effect of climate policy on the impacts of climate change on river flows in the UK', *Journal of hydrology* **510**, 424–435.

Beven, K. & Binley, A. (1992), 'The future of distributed models: model calibration and uncertainty prediction', *Hydrological Processes* **6**(3), 279–298.

Beven, K. J. (2012), *Rainfall-runoff modelling: the primer*, John Wiley & Sons Ltd, New York.

Beven, K. J. & Kirkby, M. J. (1979), 'A physically based, variable contributing area model of basin hydrology/un modle base physique de zone d'appel variable de l'hydrologie du bassin versant', *Hydrological Sciences Journal* **24**(1), 43–69.

BGS (2014), 'British geological survey, 1:625 000 scale digital hydrogeological data.'.
URL: *http://www.bgs.ac.uk/products/hydrogeology/maps.html.*

BGS (2015*a*), 'British geological survey'.
URL: *http://www.bgs.ac.uk/research/groundwater/waterResources/thames/overview.html*

BGS (2015*b*), 'British geological survey, aquifers in the thames basin'.
URL: *http://www.bgs.ac.uk/research/groundwater/waterResources/thames/aquifers.html*

Birkinshaw, S. J., Bathurst, J. C., Iroum, A. & Palacios, H. (2011), 'The effect of forest cover on peak flow and sediment dischargean integrated field and modelling study in centralsouthern chile', *Hydrological Processes* **25**(8), 1284–1297.

Birkinshaw, S. J., Bathurst, J. C. & Robinson, M. (2014), '45 years of non-stationary hydrology over a forest plantation growth cycle, coalburn catchment, northern england', *Journal of Hydrology* **519**, 559–573.

Birkinshaw, S. J., James, P. & Ewen, J. (2010), 'Graphical user interface for rapid set-up of shetran physically-based river catchment model', *Environmental Modelling & Software* **25**(4), 609–610.

Boberg, F. & Christensen, J. H. (2012), 'Overestimation of mediterranean summer temperature projections due to model deficiencies', *Nature Climate Change* **2**(6), 433–436.

Borgomeo, E., Hall, J. W., Fung, F., Watts, G., Colquhoun, K. & Lambert, C. (2014), 'Risk-based water resources planning: Incorporating probabilistic nonstationary climate uncertainties', *Water Resources Research* **50**(8), 6850–6873.

Bormann, H., Breuer, L., Giertz, S., Huisman, J. & Viney, N. (2009), *Spatially explicit versus lumped models in catchment hydrology experiences from two case studies*, NATO Science for Peace and Security Series C: Environmental Security, Springer Netherlands, book section 1, pp. 3–26.
URL: $http://dx.doi.org/10.1007/978-90-481-2636-1$

Box, G. E. P. & Jenkins, G. M. (1976), *Time series analysis: forecasting and control, revised ed*, Holden-Day.

Breuer, L., Huisman, J. A., Willems, P., Bormann, H., Bronstert, A., Croke, B. F. W., Frede, H. G., Grff, T., Hubrechts, L. & Jakeman, A. J. (2009), 'Assessing the impact of land use change on hydrology by ensemble modeling (luchem). i: Model intercomparison with current land use', *Advances in Water Resources* **32**(2), 129–146.

Brown, C., Ghile, Y., Laverty, M. & Li, K. (2012), 'Decision scaling: Linking bottom-up vulnerability analysis with climate projections in the water sector', *Water Resources Research* **48**(9).

Brown, C. & Wilby, R. L. (2012), 'An alternate approach to assessing climate risks', *Eos* **93**(41), 401–402.

Burke, E. J. & Brown, S. J. (2010), 'Regional drought over the uk and changes in the future', *Journal of Hydrology* **394**(3), 471–485.

Burnash, R. J. C., Ferral, R. L. & McGuire, R. A. (1973), 'A generalized streamflow simulation system, conceptual modeling for digital computers'.

Burton, A., Glenis, V., Jones, M. & Kilsby, C. (2013), 'Models of daily rainfall cross-correlation for the united kingdom', *Environmental Modelling & Software* **49**, 22–33.

Burton, A., Kilsby, C. G., Fowler, H. J., Cowpertwait, P. S. P. & O'Connell, P. E. (2008), 'Rainsim A spatialtemporal stochastic rainfall modelling system', *Environmental Modelling & Software* **23**(12), 1356–1369.

Calver, A. & Wood, W. L. (1995), 'Chapter 17: The institute for hydrology distributed model', *Water Resources Publications, Littleton, Colo* .

Carter, T. R., La Rovere, E. L., Jones, R., Leemans, R., Mearns, L., Nakicenovic, N., Pittock, A., Semenov, S. & Skea, J. (2001), 'Developing and applying scenarios', *Climate change* pp. 145–190.

Cetinkaya, C. P., Fistikoglu, O., Harmancioglu, N. B. & Fedra, K. (2008), 'Optimization methods applied for sustainable management of water-scarce basins', *Journal of Hydroinformatics* **10**(1), 69–95.

Christierson, B. v., Vidal, J.-P. & Wade, S. D. (2012), 'Using ukcp09 probabilistic climate information for uk water resource planning', *Journal of Hydrology* **424**, 48–67.

CIP (2015), 'Climate information portal (cip)'.
URL: *http* : *//cip.csag.uct.ac.za/webclient*2*/app/*

Clark, M. P., Wilby, R. L., Gutmann, E. D., Vano, J. A., Gangopadhyay, S., Wood, A. W., Fowler, H. J., Prudhomme, C., Arnold, J. R. & Brekke, L. D. (2016), 'Characterizing uncertainty of the hydrologic impacts of climate change', *Current Climate Change Reports* **2**(2), 55–64.

Cowpertwait, P. S. P. (1995), A generalized spatial-temporal model of rainfall based on a clustered point process, *in* 'Proceedings of the Royal Society of London A: Mathematical, Physical and Engineering Sciences', Vol. 450, The Royal Society, pp. 163–175. 1938.

Cowpertwait, P. S. P., Kilsby, C. G. & O'Connell, P. E. (2002), 'A space time neyman scott model of rainfall: Empirical analysis of extremes', *Water Resources Research* **38**(8).

Cowpertwait, P. S. P., O'Connell, P. E., Metcalfe, A. V. & Mawdsley, J. A. (1996*a*), 'Stochastic point process modelling of rainfall. i. single-site fitting and validation', *Journal of Hydrology* **175**(1), 17–46.

Cowpertwait, P. S. P., O'Connell, P. E., Metcalfe, A. V. & Mawdsley, J. A. (1996*b*), 'Stochastic point process modelling of rainfall. ii. regionalisation and disaggregation', *Journal of Hydrology* **175**(1), 47–65.

Crawford, N. H. & Linsley, R. K. (1966), 'Digital simulation in Hydrology Stanford Watershed Model 4'.

Cui, W. & Blockley, D. I. (1990), 'Interval probability theory for evidential support', *International Journal of Intelligent Systems* **5**(2), 183–192.

Curry, J. A. & Webster, P. J. (2011), 'Climate science and the uncertainty monster', *Bulletin of the American Meteorological Society* **92**(12), 1667–1682.

Davis, R. J. (2001), 'The effects of climate change on river flows in the thames region', *Water Resources Hydrology and Hydrometry Report 00/04, Environment Agency, Reading, UK* .

Defra (2008), 'Future water: The governments water strategy for England'.

Defra (2009), 'Adapting to climate change: UK Climate Projections 2009'.
URL: *https://www.gov.uk/government/uploads/system/uploads/attachment_data/file/69257/pb13274-uk-climate-projections-090617.pdf*

Dessai, S. & Hulme, M. (2007), 'Assessing the robustness of adaptation decisions to climate change uncertainties: A case study on water resources management in the east of england', *Global Environmental Change* **17**(1), 59–72.

Diaz-Nieto, J. & Wilby, R. (2005), 'A comparison of statistical downscaling and climate change factor methods: impacts on low flows in the river thames, united kingdom', *Climatic Change* **69**(2-3), 245–268.
URL: *http://dx.doi.org/10.1007/s10584-005-1157-6*

Draper, A. J., Munvar, A., Arora, S. K., Reyes, E., Parker, N. L., Chung, F. I. & Peterson, L. E. (2004), 'Calsim: Generalized model for reservoir system analysis', *Journal of Water Resources Planning and Management* **130**(6), 480–489.

EA (2007), 'Environment Agency: Areas of water stress: final classification'.
URL: *https://www.iwight.com/azservices/documents/2782-FE1-Areas-of-Water-Stress.pdf*

EA (2012), 'Environment Agency, Water Resources Planning Guideline'.

EA (2016), 'Management of the London Basin Chalk Aquifer', *Environment Agency, Bristol, UK* .

Europen Soil Data, . (2006), 'European Soil Database v2 Raster Library 1kmx1km'.
URL: *http://esdac.jrc.ec.europa.eu/content/european-soil-database-v2-raster-library-1kmx1km*

Ewen, J. & Parkin, G. (1996), 'Validation of catchment models for predicting land-use and climate change impacts. 1. method', *Journal of Hydrology* **175**(14), 583–594.
URL: *http://www.sciencedirect.com/science/article/pii/S0022169496800266*

Ewen, J., Parkin, G. & O'Connell, P. (2000), 'Shetran: Distributed river basin flow and transport modeling system', *Journal of Hydrologic Engineering* **5**(3), 250–258.
URL: *http://ascelibrary.org/doi/abs/10.1061/%28ASCE%291084-0699%282000%295%3A3%28250%29*

Fisher, R. (1918), 'Studies in crop variation. i. an examination of the yield of dressed grain from broadbalk', *Journal of Agricultural Science* **11**, 107–135.
URL: *https://web.archive.org/web/20010612211752/http://www.library.adelaide.edu.au/digitised/fisher/15.pdf*

Fowler, H. J., Blenkinsop, S. & Tebaldi, C. (2007), 'Linking climate change modelling to impacts studies: recent advances in downscaling techniques for hydrological modelling', *International Journal of Climatology* **27**(12), 1547–1578.

Fowler, M. R., Cook, S. C. & Lumbers, J. P. (1999), 'Practical experience in the successful implementation of optimisation systems for water supply management', *Computing and Control for the Water Industry. Tynemarch Ltd., Exeter, UK* .

Franchini, M., Wendling, J., Obled, C. & Todini, E. (1996), 'Physical interpretation and sensitivity analysis of the topmodel', *Journal of Hydrology* **175**(1), 293–338.

Freeze, R. A. & Harlan, R. L. (1969), 'Blueprint for a physically-based, digitally-simulated hydrologic response model', *Journal of Hydrology* **9**(3), 237–258.

Garcia-Bartual, R. (2002), 'Short term river flood forecasting with neural networks', *Universidad Politecnica de Valencia, Spain* pp. 160–165.

GLA (2014*a*), 2013 round population projections, Greater London Authority.
URL: *http://data.london.gov.uk/dataset/2013 − round − populationprojections*

GLA (2014*b*), London labor market projections, Greater London Authority.
URL: *https://lep.london/sites/default/files/documents/publication/London%20Labour%20Market%20Projections_reduced_filesize.pdf*

Glenis, V., Pinamonti, V., Hall, J. W. & Kilsby, C. G. (2015), 'A transient stochastic weather generator incorporating climate model uncertainty', *Advances in Water Resources* **85**, 14–26.

Grayson, R., Blschl, G., Moore, I. D. & Singh, V. P. (1995), 'Distributed parameter hydrologic modelling using vector elevation data: Thales and tapes-c', *Computer Models of Watershed Hydrology.* pp. 669–696.

Haasnoot, M., Kwakkel, J. H., Walker, W. E. & ter Maat, J. (2013), 'Dynamic adaptive policy pathways A method for crafting robust decisions for a deeply uncertain world', *Global environmental change* **23**(2), 485–498.

Hall, J. W., Davis, J. P. & Blockley, D. I. (1999), Uncertainty analysis of coastal projects, *in* 'Coastal Engineering 1998', pp. 1461–1474.

Hall, J. W., Dawson, R. J., Walsh, C. L., Barker, T., Barr, S. L., Batty, M., Bristow, A. L., Burton, A., Carney, S. & Dagoumas, A. (2009), 'Engineering cities: how can cities grow whilst reducing emissions and vulnerability', *Newcastle University, Newcastle* .

Hall, J. W., Watts, G., Keil, M., de Vial, L., Street, R., Conlan, K., O'Connell, P. E., Beven, K. J. & Kilsby, C. G. (2012), 'Towards risk-based water resources planning in England and Wales under a changing climate', *Water and Environment Journal* **26**(1), 118–129.

Hall, M. J. (2001), 'How well does your model fit the data?', *Journal of Hydroinformatics* **3**(1), 49–55.

Hallegatte, S. (2009), 'Strategies to adapt to an uncertain climate change', *Global environmental change* **19**(2), 240–247.

Hamby, D. (1994), 'A review of techniques for parameter sensitivity analysis of environmental models', *Environmental Monitoring and Assessment* **32**(2), 135–154.

Hamm, N. A. S., Hall, J. W. & Anderson, M. G. (2006), 'Variance-based sensitivity analysis of the probability of hydrologically induced slope instability', *Computers & Geosciences* **32**(6), 803–817.
URL: *urlhttp://www.sciencedirect.com/science/article/pii/S0098300405002335*

Harou, J. J., Pulido-Velazquez, M., Rosenberg, D. E., Medellin-Azuara, J., Lund, J. R. & Howitt, R. E. (2009), 'Hydro-economic models: Concepts, design, applications, and future prospects', *Journal of Hydrology* **375**(3), 627–643.

Harris, C. N. P., Quinn, A. D. & Bridgeman, J. (2013), 'Quantification of uncertainty sources in a probabilistic climate change assessment of future water shortages', *Climatic Change* **121**(2), 317–329.
URL: *http://dx.doi.org/10.1007/s10584-013-0871-8*

Hipel, K. W. & Ben-Haim, Y. (1999), 'Decision making in an uncertain world: information-gap modeling in water resources management', *IEEE Transactions on Systems, Man and Cybernetics Part C: Applications and Reviews* **29**(4), 506–517.
URL: *http://www.scopus.com/inward/record.url?eid=2-s2.0-00332215526partnerID=40&md5=519d4b5235e54cd194eb416bdc15baf5*

Hough, M. N. & Jones, R. J. A. (1997), 'The united kingdom meteorological office rainfall and evaporation calculation system: Morecs version 2.0-an overview', *Hydrology and Earth System Sciences Discussions* **1**(2), 227–239.

Hulme, M., Wigley, T. M. L., Barrow, E., Raper, S., Centella, A., Smith, S. & Chipanshi, A. (2000), *Using a climate scenario generator for vulnerability and adaptation assessments: MAGICC and SCENGEN: version 2.4 workbook*, Climatic Research Unit.

IPCC (2007), 'Contribution of working group i to the fourth assessment report of the intergovernmental panel on climate change, 2007'.

IWR (2008), Identification, estimation, quantification and incorporation of risk and uncertainty in water resources management tools in south africa, water research commission project no: K5/1838, Report, Institute for Water Research, Rhodes University, School of Bioresources Engineering and Environmental Hydrology, University of KwaZulu-Natal and Water for Africa.
URL: *http://www.ru.ac.za/static/institutes/iwr/uncertainty/k51838/DEL2_Literature_Review.pdf*

Jenkins, G. J., Murphy, J., Sexton, D., A., L. J., Jones, P. & Kilsby, C. (2010), *UK climate projections: briefing report*, Met Office Hadley Centre.

Jenkins, G. J., Perry, M. & Prior, J. (2009), *The climate of the United Kingdom and recent trends*, Exeter: Met Office Hadley Centre.

Jha, M. K. & Gupta, A. D. (2003), 'Application of mike basin for water management strategies in a watershed', *Water International* **28**(1), 27–35.

Jones, P. D., Kilsby, C. G., Harpham, C., Glenis, V. & Burton, A. (2009), 'Uk climate projections science report: Projections of future daily climate for the uk from the weather generator', *University of Newcastle, UK* .

Kay, A. L., Bell, V. A., Blyth, E. M., Crooks, S. M., Davies, H. N. & Reynard, N. S. (2013), 'A hydrological perspective on evaporation: historical trends and future projections in britain', *Journal of Water and Climate Change* **4**(3), 193–208.

Kendon, M., Marsh, T. & Parry, S. (2013), 'The 2010-2012 drought in England and Wales', *Weather* **68**(4), 88–95.

Kilsby, C. G., Jones, P. D., Burton, A., Ford, A. C., Fowler, H. J., Harpham, C., James, P., Smith, A. & Wilby, R. L. (2007), 'A daily weather generator for use in climate change studies', *Environmental Modelling & Software* **22**(12), 1705–1719.

Klipsch, J. D. & Hurst, M. B. (2007), 'Hec-ressim reservoir system simulation user's manual version 3.0', *USACE, Davis, CA* p. 512.

Krause, P., Boyle, D. P. & Base, F. (2005), 'Comparison of different efficiency criteria for hydrological model assessment', *Advances in Geosciences* **5**, 89–97.

Kuczera, G. (1992), 'Water supply headworks simulation using network linear programming', *Advances in Engineering Software* **14**(1), 55–60.

Kundzewicz, Z. W. & Stakhiv, E. Z. (2010), 'Are climate models ready for prime time in water resources management applications, or is more research needed?', *Hydrological Sciences JournalJournal des Sciences Hydrologiques* **55**(7), 1085–1089.

Labadie, J. W. (2004), 'Optimal operation of multireservoir systems: state-of-the-art review', *Journal of Water Resources Planning and Management* **130**(2), 93–111.

Labadie, J. W., Baldo, M. L. & Larson, R. (2000), 'Modsim: Decision support system for river basin management', *Available at: modsim. engr. colostate. edu* .

Lempert, R. J. & Groves, D. G. (2010), 'Identifying and evaluating robust adaptive policy responses to climate change for water management agencies in the american west', *Technological Forecasting and Social Change* **77**(6), 960–974.

Lempert, Robert, J., Groves, David, G., Popper, Steven, W. & Bankes, Steve, C. (2006), 'A general, analytic method for generating robust strategies and narrative scenarios', *Management Science* **52**(4), 514–528.
URL: *http://pubsonline.informs.org/doi/abs/10.1287/mnsc.1050.0472*

Lewis, E. A. (2016), 'A robust multi-purpose hydrological model for Great Britain', *Newcastle University, PhD Thesis* .

Liang, X., Lettenmaier, D. P., Wood, E. F. & Burges, S. J. (1994), 'A simple hydrologically based model of land surface water and energy fluxes for general circulation models', *Journal of Geophysical Research: Atmospheres* **99**(D7), 14415–14428.

Lopez, A., Fung, F., New, M., Watts, G., Weston, A. & Wilby, R. L. (2009), 'From climate model ensembles to climate change impacts and adaptation: A case study of water resource management in the southwest of england', *Water Resources Research* **45**(8).

Loucks, D. P., French, P. N. & Taylor, M. R. (1995), 'Iras interactive river-aquifer simulation program description and operation', *Civ. and Environ. Eng., Cornell Univ., Ithaca, NY* .

Loucks, D. P., Stedinger, J. R. & Haith, D. A. (1981), *Water Resource Systems Planning and Analysis*, Prentice-Hall.

Loucks, D. P. & Van Beek, E. (2005), 'Water Resources Systems Planning and Management-Facts about Water', *UNESCO* .

Manning, L. J., Hall, J. W., Fowler, H. J., Kilsby, C. G. & Tebaldi, C. (2009), 'Using probabilistic climate change information from a multimodel ensemble for water resources assessment', *Water Resources Research* **45**(11).

Marsh, T., Cole, G. & Wilby, R. (2007), 'Major droughts in england and wales, 1800–2006', *Weather* **62**(4), 87–93.

Matrosov, E. S. & Harou, J. J. (2010), Simulating the Thames water resource system using IRAS-2010, Thesis.

Matrosov, E. S., Woods, A. M. & Harou, J. J. (2013), 'Robust decision making and info-gap decision theory for water resource system planning', *Journal of Hydrology* **494**, 43–58.

McKay, M. D., Beckman, R. J. & Conover, W. J. (1979), 'Comparison of three methods for selecting values of input variables in the analysis of output from a computer code', *Technometrics* **21**(2), 239–245.

Meinshausen, M., Raper, S. C. B. & Wigley, T. M. L. (2011), 'Emulating coupled atmosphere-ocean and carbon cycle models with a simpler model, magicc6part 1: Model description and calibration', *Atmospheric Chemistry and Physics* **11**(4), 1417–1456.

Met Office, . (2016), '2015: the warmest year on record, say scientists'.
URL: $http : //www.metoffice.gov.uk/news/releases/2016/2015 - global - temperature4$

Miller, K. & Yates, D. (2006), 'Climate change and water resources: A primer for municipal water providers,'.

Milly, Betancourt, J., Falkenmark, M. & Robert M. Hirsch, Zbigniew W. Kundzewicz, D. P. L. R. J. S. (2008), 'Stationarity is dead: Whither water management?', **VOL 319**.
URL: $http : //wwwpaztcn.wr.usgs.gov/julio_pdf/milly_et_al.pdf$

Moriasi, D. N., Arnold, J. G., Van Liew, M. W., Bingner, R. L., Harmel, R. D. & Veith, T. L. (2007), 'Model evaluation guidelines for systematic quantification of accuracy in watershed simulations', *Transactions of the ASABE* **50**(3), 885–900.

Mourato, S., Moreira, M. & Corte-Real, J. (2015), 'Water resources impact assessment under climate change scenarios in mediterranean watersheds', *Water Resources Management* **29**(7), 2377–2391.

Mulvany, T. J. (1850), 'On the use of self-registering rain and flood gauges', *Making Observations of the Relations of Rain Fall and Flood Discharges in a Given Catchment. Transactions and Minutes of the Proceedings of the Institute of Civil Engineers of Ireland, Dublin, Ireland, Session* **1**.

Murphy, J. M., Sexton, D. M. H., Jenkins, G. J., Booth, B. B. B., Brown, C. C., Clark, R. T., Collins, M., Harris, G. R., Kendon, E. J. & Betts, R. A. (2009), 'UK climate projections science report: climate change projections'.

Naghettini, M. (2016), 'Fundamentals of statistical hydrology'.

Nash, J. E. & Sutcliffe, J. V. (1970), 'River flow forecasting through conceptual models part ia discussion of principles', *Journal of Hydrology* **10**(3), 282–290.

New, M., Lopez, A., Dessai, S. & Wilby, R. (2007), 'Challenges in using probabilistic climate change information for impact assessments: an example from the water sector', *Philosophical Transactions of the Royal Society of London A: Mathematical, Physical and Engineering Sciences* **365**(1857), 2117–2131.

NRFA (2012), 'National river flow archive'.
URL: *http://nrfa.ceh.ac.uk/data/search*

OConnell, P. E. (1991), *A historical perspective*, Springer, pp. 3–30.

Ofwat (2009), *Future Water and Sewerage Charges 2010-15: Final Determinations*, Office of Water Services.
URL: *https://books.google.co.uk/books?id=u48JcgAACAAJ*

O'Hagan, A. (2012), 'Probabilistic uncertainty specification: Overview, elaboration techniques and their application to a mechanistic model of carbon flux', *Environmental Modelling & Software* **36**, 35–48.

O'Hagan, A., Buck, C. E., Daneshkhah, A., Eiser, J. R., Garthwaite, P. H., Jenkinson, D. J., Oakley, J. E. & Rakow, T. (2006), *Uncertain judgements: eliciting experts' probabilities*, John Wiley & Sons.

Oki, T., Agata, Y., Kanae, S., Saruhashi, T. & Musiake, K. (2003), 'Global water resources assessment under climatic change in 2050 using trip', *International Association of Hydrological Sciences, Publication* (280), 124–133.

ONS (2013), 'Office of national statistic'.
URL: *http://www.ons.gov.uk/ons/index.html*

Oxford Scientific Software, . (2008), 'A guide to aquator, 1. application, version 3.0, oxford scientific software, oxford, uk.'.
URL: *http://www.oxscisoft.com/aquator/manual/01Aquator.pdf*

Parkin, G. (1996), A three-dimensional variably-saturated subsurface modelling system for river basins, Thesis.

Perera, B. J. C., James, B. & Kularathna, M. D. U. (2005), 'Computer software tool realm for sustainable water allocation and management', *Journal of Environmental Management* **77**(4), 291–300.

Pianosi, F., Beven, K., Freer, J., Hall, J. W., Rougier, J., Stephenson, D. B. & Wagener, T. (2016), 'Sensitivity analysis of environmental models: A systematic review with practical workflow', *Environmental Modelling & Software* **79**, 214–232.

Prudhomme, C., Wilby, R., Crooks, S., Kay, A. & Reynard, N. (2010), 'Scenario-neutral approach to climate change impact studies: application to flood risk', *Journal of Hydrology* **390**(3), 198–209.

Racsko, P., Szeidl, L. & Semenov, M. (1991), 'A serial approach to local stochastic weather models', *Ecological Modelling* **57**(1-2), 27–41.

Randall, D., Cleland, L., Kuehne, C. S., Link, G. W. & Sheer, D. P. (1997), 'Water supply planning simulation model using mixed-integer linear programming engine', *Journal of Water Resources Planning and Management* **123**(2), 116–124.

Ranger, N., Reeder, T. & Lowe, J. (2013), 'Addressing deep uncertainty over long-term climate in major infrastructure projects four innovations of the Thames Estuary 2100 project', *EURO Journal on Decision Processes* **1**(3-4), 233–262.

Refsgaard, J. & Storm, B. (1995), *MIKE SHE.*, Water Resource Publications, CO, USA, pp. 806846.

Richardson, C. W. & Wright, D. A. (1984), 'WGEN: A model for generating daily weather variables'.

Rockwood, D. M. (1968), *Application of Streamflow Synthesis and Reservoir Regulation-" SSARR"-program to the Lower Mekong River*, US Army Corps of Engineers.

Rodda, J. C. & Marsh, T. J. (2011), 'The 1975-76 drought-a contemporary and retrospective review', *National Hydrological Monitoring Programme series* .

Salas, J., Rajagopalan, B., Saito, L. & Brown, C. (2012), 'Special section on climate change and water resources: Climate nonstationarity and water resources management', *Journal of Water Resources Planning and Management* **138**(5), 385–388.
URL: $http://dx.doi.org/10.1061/(ASCE)WR.1943-5452.0000279$

Salath, E. P. (2003), 'Comparison of various precipitation downscaling methods for the simulation of streamflow in a rainshadow river basin', *International Journal of Climatology* **23**(8), 887–901.

Saltelli, A., Annoni, P., Azzini, I., Campolongo, F., Ratto, M. & Tarantola, S. (2010), 'Variance based sensitivity analysis of model output. design and estimator for the total sensitivity index', *Computer Physics Communications* **181**(2), 259–270.
URL: *http://www.sciencedirect.com/science/article/pii/S0010465509003087*

Sechi, G. M. & Sulis, A. (2009), 'Water system management through a mixed optimization-simulation approach', *Journal of Water Resources Planning and Management* **135**(3), 160–170.

Semenov, M. A. & Barrow, E. M. (1997), 'Use of a stochastic weather generator in the development of climate change scenarios', *Climatic Change* **35**(4), 397–414.

Semenov, M. A., Brooks, R. J., Barrow, E. M. & Richardson, C. W. (1998), 'Comparison of the wgen and lars-wg stochastic weather generators for diverse climates', *Climate Research* **10**(2), 95–107.

Serinaldi, F. & Kilsby, C. G. (2012), 'A modular class of multisite monthly rainfall generators for water resource management and impact studies', *Journal of hydrology* **464**, 528–540.

Serrat-Capdevila, A., Valdes, J. B. & Gupta, H. V. (2011), 'Decision support systems in water resources planning and management: stakeholder participation and the

sustainable path to science-based decision making', *Efficient Decision Support Systems: Practice and ChallengesFrom Current to Future. Open Access Publisher* .

Shaw, E. M., Beven, K. J., Chappell, N. A. & Lamb, R. (2010), *Hydrology in practice*, CRC Press.

Sherman, J. (1932), 'Crystal energies of ionic compounds and thermochemical applications', *Chemical Reviews* **11**(1), 93–170.

Shiklomanov, I. A. & Rodda, J. C. (2003), 'World Water Resources at the beginning of the 21th century', *International Hydrology Series* .

Singh, J., Knapp, H. V. & Demissie, M. (2004), 'Hydrological modeling of the iroquois river watershed using hspf and swat'.

Singh, R., Subramanian, K. & Refsgaard, J. C. (1999), 'Hydrological modelling of a small watershed using mike she for irrigation planning', *Agricultural Water Management* **41**(3), 149–166.

Spearman, C. (1904), 'The proof and measurement of association between two things', *The American Journal of Psychology* **15**(1), 72–101.

Stakhiv, E. Z. (2011), 'Pragmatic approaches for water management under climate change uncertainty', *JAWRA Journal of the American Water Resources Association* **47**(6), 1183–1196.

Stott, P. A., Tett, S. F. B., Jones, G. S., Allen, M. R., Mitchell, J. F. B. & Jenkins, G. J. (2000), 'External control of 20th century temperature by natural and anthropogenic forcings', *Science* **290**(5499), 2133–2137.

Sugawara, M., Watanabe, I., Ozaki, E. & Katsuyame, Y. (1983), 'Reference manual for the tank model', *National Research Center for Disaster Prevention, Japan* .

Tanguy, M., Dixon, H., Prosdocimi, I., Morris, D. & Keller, V. (2014), 'Gridded estimates of daily and monthly areal rainfall for the united kingdom (1890–2012)[ceh-gear]', *NERC Environmental Information Data Centre, doi* **10**.

Thames Water, . (2012), 'Water-Planning for The Future. Final Water Resources Management Plan'.
URL: *http://www.thameswater.co.uk/tw/common/downloads/wrmp/wrmp-vol-1-executive-summary.pdf*

Thames Water, . (2013), 'Water resources management plan 2015 - 2040', *Thames Water Utilities Ltd., Reading, UK* .
URL: $http://www.thameswater.co.uk/about-us/5392.htm$

Thames Water, . (2017), 'Previous performance reports'.
URL: *https://corporate.thameswater.co.uk/about-us/our-business/previous-performance-reports*

Todini, E. (1996), 'The arno rainfallrunoff model', *Journal of Hydrology* **175**(1), 339–382.

UKCIP (2008), Your home in a changing climate, Report.
URL: $http://www.ukcip.org.uk/wp-content/PDFs/3Regions_Retrofitting.pdf$

UKCP09 UI, . (2009), 'UKCP09 User Interface manual'.
URL: *http://ukclimateprojections-ui.metoffice.gov.uk/ui/manual/pdf/ui_manual.pdf*

Uusitalo, L., Lehikoinen, A., Helle, I. & Myrberg, K. (2015), 'An overview of methods to evaluate uncertainty of deterministic models in decision support', *Environmental Modelling & Software* **63**, 24–31.

Vertessy, R. A., Hatton, T. J., O'Shaughnessy, P. J. & Jayasuriya, M. D. A. (1993), 'Predicting water yield from a mountain ash forest catchment using a terrain analysis based catchment model', *Journal of Hydrology* **150**(2), 665–700.

Viney, N., Croke, B., Breuer, L., Bormann, H., Bronstert, A., Frede, H., Graff, T., Hubrechts, L., Huisman, J. A. & Jakeman, A. (2005), 'Ensemble modelling of the hydrological impacts of land use change', *Modelling and Simulation Society of Australia and New Zealand Inc.* .

Vorosmarty, C. J., Green, P., Salisbury, J. & Lammers, R. B. (2000), 'Global water resources: vulnerability from climate change and population growth', *Science* **289**(5477), 284–288.

Wade, S., Hossell, J., Hough, M. & Fenn, C. (1999), 'Rising to the challenge: the impacts of climate change in the south east: Technical report, 94pp'.

Walsh, C. L., Blenkinsop, S., Fowler, H. J., Burton, A., Dawson, R. J., Glenis, V., Manning, L. J., Jahanshahi, G. & Kilsby, C. G. (2016), 'Adaptation of water resource systems to an uncertain future', *Hydrol. Earth Syst. Sci.* **20**(5), 1869–1884. HESS.
URL: *http://www.hydrol-earth-syst-sci.net/20/1869/2016/*

WEF (2016), The global risks report 2016, World Economic Forum.

Wheater, H. S., Jakeman, A. J. & Beven, K. J. (1993), 'Progress and directions in rainfall-runoff modelling'.

Wigley, T. M. L. & Raper, S. C. B. (1987), 'Thermal expansion of sea water associated with global warming', *Nature* **330**(6144), 127–131.

Wilby, R., Greenfield, B. & Glenny, C. (1994), 'A coupled synoptic hydrological model for climate-change impact assessment', *Journal of Hydrology* **153**(1-4), 265–290.

Wilby, R. L. (2005), 'Uncertainty in water resource model parameters used for climate change impact assessment', *Hydrological Processes* **19**(16), 3201–3219.

Wilby, R. L. & Dawson, C. W. (2013), 'The statistical downscaling model: insights from one decade of application', *International Journal of Climatology* **33**(7), 1707–1719.

Wilby, R. L., Dawson, C. W. & Barrow, E. M. (2002), 'SDSM- a decision support tool for the assessment of regional climate change impacts', *Environmental Modelling & Software* **17**(2), 145–157.

Wilby, R. L. & Dessai, S. (2010), 'Robust adaptation to climate change', *Weather* **65**(7), 180–185.
URL: *urlhttp://dx.doi.org/10.1002/wea.543*

Wilby, R. L. & Harris, I. (2006), 'A framework for assessing uncertainties in climate change impacts: Low-flow scenarios for the River Thames, UK', *Water Resources Research* **42**(2).

Wood, E. F., Lettenmaier, D. P. & Zartarian, V. G. (1992), 'A land surface hydrology parameterization with subgrid variability for general circulation models', *Journal of Geophysical Research: Atmospheres* **97**(D3), 2717–2728.

Wurbs, R. A. (2005), 'Comparative evaluation of generalized reservoir/river system models', *Texas. USA Internet Websites* .

WWAP (2009), 'World Water Assessment Programme: The United Nations World Water Development Report 3, Water in a Changing World'.

Xevi, E., Christiaens, K., Espino, A., Sewnandan, W., Mallants, D., Srensen, H. & Feyen, J. (1997), 'Calibration, validation and sensitivity analysis of the mike-she model using the neuenkirchen catchment as case study', *Water Resources Management* **11**(3), 219–242.

Yang, D., Herath, S. & Musiake, K. (2000), 'Comparison of different distributed hydrological models for characterization of catchment spatial variability', *Hydrological Processes* **14**(3), 403–416.

Yang, J. (2011), 'Convergence and uncertainty analyses in monte-carlo based sensitivity analysis', *Environmental Modelling & Software* **26**(4), 444–457.

Yates, D. N., Miller, K. A., Wilby, R. L. & Kaatz, L. (2015), 'Decision-centric adaptation appraisal for water management across colorados continental divide', *Climate Risk Management* **10**, 35–50.

Yates, D., Sieber, J., Purkey, D. & Huber-Lee, A. (2005), 'WEAP21-A demand-, priority-, and preference-driven water planning model: part 1: Model characteristics', *Water International* **30**(4), 487–500.

Young, P. C. & Beven, K. J. (1994), 'Data based mechanistic modelling and the rainfall flow non linearity', *Environmetrics* **5**(3), 335–363.

Zadeh, L. A. (1978), 'Fuzzy sets as a basis for a theory of possibility', *Fuzzy Sets and Systems* **1**(1), 3–28.
URL: *http://www.sciencedirect.com/science/article/pii/0165011478900295*

Zagona, E. A., Fulp, T. J., Shane, R., Magee, T. & Goranflo, H. M. (2001), 'Riverware: A generalized tool for complex reservoir system modeling1'.

Zhao, R. J., Liu, X. R. & Singh, V. P. (1995), 'The Xinanjiang model', *Computer Models of Watershed Hydrology.* pp. 215–232.

Appendices

Appendix A

Supporting documents for Chapter 3

Months	Rainfall (mm)			Change (mm)			Change (%)		
	Historical (1961-1990)	SWG	SSWG	Historical (1961-1990)	SWG	SSWG	Historical (1961-1990)	SWG	SSWG
Jan	2.20	2.24	1.91	0.00	0.04	-0.30	0.0	1.7	-13.5
Feb	1.69	1.69	1.51	0.00	-0.01	-0.18	0.0	-0.3	-10.6
Mar	1.89	1.89	1.73	0.00	0.00	-0.16	0.0	-0.1	-8.6
Apr	1.70	1.70	1.61	0.00	0.01	-0.09	0.0	0.4	-5.1
May	1.86	1.80	1.54	0.00	-0.06	-0.32	0.0	-3.1	-17.3
Jun	1.84	1.81	1.96	0.00	-0.03	0.12	0.0	-1.4	6.7
Jul	1.58	1.43	1.37	0.00	-0.15	-0.20	0.0	-9.3	-12.8
Aug	1.93	1.86	1.70	0.00	-0.06	-0.22	0.0	-3.3	-11.5
Sep	2.04	2.02	1.90	0.00	-0.02	-0.14	0.0	-0.7	-6.9
Oct	2.09	2.20	1.99	0.00	0.11	-0.10	0.0	5.3	-4.8
Nov	2.22	2.24	1.97	0.00	0.02	-0.26	0.0	1.0	-11.6
Dec	2.38	2.37	2.08	0.00	-0.01	-0.31	0.0	-0.4	-12.9
Average	1.95	1.94	1.77	0.00	-0.01	-0.18	0.0	-0.5	-9.2

Table A.1: Mean rainfall comparison between historical (1961-1990) and simulated values from SWG and SSWG control scenario for Kingston sub-catchment.

Months	PET (mm)			Change (mm)			Change (%)		
	Historical (1961-1990)	SWG	SSWG	Historical (1961-1990)	SWG	SSWG	Historical (1961-1990)	SWG	SSWG
Jan	0.44	0.57	0.57	0.00	0.13	0.13	0.0	30.6	30.8
Feb	0.66	0.71	0.69	0.00	0.05	0.04	0.0	8.0	5.6
Mar	1.18	1.22	1.21	0.00	0.04	0.02	0.0	3.1	1.8
Apr	1.89	1.84	1.82	0.00	-0.05	-0.07	0.0	-2.7	-3.7
May	2.68	2.61	2.56	0.00	-0.07	-0.12	0.0	-2.6	-4.4
Jun	3.22	3.08	3.00	0.00	-0.14	-0.22	0.0	-4.3	-6.7
Jul	3.34	3.27	3.19	0.00	-0.07	-0.15	0.0	-2.1	-4.5
Aug	2.79	2.74	2.75	0.00	-0.05	-0.04	0.0	-1.9	-1.5
Sep	1.84	1.83	1.82	0.00	-0.02	-0.03	0.0	-1.0	-1.6
Oct	0.96	1.02	1.01	0.00	0.05	0.04	0.0	5.3	4.3
Nov	0.50	0.61	0.59	0.00	0.12	0.10	0.0	23.2	19.2
Dec	0.38	0.51	0.50	0.00	0.12	0.11	0.0	31.9	28.9
Average	1.66	1.67	1.64	0.00	0.01	-0.02	0.0	0.5	-0.9

Table A.2: Mean PET comparison between historical (1961-1990) and simulated values from SWG and SSWG control scenario for Kingston sub-catchment.

Months	Rainfall (mm)			Change (mm)			Change (%)		
	Historical (1961-1990)	SWG	SSWG	Historical (1961-1990)	SWG	SSWG	Historical (1961-1990)	SWG	SSWG
Jan	1.77	1.80	1.91	0.00	0.03	0.14	0.0	1.5	7.7
Feb	1.42	1.42	1.51	0.00	-0.01	0.09	0.0	-0.5	6.3
Mar	1.58	1.58	1.73	0.00	0.00	0.14	0.0	-0.1	9.1
Apr	1.61	1.62	1.61	0.00	0.01	0.00	0.0	0.3	-0.2
May	1.57	1.53	1.54	0.00	-0.04	-0.03	0.0	-2.8	-1.9
Jun	1.77	1.75	1.96	0.00	-0.02	0.20	0.0	-1.2	11.2
Jul	1.66	1.51	1.37	0.00	-0.15	-0.29	0.0	-9.1	-17.4
Aug	1.77	1.71	1.70	0.00	-0.06	-0.07	0.0	-3.7	-3.8
Sep	1.75	1.74	1.90	0.00	-0.01	0.15	0.0	-0.8	8.5
Oct	1.82	1.92	1.99	0.00	0.09	0.17	0.0	5.2	9.3
Nov	1.97	1.99	1.97	0.00	0.02	0.00	0.0	1.0	0.0
Dec	1.91	1.90	2.08	0.00	-0.01	0.17	0.0	-0.6	8.8
Average	1.72	1.70	1.77	0.00	-0.01	0.06	0.0	-0.8	3.2

Table A.3: Mean rainfall comparison between historical (1961-1990) and simulated values from SWG and SSWG control scenario for Lee sub-catchment.

Months	PET (mm)			Change (mm)			Change (%)		
	Historical (1961-1990)	SWG	SSWG	Historical (1961-1990)	SWG	SSWG	Historical (1961-1990)	SWG	SSWG
Jan	0.40	0.57	0.57	0.00	0.17	0.17	0.0	42.5	41.7
Feb	0.62	0.70	0.69	0.00	0.08	0.07	0.0	12.4	10.9
Mar	1.17	1.24	1.21	0.00	0.07	0.04	0.0	6.2	3.4
Apr	1.85	1.85	1.82	0.00	-0.01	-0.03	0.0	-0.5	-1.9
May	2.64	2.63	2.56	0.00	-0.01	-0.08	0.0	-0.3	-2.9
Jun	3.18	3.13	3.00	0.00	-0.05	-0.18	0.0	-1.5	-5.6
Jul	3.29	3.31	3.19	0.00	0.02	-0.10	0.0	0.7	-2.9
Aug	2.81	2.82	2.75	0.00	0.01	-0.06	0.0	0.4	-2.0
Sep	1.87	1.88	1.82	0.00	0.01	-0.05	0.0	0.8	-2.9
Oct	0.96	1.05	1.01	0.00	0.09	0.04	0.0	9.6	4.6
Nov	0.47	0.61	0.59	0.00	0.14	0.13	0.0	30.1	26.8
Dec	0.35	0.51	0.50	0.00	0.15	0.14	0.0	43.8	40.4
Average	1.63	1.69	1.64	0.00	0.06	0.01	0.0	3.5	0.5

Table A.4: Mean PET comparison between historical (1961-1990) and simulated values from SWG and SSWG control scenario for Lee sub-catchment.

Month	Validation (1961-1990)				Calibration (1991-2001)			
	Historical (m^3/s)	Simulated (m^3/s)	Change (m^3/s)	Change (%)	Historical (m^3/s)	Simulated (m^3/s)	Change (m^3/s)	Change (%)
Jan	138.03	144.07	6.05	4.38	160.44	171.94	11.50	7.17
Feb	135.52	145.52	10.00	7.38	128.86	132.48	3.62	2.81
Mar	123.22	114.38	-8.84	-7.17	103.65	98.70	-4.95	-4.77
Apr	95.62	82.10	-13.52	-14.14	106.02	91.81	-14.21	-13.41
May	74.51	57.99	-16.51	-22.17	66.84	52.51	-14.33	-21.43
Jun	57.85	47.12	-10.72	-18.54	49.20	41.31	-7.89	-16.03
Jul	40.83	35.44	-5.39	-13.19	36.54	33.22	-3.32	-9.10
Aug	37.99	33.69	-4.29	-11.30	32.12	30.40	-1.72	-5.36
Sep	39.99	36.47	-3.53	-8.82	38.32	34.90	-3.42	-8.93
Oct	54.18	55.07	0.89	1.64	62.66	59.79	-2.87	-4.59
Nov	76.64	81.83	5.19	6.77	96.72	110.35	13.62	14.08
Dec	105.99	114.63	8.63	8.14	133.16	143.91	10.76	8.08
Average	81.70	79.03	-2.67	-5.58	84.54	83.44	-1.10	-4.29

Table A.5: Mean flow comparison between historical (1961-1990) and simulated values for calibration and validation period in Kingston sub-catchment.

Month	Validation (1961-1990)				Calibration (1991-2001)			
	Historical (m^3/s)	Simulated (m^3/s)	Change (m^3/s)	Change (%)	Historical (m^3/s)	Simulated (m^3/s)	Change (m^3/s)	Change (%)
Jan	8.29	8.75	0.46	5.54	9.06	8.65	-0.41	-4.50
Feb	7.49	8.95	1.46	19.48	7.99	8.74	0.75	9.42
Mar	7.49	7.65	0.16	2.09	6.62	6.56	-0.07	-0.99
Apr	6.41	6.15	-0.26	-4.02	7.22	6.09	-1.13	-15.62
May	5.30	4.37	-0.93	-17.58	4.77	3.94	-0.84	-17.53
Jun	4.08	3.80	-0.28	-6.82	4.09	3.35	-0.74	-18.04
Jul	3.24	3.35	0.12	3.64	3.28	2.87	-0.41	-12.50
Aug	2.99	3.06	0.07	2.33	2.81	2.44	-0.37	-13.31
Sep	3.08	3.46	0.39	12.55	3.10	3.13	0.02	0.80
Oct	4.25	4.97	0.72	16.85	5.83	5.82	-0.01	-0.18
Nov	5.20	5.98	0.78	15.05	6.37	7.62	1.25	19.68
Dec	6.40	7.30	0.90	13.99	7.09	7.43	0.34	4.86
Average	5.35	5.65	0.28	4.80	5.69	5.55	-0.13	-3.99

Table A.6: Mean flow comparison between historical (1961-1990) and simulated values for calibration and validation period in Lee sub-catchment.

Month	Historical (1961-1990)	Simulated					
	$\mathbf{Q_{Obs}}$ (m^3/s)	$\mathbf{Q_S^{Obs}}$ (m^3/s)	Change (m^3/s)	Change (%)	$\mathbf{Q_S^{SWG}}$ (m^3/s)	Change (m^3/s)	Change (%)
Jan	138.03	144.07	6.05	4.38	139.51	1.48	1.07
Feb	135.52	145.52	10	7.38	128.12	-7.4	-5.46
Mar	123.22	114.38	-8.84	-7.17	108.83	-14.39	-11.68
Apr	95.62	82.1	-13.52	-14.14	77.66	-17.96	-18.78
May	74.51	57.99	-16.51	-22.17	53.9	-20.6	-27.65
Jun	57.85	47.12	-10.72	-18.54	42.87	-14.98	-25.89
Jul	40.83	35.44	-5.39	-13.19	35.53	-5.29	-12.97
Aug	37.99	33.69	-4.29	-11.3	33.37	-4.61	-12.14
Sep	39.99	36.47	-3.53	-8.82	36.78	-3.21	-8.02
Oct	54.18	55.07	0.89	1.64	49.24	-4.94	-9.12
Nov	76.64	81.83	5.19	6.77	73.18	-3.45	-4.51
Dec	105.99	114.63	8.63	8.14	112.96	6.97	6.57
Average	81.7	79.03	-2.67	-5.58	74.33	-7.37	-10.72

Table A.7: Mean flow comparison between historical (1961-1990) and simulated values in Kingston sub-catchment.

Month	Historical (1961-1990)	Simulated					
	$\mathbf{Q_{Obs}}$ (m^3/s)	$\mathbf{Q_S^{Obs}}$ (m^3/s)	Change (m^3/s)	Change (%)	$\mathbf{Q_S^{SWG}}$ (m^3/s)	Change (m^3/s)	Change (%)
Jan	8.29	8.75	0.45	5.47	7.17	-1.12	-13.55
Feb	7.49	8.95	1.46	19.5	6.81	-0.69	-9.17
Mar	7.49	7.65	0.16	2.09	6.29	-1.21	-16.08
Apr	6.41	6.15	-0.26	-4	5.13	-1.28	-19.97
May	5.3	4.37	-0.93	-18	3.95	-1.35	-25.54
Jun	4.08	3.8	-0.28	-6.8	3.66	-0.42	-10.29
Jul	3.24	3.35	0.12	3.64	3.27	0.03	1.01
Aug	2.99	3.06	0.07	2.33	2.98	0	-0.10
Sep	3.08	3.46	0.39	12.6	3.11	0.03	1.02
Oct	4.25	4.97	0.72	16.9	3.59	-0.66	-15.63
Nov	5.2	5.98	0.78	15.1	4.61	-0.59	-11.28
Dec	6.4	7.3	0.9	14	6.27	-0.13	-2.11
Average	5.35	5.65	0.3	5.25	4.74	-0.62	-10.14

Table A.8: Mean flow comparison between historical (1961-1990) and simulated values in Lee sub-catchment

Months	Flow (m^3/s)				Change (m^3/s)			change (%)		
	Historical (1961-1990)	SWG	SWG-mean	SSWG	SWG	SWG-mean	SSWG	SWG	SWG-mean	SSWG
Jan	138.03	139.51	145.52	113.75	1.48	7.49	-24.27	1.1	5.4	-17.6
Feb	135.52	128.12	129.83	103.60	-7.40	-5.69	-31.92	-5.5	-4.2	-23.6
Mar	123.22	108.83	108.25	89.98	-14.39	-14.97	-33.24	-11.7	-12.1	-27.0
Apr	95.62	77.66	75.34	64.17	-17.96	-20.28	-31.45	-18.8	-21.2	-32.9
May	74.51	53.90	49.90	41.80	-20.60	-24.61	-32.71	-27.7	-33.0	-43.9
Jun	57.85	42.87	38.70	37.01	-14.98	-19.14	-20.83	-25.9	-33.1	-36.0
Jul	40.83	35.53	31.78	30.38	-5.29	-9.05	-10.45	-13.0	-22.2	-25.6
Aug	37.99	33.37	30.01	29.05	-4.61	-7.97	-8.94	-12.1	-21.0	-23.5
Sep	39.99	36.78	33.87	33.27	-3.21	-6.12	-6.72	-8.0	-15.3	-16.8
Oct	54.18	49.24	48.11	43.36	-4.94	-6.07	-10.82	-9.1	-11.2	-20.0
Nov	76.64	73.18	76.78	63.56	-3.45	0.15	-13.07	-4.5	0.2	-17.1
Dec	105.99	112.96	121.13	96.62	6.97	15.14	-9.38	6.6	14.3	-8.8
Average	81.70	74.33	74.10	62.21	-7.37	-7.59	-19.48	-9.0	-9.3	-23.8

Table A.9: Mean flow comparison between historical, SWG, SWG-mean and SSWG, in Kingston sub-catchment.

Months	Flow (m^3/s)				Change (m^3/s)			change (%)		
	Historical (1961-1990)	SWG	SWG-mean	SSWG	SWG	SWG-mean	SSWG	SWG	SWG-mean	SSWG
Jan	8.29	7.17	7.60	9.66	-1.12	-0.70	1.37	-13.5	-8.4	16.5
Feb	7.49	6.81	7.26	8.95	-0.69	-0.23	1.45	-9.2	-3.1	19.4
Mar	7.49	6.29	6.59	8.32	-1.21	-0.90	0.83	-16.1	-12.1	11.1
Apr	6.41	5.13	5.22	6.02	-1.28	-1.19	-0.39	-20.0	-18.6	-6.0
May	5.30	3.95	3.87	4.19	-1.35	-1.43	-1.11	-25.5	-27.0	-20.9
Jun	4.08	3.66	3.52	4.32	-0.42	-0.56	0.24	-10.3	-13.7	5.9
Jul	3.24	3.27	3.08	3.17	0.03	-0.16	-0.06	1.0	-4.9	-2.0
Aug	2.99	2.98	2.89	3.44	0.00	-0.10	0.46	-0.1	-3.4	15.3
Sep	3.08	3.11	3.01	3.83	0.03	-0.07	0.76	1.0	-2.3	24.7
Oct	4.25	3.59	3.50	4.19	-0.66	-0.75	-0.06	-15.6	-17.5	-1.4
Nov	5.20	4.61	4.65	5.52	-0.59	-0.54	0.33	-11.3	-10.5	6.3
Dec	6.40	6.27	6.48	8.47	-0.13	0.08	2.07	-2.1	1.3	32.4
Average	5.35	4.74	4.81	5.84	-0.62	-0.55	0.49	-11.5	-10.2	9.2

Table A.10: Mean flow comparison between historical, SWG, SWG-mean and SSWG, in Lee sub-catchment.

Appendix B

Supporting documents for Chapter 4

Months	Average				90th Percentile				10th Percentile			
	Control (1961-90)	2020s	2050s	2080s	Control (1961-90)	2020s	2050s	2080s	Control (1961-90)	2020s	2050s	2080s
Jan	2.24	2.24	2.47	2.48	2.32	2.65	3.12	3.41	2.15	1.92	1.95	1.81
Feb	1.69	1.86	2.00	2.22	1.77	2.18	2.42	2.89	1.59	1.54	1.65	1.70
Mar	1.89	2.00	2.03	2.14	1.98	2.29	2.37	2.45	1.81	1.66	1.73	1.79
Apr	1.70	1.71	1.75	1.74	1.78	1.86	1.90	1.90	1.63	1.56	1.55	1.57
May	1.80	1.83	1.70	1.62	1.88	2.19	2.04	1.93	1.73	1.54	1.33	1.33
Jun	1.81	1.71	1.62	1.52	1.94	2.18	2.04	2.31	1.70	1.32	1.13	0.95
Jul	1.43	1.39	1.27	1.24	1.54	1.76	1.68	1.77	1.33	0.97	0.80	0.72
Aug	1.86	1.71	1.34	1.42	1.98	2.28	1.90	2.23	1.75	1.27	0.85	0.72
Sep	2.02	1.92	1.80	1.63	2.14	2.35	2.36	2.11	1.89	1.46	1.18	1.15
Oct	2.20	2.10	2.13	2.13	2.27	2.41	2.49	2.49	2.11	1.85	1.75	1.84
Nov	2.24	2.37	2.49	2.54	2.34	2.79	3.03	3.24	2.14	1.99	1.91	1.85
Dec	2.37	2.56	2.74	2.85	2.48	3.07	3.20	3.51	2.25	2.09	2.32	2.24

Table B.1: Mean, 90th and 10th percentile of rainfall, for control and future scenarios in Kingston sub-catchment.

Months	Average				90th Percentile				10th Percentile			
	Control (1961-90)	2020s	2050s	2080s	Control (1961-90)	2020s	2050s	2080s	Control (1961-90)	2020s	2050s	2080s
Jan	0.00	0.14	10.48	10.89	0.00	14.01	34.65	47.01	0.00	-10.34	-8.97	-15.52
Feb	0.00	10.56	18.82	31.82	0.00	23.40	37.26	63.39	0.00	-2.87	3.93	6.86
Mar	0.00	5.71	7.19	13.47	0.00	15.95	19.57	24.07	0.00	-8.00	-4.14	-0.78
Apr	0.00	0.50	2.89	1.89	0.00	4.23	6.79	6.55	0.00	-4.24	-4.81	-3.39
May	0.00	1.79	-5.93	-10.11	0.00	16.56	8.56	2.98	0.00	-10.64	-22.73	-23.10
Jun	0.00	-5.99	-10.86	-16.47	0.00	12.54	5.07	19.02	0.00	-22.21	-33.29	-43.85
Jul	0.00	-2.93	-10.91	-13.08	0.00	14.55	9.66	15.40	0.00	-27.41	-39.65	-46.00
Aug	0.00	-8.10	-28.15	-23.95	0.00	15.24	-3.85	12.84	0.00	-27.64	-51.27	-59.08
Sep	0.00	-5.19	-11.07	-19.22	0.00	9.69	10.34	-1.34	0.00	-22.83	-37.49	-39.28
Oct	0.00	-4.51	-3.41	-3.33	0.00	6.01	9.70	9.44	0.00	-12.27	-17.20	-12.75
Nov	0.00	5.80	10.71	13.20	0.00	19.12	29.11	38.20	0.00	-7.03	-10.89	-13.56
Dec	0.00	7.75	15.33	20.03	0.00	23.53	29.10	41.40	0.00	-7.04	3.18	-0.39

Table B.2: % change in mean, 90th and 10th percentile of projected rainfall from mean control in Kingston sub-catchment.

Months	Average				90th Percentile				10th Percentile			
	Control (1961-1990)	2020s	2050s	2080s	Control (1961-1990)	2020s	2050s	2080s	Control (1961-1990)	2020s	2050s	2080s
Jan	0.57	0.56	0.61	0.62	0.57	0.60	0.67	0.71	0.56	0.52	0.54	0.54
Feb	0.71	0.74	0.77	0.81	0.71	0.78	0.82	0.89	0.70	0.69	0.71	0.74
Mar	1.22	1.34	1.41	1.48	1.23	1.39	1.52	1.63	1.22	1.28	1.32	1.34
Apr	1.84	2.00	2.14	2.24	1.85	2.14	2.34	2.54	1.83	1.85	1.97	2.00
May	2.61	2.87	3.14	3.30	2.62	3.17	3.56	3.84	2.59	2.58	2.81	2.84
Jun	3.08	3.55	3.77	4.07	3.10	3.97	4.25	4.84	3.06	3.16	3.25	3.49
Jul	3.27	3.70	4.07	4.42	3.29	4.19	4.80	5.44	3.25	3.28	3.37	3.63
Aug	2.74	3.22	3.64	3.96	2.75	3.66	4.26	4.78	2.72	2.85	3.13	3.15
Sep	1.83	2.02	2.20	2.38	1.83	2.27	2.54	2.85	1.82	1.75	1.80	1.90
Oct	1.02	1.12	1.23	1.30	1.02	1.20	1.35	1.45	1.01	1.04	1.12	1.18
Nov	0.61	0.69	0.74	0.78	0.62	0.73	0.82	0.88	0.61	0.65	0.66	0.67
Dec	0.51	0.53	0.56	0.59	0.51	0.57	0.60	0.65	0.50	0.49	0.52	0.52

Table B.3: Mean, 90th and 10th percentile of PET, for control and future scenarios in Kingston sub-catchment.

Months	Average				90th Percentile				10th Percentile			
	Control (1961-90)	2020s	2050s	2080s	Control (1961-90)	2020s	2050s	2080s	Control (1961-90)	2020s	2050s	2080s
Jan	0.00	-0.87	6.53	9.22	0.00	5.27	16.66	24.54	0.00	-6.93	-3.62	-3.49
Feb	0.00	4.55	8.46	14.63	0.00	9.34	14.80	25.09	0.00	-1.61	1.68	4.63
Mar	0.00	9.80	15.24	21.42	0.00	13.50	23.72	33.23	0.00	5.47	8.33	10.33
Apr	0.00	8.84	16.21	21.64	0.00	15.84	26.62	37.37	0.00	1.24	7.71	9.12
May	0.00	10.02	20.48	26.57	0.00	20.95	35.78	46.42	0.00	-0.44	8.43	9.47
Jun	0.00	15.20	22.45	32.21	0.00	28.09	37.14	56.20	0.00	3.16	6.00	13.89
Jul	0.00	13.20	24.53	35.16	0.00	27.44	45.91	65.30	0.00	0.96	3.80	11.67
Aug	0.00	17.58	33.00	44.60	0.00	32.91	54.68	73.77	0.00	4.67	14.89	15.74
Sep	0.00	10.65	20.44	30.13	0.00	23.88	38.41	55.73	0.00	-3.64	-1.10	4.54
Oct	0.00	10.54	21.22	28.28	0.00	18.20	32.08	42.13	0.00	2.46	10.22	16.23
Nov	0.00	12.06	20.31	27.02	0.00	18.34	32.46	43.10	0.00	6.42	8.34	10.81
Dec	0.00	4.96	10.21	15.41	0.00	10.78	16.78	26.02	0.00	-1.72	3.01	4.35

Table B.4: % change in mean, 90th and 10th percentile of projected PET from mean control in Kingston sub-catchment.

Months	Average				90th Percentile (Q10)				10th Percentile (Q90)			
	Control (1961-90)	2020s	2050s	2080s	Control (1961-90)	2020s	2050s	2080s	Control (1961-90)	2020s	2050s	2080s
Jan	139.51	122.17	111.16	101.70	146.60	152.83	143.63	135.83	132.70	91.45	80.91	72.46
Feb	128.12	120.43	117.06	114.18	134.21	143.23	145.15	160.50	122.20	98.40	93.70	81.54
Mar	108.83	106.59	103.27	104.92	113.45	122.80	124.22	130.02	104.30	89.29	85.14	80.93
Apr	77.66	73.53	71.46	69.22	80.76	86.60	87.23	85.86	73.83	63.31	59.40	56.42
May	53.90	50.74	47.76	45.18	56.22	58.55	55.30	53.07	51.37	43.04	41.10	38.44
Jun	42.87	40.39	37.57	35.95	44.64	46.02	43.59	43.19	41.24	34.93	32.13	30.09
Jul	35.53	32.87	30.16	28.55	37.09	37.44	35.25	33.97	34.18	27.84	25.64	23.19
Aug	33.37	30.22	26.08	24.58	34.86	37.08	33.73	32.27	31.98	23.93	21.09	17.47
Sep	36.78	31.37	25.67	23.27	39.23	40.28	34.94	32.13	34.92	23.85	19.18	15.62
Oct	49.24	38.32	31.17	27.51	52.87	50.33	45.30	37.45	46.00	28.04	23.17	19.29
Nov	73.18	57.28	45.91	40.61	78.12	80.34	67.58	55.67	68.53	40.10	32.58	27.31
Dec	112.96	95.03	78.77	70.96	118.79	129.42	117.54	101.08	104.71	68.51	54.93	45.97

Table B.5: Mean, 90th and 10th percentile projections of flow, for control and future scenarios in Kingston sub-catchment.

Months	Average				90th Percentile (Q10)				10th Percentile (Q90)			
	Control (1961-90)	2020s	2050s	2080s	Control (1961-90)	2020s	2050s	2080s	Control (1961-90)	2020s	2050s	2080s
Jan	0.00	-12.43	-20.32	-27.10	0.00	4.25	-2.03	-7.34	0.00	-31.08	-39.03	-45.40
Feb	0.00	-6.01	-8.64	-10.88	0.00	6.73	8.15	19.60	0.00	-19.48	-23.32	-33.27
Mar	0.00	-2.06	-5.11	-3.59	0.00	8.25	9.50	14.61	0.00	-14.39	-18.36	-22.41
Apr	0.00	-5.32	-7.98	-10.87	0.00	7.23	8.02	6.31	0.00	-14.24	-19.53	-23.57
May	0.00	-5.86	-11.39	-16.18	0.00	4.14	-1.64	-5.61	0.00	-16.20	-19.98	-25.16
Jun	0.00	-5.78	-12.35	-16.14	0.00	3.10	-2.34	-3.24	0.00	-15.30	-22.08	-27.04
Jul	0.00	-7.48	-15.12	-19.66	0.00	0.92	-4.97	-8.42	0.00	-18.56	-24.99	-32.14
Aug	0.00	-9.44	-21.85	-26.36	0.00	6.38	-3.23	-7.41	0.00	-25.17	-34.05	-45.39
Sep	0.00	-14.71	-30.20	-36.74	0.00	2.66	-10.93	-18.10	0.00	-31.70	-45.07	-55.26
Oct	0.00	-22.17	-36.69	-44.14	0.00	-4.80	-14.32	-29.17	0.00	-39.05	-49.63	-58.06
Nov	0.00	-21.73	-37.27	-44.51	0.00	2.83	-13.50	-28.75	0.00	-41.48	-52.46	-60.15
Dec	0.00	-15.88	-30.27	-37.18	0.00	8.94	-1.06	-14.91	0.00	-34.57	-47.54	-56.09

Table B.6: % change in mean, 90th and 10th percentile of projected flow from mean control in Kingston.

Months	Average				90th Percentile				10th Percentile			
	Control (1961-90)	2020s	2050s	2080s	Control (1961-90)	2020s	2050s	2080s	Control (1961-90)	2020s	2050s	2080s
Jan	4856.25	4841.99	4829.04	4818.41	4859.78	4861.96	4856.97	4850.13	4851.96	4820.72	4804.97	4788.34
Feb	4861.55	4851.00	4842.74	4835.11	4864.52	4868.41	4863.67	4860.46	4858.06	4830.60	4820.95	4810.98
Mar	4861.84	4853.59	4846.90	4841.82	4865.07	4869.26	4865.57	4863.45	4858.12	4836.85	4827.70	4821.86
Apr	4857.15	4848.79	4842.05	4836.94	4860.34	4862.02	4860.96	4856.56	4853.65	4831.95	4823.18	4816.46
May	4844.91	4834.05	4823.76	4816.26	4847.83	4847.53	4843.75	4839.67	4841.32	4816.50	4805.52	4794.69
Jun	4826.23	4810.31	4795.21	4783.04	4829.53	4827.66	4819.84	4813.75	4822.45	4790.84	4773.73	4753.33
Jul	4801.34	4778.85	4758.35	4741.53	4805.54	4799.95	4794.58	4780.78	4796.60	4754.16	4731.20	4703.52
Aug	4783.31	4753.78	4724.80	4706.22	4788.70	4784.68	4773.94	4759.56	4778.07	4718.65	4689.92	4659.26
Sep	4783.50	4749.04	4713.70	4693.89	4788.76	4787.41	4770.40	4749.40	4777.53	4710.63	4673.11	4640.38
Oct	4800.74	4765.53	4730.79	4708.94	4806.45	4801.39	4786.32	4766.22	4794.74	4728.34	4687.79	4649.34
Nov	4822.24	4792.31	4762.47	4742.87	4827.09	4823.07	4811.67	4796.19	4816.78	4758.67	4724.06	4688.85
Dec	4842.00	4820.89	4799.15	4784.29	4846.37	4846.62	4841.10	4827.88	4837.60	4794.53	4768.13	4740.37
Average	4828.42	4808.34	4789.08	4775.78	4832.50	4831.66	4824.06	4813.67	4823.91	4782.70	4760.86	4738.95

Table B.7: Mean, 90th and 10th percentile of subsurface storage, for control and future scenarios in Kingston sub-catchment.

Months	Average				90th Percentile				10th Percentile			
	Control (1961-90)	2020s	2050s	2080s	Control (1961-90)	2020s	2050s	2080s	Control (1961-90)	2020s	2050s	2080s
Jan	0.00	-0.29	-0.56	-0.78	0.00	0.04	-0.06	-0.20	0.00	-0.64	-0.97	-1.31
Feb	0.00	-0.22	-0.39	-0.54	0.00	0.08	-0.02	-0.08	0.00	-0.57	-0.76	-0.97
Mar	0.00	-0.17	-0.31	-0.41	0.00	0.09	0.01	-0.03	0.00	-0.44	-0.63	-0.75
Apr	0.00	-0.17	-0.31	-0.42	0.00	0.03	0.01	-0.08	0.00	-0.45	-0.63	-0.77
May	0.00	-0.22	-0.44	-0.59	0.00	-0.01	-0.08	-0.17	0.00	-0.51	-0.74	-0.96
Jun	0.00	-0.33	-0.64	-0.89	0.00	-0.04	-0.20	-0.33	0.00	-0.66	-1.01	-1.43
Jul	0.00	-0.47	-0.90	-1.25	0.00	-0.12	-0.23	-0.52	0.00	-0.88	-1.36	-1.94
Aug	0.00	-0.62	-1.22	-1.61	0.00	-0.08	-0.31	-0.61	0.00	-1.24	-1.84	-2.49
Sep	0.00	-0.72	-1.46	-1.87	0.00	-0.03	-0.38	-0.82	0.00	-1.40	-2.19	-2.87
Oct	0.00	-0.73	-1.46	-1.91	0.00	-0.11	-0.42	-0.84	0.00	-1.38	-2.23	-3.03
Nov	0.00	-0.62	-1.24	-1.65	0.00	-0.08	-0.32	-0.64	0.00	-1.21	-1.92	-2.66
Dec	0.00	-0.44	-0.88	-1.19	0.00	0.01	-0.11	-0.38	0.00	-0.89	-1.44	-2.01
Average	0.00	-0.42	-0.82	-1.09	0.00	-0.02	-0.18	-0.39	0.00	-0.86	-1.31	-1.77

Table B.8: % change in mean, 90th and 10th percentile of projected subsurface storage from control in Kingston sub-catchment.

Months	Average				90th Percentile				10th Percentile			
	Control (1961-90)	2020s	2050s	2080s	Control (1961-90)	2020s	2050s	2080s	Control (1961-90)	2020s	2050s	2080s
Jan	1.80	1.80	1.99	1.98	1.87	2.13	2.51	2.63	1.72	1.54	1.58	1.47
Feb	1.42	1.56	1.69	1.87	1.49	1.86	2.04	2.45	1.32	1.29	1.37	1.42
Mar	1.58	1.67	1.70	1.79	1.66	1.94	1.98	2.04	1.52	1.40	1.44	1.49
Apr	1.62	1.63	1.67	1.65	1.70	1.79	1.82	1.80	1.55	1.47	1.50	1.52
May	1.53	1.54	1.43	1.37	1.60	1.83	1.69	1.68	1.46	1.29	1.14	1.11
Jun	1.75	1.63	1.56	1.46	1.86	2.05	1.98	2.17	1.63	1.26	1.11	0.92
Jul	1.51	1.47	1.34	1.31	1.63	1.86	1.80	1.87	1.39	1.04	0.86	0.78
Aug	1.71	1.58	1.24	1.30	1.82	2.11	1.72	2.07	1.61	1.14	0.80	0.67
Sep	1.74	1.64	1.55	1.41	1.86	2.05	2.06	1.83	1.61	1.26	1.01	0.99
Oct	1.92	1.83	1.85	1.86	2.01	2.10	2.14	2.17	1.83	1.61	1.51	1.59
Nov	1.99	2.10	2.19	2.24	2.08	2.51	2.68	2.86	1.91	1.77	1.65	1.62
Dec	1.90	2.05	2.20	2.28	1.99	2.47	2.56	2.79	1.79	1.68	1.87	1.81

Table B.9: Mean, 90th and 10th percentiles of rainfall, for control and future scenarios in Lee sub-catchment.

Months	Average				90th Percentile				10th Percentile			
	Control (1961-90)	2020s	2050s	2080s	Control (1961-90)	2020s	2050s	2080s	Control (1961-90)	2020s	2050s	2080s
Jan	0.00	0.10	10.80	10.57	0.00	14.32	34.32	40.96	0.00	-10.65	-8.40	-14.70
Feb	0.00	10.41	19.07	32.01	0.00	24.93	36.52	64.06	0.00	-2.46	3.68	7.09
Mar	0.00	5.68	7.22	13.28	0.00	16.67	19.31	23.11	0.00	-7.89	-5.25	-1.54
Apr	0.00	0.53	3.19	1.88	0.00	5.52	7.16	5.97	0.00	-5.12	-3.02	-1.56
May	0.00	1.18	-6.05	-10.31	0.00	14.48	5.95	5.04	0.00	-11.61	-21.61	-23.82
Jun	0.00	-6.80	-10.80	-16.17	0.00	10.37	6.63	16.37	0.00	-23.17	-32.21	-43.77
Jul	0.00	-2.78	-11.66	-13.35	0.00	14.26	10.34	14.85	0.00	-25.09	-38.45	-44.02
Aug	0.00	-7.67	-27.55	-23.58	0.00	16.06	-5.47	13.93	0.00	-29.51	-50.13	-58.30
Sep	0.00	-5.26	-10.61	-18.90	0.00	10.20	10.60	-1.86	0.00	-21.50	-37.39	-38.84
Oct	0.00	-4.53	-3.56	-3.05	0.00	4.80	6.47	8.33	0.00	-11.85	-17.40	-13.18
Nov	0.00	5.78	10.57	13.03	0.00	20.45	28.57	37.20	0.00	-7.10	-13.32	-15.16
Dec	0.00	7.95	15.79	20.40	0.00	24.07	28.73	40.36	0.00	-6.12	4.06	0.80

Table B.10: % change in mean, 90th and 10th percentile of projected rainfall from mean control in Lee sub-catchment.

Months	Average				90th Percentile				10th Percentile			
	Control (1961-90)	2020s	2050s	2080s	Control (1961-90)	2020s	2050s	2080s	Control (1961-90)	2020s	2050s	2080s
Jan	0.57	0.56	0.61	0.62	0.58	0.61	0.67	0.71	0.57	0.52	0.55	0.54
Feb	0.70	0.73	0.76	0.80	0.71	0.77	0.81	0.89	0.70	0.68	0.71	0.72
Mar	1.24	1.36	1.43	1.50	1.24	1.41	1.54	1.65	1.23	1.29	1.33	1.36
Apr	1.85	2.01	2.15	2.25	1.85	2.15	2.35	2.55	1.84	1.86	1.98	2.01
May	2.63	2.90	3.18	3.34	2.65	3.21	3.60	3.89	2.62	2.61	2.84	2.87
Jun	3.13	3.61	3.84	4.14	3.15	4.04	4.32	4.92	3.12	3.20	3.30	3.53
Jul	3.31	3.75	4.13	4.49	3.33	4.25	4.88	5.53	3.29	3.32	3.42	3.68
Aug	2.82	3.31	3.74	4.07	2.83	3.77	4.38	4.92	2.80	2.93	3.21	3.24
Sep	1.88	2.09	2.27	2.46	1.89	2.35	2.63	2.95	1.88	1.80	1.86	1.97
Oct	1.05	1.17	1.28	1.35	1.06	1.25	1.40	1.50	1.05	1.08	1.16	1.22
Nov	0.61	0.68	0.73	0.77	0.61	0.72	0.81	0.88	0.60	0.64	0.65	0.67
Dec	0.51	0.53	0.56	0.58	0.51	0.57	0.60	0.64	0.50	0.49	0.52	0.52

Table B.11: Mean, 90th and 10th percentiles of PET, for control and future scenarios in Lee sub-catchment.

Months	Average				90th Percentile				10th Percentile			
	Control (1961-90)	2020s	2050s	2080s	Control (1961-90)	2020s	2050s	2080s	Control (1961-90)	2020s	2050s	2080s
Jan	0.00	-1.37	5.97	8.30	0.00	4.84	16.17	23.12	0.00	-7.74	-3.84	-3.93
Feb	0.00	4.32	8.19	14.27	0.00	9.31	14.67	25.51	0.00	-1.73	1.28	3.88
Mar	0.00	9.66	15.13	21.18	0.00	13.11	23.62	32.74	0.00	5.05	8.22	10.69
Apr	0.00	8.86	16.35	21.81	0.00	16.06	26.76	37.64	0.00	1.14	7.84	9.33
May	0.00	10.13	20.69	26.85	0.00	21.34	36.02	47.05	0.00	-0.57	8.44	9.58
Jun	0.00	15.12	22.35	32.10	0.00	28.16	37.21	56.13	0.00	2.64	5.80	13.37
Jul	0.00	13.34	24.80	35.55	0.00	27.71	46.60	66.23	0.00	0.97	4.06	11.86
Aug	0.00	17.46	32.81	44.47	0.00	33.19	54.75	73.92	0.00	4.52	14.31	15.67
Sep	0.00	10.79	20.75	30.57	0.00	24.13	38.91	56.22	0.00	-3.85	-0.84	4.84
Oct	0.00	10.70	21.43	28.52	0.00	18.31	32.16	42.17	0.00	2.71	10.31	16.34
Nov	0.00	12.07	20.29	26.90	0.00	18.40	32.12	43.44	0.00	6.57	8.27	10.75
Dec	0.00	4.70	9.73	14.48	0.00	10.92	16.16	24.06	0.00	-1.86	3.31	4.08

Table B.12: % change in mean, 90th and 10th percentile of projected PET from mean control in Lee sub-catchment.

Months	Average				90th Percentile				10th Percentile			
	Control (1961-90)	2020s	2050s	2080s	Control (1961-90)	2020s	2050s	2080s	Control (1961-90)	2020s	2050s	2080s
Jan	7.17	5.81	5.39	5.10	7.68	7.20	6.95	6.78	6.67	4.34	4.14	3.80
Feb	6.81	5.91	5.64	5.67	7.26	7.29	6.98	7.37	6.23	4.66	4.58	4.28
Mar	6.29	5.65	5.36	5.30	6.66	6.83	6.61	6.30	5.91	4.64	4.42	4.38
Apr	5.13	4.68	4.56	4.35	5.41	5.51	5.36	5.03	4.88	4.06	4.02	3.77
May	3.95	3.74	3.64	3.47	4.10	4.17	4.12	3.92	3.79	3.34	3.19	3.06
Jun	3.66	3.43	3.19	3.09	3.83	4.10	3.87	4.01	3.50	2.87	2.51	2.35
Jul	3.27	2.99	2.66	2.51	3.47	3.80	3.30	3.49	3.07	2.31	2.07	1.84
Aug	2.98	2.73	2.27	2.20	3.20	3.68	3.59	3.49	2.80	1.88	1.54	1.37
Sep	3.11	2.65	2.21	1.95	3.38	3.48	3.17	2.60	2.90	1.92	1.51	1.35
Oct	3.59	2.90	2.48	2.27	3.83	3.47	3.24	2.88	3.33	2.28	1.87	1.67
Nov	4.61	3.91	3.46	3.27	4.86	5.10	4.55	4.40	4.27	2.98	2.51	2.16
Dec	6.27	5.40	4.92	4.76	6.70	7.26	6.38	6.36	5.73	4.11	3.71	3.51

Table B.13: Mean, 90th and 10th percentiles of flow, for control and future scenarios in Lee sub-catchment.

Months	Average				90th Percentile				10th Percentile			
	Control (1961-90)	2020s	2050s	2080s	Control (1961-90)	2020s	2050s	2080s	Control (1961-90)	2020s	2050s	2080s
Jan	0.00	-19.02	-24.82	-28.82	0.00	-6.23	-9.51	-11.65	0.00	-34.85	-37.90	-43.09
Feb	0.00	-13.25	-17.14	-16.74	0.00	0.32	-3.91	1.45	0.00	-25.25	-26.57	-31.36
Mar	0.00	-10.17	-14.79	-15.75	0.00	2.49	-0.81	-5.45	0.00	-21.52	-25.21	-26.01
Apr	0.00	-8.79	-11.01	-15.24	0.00	1.88	-0.92	-6.89	0.00	-16.79	-17.70	-22.84
May	0.00	-5.25	-7.87	-11.94	0.00	1.63	0.42	-4.56	0.00	-11.92	-15.87	-19.22
Jun	0.00	-6.16	-12.92	-15.62	0.00	7.15	1.15	4.80	0.00	-17.97	-28.25	-32.89
Jul	0.00	-8.52	-18.69	-23.24	0.00	9.73	-4.73	0.60	0.00	-24.91	-32.74	-40.16
Aug	0.00	-8.58	-24.01	-26.37	0.00	15.26	12.20	9.18	0.00	-32.73	-44.98	-51.02
Sep	0.00	-14.74	-29.02	-37.34	0.00	2.87	-6.18	-22.92	0.00	-33.69	-48.03	-53.42
Oct	0.00	-19.16	-30.82	-36.82	0.00	-9.46	-15.51	-24.73	0.00	-31.39	-43.72	-49.99
Nov	0.00	-15.25	-25.03	-29.01	0.00	4.90	-6.42	-9.49	0.00	-30.27	-41.23	-49.43
Dec	0.00	-13.82	-21.52	-24.11	0.00	8.42	-4.74	-5.07	0.00	-28.30	-35.28	-38.79

Table B.14: % change in mean, 90th and 10th percentile of projected flow from mean control in Lee sub-catchment.

Months	Average				90th Percentile				10th Percentile			
	Control (1961-90)	2020s	2050s	2080s	Control (1961-90)	2020s	2050s	2080s	Control (1961-90)	2020s	2050s	2080s
Jan	6588.73	6542.17	6513.73	6497.11	6597.42	6584.10	6569.89	6546.15	6580.98	6498.63	6475.07	6457.54
Feb	6601.17	6559.43	6535.70	6521.34	6608.33	6596.85	6585.65	6565.48	6593.96	6517.08	6498.99	6485.07
Mar	6605.43	6567.21	6545.40	6533.98	6611.90	6604.12	6588.38	6572.67	6598.47	6527.17	6509.63	6499.64
Apr	6601.32	6563.15	6541.02	6529.38	6607.91	6600.07	6584.07	6568.10	6594.98	6524.45	6505.42	6494.76
May	6585.34	6543.99	6517.48	6502.80	6591.70	6581.23	6564.59	6543.58	6578.66	6503.44	6480.64	6467.50
Jun	6559.79	6512.29	6481.04	6461.90	6566.15	6551.37	6537.93	6515.51	6553.06	6469.31	6442.98	6421.28
Jul	6530.00	6476.67	6442.05	6420.20	6537.38	6520.77	6504.19	6479.14	6523.15	6430.19	6401.61	6377.48
Aug	6507.20	6449.66	6410.05	6388.78	6514.53	6502.14	6482.52	6445.87	6499.50	6398.94	6368.25	6342.10
Sep	6500.96	6440.76	6398.19	6376.96	6509.72	6495.40	6473.11	6428.48	6492.62	6390.16	6352.74	6329.19
Oct	6514.74	6453.25	6411.33	6388.86	6524.16	6502.90	6484.97	6443.74	6506.85	6399.04	6368.13	6338.35
Nov	6539.39	6480.30	6440.80	6419.55	6549.13	6529.40	6514.95	6475.73	6531.37	6429.96	6398.79	6370.14
Dec	6566.30	6513.28	6478.22	6459.40	6575.70	6562.62	6543.93	6513.47	6558.33	6464.85	6436.87	6414.52
Average	6558.36	6508.51	6476.25	6458.35	6566.17	6552.58	6536.18	6508.16	6550.99	6462.77	6436.59	6416.46

Table B.15: Mean, 90th and 10th percentile of subsurface storage, for control and future scenarios in Lee sub-catchment.

Months	Average				90th Percentile				10th Percentile			
	Control (1961-90)	2020s	2050s	2080s	Control (1961-90)	2020s	2050s	2080s	Control (1961-90)	2020s	2050s	2080s
Jan	0.00	-0.71	-1.14	-1.39	0.00	-0.20	-0.42	-0.78	0.00	-1.25	-1.61	-1.88
Feb	0.00	-0.63	-0.99	-1.21	0.00	-0.17	-0.34	-0.65	0.00	-1.17	-1.44	-1.65
Mar	0.00	-0.58	-0.91	-1.08	0.00	-0.12	-0.36	-0.59	0.00	-1.08	-1.35	-1.50
Apr	0.00	-0.58	-0.91	-1.09	0.00	-0.12	-0.36	-0.60	0.00	-1.07	-1.36	-1.52
May	0.00	-0.63	-1.03	-1.25	0.00	-0.16	-0.41	-0.73	0.00	-1.14	-1.49	-1.69
Jun	0.00	-0.72	-1.20	-1.49	0.00	-0.23	-0.43	-0.77	0.00	-1.28	-1.68	-2.01
Jul	0.00	-0.82	-1.35	-1.68	0.00	-0.25	-0.51	-0.89	0.00	-1.43	-1.86	-2.23
Aug	0.00	-0.88	-1.49	-1.82	0.00	-0.19	-0.49	-1.05	0.00	-1.55	-2.02	-2.42
Sep	0.00	-0.93	-1.58	-1.91	0.00	-0.22	-0.56	-1.25	0.00	-1.58	-2.15	-2.52
Oct	0.00	-0.94	-1.59	-1.93	0.00	-0.33	-0.60	-1.23	0.00	-1.66	-2.13	-2.59
Nov	0.00	-0.90	-1.51	-1.83	0.00	-0.30	-0.52	-1.12	0.00	-1.55	-2.03	-2.47
Dec	0.00	-0.81	-1.34	-1.63	0.00	-0.20	-0.48	-0.95	0.00	-1.43	-1.85	-2.19
Average	0.00	-0.76	-1.25	-1.53	0.00	-0.21	-0.46	-0.88	0.00	-1.35	-1.75	-2.06

Table B.16: % change in mean, 90th and 10th percentiles of projected subsurface from control in Lee sub-catchment.

Population Scenarios	Climate scenarios	Month												Annual
		Jan	Feb	Mar	Apr	May	Jun	Jul	Aug	Sep	Oct	Nov	Dec	
Current (2010)	Control	99.64	99.95	99.99	99.97	99.79	99.14	97.24	92.75	87.66	86.96	92.25	97.73	96.09
	2020s	96.44	98.92	99.62	99.73	99.26	97.84	94.18	86.91	78.55	75	79.96	89.67	91.34
	2050s	91.98	97.67	99.27	99.58	98.86	96.55	91.3	81.32	69.32	63.01	66.84	79.47	86.26
	2080s	87.35	95.54	98.37	99.03	98.21	95.25	88.67	77.22	64.18	56.1	58.72	71.93	82.55
2020	Control	99.29	99.89	99.97	99.95	99.59	98.39	95.44	89.50	83.31	82.41	88.90	96.23	94.41
	2020s	94.75	98.33	99.39	99.57	98.82	96.58	91.61	82.88	73.47	69.23	74.45	85.86	88.75
	2050s	89.02	96.62	98.87	99.32	98.24	94.87	88.15	76.72	63.72	56.49	60.00	73.83	82.99
	2080s	83.69	93.99	97.73	98.61	97.40	93.28	85.20	72.41	58.43	49.44	51.64	65.74	78.96
2050	Control	98.18	99.69	99.91	99.85	99.00	96.45	91.34	82.73	74.74	73.72	82.03	92.56	90.85
	2020s	91.12	97.02	98.85	99.15	97.68	93.73	86.36	75.15	64.03	58.95	64.56	78.44	83.75
	2050s	83.31	94.38	97.98	98.66	96.71	91.28	82.00	68.22	53.60	45.34	48.62	64.01	77.01
	2080s	77.12	90.93	96.40	97.66	95.53	89.24	78.67	63.73	48.29	38.46	40.40	55.55	72.67
2080	Control	95.42	99.05	99.73	99.58	97.62	92.51	84.12	72.30	62.26	60.55	70.36	85.10	84.88
	2020s	84.99	94.55	97.81	98.27	95.42	88.67	78.07	64.06	51.04	45.00	50.85	67.35	76.34
	2050s	74.94	90.48	96.36	97.37	93.87	85.33	72.84	56.55	40.30	31.57	34.93	51.53	68.84
	2080s	68.23	86.14	94.16	95.97	92.24	82.80	69.16	51.96	35.32	25.61	27.74	43.44	64.40

Table B.17: Mean total reservoir storage for different population and climate change scenarios.

Population Scenarios	Climate scenarios	Month												Annual
		Jan	Feb	Mar	Apr	May	Jun	Jul	Aug	Sep	Oct	Nov	Dec	
Current (2010)	Control	0.00	0.00	0.00	0.00	0.00	0.00	0.00	0.00	0.00	0.00	0.00	0.00	0.00
	2020s	-3.21	-1.03	-0.37	-0.24	-0.53	-1.31	-3.15	-6.30	-10.39	-13.75	-13.32	-8.25	-4.94
	2050s	-7.69	-2.28	-0.72	-0.39	-0.93	-2.61	-6.11	-12.32	-20.92	-27.54	-27.54	-18.68	-10.22
	2080s	-12.33	-4.41	-1.62	-0.94	-1.58	-3.92	-8.81	-16.74	-26.79	-35.49	-36.35	-26.40	-14.09
2020	Control	0.00	0.00	0.00	0.00	0.00	0.00	0.00	0.00	0.00	0.00	0.00	0.00	0.00
	2020s	-4.57	-1.56	-0.58	-0.38	-0.77	-1.84	-4.01	-7.40	-11.82	-16.00	-16.25	-10.78	-6.00
	2050s	-10.34	-3.27	-1.10	-0.62	-1.35	-3.58	-7.64	-14.28	-23.52	-31.45	-32.50	-23.28	-12.09
	2080s	-15.71	-5.91	-2.23	-1.34	-2.20	-5.19	-10.73	-19.10	-29.87	-40.01	-41.91	-31.69	-16.36
2050	Control	0.00	0.00	0.00	0.00	0.00	0.00	0.00	0.00	0.00	0.00	0.00	0.00	0.00
	2020s	-7.18	-2.69	-1.06	-0.70	-1.33	-2.82	-5.45	-9.16	-14.33	-20.02	-21.29	-15.26	-7.81
	2050s	-15.14	-5.33	-1.93	-1.19	-2.31	-5.36	-10.23	-17.53	-28.29	-38.50	-40.73	-30.84	-15.23
	2080s	-21.45	-8.79	-3.51	-2.19	-3.50	-7.47	-13.87	-22.96	-35.39	-47.83	-50.75	-39.98	-20.01
2080	Control	0.00	0.00	0.00	0.00	0.00	0.00	0.00	0.00	0.00	0.00	0.00	0.00	0.00
	2020s	-10.94	-4.55	-1.93	-1.32	-2.25	-4.16	-7.20	-11.41	-18.03	-25.68	-27.73	-20.85	-10.07
	2050s	-21.47	-8.65	-3.38	-2.22	-3.84	-7.77	-13.41	-21.79	-35.27	-47.86	-50.35	-39.45	-18.90
	2080s	-28.50	-13.04	-5.58	-3.62	-5.51	-10.50	-17.78	-28.13	-43.27	-57.71	-60.57	-48.96	-24.13

Table B.18: % change in mean total reservoir storage for different population and climate change scenarios.

Population Scenario	Climate scenarios	Average					change (%)				
		Lovel of services				Total	Level of services				Total
		Level 1	Level 2	Level 3	Level 4		Level 1	Level 2	Level 3	Level 4	
Current (2010)	Control	14.43	0.62	0.3	0.02	15.37	0.00	0.00	0.00	0.00	0.00
	2020s	35.1	5.67	4.74	1.19	46.70	143.24	814.52	1480.00	5850.00	203.84
	2050s	49.68	11.51	12.45	4.63	78.27	244.28	1756.45	4050.00	23050.00	409.24
	2080s	53.78	14.69	19.09	11.06	98.62	272.70	2269.35	6263.33	55200.00	541.64
2020	Control	21.23	1.44	0.75	0.08	23.49	0.00	0.00	0.00	0.00	0.00
	2020s	41.55	7.98	8.18	2.57	60.28	95.74	455.98	995.36	2953.12	156.58
	2050s	53.52	14.08	17.95	8.82	94.36	152.13	880.88	2303.35	10373.50	301.65
	2080s	55.86	16.96	24.68	17.88	115.38	163.15	1081.85	3204.57	21134.89	391.10
2050	Control	35.59	4.65	3.14	0.56	43.94	0.00	0.00	0.00	0.00	0.00
	2020s	50.77	12.54	16.23	7.94	87.47	42.64	169.57	416.72	1322.39	99.07
	2050s	56.58	18.41	27.74	21.02	123.75	58.98	295.82	783.22	3664.92	181.62
	2080s	56.52	20.10	33.49	34.67	144.78	58.82	332.27	966.24	6110.58	229.50
2080	Control	51.82	11.13	12.43	3.63	79.02	0.00	0.00	0.00	0.00	0.00
	2020s	57.69	17.95	27.63	22.79	126.07	11.34	61.19	122.23	527.12	59.54
	2050s	57.19	21.30	37.81	46.04	162.33	10.36	91.28	204.04	1166.79	105.43
	2080s	54.45	22.07	41.32	64.00	181.84	5.09	98.17	232.28	1661.05	130.12

Table B.19: Mean number of demand saving days (in 100 years) for different population and climate scenarios and % change from mean of control scenarios.

Climate & population scenarios	Level of services	Adaptation options							
		No adaptation	Desalination plant	Reduced leakage	New reservoir	Desalination & leakage	Desalination & New reservoir	Leakage & New reservoir	Desalination & Leakage & New reservoir
2020s	Level 1	41.55	39.74	40.09	-	38.19	-	-	-
	Level 2	7.98	6.55	7.44	-	5.99	-	-	-
	Level 3	8.18	5.61	7.30	-	4.90	-	-	-
	Level 4	2.57	1.34	2.18	-	1.11	-	-	-
2050s	Level 1	56.58	58.39	55.56	37.28	56.62	64.70	60.88	60.51
	Level 2	18.41	17.26	16.33	10.52	14.92	16.26	15.01	12.99
	Level 3	27.74	24.32	22.76	14.03	19.01	16.86	15.32	11.53
	Level 4	21.02	14.25	13.81	9.78	8.83	4.85	4.63	2.50
2080s	Level 1	54.45	57.24	56.16	44.38	58.76	68.38	66.63	68.62
	Level 2	22.07	21.95	20.77	17.62	20.51	25.92	23.47	22.06
	Level 3	41.32	40.13	36.52	30.65	34.18	40.53	34.31	30.28
	Level 4	64.00	52.16	43.02	42.87	33.02	30.82	23.67	16.55

Table B.20: Number of demand saving days (in 100 years) for different adaptation options, under climate and population scenarios (without demand reduction).

Climate & population scenarios	Level of services	Adaptation options							
		No adaptation	Desalination plant	Reduced leakage	New reservoir	Desalination & leakage	Desalination & New reservoir	Leakage & New reservoir	Desalination & Leakage & New reservoir
2020s	Level 1	0.00	-4.35	-3.52		-8.08			
	Level 2	0.00	-17.89	-6.78	-	-24.86	-	-	-
	Level 3	0.00	-31.37	-10.80	-	-40.13	-	-	-
	Level 4	0.00	-47.86	-15.38	-	-56.71	-	-	-
2050s	Level 1	0.00	3.20	-1.82	-34.11	0.07	14.34	7.59	6.95
	Level 2	0.00	-6.21	-11.27	-42.84	-18.93	-11.69	-18.45	-29.44
	Level 3	0.00	-12.33	-17.95	-49.44	-31.46	-39.22	-44.76	-58.43
	Level 4	0.00	-32.18	-34.30	-53.45	-57.97	-76.93	-77.95	-88.09
2080s	Level 1	0.00	5.12	3.13	-18.49	7.90	25.58	22.37	26.01
	Level 2	0.00	-0.51	-5.89	-20.15	-7.06	17.46	6.35	-0.04
	Level 3	0.00	-2.87	-11.62	-25.81	-17.28	-1.90	-16.96	-26.73
	Level 4	0.00	-18.51	-32.78	-33.02	-48.40	-51.85	-63.02	-74.15

Table B.21: % change in mean number of demand saving days (in 100 years) for different adaptation options compared to no adaptation, under different climate and population scenarios (without demand reduction).

Climate & population scenarios	Level of services	Adaptation options							
		No adaptation	Desalination plant	Reduced leakage	New reservoir	Desalination & leakage	Desalination & New reservoir	Leakage & New reservoir	Desalination & Leakage & New reservoir
2020s	Level 1	0.00	0.00	0.00	0.00	0.00	0.00	0.00	0.00
	Level 2	0.00	0.00	0.00	0.00	0.00	0.00	0.00	0.00
	Level 3	0.00	0.00	0.00	0.00	0.00	0.00	0.00	0.00
	Level 4	0.00	0.00	0.00	0.00	0.00	0.00	0.00	0.00
2050s	Level 1	0.00	0.00	0.00	0.00	0.00	0.00	0.00	0.00
	Level 2	0.00	0.00	0.00	0.00	0.00	0.00	0.00	0.00
	Level 3	0.00	0.00	0.00	0.00	0.00	0.00	0.00	0.00
	Level 4	0.00	0.00	0.00	0.00	0.00	0.00	0.00	0.00
2080s	Level 1	56.09	57.77	52.56	35.21	52.91	62.84	55.20	54.09
	Level 2	17.40	16.19	13.65	9.49	11.95	15.06	11.34	9.51
	Level 3	25.74	22.20	16.84	12.57	13.38	15.33	10.27	7.31
	Level 4	19.42	13.25	8.96	9.85	5.42	4.94	3.08	1.65

Table B.22: Number of demand saving days (in 100 years) for combination of demand and supply adaptation options, under climate and population scenarios, after 25% reduction in per person demand.

Climate & population scenarios	Level of services	Adaptation options							
		No adaptation	Desalination plant	Reduced leakage	New reservoir	Desalination & leakage	Desalination & New reservoir	Leakage & New reservoir	Desalination & Leakage & New reservoir
2020s	Level 1	0.00	0.00	0.00	0.00	0.00	0.00	0.00	0.00
	Level 2	0.00	0.00	0.00	0.00	0.00	0.00	0.00	0.00
	Level 3	0.00	0.00	0.00	0.00	0.00	0.00	0.00	0.00
	Level 4	0.00	0.00	0.00	0.00	0.00	0.00	0.00	0.00
2050s	Level 1	0.00	0.00	0.00	0.00	0.00	0.00	0.00	0.00
	Level 2	0.00	0.00	0.00	0.00	0.00	0.00	0.00	0.00
	Level 3	0.00	0.00	0.00	0.00	0.00	0.00	0.00	0.00
	Level 4	0.00	0.00	0.00	0.00	0.00	0.00	0.00	0.00
2080s	Level 1	0.00	2.99	-6.30	-37.23	-5.67	12.02	-1.59	-3.58
	Level 2	0.00	-6.95	-21.54	-45.49	-31.35	-13.45	-34.84	-45.32
	Level 3	0.00	-13.72	-34.57	-51.17	-48.03	-40.42	-60.10	-71.61
	Level 4	0.00	-31.77	-53.88	-49.30	-72.08	-74.58	-84.17	-91.49

Table B.23: % change in mean number of demand saving days (in 100 years) after 25% reduction in per person demand, for different adaptation options compared to no adaptation, under climate and population scenarios, after 25% reduction in per person demand.

Impacts of different adaptation option on number of drought days, for different combinations of population and climate scenarios:

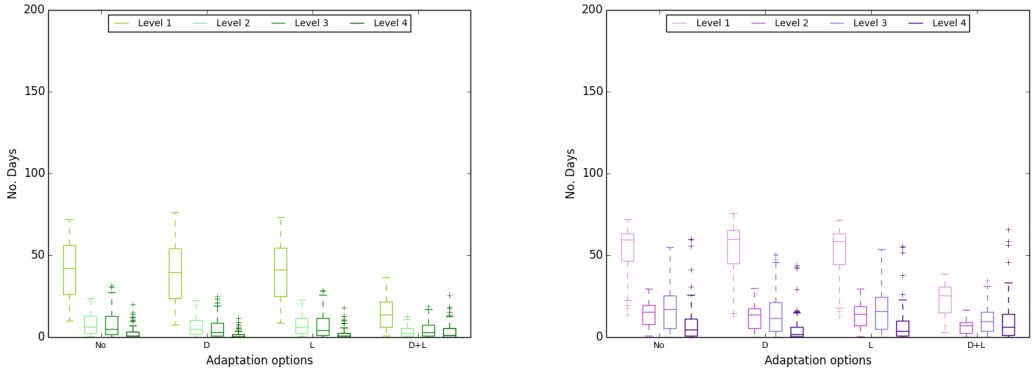

(a) (b)

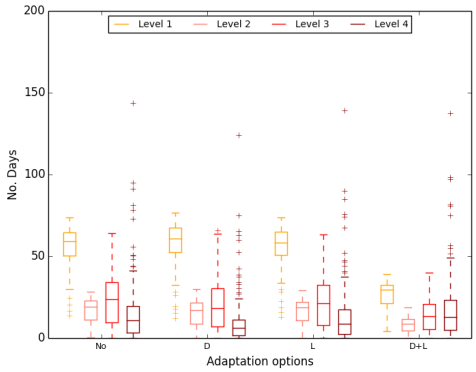

(c)

Figure B.1: Boxplots of number of demand saving days for different adaptation options, population scenario of 2020s and climate change scenarios: (a) 2020s, (b) 2050s, (c) 2080s.

Climate scenarios	Level of services	Adaptation Options			
		No adaptation	Desalination plant	Reduced leakage	Desalination and leakage
2020	Level 1	41.55	39.74	40.09	38.19
	Level 2	7.98	6.55	7.44	5.99
	Level 3	8.18	5.61	7.30	4.90
	Level 4	2.57	1.34	2.18	1.11
2050	Level 1	53.52	53.87	52.83	52.89
	Level 2	14.08	12.70	13.47	12.05
	Level 3	17.95	14.13	16.62	12.94
	Level 4	8.82	5.23	7.72	4.46
2080	Level 1	55.86	57.42	55.55	56.87
	Level 2	16.96	15.73	16.42	15.23
	Level 3	24.68	21.08	23.40	19.72
	Level 4	17.88	12.04	16.17	10.73

Table B.24: Number of demand saving days (in 100 years) for different adaptation options, population scenario of 2020s.

Climate scenarios	Level of services	Adaptation Options			
		No adaptation	Desalination plant	Reduced leakage	Desalination and leakage
2020	Level 1	0.00	-4.35	-3.52	-8.08
	Level 2	0.00	-17.89	-6.78	-24.86
	Level 3	0.00	-31.37	-10.80	-40.13
	Level 4	0.00	-47.86	-15.38	-56.71
2050	Level 1	0.00	0.65	-1.29	-1.17
	Level 2	0.00	-9.76	-4.32	-14.40
	Level 3	0.00	-21.28	-7.43	-27.89
	Level 4	0.00	-40.72	-12.42	-49.38
2080	Level 1	0.00	2.79	-0.55	1.81
	Level 2	0.00	-7.27	-3.16	-10.18
	Level 3	0.00	-14.59	-5.18	-20.09
	Level 4	0.00	-32.64	-9.55	-39.99

Table B.25: % change in number of demand saving days (in 100 years) for different adaptation options (compared to No adaptation option), population scenario of 2020s.

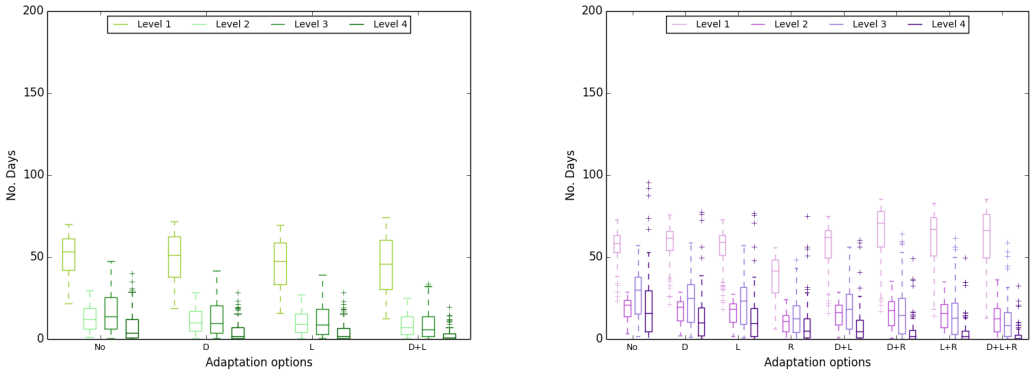

(a)

(b)

(c)

Figure B.2: Boxplots of number of demand saving days for different adaptation options, population scenario of 2050s and climate change scenarios: (a) 2020s, (b) 2050s, (c) 2080s.

Climate scenarios	Level of services	Adaptation options							
		No adaptation	Desalination plant	Reduced leakage	New reservoir	Desalination & leakage	Desalination & New reservoir	Leakage & New reservoir	Desalination & Leakage & New reservoir
2020s	Level 1	50.77	50.16	46.32	-	45.30	-	-	-
	Level 2	12.54	11.16	10.28	-	8.59	-	-	-
	Level 3	16.23	12.79	11.78	-	8.75	-	-	-
	Level 4	7.94	4.74	4.59	-	2.55	-	-	-
2050s	Level 1	56.58	58.39	55.56	37.28	56.62	64.70	60.88	60.51
	Level 2	18.41	17.26	16.33	10.52	14.92	16.26	15.01	12.99
	Level 3	27.74	24.32	22.76	14.03	19.01	16.86	15.32	11.53
	Level 4	21.02	14.25	13.81	9.78	8.83	4.85	4.63	2.50
2080s	Level 1	56.52	58.92	56.52	41.09	58.61	67.69	64.62	65.33
	Level 2	20.10	19.66	18.81	13.07	17.78	19.95	18.73	17.17
	Level 3	33.49	30.70	29.15	19.89	25.84	25.49	23.65	19.42
	Level 4	34.67	25.73	25.17	19.71	17.86	11.85	11.56	7.27

Table B.26: Number of demand saving days (in 100 years) for different adaptation options, population scenario of 2050s.

Climate scenarios	Level of services	Adaptation options							
		No adaptation	Desalination plant	Reduced leakage	New reservoir	Desalination & leakage	Desalination & New reservoir	Leakage & New reservoir	Desalination & Leakage & New reservoir
2020s	Level 1	0.00	-1.21	-8.75	-	-10.78	-	-	-
	Level 2	0.00	-10.96	-17.96	-	-31.45	-	-	-
	Level 3	0.00	-21.17	-27.39	-	-46.09	-	-	-
	Level 4	0.00	-40.36	-42.20	-	-67.91	-	-	-
2050s	Level 1	0.00	3.20	-1.82	-34.11	0.07	14.34	7.59	6.95
	Level 2	0.00	-6.21	-11.27	-42.84	-18.93	-11.69	-18.45	-29.44
	Level 3	0.00	-12.33	-17.95	-49.44	-31.46	-39.22	-44.76	-58.43
	Level 4	0.00	-32.18	-34.30	-53.45	-57.97	-76.93	-77.95	-88.09
2080s	Level 1	0.00	4.24	-0.01	-27.31	3.68	19.76	14.32	15.58
	Level 2	0.00	-2.20	-6.43	-34.97	-11.54	-0.76	-6.84	-14.60
	Level 3	0.00	-8.33	-12.97	-40.59	-22.85	-23.89	-29.39	-42.02
	Level 4	0.00	-25.78	-27.40	-43.15	-48.49	-65.81	-66.66	-79.03

Table B.27: % change in number of demand saving days (in 100 years) for different adaptation options (compared to no adaptation option), population scenario of 2050s.

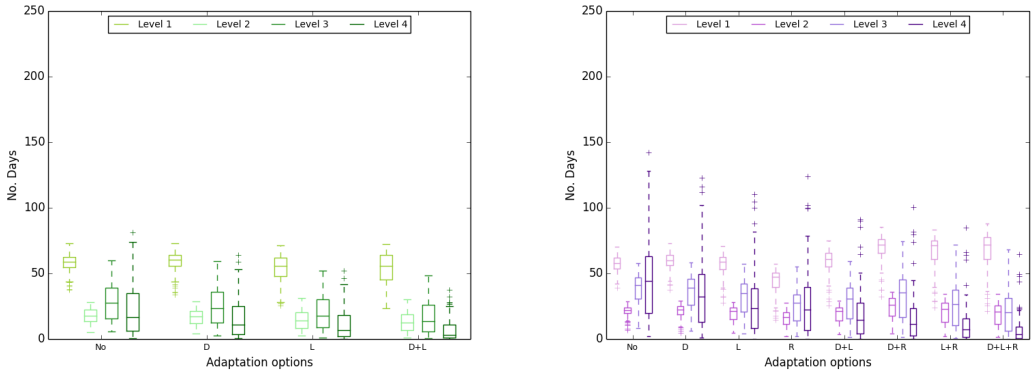

(a) (b)

(c)

Figure B.3: Boxplots of number of demand saving days (in 100 years) for different adaptation options, population scenario of 2080s and climate change scenarios: (a) 2020s, (b) 2050s, (c) 2080s.

Climate scenarios	Level of services	Adaptation options							
		No adaptation	Desalination plant	Reduced leakage	New reservoir	Desalination & leakage	Desalination & New reservoir	Leakage & New reservoir	Desalination & Leakage & New reservoir
2020s	Level 1	57.69	58.60	53.59	-	53.46	-	-	-
	Level 2	17.95	16.63	14.21	-	12.86	-	-	-
	Level 3	27.63	24.44	19.80	-	16.39	-	-	-
	Level 4	22.79	16.06	11.54	-	7.28	-	-	-
2050s	Level 1	57.19	59.23	57.09	43.72	58.96	69.52	66.06	66.97
	Level 2	21.30	21.01	19.41	15.65	18.81	23.65	20.53	18.73
	Level 3	37.81	35.91	31.45	25.36	28.27	32.73	26.21	21.61
	Level 4	46.04	35.56	27.77	27.40	19.77	17.23	12.05	7.57
2080s	Level 1	54.45	57.24	56.16	44.38	58.76	68.38	66.63	68.62
	Level 2	22.07	21.95	20.77	17.62	20.51	25.92	23.47	22.06
	Level 3	41.32	40.13	36.52	30.65	34.18	40.53	34.31	30.28
	Level 4	64.00	52.16	43.02	42.87	33.02	30.82	23.67	16.55

Table B.28: Number of demand saving days (in 100 years) for different adaptation options, population scenario of 2080s.

Climate scenarios	Level of services	Adaptation options							
		No adaptation	Desalination plant	Reduced leakage	New reservoir	Desalination & leakage	Desalination & New reservoir	Leakage & New reservoir	Desalination & Leakage & New reservoir
2020s	Level 1	0.00	1.57	-7.11	-	-7.34	-	-	-
	Level 2	0.00	-7.32	-20.85	-	-28.37	-	-	-
	Level 3	0.00	-11.54	-28.35	-	-40.70	-	-	-
	Level 4	0.00	-29.55	-49.38	-	-68.06	-	-	-
2050s	Level 1	0.00	3.57	-0.17	-23.55	3.10	21.57	15.52	17.12
	Level 2	0.00	-1.36	-8.86	-26.53	-11.66	11.04	-3.62	-12.05
	Level 3	0.00	-5.02	-16.81	-32.93	-25.22	-13.44	-30.67	-42.84
	Level 4	0.00	-22.77	-39.69	-40.49	-57.06	-62.57	-73.83	-83.55
2080s	Level 1	0.00	5.12	3.13	-18.49	7.90	25.58	22.37	26.01
	Level 2	0.00	-0.51	-5.89	-20.15	-7.06	17.46	6.35	-0.04
	Level 3	0.00	-2.87	-11.62	-25.81	-17.28	-1.90	-16.96	-26.73
	Level 4	0.00	-18.51	-32.78	-33.02	-48.40	-51.85	-63.02	-74.15

Table B.29: % change in number of demand saving days (in 100 years) for different adaptation options (compared to no adaptation option), population scenario of 2080s.

Appendix C

Supporting documents for Chapter 5

Year	Flow (mm/year)		Change (%)
	Current land cover	Increased urban developments	
1991	46841.03	55225.24	17.90
1992	83344.21	92200.86	10.63
1993	96238.65	104716.76	8.81
1994	101132.50	108245.51	7.03
1995	94821.27	102341.87	7.93
1996	56707.68	63879.56	12.65
1997	44632.45	53610.23	20.11
1998	102264.09	113207.27	10.70
1999	102750.07	111355.58	8.38
2000	151618.68	162571.37	7.22
2001	138512.23	143178.86	3.37

Table C.1: Total annual flow before and after increasing the urban area in Kingston sub-catchment.

Year	Flow (mm/year)		Change (%)
	Current land cover	Increased urban developments	
1991	3617.96	3724.49	2.94
1992	4909.06	6041.10	23.06
1993	6370.31	7833.07	22.96
1994	6475.43	6951.08	7.35
1995	5907.04	6635.13	12.33
1996	3056.84	3197.74	4.61
1997	2787.29	2936.46	5.35
1998	5187.93	6483.89	24.98
1999	5196.45	6493.21	24.95
2000	11293.68	12533.68	10.98
2001	12922.47	13412.23	3.79

Table C.2: Total annual flow before and after increasing the urban area in Lee sub-catchment.

Climate scenario	Mean No drought days			Change (%)
	Level of services	New land cover	Current land cover	
1970	Level 1	4.98	14.43	-65.48
	Level 2	0.15	0.62	-75.25
	Level 3	0.04	0.30	-86.71
	Level 4	0.00	0.02	-100.00
2020	Level 1	20.20	35.10	-42.47
	Level 2	2.02	5.67	-64.34
	Level 3	1.31	4.74	-72.45
	Level 4	0.23	1.19	-81.05
2050	Level 1	35.14	49.68	-29.27
	Level 2	5.43	11.51	-52.84
	Level 3	4.68	12.45	-62.41
	Level 4	1.13	4.63	-75.62
2080	Level 1	42.17	53.78	-21.59
	Level 2	8.45	14.69	-42.47
	Level 3	9.00	19.09	-52.84
	Level 4	3.71	11.06	-66.43

Table C.3: Mean number of demand saving days (in 100 years) for increased urban development and the percentage of change compared to the current land cover .

Months	Current				New land cover				Change (%) (new land cover vs current)			
	Control (1961-1990)	2020s	2050s	2080s	Control (1961-1990)	2020s	2050s	2080s	Control (1961-1990)	2020s	2050s	2080s
Jan	99.64	96.44	91.98	87.35	99.94	99.01	97.41	95.03	0.30	2.66	5.91	8.79
Feb	99.95	98.92	97.67	95.54	99.99	99.77	99.52	98.70	0.04	0.86	1.89	3.31
Mar	99.99	99.62	99.27	98.37	100.00	99.92	99.88	99.58	0.01	0.30	0.61	1.23
Apr	99.97	99.73	99.58	99.03	99.99	99.91	99.88	99.70	0.02	0.18	0.30	0.68
May	99.79	99.26	98.86	98.21	99.89	99.65	99.46	99.18	0.10	0.39	0.61	0.99
Jun	99.14	97.84	96.55	95.25	99.56	98.84	98.06	97.29	0.42	1.02	1.57	2.14
Jul	97.24	94.18	91.3	88.67	98.47	96.44	94.44	92.46	1.27	2.40	3.44	4.28
Aug	92.75	86.91	81.32	77.22	95.59	91.07	86.57	83.13	3.07	4.79	6.46	7.66
Sep	87.66	78.55	69.32	64.18	92.37	84.71	76.53	71.99	5.38	7.84	10.41	12.16
Oct	86.96	75	63.01	56.1	92.67	82.98	72.34	65.99	6.56	10.65	14.81	17.62
Nov	92.25	79.96	66.84	58.72	96.65	88.74	78.81	71.66	4.77	10.98	17.90	22.04
Dec	97.73	89.67	79.47	71.93	99.41	95.88	90.36	84.86	1.72	6.92	13.70	17.98

Table C.4: Total reservoir level for current and new land cover [A1-P (0%)-D (0%)-L (0%)-U2 vs U1].

	Population			% Change (Relative to 2010)		
Year	Low	Central	High	Low	Central	High
2010	8,107,073	8,107,073	8,107,073	-	-	-
2011	8,217,475	8,217,475	8,217,475	1.36	1.36	1.36
2020	9,071,303	9,127,567	9,184,047	11.89	12.59	13.28
2030	9,571,176	9,782,155	9,997,220	18.06	20.66	23.31
2040	9,976,895	10,307,871	10,649,201	23.06	27.15	31.36
2050	10,342,890	10,776,890	11,228,103	27.58	32.93	38.50
2060	10,708,886	11,245,909	11,807,006	32.09	38.72	45.64
2070	11,074,881	11,714,929	12,385,909	36.61	44.50	52.78
2080	11,440,877	12,183,948	12,964,812	41.12	50.29	59.92

Table C.5: Population projections (GLA 2014*a*).

Time slice	Level of services	Population scenarios								
		P (-15%)	P (-10%)	P (-5%)	P (0%)	P (+5%)	P (10%)	P (25%)	P (+50%)	P (+75%)
1970	Level 1	6.22	8.47	11.25	14.43	17.98	21.92	34.54	52.44	62.14
	Level 2	0.16	0.26	0.39	0.62	1.00	1.51	4.30	11.62	18.54
	Level 3	0.03	0.09	0.17	0.30	0.49	0.77	2.81	13.14	28.02
	Level 4	0.00	0.00	0.00	0.02	0.04	0.09	0.48	3.97	17.41
2020	Level 1	24.43	28.02	31.64	35.10	38.56	41.89	50.00	57.49	59.17
	Level 2	2.52	3.45	4.48	5.67	6.93	8.15	12.23	18.23	22.16
	Level 3	1.64	2.36	3.41	4.74	6.37	8.35	15.45	28.24	39.28
	Level 4	0.26	0.47	0.77	1.19	1.80	2.64	7.23	23.83	50.87
2050	Level 1	41.09	44.36	47.26	49.68	51.84	53.48	56.09	56.56	54.50
	Level 2	6.80	8.19	9.86	11.51	12.95	14.27	18.15	21.33	23.42
	Level 3	5.78	7.78	9.92	12.45	15.18	18.21	26.93	38.20	44.20
	Level 4	1.26	2.05	3.16	4.63	6.58	8.98	19.57	47.55	82.44
2080	Level 1	47.89	50.23	52.10	53.78	54.96	55.68	56.14	53.71	50.49
	Level 2	10.23	11.86	13.39	14.69	15.88	17.10	19.94	22.05	22.86
	Level 3	11.10	13.54	16.26	19.09	22.02	24.92	32.78	41.57	45.73
	Level 4	4.35	6.13	8.34	11.06	14.33	18.11	32.80	65.61	102.27

Table C.6: Mean number of demand saving days in 100 years [A1-P (all)-D (0%)-L (0%)-U1].

Time slice	Level of services	Population scenarios								
		P (-15%)	P (-10%)	P (-5%)	P (0%)	P (+5%)	P (10%)	P (25%)	P (+50%)	P (+75%)
1970	Level 1	-56.91	-41.30	-22.05	-	24.58	51.90	139.37	263.37	330.60
	Level 2	-73.80	-58.54	-36.79	-	59.94	142.32	591.71	1767.96	2879.85
	Level 3	-89.68	-69.44	-43.39	-	63.09	154.81	831.16	4246.66	9172.65
	Level 4	-100.00	-97.32	-67.11	-	148.32	496.64	3088.59	26276.51	115677.18
2020	Level 1	-30.41	-20.17	-9.88	-	9.85	19.32	42.44	63.78	68.55
	Level 2	-55.52	-39.04	-21.02	-	22.33	43.74	115.77	221.65	290.91
	Level 3	-65.37	-50.15	-28.17	-	34.26	76.05	225.81	495.69	728.51
	Level 4	-77.98	-60.48	-35.16	-	51.21	120.96	506.51	1898.17	4165.59
2050	Level 1	-17.30	-10.70	-4.88	-	4.34	7.65	12.91	13.85	9.70
	Level 2	-40.93	-28.84	-14.35	-	12.43	23.94	57.65	85.26	103.43
	Level 3	-53.55	-37.53	-20.31	-	21.93	46.26	116.21	206.76	254.92
	Level 4	-72.78	-55.72	-31.71	-	42.02	93.69	322.17	926.14	1678.93
2080	Level 1	-10.95	-6.61	-3.13	-	2.18	3.54	4.39	-0.12	-6.13
	Level 2	-30.36	-19.25	-8.82	-	8.13	16.39	35.78	50.10	55.65
	Level 3	-41.82	-29.09	-14.79	-	15.34	30.55	71.73	117.76	139.58
	Level 4	-60.69	-44.61	-24.56	-	29.59	63.74	196.56	493.28	824.78

Table C.7: % change in mean number of drought days relative to P (0%) [A1-P (all)-D (0%)-L (0%)-U1].

Time slice	Level of services	PCC scenarios														
		D (-50%)	D (-40%)	D (-38%)	D (-30%)	D (-25%)	D (-20%)	D (-15%)	D (-10%)	D (-5%)	D (0%)	D (+0.5%)	D (+5%)	D (+10%)	D (+15%)	D (+20%)
1970	Level 1	0.29	0.84	1.06	2.02	3.01	4.39	6.22	8.47	11.25	14.43	14.78	17.98	21.92	26.13	30.37
	Level 2	0.00	0.00	0.00	0.02	0.03	0.09	0.16	0.26	0.39	0.62	0.65	1.00	1.51	2.15	3.09
	Level 3	0.00	0.00	0.00	0.00	0.00	0.01	0.03	0.09	0.17	0.30	0.32	0.49	0.77	1.24	1.89
	Level 4	0.00	0.00	0.00	0.00	0.00	0.00	0.00	0.00	0.00	0.02	0.02	0.04	0.09	0.17	0.29
2020	Level 1	4.90	8.80	9.99	14.21	17.42	20.88	24.43	28.02	31.64	35.10	35.46	38.56	41.89	44.85	47.52
	Level 2	0.11	0.38	0.47	0.83	1.22	1.76	2.52	3.45	4.48	5.67	5.78	6.93	8.15	9.55	11.01
	Level 3	0.02	0.12	0.18	0.45	0.72	1.10	1.64	2.36	3.41	4.74	4.89	6.37	8.35	10.52	12.87
	Level 4	0.00	0.00	0.00	0.03	0.07	0.14	0.26	0.47	0.77	1.19	1.24	1.80	2.64	3.79	5.29
2050	Level 1	14.25	21.50	23.40	29.48	33.46	37.36	41.09	44.36	47.26	49.68	49.92	51.84	53.48	54.75	55.62
	Level 2	0.56	1.54	1.91	3.18	4.28	5.52	6.80	8.19	9.86	11.51	11.65	12.95	14.27	15.68	17.00
	Level 3	0.17	0.61	0.83	1.83	2.85	4.15	5.78	7.78	9.92	12.45	12.72	15.18	18.21	21.18	24.10
	Level 4	0.02	0.08	0.10	0.23	0.41	0.75	1.26	2.05	3.16	4.63	4.81	6.58	8.98	11.89	15.42
2080	Level 1	22.89	30.67	32.66	38.34	41.83	45.07	47.89	50.23	52.10	53.78	53.92	54.96	55.68	56.07	56.21
	Level 2	1.93	3.67	4.20	6.10	7.46	8.81	10.23	11.86	13.39	14.69	14.80	15.88	17.10	18.29	19.24
	Level 3	1.05	2.52	3.04	5.04	6.75	8.75	11.10	13.54	16.26	19.09	19.39	22.02	24.92	27.70	30.33
	Level 4	0.13	0.43	0.57	1.25	1.99	3.01	4.35	6.13	8.34	11.06	11.35	14.33	18.11	22.44	27.35

Table C.8: Mean number of demand saving days in 100 years [A1- P (0%)-D (All)- L(0%)-U1].

Time slice	Level of services	PCC scenarios)														
		D (-50%)	D (-40%)	D (-38%)	D (-30%)	D (-25%)	D (-20%)	D (-15%)	D (-10%)	D (-5%)	D (0%)	D (+0.5%)	D (+5%)	D (+10%)	D (+15%)	D (+20%)
1970	Level 1	-97.98	-94.20	-92.66	-85.97	-79.11	-69.60	-56.91	-41.30	-22.05	-	2.39	24.58	51.90	81.09	110.44
	Level 2	-100.00	-100.00	-99.77	-97.21	-95.09	-85.73	-73.80	-58.54	-36.79	-	4.38	59.94	142.32	245.11	396.64
	Level 3	-100.00	-100.00	-100.00	-100.00	-98.90	-95.26	-89.68	-69.44	-43.39	-	5.54	63.09	154.81	311.02	526.45
	Level 4	-100.00	-100.00	-100.00	-100.00	-100.00	-100.00	-100.00	-97.32	-67.11	-	10.07	148.32	496.64	1000.67	1835.57
2020	Level 1	-86.05	-74.93	-71.53	-59.52	-50.37	-40.51	-30.41	-20.17	-9.88	-	1.01	9.85	19.32	27.75	35.36
	Level 2	-98.04	-93.35	-91.69	-85.43	-78.51	-69.01	-55.52	-39.04	-21.02	-	2.05	22.33	43.74	68.46	94.27
	Level 3	-99.62	-97.41	-96.17	-90.56	-84.84	-76.85	-65.37	-50.15	-28.17	-	3.17	34.26	76.05	121.80	171.49
	Level 4	-100.00	-100.00	-99.90	-97.69	-94.50	-88.33	-77.98	-60.48	-35.16	-	4.24	51.21	120.96	217.99	343.97
2050	Level 1	-71.32	-56.72	-52.89	-40.66	-32.65	-24.80	-17.30	-10.70	-4.88	-	0.47	4.34	7.65	10.20	11.94
	Level 2	-95.15	-86.59	-83.39	-72.40	-62.86	-52.06	-40.93	-28.84	-14.35	-	1.20	12.43	23.94	36.14	47.63
	Level 3	-98.61	-95.13	-93.33	-85.29	-77.13	-66.68	-53.55	-37.53	-20.31	-	2.16	21.93	46.26	70.06	93.54
	Level 4	-99.61	-98.27	-97.78	-95.06	-91.07	-83.90	-72.78	-55.72	-31.71	-	3.82	42.02	93.69	156.55	232.69
2080	Level 1	-57.45	-42.97	-39.27	-28.72	-22.22	-16.19	-10.95	-6.61	-3.13	-	0.27	2.18	3.54	4.25	4.52
	Level 2	-86.86	-74.99	-71.43	-58.50	-49.23	-40.03	-30.36	-19.25	-8.82	-	0.78	8.13	16.39	24.53	31.00
	Level 3	-94.52	-86.82	-84.05	-73.61	-64.64	-54.15	-41.82	-29.09	-14.79	-	1.59	15.34	30.55	45.14	58.89
	Level 4	-98.82	-96.11	-94.84	-88.73	-82.02	-72.81	-60.69	-44.61	-24.56	-	2.68	29.59	63.74	102.88	147.33

Table C.9: % change in mean number of drought days relative to D (0%) [A1- P(0%)-D (All)- L(0%)-U1].

Time slice	Level of services	Leakage scenarios									
		L (-40%)	L (-20%)	L (-17%)	L (-15%)	L (-10%)	L (-5%)	L (0%)	L (+5%)	L (+10%)	L (+15%)
1970	Level 1	8.45	9.66	10.32	10.75	11.94	13.15	14.43	15.74	17.13	18.56
	Level 2	0.26	0.31	0.34	0.36	0.44	0.52	0.62	0.74	0.90	1.07
	Level 3	0.09	0.13	0.14	0.16	0.19	0.24	0.30	0.37	0.44	0.53
	Level 4	0.00	0.00	0.00	0.00	0.01	0.01	0.02	0.02	0.03	0.04
2020	Level 1	27.99	29.66	30.49	31.04	32.42	33.73	35.10	36.45	37.80	39.11
	Level 2	3.45	3.90	4.13	4.29	4.75	5.20	5.67	6.13	6.64	7.10
	Level 3	2.35	2.80	3.05	3.22	3.68	4.18	4.74	5.32	5.97	6.65
	Level 4	0.47	0.59	0.67	0.72	0.85	1.01	1.19	1.40	1.65	1.92
2050	Level 1	44.33	45.70	46.40	46.83	47.84	48.78	49.68	50.54	51.40	52.14
	Level 2	8.18	8.95	9.30	9.55	10.25	10.89	11.51	12.08	12.64	13.12
	Level 3	7.76	8.71	9.21	9.54	10.46	11.40	12.45	13.47	14.53	15.66
	Level 4	2.04	2.51	2.77	2.95	3.47	4.02	4.63	5.32	6.10	6.92
2080	Level 1	50.20	51.11	51.52	51.79	52.49	53.16	53.78	54.30	54.75	55.08
	Level 2	11.85	12.58	12.92	13.16	13.73	14.22	14.69	15.11	15.60	16.07
	Level 3	13.51	14.74	15.39	15.81	16.87	17.94	19.09	20.24	21.36	22.48
	Level 4	6.11	7.07	7.58	7.93	8.92	9.94	11.06	12.23	13.54	14.88

Table C.10: Mean number of demand saving days in 100 years [A1- P (0%)-D (0%)- L(All)-U1].

Time slice	Level of services	Leakage scenarios									
		L (-40%)	L (-20%)	L (-17%)	L (-15%)	L (-10%)	L (-5%)	L (0%)	L (+5%)	L (+10%)	L (+15%)
1970	Level 1	-41.46	-33.03	-28.49	-25.50	-17.26	-8.88	-	9.10	18.73	28.62
	Level 2	-58.73	-50.12	-45.24	-41.48	-29.62	-16.33	-	18.88	44.80	71.63
	Level 3	-69.64	-58.15	-52.14	-47.90	-35.60	-19.27	-	22.65	46.76	74.28
	Level 4	-97.99	-86.58	-79.87	-74.50	-54.36	-34.90	-	36.24	95.30	184.56
2020	Level 1	-20.26	-15.52	-13.13	-11.58	-7.64	-3.91	-	3.82	7.68	11.41
	Level 2	-39.15	-31.12	-27.11	-24.35	-16.20	-8.20	-	8.17	17.07	25.31
	Level 3	-50.34	-40.92	-35.58	-32.13	-22.42	-11.74	-	12.15	25.87	40.36
	Level 4	-60.65	-50.14	-44.19	-40.03	-28.34	-15.41	-	17.39	38.06	60.63
2050	Level 1	-10.77	-8.01	-6.60	-5.73	-3.71	-1.81	-	1.73	3.45	4.94
	Level 2	-28.98	-22.28	-19.22	-17.03	-10.99	-5.43	-	4.90	9.75	13.96
	Level 3	-37.67	-30.03	-26.03	-23.40	-16.04	-8.49	-	8.16	16.71	25.78
	Level 4	-55.90	-45.81	-40.20	-36.28	-25.11	-13.28	-	14.86	31.59	49.38
2080	Level 1	-5.58	-3.86	-3.08	-2.58	-1.26	-1.15	-	0.97	1.80	2.42
	Level 2	-16.72	-11.57	-9.14	-7.48	-3.50	-3.16	-	2.89	6.18	9.37
	Level 3	-24.69	-17.85	-14.20	-11.88	-5.96	-6.01	-	6.03	11.92	17.78
	Level 4	-38.55	-28.83	-23.70	-20.19	-10.24	-10.13	-	10.55	22.42	34.55

Table C.11: % change in mean number of drought days relative to L (0%) [A1- P (0%)-D (0%)- L(All)-U1].

Appendix D

Supporting documents for Chapter 6

Climate scenario	Level of services	Water use scenarios		Difference (%)
		Current	High	
1970	Level 1	14.43	64.79	349.00
	Level 2	0.62	27.17	4282.26
	Level 3	0.30	46.47	15390.00
	Level 4	0.02	62.47	312250.00
2020	Level 1	35.10	55.48	58.06
	Level 2	5.67	27.51	385.19
	Level 3	4.74	51.11	978.27
	Level 4	1.19	105.17	8737.82
2050	Level 1	49.68	47.52	-4.35
	Level 2	11.51	26.94	134.06
	Level 3	12.45	52.93	325.14
	Level 4	4.63	137.95	2879.48
2080	Level 1	53.78	43.04	-19.97
	Level 2	14.69	25.31	72.29
	Level 3	19.09	52.54	175.22
	Level 4	11.06	156.64	1316.27

Table D.1: Impact of High water use scenario on mean number of demand saving days (in 100 years) with current land cover.

Climate scenario	Level of services	Water use scenarios		Change (%)
		Current	Low	
1970	Level 1	14.43	0.03	-99.82
	Level 2	0.62	0.00	-100.00
	Level 3	0.30	0.00	-100.00
	Level 4	0.02	0.00	-100.00
2020	Level 1	35.10	1.27	-96.37
	Level 2	5.67	0.00	-99.99
	Level 3	4.74	0.00	-100.00
	Level 4	1.19	0.00	-100.00
2050	Level 1	49.68	5.25	-89.44
	Level 2	11.51	0.07	-99.42
	Level 3	12.45	0.02	-99.87
	Level 4	4.63	0.00	-100.00
2080	Level 1	53.78	11.10	-79.36
	Level 2	14.69	0.40	-97.30
	Level 3	19.09	0.12	-99.36
	Level 4	11.06	0.00	-99.98

Table D.2: Impact of Low water use scenario on mean number of demand saving days (in 100 years) with current land cover.

Climate scenario	Level of services	Adaptation options			
		No adaptation	Desalination plant	New Reservoir	Desalination and New reservoir
1970	Level 1	64.86	66.20	78.49	78.49
	Level 2	23.49	22.11	26.92	24.25
	Level 3	38.70	35.91	36.29	30.60
	Level 4	38.78	29.37	17.69	11.82
2020	Level 1	57.94	60.09	70.35	72.35
	Level 2	24.96	24.29	30.95	29.56
	Level 3	45.79	44.33	53.26	49.08
	Level 4	79.15	67.40	55.96	44.74
2050	Level 1	51.50	54.06	61.41	64.75
	Level 2	25.14	24.67	31.77	31.26
	Level 3	48.25	47.41	62.23	59.40
	Level 4	112.65	100.47	91.25	77.19
2080	Level 1	46.78	49.49	55.32	58.59
	Level 2	24.23	24.04	30.06	30.10
	Level 3	48.56	47.93	63.65	61.60
	Level 4	132.27	120.19	114.16	99.55

Table D.3: Mean number of demand saving days (in 100 years) for High water use scenario with current land cover.

Climate scenarios	Level of services	Adaptaion options			
		No adaptation	Desalination plant	New Reservoir	Desalination and New reservoir
1970	Level 1	-	2.07	21.01	21.02
	Level 2	-	-5.87	14.60	3.22
	Level 3	-	-7.21	-6.24	-20.94
	Level 4	-	-24.27	-54.39	-69.51
2020	Level 1	-	3.72	21.42	24.87
	Level 2	-	-2.66	24.02	18.42
	Level 3	-	-3.19	16.31	7.19
	Level 4	-	-14.84	-29.30	-43.47
2050	Level 1	-	4.96	19.24	25.73
	Level 2	-	-1.86	26.38	24.35
	Level 3	-	-1.74	28.98	23.12
	Level 4	-	-10.82	-19.00	-31.48
2080	Level 1	-	5.79	18.24	25.23
	Level 2	-	-0.79	24.08	24.24
	Level 3	-	-1.30	31.08	26.87
	Level 4	-	-9.13	-13.69	-24.74

Table D.4: % change in mean number of demand saving days (in 100 years) for High water use scenario with current land cover, relative to No adaptation option.

Climate scenario	Level of services	Adaptation options			
		No adaptation	Desalination plant	New Reservoir	Desalination and New reservoir
1970	Level 1	65.37	64.87	74.13	71.82
	Level 2	19.76	17.89	19.65	16.48
	Level 3	28.84	24.69	21.04	16.03
	Level 4	18.80	12.95	5.87	3.47
2020	Level 1	62.20	63.54	73.95	74.63
	Level 2	23.96	22.93	27.90	25.72
	Level 3	40.58	37.38	41.13	35.98
	Level 4	48.40	39.14	28.21	20.86
2050	Level 1	57.64	59.82	69.38	71.78
	Level 2	25.67	25.04	32.09	30.81
	Level 3	46.44	44.45	55.27	50.72
	Level 4	76.64	65.51	52.83	41.89
2080	Level 1	53.73	56.26	64.18	67.08
	Level 2	25.53	25.14	31.97	31.45
	Level 3	48.80	47.17	60.19	56.41
	Level 4	94.02	82.54	71.82	59.48

Table D.5: Mean mean number of demand saving days (in 100 years) for High water use scenario with increased urbanization.

Climate scenario	Level of services	Adaptation options			
		No adaptation	Desalination plant	New Reservoir	Desalination and New reservoir
1970	Level 1	0.00	-0.77	13.40	9.87
	Level 2	0.00	-9.47	-0.56	-16.62
	Level 3	0.00	-14.38	-27.02	-44.41
	Level 4	0.00	-31.11	-68.80	-81.55
2020	Level 1	0.00	2.15	18.89	19.99
	Level 2	0.00	-4.27	16.44	7.35
	Level 3	0.00	-7.88	1.37	-11.34
	Level 4	0.00	-19.13	-41.70	-56.89
2050	Level 1	0.00	3.78	20.37	24.53
	Level 2	0.00	-2.43	25.02	20.05
	Level 3	0.00	-4.29	19.01	9.21
	Level 4	0.00	-14.51	-31.07	-45.34
2080	Level 1	0.00	4.72	19.45	24.86
	Level 2	0.00	-1.50	25.22	23.19
	Level 3	0.00	-3.34	23.34	15.60
	Level 4	0.00	-12.20	-23.61	-36.74

Table D.6: % change in mean number of demand saving days (in 100 years) for High scenario with increased urbanization, relative to No adaptation option.

Months	Current				Low				High			
	Control (1961-1990)	2020s	2050s	2080s	Control (1961-1990)	2020s	2050s	2080s	Control (1961-1990)	2020s	2050s	2080s
Jan	99.64	96.44	91.98	87.35	100	99.96	99.87	99.48	76.9	61.62	50.49	44.53
Feb	99.95	98.92	97.67	95.54	100	100	99.99	99.9	91.13	80.09	72.23	66.5
Mar	99.99	99.62	99.27	98.37	100	100	100	99.98	96.9	90.5	86.13	82.12
Apr	99.97	99.73	99.58	99.03	100	100	100	99.99	96.71	92.22	89.29	86.52
May	99.79	99.26	98.86	98.21	100	100	99.99	99.99	88.97	83.69	80.24	77.27
Jun	99.14	97.84	96.55	95.25	100	99.99	99.97	99.92	74.45	68.29	63.3	59.69
Jul	97.24	94.18	91.3	88.67	99.99	99.92	99.77	99.45	57.3	50.15	44.13	40.24
Aug	92.75	86.91	81.32	77.22	99.95	99.48	98.6	97.46	38.99	31.32	24.56	21.13
Sep	87.66	78.55	69.32	64.18	99.82	98.47	95.93	93.56	25.45	17.62	10.88	8.9
Oct	86.96	75	63.01	56.1	99.79	97.94	94.34	91.05	22.99	13.93	7.5	5.45
Nov	92.25	79.96	66.84	58.72	99.91	98.66	96.05	93.17	33.47	20.27	11.63	8.49
Dec	97.73	89.67	79.47	71.93	99.99	99.67	98.84	97.44	54.28	37.76	26.09	21.12

Table D.7: Mean total reservoir storage (%) for current, Low and High water use scenarios.

Months	Low change (%)				High change (%)			
	Control (1961-1990)	2020s	2050s	2080s	Control (1961-1990)	2020s	2050s	2080s
Jan	0.36	3.65	8.58	13.89	-22.82	-36.11	-45.11	-49.02
Feb	0.05	1.09	2.38	4.56	-8.82	-19.04	-26.05	-30.40
Mar	0.01	0.38	0.74	1.64	-3.09	-9.15	-13.24	-16.52
Apr	0.03	0.27	0.42	0.97	-3.26	-7.53	-10.33	-12.63
May	0.21	0.75	1.14	1.81	-10.84	-15.69	-18.83	-21.32
Jun	0.87	2.20	3.54	4.90	-24.90	-30.20	-34.44	-37.33
Jul	2.83	6.09	9.28	12.16	-41.07	-46.75	-51.66	-54.62
Aug	7.76	14.46	21.25	26.21	-57.96	-63.96	-69.80	-72.64
Sep	13.87	25.36	38.39	45.78	-70.97	-77.57	-84.30	-86.13
Oct	14.75	30.59	49.72	62.30	-73.56	-81.43	-88.10	-90.29
Nov	8.30	23.39	43.70	58.67	-63.72	-74.65	-82.60	-85.54
Dec	2.31	11.15	24.37	35.47	-44.46	-57.89	-67.17	-70.64

Table D.8: % change in mean total reservoir storage for High and Low water use scenarios compared to current scenario.

Flow (m^3/s)	Level of services				Total number of drought days
	Level 1	Level 2	Level 3	Level 4	
0.00	0.19	0.07	0.14	368.06	368.46
7.23	0.26	0.09	0.18	367.90	368.43
12.52	0.33	0.13	0.25	367.69	368.40
14.41	0.36	0.14	0.29	367.58	368.38
16.80	0.41	0.15	0.34	367.46	368.37
17.01	0.43	0.17	0.36	367.39	368.36
22.11	0.63	0.22	78.60	288.85	368.30
23.15	0.67	0.49	155.02	212.10	368.28
27.66	191.91	57.77	118.22	0	367.90
28.77	206.07	100.45	36.46	0	342.97
30.70	239.07	27.29	0	0	266.36
33.94	95.24	0	0	0	95.24
36.00	22.47	0	0	0	22.47
36.52	2.57	0	0	0	2.57
36.78	0	0	0	0	0
37.03	0	0	0	0	0
37.30	0	0	0	0	0
37.50	0	0	0	0	0
37.80	0	0	0	0	0
37.90	0	0	0	0	0
37.95	0	0	0	0	0
37.99	0	0	0	0	0
38.00	0	0	0	0	0
38.07	0	0	0	0	0
38.58	0	0	0	0	0
38.89	0	0	0	0	0
39.00	0	0	0	0	0
39.10	0	0	0	0	0
41.16	0	0	0	0	0
43.23	0	0	0	0	0

Table D.9: Number of demand saving days in 100 years (stress test, including demand saving measures).

Flow (m^3/s)	Level of services				Total number of drought days
	Level 1	Level 2	Level 3	Level 4	
0.00	0.17	0.06	0.11	368.13	368.47
3.40	0.19	0.06	0.12	368.08	368.45
7.23	0.21	0.08	0.13	368.01	368.43
12.52	0.27	0.09	0.17	367.87	368.40
14.41	0.30	0.10	0.19	367.80	368.39
16.80	0.32	0.11	0.20	367.74	368.37
17.01	0.34	0.12	0.21	367.70	368.37
19.54	0.38	0.14	0.26	367.55	368.34
22.11	0.45	0.16	0.32	367.37	368.31
23.15	0.47	0.17	0.35	367.29	368.29
27.66	0.65	0.24	0.68	366.64	368.20
28.77	0.70	0.27	0.87	366.32	368.16
30.70	1.68	1.04	1.32	364.06	368.10
33.94	10.60	6.58	20.65	328.28	366.11
36.00	160.84	0	0	0	160.84
36.52	103.11	0	0	0	103.11
36.78	73.85	0	0	0	73.85
37.03	46.51	0	0	0	46.51
37.30	17.33	0	0	0	17.33
37.50	0	0	0	0	0
37.80	0	0	0	0	0
37.90	0	0	0	0	0
37.95	0	0	0	0	0
37.99	0	0	0	0	0
38.00	0	0	0	0	0
38.07	0	0	0	0	0
38.58	0	0	0	0	0
38.89	0	0	0	0	0
39.00	0	0	0	0	0
39.10	0	0	0	0	0
41.16	0	0	0	0	0
43.23	0	0	0	0	0

Table D.10: Number of demand saving days in 100 years (stress test, without demand saving measures).